The Complement System and invariant Natural Killer T (iNKT) Cell Responses





Nazish Malik

Radcliffe Department of Medicine
St Anne's College
University of Oxford

Biology Group 2
Adaptive Immunity Research Unit
GSK

This thesis is submitted as part of the requirements for the degree of
Doctor of Philosophy in Medical Sciences

Hilary Term 2021

Abstract

The recent discovery of intracellular complement activation, specifically anaphylatoxin generation and downstream autocrine receptor engagement in conventional α/β CD4+ T cells has provided new insights into mechanisms of T cell activation, polarisation, and homeostatic survival. Anaphylatoxin generation by antigen-presenting cells (APCs) which leads to paracrine signalling via anaphylatoxin receptors on T cells has also been observed but is less extensively described. It is speculated that cell-derived complement may also influence the activity of non-conventional α/β T cells, specifically invariant Natural Killer T (iNKT) cells. The modulation of iNKT cell effector function by cell-derived complement may manifest in two ways, either through autocrine signalling events or via paracrine signalling by neighbouring APCs. Through a combination of molecular biology approaches, a thorough appraisal of iNKT complement expression profiles was performed. Specifically, iNKT cells were shown to up-regulate C3 and the anaphylatoxin receptors C3aR and C5aR1 on their cell surface upon activation with the canonical ligand α-GalCer. Moreover, iNKT cells may 'recycle' C3 from the extracellular space, to potentially regulate complement in their local microenvironment. As iNKT cells mature dendritic cells (DC) in a CD40L-dependent manner, subsequent work showed that engagement of the CD40-CD40L axis also influenced DC complement expression profiles. Specifically, the alternative pathway (AP) complement protein Factor B (FB) along with C3 were positively modulated by CD40 ligation. Moreover, pharmacological inhibition of FB by proprietary GSK inhibitors, specifically cell-permeable small molecules was shown to suppress DC effector function. Subsequent work which assessed cell-derived anaphylatoxin generation was undertaken to validate the specificity of pharmacological inhibition. In conclusion, potential crosstalk mechanisms between the CD40-CD40L axis and FB may underscore DC activation profiles. Modulation of DC effector function may in turn influence iNKT activation at the iNKT-APC interface.

Laboratory work performed

- Dawn Shepherd, Uzi Gileadi and Andrea Tarlton generated the CD1d and β2M monomers, used for iNKT cell sorting.
- Claudia Gonzalez-Lopez generated the biotinylated CD1d monomer used for plate-bound activation of iNKT cells.
- Prathiba Kurupati collected and froze IL-2 and IL-4 from supernatants, which were subsequently thawed and used for cell culture.
- Craig Waugh, Sally-Ann Clark, Kevin Clark and Paul Sopp performed fluorescence-activated cell sorting of iNKT cells.
- Jana Koth set up the Confocal Laser Scanning Microscope (Zeiss LSM 880) for co-localisation experiments in iNKT cells.
- Fraser Cunningham (along with other members of GSK's Medicinal Chemistry department) generated the small-molecule Factor B inhibitors and the Factor B blocking antibodies used for alternative pathway inhibition.
- Claire Cattermole ruthenylated the anti-human C3a and C5a antibodies which were used for MSD detection of anaphylatoxins.
- Isabelle Osuch tested the Factor B blocking antibodies in a haemolysis assay.
- Mass spectrometry was performed by members of GSK's Medicinal Chemistry Department.

Common Abbreviations

α-GalCer	alpha-galactosylceramide
ANOVA	Analysis of variance
AP	Alternative Pathway
APC	Antigen presenting cell
β2M	β2 Microglobulin
C3	Complement component 3
C3a	Complement component 3 anaphylatoxin
C5	Complement component 5
C5a	Complement component 5 anaphylatoxin
CD	Cluster of differentiation
CM	Complete Medium
fB	Factor B
FCS	Foetal calf serum
fD	Factor D
IFN	Interferon
Ig	Immunoglobulin
IL	Interleukin
IMDM	Iscove's Modified Dulbecco's Medium
MAC	Membrane attack complex
MdDC	Monocyte-derived dendritic cell
MHC	Major histocompatibility complex
Min	Minute
MSD	MesoScale Discovery
NHS	Normal Human Serum
iNKT	Invariant Natural killer T cell
ns	non-significant
PBMC	Peripheral blood mononuclear cell
PBS	Phosphate buffered saline
PCR	Polymerase chain reaction
PFA	Paraformaldehyde

qRT	Quantitative Real Time
RPMI	Roswell Park Memorial Institute (Medium)
RT	Room temperature
SFM	Serum-free Medium
SD	Standard Deviation
TCR	T cell receptor
TLR	Toll-like receptor

Table of Contents

1 INTRODUCTION 11

1.1 OVERVIEW OF THE IMMUNE SYSTEM 11

1.2 THE COMPLEMENT SYSTEM 14

1.2.1 AN OVERVIEW OF EXTRACELLULAR COMPLEMENT ACTIVATION 14

1.2.2 CELLULAR COMPLEMENT AND INNATE IMMUNITY 20

1.2.3 CELLULAR COMPLEMENT AND ADAPTIVE IMMUNE RESPONSES 26

1.3 CONTROVERSIAL ASPECTS OF INTRACELLULAR COMPLEMENT GENERATION AND SIGNALLING 39

1.4 NON-CONVENTIONAL T CELLS 45

1.4.1 INVARIANT NATURAL KILLER T (iNKT) CELLS 45

1.4.2 CD1D STRUCTURE AND FUNCTION 49

1.4.3 CD1D-DEPENDENT AND INDEPENDENT iNKT CELL ACTIVATION 49

1.4.4 THE CD40-CD40L SIGNALLING AXIS 51

1.4.5 iNKT CELL EFFECTOR FUNCTIONS 52

1.4.6 iNKT CELLS AND COMPLEMENT 54

1.5 COMPLEMENT PATHOLOGY AND THERAPEUTIC POTENTIAL 55

1.5.1 KIDNEY DISEASE 55

1.5.2 AGE-RELATED MACULAR DEGENERATION (AMD) 56

1.5.3 SYSTEMIC LUPUS ERYTHEMATOSUS (SLE) 56

1.5.4 HAEMATOLOGICAL DISORDERS 57

1.5.5 TRANSPLANT REJECTION 58

1.5.6 ISCHAEMIA-REPERFUSION INJURY (IRI) 58

1.5.7 LEVERAGING iNKT CELLS AS A THERAPEUTIC STRATEGY 59

1.6 MAIN HYPOTHESIS & PROJECT AIMS 61

2 MATERIALS AND METHODS 62

2.1 CELL CULTURE MEDIA 62

2.2 SAMPLE PROCESSING 62

2.3 GENERATION OF MONOCYTE-DERIVED DENDRITIC CELLS (MDDCS) 63

2.3.1 SEPARATION USING THE MACS® MICROBEADS (MILTENYI BIOTEC): 63

2.3.2 SEPARATION USING THE EASYSEP™ HUMAN CD14 POSITIVE SELECTION KIT II (STEMCELL): 64

2.4 GENERATION OF iNKT CELLS 64

2.5 STIMULATION AND INHIBITION ASSAYS 65

2.5.1 CD40L (CD154) BLOCKADE 65

2.5.2 CD40L-INDUCED MDDC MATURATION 66

2.5.3 CD1D PLATE-BOUND ASSAY 66

2.5.4 SMALL-MOLECULE OR ANTIBODY-MEDIATED INHIBITION OF AP 67

2.6 FLOW CYTOMETRY AND CELL SORTING 67

2.6.1 CELL VIABILITY AND SURFACE STAINING 67

2.6.2 INTRACELLULAR STAINING 68

2.6.3 FLOW CYTOMETRY ANTIBODIES 68

2.6.4 ANALYSERS AND CELL SORTERS 69

2.7 ENZYME-LINKED IMMUNOSORBENT ASSAY (ELISA) OF IFN-GAMMA AND IL-12P40/70 70

2.7.1 CAPTURE AND DETECTION ANTIBODIES 71

2.7.2 CYTOKINE STANDARDS 72

2.8 COMPLEMENT C3 AND FACTOR B DETECTION (ELISA KITS) 72

2.9 MESOSCALE DISCOVERY (MSD) FOR ANAPHYLATOXIN DETECTION 73

2.9.1 SAMPLE GENERATION I.E. ALTERNATIVE PATHWAY ACTIVATION IN PLASMA 73

2.9.2 ANALYSIS OF ANAPHYLATOXIN (C3A AND C5A) GENERATION 74

2.10 CYTOKINE BEAD ARRAY 75

2.11 QUANTITATIVE REVERSE TRANSCRIPTION (RT-QPCR) 77

2.11.1 PROBES USED FOR RT-QPCR 81

2.12 CONFOCAL MICROSCOPY 82

2.12.1 ANTIBODIES USED FOR CONFOCAL MICROSCOPY 83

2.13 ASSESSMENT OF CO-LOCALISATION 83

2.14 WESTERN BLOT 84

2.14.1 PRIMARY ANTIBODIES FOR WESTERN BLOT 86

2.14.2 SECONDARY ANTIBODIES FOR WESTERN BLOT 86

2.15 CELL-FREE ASSAY (SILVER STAIN) 87

2.16 CRISPR/CAS 9 88

2.16.1 TRANSFECTION PROTOCOL 88

2.16.2 GUIDE RNA (GRNA) SEQUENCES 89

2.16.3 ASSESSMENT OF GENE AND PROTEIN EXPRESSION POST-CRISPR 89

2.17 STATISTICAL DATA ANALYSIS (IMPLEMENTATION STRATEGY) 90

2.17.1 ASSESSMENT OF NORMALITY 90

2.17.2 STATISTICAL ANALYSIS (ON NORMALLY DISTRIBUTED DATA): 91

2.17.3 STATISTICAL ANALYSIS (ON DATA WHICH WAS NOT NORMALLY DISTRIBUTED): 91

RESULTS 92

3 CHARACTERISATION OF INKT CELL AND DENDRITIC CELL COMPLEMENT EXPRESSION PROFILES 92

3.1 SURFACE ANAPHYLATOXIN RECEPTOR EXPRESSION IN INKT CELLS 96

3.2 INKT ANAPHYLATOXIN RECEPTORS AND THEIR COGNATE LIGANDS 104

3.3 INKT NATIVE COMPLEMENT EXPRESSION 111

3.4 COMPLEMENT RECYCLING PATHWAYS IN INKT CELLS 114

3.5 MODULATION OF INKT CELL EFFECTOR FUNCTION BY ANAPHYLATOXINS 120

3.6 THE CD40-CD40L AXIS AND POTENTIAL IMPLICATIONS FOR COMPLEMENT SIGNALLING PATHWAYS 123

3.7 CD40L-INDUCED MDDC COMPLEMENT EXPRESSION PROFILES 125

3.8 CD40L-INDUCTION OF MDDC COMPLEMENT SECRETION PROFILES 128

3.9 CD40L-INDUCED COMPLEMENT CLEAVAGE 131

3.10 DISCUSSION 134

3.10.1 WHAT COMPLEMENT PROTEINS DO INKT CELLS EXPRESS? 134

3.10.2 IS INKT CELL EFFECTOR FUNCTION MODULATED BY COMPLEMENT? 135

3.10.3 DO NEIGHBOURING ANTIGEN-PRESENTING CELLS EXPRESS AND SECRETE COMPLEMENT AP PROTEINS? 136

4 ALTERNATIVE PATHWAY (AP) INHIBITION IN MONOCYTE-DERIVED DENDRITIC CELLS (MDDCS) 138

4.1 PROFILING OF FACTOR B INHIBITORS IN THE MODULATION OF ALTERNATIVE PATHWAY ACTIVATION 140

4.2 ANTIBODY-MEDIATED BLOCKADE OF FACTOR B 144

4.3 SMALL MOLECULE-MEDIATED INHIBITION OF FACTOR B 149

4.4 ATTEMPT AT VALIDATION OF SMALL MOLECULE INHIBITION OF FACTOR B BY ASSESSMENT OF ANAPHYLATOXIN GENERATION 154

4.4.1 APPROACH 1: ASSESSMENT OF C3A AND C5A SECRETION BY MSD 154

4.4.2 APPROACH 2: ASSESSMENT OF C3A GENERATION BY WESTERN BLOT 156

4.4.3 APPROACH 3: ATTEMPT AT ASSESSMENT OF C3A GENERATION IN A CELL-FREE ASSAY 160

4.5 ASSESSMENT OF COMPLEMENT EXPRESSION PROFILES IN THP-1 CELLS 164

4.6 CRISPR-CAS9 TARGETING OF COMPLEMENT C3 IN THP-1 CELLS 167

4.7 DISCUSSION 177

4.7.1 PART 1: PHARMACOLOGICAL BLOCKADE OF AP 177

4.7.2 PART 2: ASSESSMENT OF PHARMACOLOGICAL BLOCKADE OF AP IN CELLS 178

4.7.3 PART 3: EFFECT OF GENETIC ABLATION OF C3 IN CELLS 179

5 GENERAL DISCUSSION 183

5.1 INKT CELLS AND COMPLEMENT 183

5.2 DENDRITIC CELLS AND COMPLEMENT 186

5.3 POTENTIAL FUTURE EXPERIMENTS 189

5.4 POTENTIAL THERAPEUTIC IMPLICATIONS OF THIS WORK 193

6 APPENDIX 194

7 REFERENCES 197

1 INTRODUCTION

1.1 OVERVIEW OF THE IMMUNE SYSTEM

The purpose of the immune system is to recognise, defend against and eliminate non-self, without causing damage to self (Janeway, 2001). The initial response to foreign pathogen leverages the innate immune system, whereby multiple cell types including antigen-presenting cells (APCs) such as dendritic cells (DCs) recognise non-self through pattern-recognition receptors (PRRs) (Medzhitov and Janeway, 1997). PRR recognition of pathogen promotes an acute inflammatory response which attempts to eliminates these pathogens. The innate immune system comprises physical barriers such as the skin along with mucosal defences but also broad effector molecules (Coates et al., 2018). PRRs on the surface of tissue-resident cells respond to effector molecules such as damage and pathogen-associated molecular patterns (DAMPs and PAMPs, respectively) along with complement proteins to induce an acute inflammatory response and direct host protection (Takeuchi et al., 2010). The complement system which consists of over 50 liver-derived serum-circulating proteins, intracellular and cell-surface bound proteins (Freeley et al., 2016), is discussed in further detail below.

Professional APCs such as DCs also facilitate pathogen acquisition, degradation and subsequent presentation by major histocompatibility (MHC) molecules on their cell surface (Dudek et al., 2013). MHC I and II molecules present peptide antigens to the T-cell receptors (TCRs) of $CD8^+$ and $CD4^+$ T cells, respectively. DCs exist in an immature, semi-mature or fully mature state (Dudek et al., 2013). In the immature state, DCs facilitate self-tolerance through continuously presenting self-antigens to T cells and expressing ligands for the T-cell inhibitory checkpoint receptors cytotoxic T-lymphocyte-associated antigen 4 (CTLA4) and programmed cell death protein 1 (PD1) (Dudek et al., 2013). Upon pathogen encounter, DCs

mature and become stimulatory in nature. Specifically, mature DCs present antigen to T and B cells.

TCR engagement, in combination with APC effector cytokines and multiple co-stimulatory axes such as CD28-B7 and CD40-CD40L at the T cell-APC interface promote T cell effector responses, thereby initiating a long-term adaptive immune response (Bonilla and Oetgen., 2010). T cell progenitors originate from bone marrow progenitors which subsequently migrate to the thymus where they undergo T cell receptor (TCR) rearrangement to form $CD4^+CD8^+$ double positive (DP) thymocytes (Zúñiga-Pflücker et al., 2004; Kumar et al., 2018). Upon selection, $CD4^+$ or $CD8^+$ single positive (SP) thymocytes enter the periphery (Kumar et al., 2018). Peripheral T cell subsets include naïve, memory and regulatory T (T_{reg}) cells. Upon encounter with antigen, naïve T cells produce interleukin-2 (IL-2), proliferate and differentiate into effector cells. Following pathogen clearance, the majority of effector T cells die by apoptosis whilst a small fraction remain as long-term memory cells (Kumar et al., 2018). On the other hand, $Foxp3^+$ Treg cells are immunosuppressive in nature and promote both tolerance homeostasis (Li et al., 2015).

More specifically, upon recognition of cognate antigen $CD4^+$ T cells polarise toward multiple 'helper' phenotypes including T_H1, T_H2 and T_H17 and T_{FH} (follicular helper) cells which produce a pleiotropy of downstream effects including macrophage phagocytosis, cytotoxic $CD8^+$ T cell proliferation along with B cell proliferation and hence antibody-mediated immune responses (Bonilla and Oetgen., 2010).

Antigen-activated B cells undergo clonal expansion within B cell follicles in secondary lymphoid organs (Akkaya et al., 2020). Specifically, B cell receptor (BCR) diversification through somatic hypermutation is observed in the dark zone of the B cell follicle germinal centres (Kurosaki et al., 2015). B cells can in turn exit the germinal centre as either memory B

cells or antibody-secreting plasma cells (Akkaya et al., 2020). However, B cells that exit the cell cycle may also re-enter the germinal centre light zone, where affinity selection occurs via interactions with immune complex-coated follicular dendritic cells (FDCs) and antigen-specific T follicular helper cells (T_{FH} cells) (Kurosaki et al., 2015).

Finally, non-conventional α/β T cells such as invariant Natural Killer T (iNKT) cells which are activated by MHC-like molecules also play important roles in integrating innate and adaptive immune responses (Krovi and Gapin, 2018). Furthermore, a minor T cell lineage called γ/δ T cells are mainly found in peripheral tissues such as the gut mucosa, skin, lungs and uterus, where they are thought to modulate the immune responsiveness of anatomical sites that are not served by α/β T cells (Ribot et al., 2020).

1.2 THE COMPLEMENT SYSTEM

1.2.1 An overview of extracellular complement activation

The complement system is one of the most ancient host defence systems, consisting of over 50 soluble (serum-operative), cell surface and intracellular proteins (Freeley et al., 2016). It forms the first central line of defence against invading microorganisms, with the potential to eliminate both foreign cells along with modified self (Fujita et al., 2002; Zipfel et al., 2009). The complement cascade has at its core nine native liver-derived serum circulating proteins termed C1, C2 etc. up to C9, and its extracellular activation is initiated through three main pathways dependent on microbial sensing: the classical, lectin and alternative pathways (Reis et al., 2019; **Figure 1-1**).

- The classical pathway is initiated by the protein C1q (part of the C1 complex) which binds pathogen surfaces (via complement-fixing antibodies of the IgG and IgM classes) and is linked to the zymogens C1r and C1s. Through a mechanism of autocatalysis, C1r becomes activated and cleaves C1s which is a serine protease. C1s cleaves C4 into C4b, which subsequently binds C2. C1s then cleaves C2 when it is bound to C4b i.e. C4bC2 to form the C3 convertase enzyme C4bC2a (Freeley et a., 2016).
- The lectin pathway is activated when carbohydrate moieties exposed on the pathogen cell surface are bound by the following complement proteins:
    - The protein MBL (mannan-binding lectin)
    - Ficolins (of which there are 3 types: H-ficolin, L-ficolin, M-ficolin)
    - Collectin-LK (which is a heteromer consisting of collectin-10 (CL-L1) and collectin-11 (CL-K1).

  These proteins form a complex with the MBL-associated serine proteases (MASPs) 1 and 2 to cleave C4 and C2 once again, thus forming the C3 convertase C4bC2a (Fujita et al., 2002).

- Finally, alternative pathway (AP) activation exists both in steady state following spontaneous hydrolysis of the abundant serum complement protein C3 (referred to as 'tick-over') but is subsequently up-regulated during inflammation (Kemper et al., 2007). Once C3 spontaneously hydrolyses to the C3b-like molecule C3(H_2O), it forms a complex with Factor B which is cleaved by Factor D into Bb. C3(H_2O)Bb subsequently cleaves C3 into C3b which binds to target surfaces.

  Subsequent stabilisation of the AP C3 convertase C3bBb requires the positive complement regulator properdin, which promotes the association of C3b and Factor B (Hourcade et al., 2006). This alternative pathway C3 convertase is structurally distinct but functionally equivalent to the classical and lectin pathway C3 convertase. The C3 convertases cleave C3 to C3a and C3b, but also behave as scaffolds for C5 convertase formation i.e. C4b2aC3b or C3bBbC3b. The C5 convertases cleave C5 to C5a and C5b. This leads to rapid generation of the main effector molecules of the complement system; the anaphylatoxins C3a and C5a, the opsonins C3b and C5b and the final downstream membrane-attack complex (MAC; C5b-C6-C7-C8-C9) (Kolev et al., 2014; **Figure 1-1**).

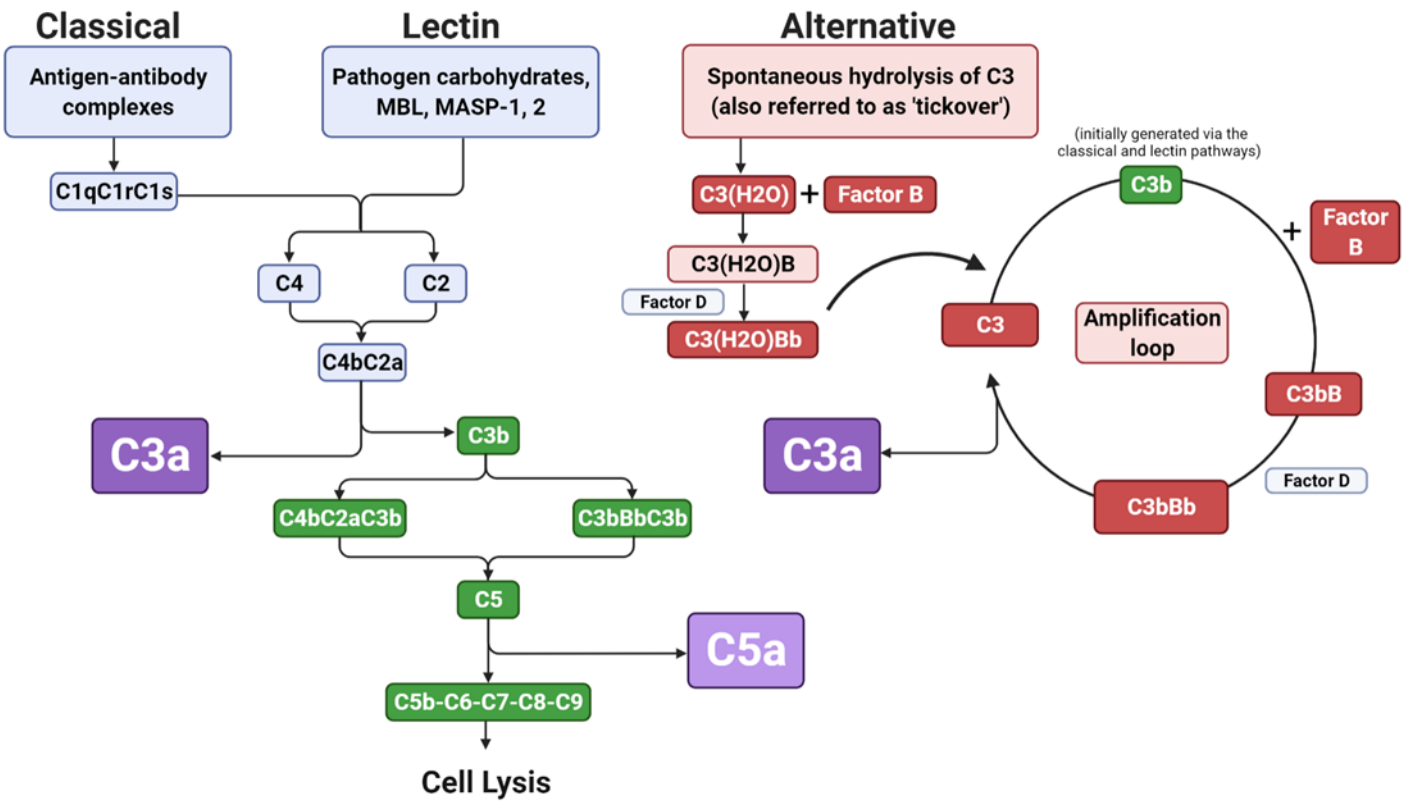


Figure 1-1 Overview of conventional (extracellular) complement activation
Complement is activated in the extracellular space by three distinct mechanisms:
1) The classical pathway leverages activation of C1q (along with to C1r and C1s) upon binding to antigen-antibody immune complexes.
2) The lectin pathway leverages mannose-binding lectin (MBL) and ficolins which recognise carbohydrate moieties on pathogen cell surfaces, prior to signalling via downstream MASP-1 and MASP-2. The classical and lectin pathways cleave C4 and C2, leading to the formation of the C3 convertase C4bC2a.
3) The alternative pathway (AP) exists at steady state, whereby serum-circulating $C3(H_2O)$ binds Factor B to form $C3(H_2O)B$. Factor D subsequently cleaves Factor B in the context of $C3(H_2O)B$ to form $C3(H_2O)Bb$ (i.e., fluid-phase AP C3 convertase). $C3(H_2O)Bb$ then cleaves serum C3 to form C3b, thus amplifying signal propagation (and hence C3b) of the classical and lectin pathways. C3b covalently binds to pathogen cell surfaces (via its exposed thioester bond), and recruits Factor B to form C3bB. Factor D then cleaves Factor B in the context of C3bB to form C3bBb (i.e., cell-surface bound AP C3 convertase).

The C3 convertases (irrespective of activation pathway) cleave serum C3 to generate C3b (opsonin) and C3a (anaphylatoxin). C3b then binds to existing C3 convertases to subsequently form the C5 convertases: C4bC2aC3b and/ or C3bBbC3b.

The C5 convertases cleave C5 into C5a and C5b. C5b in combination with C6, C7, C8 and polyC9 form the membrane-attack complex (MAC) which ultimately lyses and kills infected cells.

The **anaphylatoxins** C3a and C5a bind their cognate G-protein coupled receptors (GPCRs) C3aR and C5aR1 (CD88) which are highly expressed on both myeloid and non-myeloid cells alike (Freeley et al., 2016; Wetzel et al., 1995). This interaction modulates a pleiotropy of effects associated with the acute inflammatory response including smooth muscle contraction, increased mast cell histamine release, modulation of intracellular adhesion molecules and thus recruitment of leukocytes (Wetzel et al., 1995). C5a also binds another seven-transmembrane spanning receptor called C5aR2 (GPR77) (Li et al., 2019). Unlike C5aR1, C5aR2 does not couple to a G-protein due to the absence of highly conserved signalling motifs. However, it may function as a decoy receptor for C5a thereby exerting immunomodulatory effects towards C5aR1 (Li et al., 2019).

The **opsonins** C3b and C4b mediate phagocytosis of opsonised targets by phagocytic cells, via the receptor CR1 (CD35) and membrane bound C5b initiates the formation of the **membrane attack complex** (MAC). MAC assembly is initiated by the sequential and irreversible binding of the complement proteins C5b, C6, C7, C8 and C9 (Serna et al., 2016). Sequence similarity between perforin and MAC components has revealed a distinct protein fold termed the MAC/ perforin domain (MACPF) composed of approximately 350 amino acids. The MACPF form giant β-barrel pores which penetrate the lipid bilayer, promoting cell lysis (Kemper et al., 2007; Bayly-Jones et al., 2017).

Given that complement behaves as a key mediator of the general inflammatory response, multiple negative regulators of complement activation exist in both fluid phase and at the cell surface to avoid uncontrolled activation (Reis et al., 2019; Ricklin et al., 2016). C1 inhibitor (C1-INH) binds to and C1r and C1s, thereby inactivating C1 complex activation associated with classical pathway complement activation (Noris et al., 2013). C3b is proteolytically inactivated by the serum protease factor I (FI) with the aid of various cofactor proteins including circulating factor H (FH), and membrane bound CD46 and CR1 (Reis et al., 2019).

Inactivated C3b (iC3b) is then further cleaved into C3dg and C3c, once again by FI (Noris et al., 2013). FI also cleaves the C4b component of the C3 convertase C4bC2a, with the aid of the plasma cofactor protein C4b-binding protein (C4BP) and also CR1 (Noris et al., 2013). Moreover, decay accelerating factor (DAF, also referred to as CD55) both prevents the assembly of and promotes the disassembly of the C3 and C5 convertases, whereas CD59 inhibits MAC formation, by preventing the association of C9 with C5b-8 (Reis et al., 2019). Additional fluid phase regulators of the MAC include vitronectin (also referred to protein S) which binds C5b-7 and clusterin which binds to downstream C8 and to C9, thus inhibiting polymerisation of C9 (Noris et al., 2013; **Table 1**).

Table 1: Complement receptors and regulators

Receptor/Regulator	Location	Function
C3aR	Membrane-bound (GPCR)	▪ Binds C3a to initiate an acute pro-inflammatory response
C5aR1 (CD88)	Membrane-bound (GPCR)	▪ Binds C5a to initiate an acute pro-inflammatory response
C5aR2 (GPR77)	Membrane-bound (7 TM spanning)	▪ Potential decoy receptor for C5a ▪ Initiates an anti-inflammatory response
CR1 (CD35)	Membrane-bound (Single TM spanning)	▪ Cofactor for FI-mediated cleavage of C3b and C4b
CD59 (Protectin)	Membrane-bound (GPI-anchored)	▪ Inhibits MAC assembly by preventing association of C9 with C5b-8
CD55 (DAF)	Membrane-bound (GPI-anchored)	▪ Prevents formation of convertases ▪ Destabilises convertases
CD46 (MCP)	Membrane-bound (Single TM spanning)	▪ Cofactor for FI-mediated cleavage of C3b
Factor I	Plasma	▪ Inactivates C3b and C4b, thereby preventing downstream convertase formation
Factor H	Plasma	▪ Co-factor for FI-mediated cleavage of C3b and C4b
C4 binding protein (C4BP)	Plasma	▪ Cofactor for FI-mediated cleavage of C4b (and C3b)

C1 inhibitor (C1-INH)	Plasma	▪ Binds to C1r and C1s thereby inhibiting classical pathway complement activation ▪ Binds to MASP-1 and MASP-2 thereby inhibiting lectin pathway complement activation
Vitronectin (Protein S)	Plasma	▪ Binds C5b-7 and inhibits MAC formation
Clusterin	Plasma	▪ Binds C8 and C9 to inhibit MAC formation

1.2.2 Cellular complement and innate immunity

The ancient complement system has elaborated beyond the fluid phase, where extrahepatic complement production – specifically complement proteins expressed and secreted by various cell types into the local microenvironment have major functional implications for cellular immune responses (Lubbers et al., 2017).

Polymorphonuclear leucocytes (PMNs) such as neutrophils have been shown to express C3 and Factor B along with the positive complement regulator properdin at steady state. The complement proteins are subsequently secreted upon stimulation. It is hypothesised that secreted properdin may stabilise extracellular AP convertase and thus perpetuate 'local' complement activation. Moreover, PMNs have been shown to express multiple complement receptors on their cell surface including CR1, C3aR and C5aR1. Another cell type which expressed cytoplasmic C3 and C5 are mast cells. Moreover, the mast cell enzymes, tryptase and chymase can cleave C3 into C3a which is subsequently secreted and binds cell-surface expressed C3aR in an autocrine or paracrine manner. Additionally, skin mast cells also express C5aR1 on their cell surface, enabling direct modulation of effector function by C5a. In addition, NK cells have also been shown to express several complement receptors including C3aR, C5aR1 and C5aR2, yet their role in the modulation of effector cell function remains unclear (Lubbers et al., 2017).

Furthermore, monocytes, macrophages and DCs are considered major sources of certain complement proteins in the serum (Freeley et al., 2016). For example, monocytes have been shown to secrete C1q, C1r and C1s, C2 and C4 enabling local C1 complex assembly and hence classical pathway activation. Moreover, monocytes have also been shown to secrete multiple alternative pathway complement proteins including C3, Factor B and Factor D along with components of the terminal pathway i.e. C5, C6, C7, C8 and C9. Surface expression of the anaphylatoxin receptors C3aR and C5aR1 have also been reported. Given the large array of

complement proteins expressed by monocytes, it is perhaps unsurprising that this is couples with the expression of multiple negative complement regulators including Factor H, FI, C4BP and C1INH. Moreover, macrophages which have differentiated from monocyte precursors also exhibit a very similar complement protein expression profile (Lubbers et al., 2017).

Finally, complement is detected in multiple DC sub-types (Li et al., 2007), either constitutively or during inflammation. Downstream effects of complement on human and murine DCs include the modulation of cytokine secretion, antigen presentation and the promotion of antigen specific T cell responses (Strainic et al., 2008) – as detailed next.

1.2.2.1 Murine BMDCs and complement

In the mouse, complement and specifically anaphylatoxin deficiency in bone-marrow derived DCs (BMDCs) manifests in impaired effector function, including a reduced capacity for antigen uptake and a less activated phenotype (Li et al., 2008).

More specifically, C3-deficient BMDCs were shown to secrete less IL-12 compared to their wild-type counterparts, upon stimulation with the toll-like receptor 4 (TLR 4) ligand lipopolysaccharide (LPS). Cell surface expression of the co-stimulatory molecules MHC class II and B7.2 (CD86) were also reduced by ~30% in C3-deficient BMDCs (Peng et al., 2006). Consequently, C3-deficient DCs were less potent in stimulating downstream $CD4^+$ T cells responses, as demonstrated by reduced IFN-γ and IL-2 secretion *in vitro*. Instead these C3-deficient DCs promoted IL-10 secretion and increased Foxp3 mRNA and protein expression by CD4+ T cells, suggesting a regulatory T cell driving capacity (Peng et al., 2006). It was subsequently demonstrated by Li et al. that C3aR-deficient and C3aR-antagonist treated BMDCs exhibited a similar phenotype to that from C3-deficient mice (Li et al., 2008).

Specifically, C3aR-deficient DCs showed impaired antigen presentation, as demonstrated by reduced IFN-γ and IL-2 secretion from TCR transgenic OTI CD8+ T cells (when co-cultured

with ovalbumin-loaded C3aR-deficient DCs). Furthermore, C3aR-deficient DCs expressed increased levels of cyclic AMP and phosphorylated-Akt but reduced phosphorylated-ERK1/2, when compared to their wild-type counterparts at steady state (Li et al., 2008). Additional work by the same laboratory also demonstrated similar downstream responses upon C5aR1 engagement (Peng et al., 2009). Specifically, C5aR1-deficient BMDCs were shown to secrete less IL-12p70 but more IL-10 compared to their wild-type counterparts. In contrast, addition of exogenous C5a to wild-type DC promoted IL-12p70 secretion. As previously observed for C3aR, stimulation of C5aR1 (by exogenous C5a) decreased intracellular cAMP and downstream Protein Kinase A (PKA) phosphorylation. Moreover, phosphorylation of Akt and downstream IκBα (leading to NF-κB activation) were increased. Also, as native C5 mRNA and protein were detected inside of cells and C5a was observed in cell supernatant – the authors speculated that local autocrine C5a-C5aR1 interactions were responsible for positive modulation of BMDC activation (Li et al., 2008).

It was also demonstrated that the alternative pathway (AP) but not the classical or lectin pathways of complement activation was driving DC effector function (Peng et al., 2008). BMDCs from C3- and Factor B-deficient mice but not C4-deficient mice were shown to elicit weaker T cell responses, as demonstrated by reduced IFN-γ secretion *in vitro*. It was speculated that local AP C3 convertase and downstream anaphylatoxin generation are indispensable components of DC effector function (Peng et al. 2008).

1.2.2.2 Human Monocyte-derived dendritic cells (MdDCs) and complement

Primary C3 deficiency is a rare autosomal inherited disease, in which patients suffer from recurrent pyogenic infections, and C3 levels are undetectable in the serum. Furthermore, *in vitro* complement haemolytic activity and alloreactive responses are defective (Ghannam et al., 2008). Ghannam et al. demonstrated in a patient with C3 deficiency that differentiation of monocytes into DCs was decreased as determined by reduced CD1a and HLA-DR surface

expression when compared to healthy controls. Also, DC maturation i.e. IL-12p70 secretion in the presence of 100 ng/ml lipopolysaccharide (LPS) was also reduced when compared to healthy control.

Monocyte-derived DCs (MdDC) synthesise a diverse range of complement components and receptors at steady state (Li et al., 2011). Some of these components are up-regulated upon TLR-induced maturation (Reis et al., 2006; Cravedi et al., 2013). Specifically, treatment with LPS or TNF-α/IL-1/PGE2 (TIP) up-regulated many complement proteins, most notably C3, fB, C3aR and C5aR1 (Li et al., 2011). The authors then differentiated monocytes into DCs for six days in either heat-inactivated human serum or 'fresh' human serum. DC complement expression was suppressed when cells were cultured in heat-inactivated serum and the authors attributed this 'phenotype' to a loss of external complement signalling i.e. via auto-amplification (Li et al., 2011). However, it should be noted that Elvington et al., (2017) has previously detected stable C3 expression in heat-inactivated (56°C) serum, suggesting that the integrity of complement remains intact upon heat inactivation.

Hence, a mechanistic link between heat inactivation of serum and its influence on *de novo* complement generation remains unclear. However, one may speculate that cells internalise complement from human serum at steady state, and subsequent culture in a complement-deficient matrix may promote increases in *de novo* gene expression as a compensatory mechanism of generation.

Additional work by the same laboratory also demonstrated that MdDC stimulation by C3a (5-20 nM) and C5a (2.5-10 nM) increased co-stimulatory molecule expression, specifically HLA-DR, CD86 and CD40 (Li et al., 2012). In addition, anaphylatoxins positively modulated IL-6, TNF and IL-12 secretion. Although *de novo* anaphylatoxin receptor (C3aR and C5aR1) mRNA levels were upregulated by their respective ligands, surface expression was down-regulated (Li

et al., 2012). Whilst the authors did not comment further on this phenomenon, one may speculate that the receptors are endocytosed upon ligand binding i.e. a form of negative feedback which prevents aberrant signalling and downstream inflammatory responses. Moreover, pre-treatment of MdDCs with C3a and C5a prior to co-culture with allogeneic $CD4^+$ T cells positively correlated with downstream T cell proliferative and cytokine response (IFN-γ, IL-17A and TNF), when compared to allogeneic $CD4^+$ T cells co-cultured with non-treated DCs. Moreover, stimulation with C3a and C5a reduced intracellular cAMP but increased p-AKT, p-ERK and p-IκBα (part of the NF-κB pathway) (Li et al., 2012) (**Figure 1-2**).

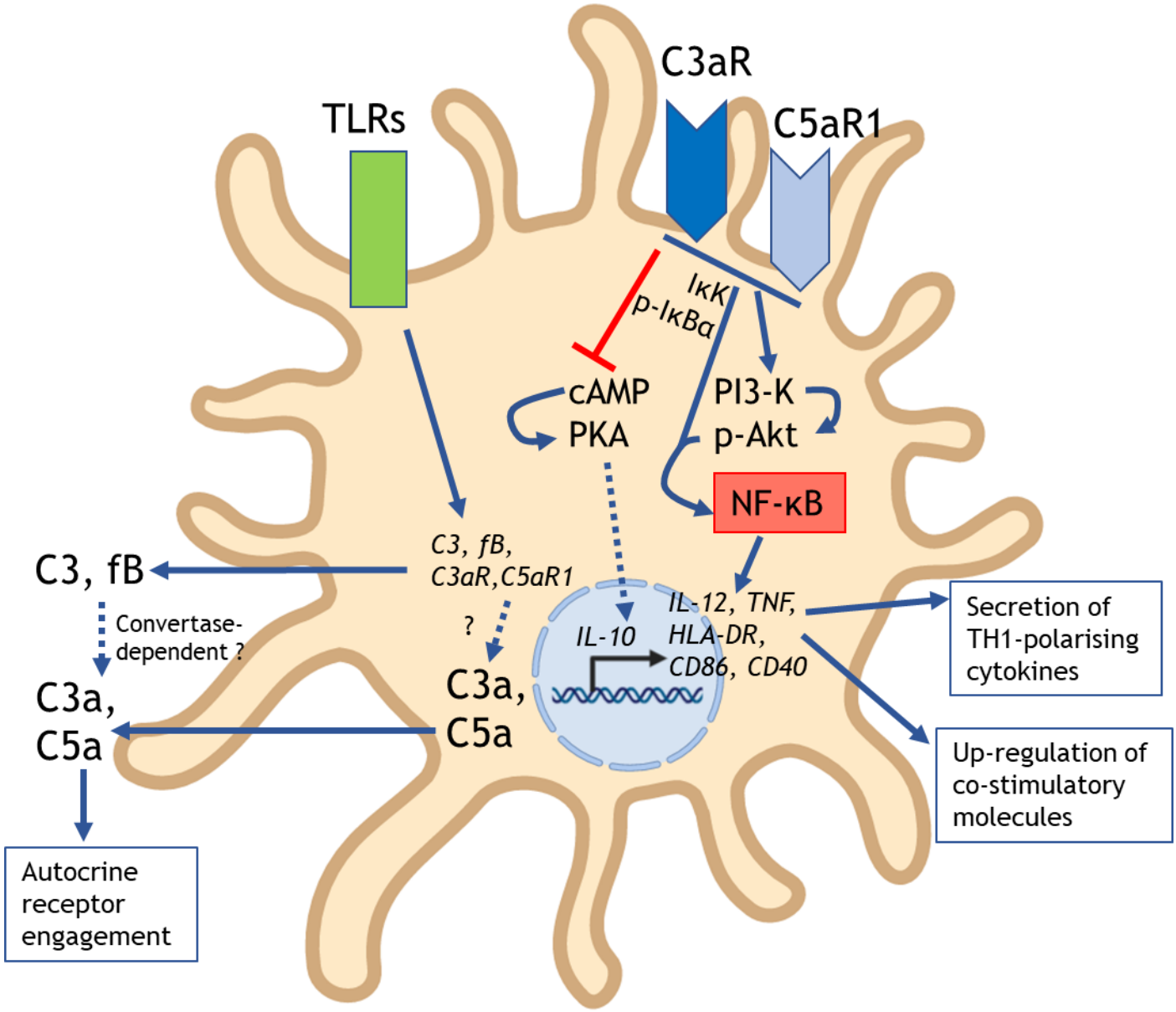


Figure 1-2 Overview of Dendritic Cells and Complement

TLR engagement positively modulates *de novo* generation of multiple complement proteins including components of the alternative pathway and anaphylatoxin receptors in human and mouse DCs. C3a and C5a are detected in cell supernatants, but the mechanism of cleavage i.e. convertase-dependent or independent and location of cleavage i.e. inside or outside of the cell remain elusive. C3aR and C5aR1 engagement (by their respective ligands) positively modulates the PI3-Kinase//p-Akt axis, but negatively regulates the cAMP-PKA axis and downstream IL-10 secretion i.e. DC tolerisation. Phosphorylation of IκBα by IKK targets it for degradation, thereby enabling nuclear translocation of NF-κB, followed by increased generation of T_H1 polarising cytokines and up-regulation of co-stimulatory molecule surface expression.

Blue arrows indicate 'direct' positive modulation. Dotted blue arrows indicate positive modulation, through an undefined mechanism. Red blunted arrows indicate inhibition. Italicised text indicate genes, whereas non-italicised text indicates protein.

cAMP: cyclic AMP, PKA: Protein Kinase A, T_H1: T helper 1, TLR: Toll-like receptor, NF-κB: nuclear factor kappa-light-chain-enhancer of activated B cells, PI3-K: Phosphoinositide 3-kinase, Akt: also called PKB (Protein Kinase B), IκB: inhibitor of nuclear factor kappa B, IκK:IκB kinase, p-: phosphorylated.

1.2.3 Cellular complement and adaptive immune responses

Work within the last decade has shown *de novo* complement generation and activation in both mouse and human α/β T cells, where it is considered to play a role in both homeostatic survival and modulation of effector function (Strainic et al., 2008; Strainic et al., 2013; Liszewski et al., 2013; Arbore et al., 2016; Arbore et al., 2018). Complement generation and signalling in conventional T cells can be depicted using the following 'models', as described next:

1) **Inside-out signalling**, where native proteins are secreted into the extracellular milieu prior to extracellular cleavage and signalling via cell-surface receptors.
2) **Intracellular C3/C3a signalling**, where intracellular cleavage of C3 generates intracellular C3a. Intracellular C3a signals intracellularly.
3) **Intracellular C5/C5a signalling**, where intracellular cleavage of C5 generates intracellular C5a. Intracellular C5a signals intracellularly.

1.2.3.1 Inside-out signalling

Initial observations by Strainic et al. (2008) revealed that TCR engagement in OT-II TCR transgenic T cells with ovalbumin (OVA) peptide and bone-marrow-derived DCs as APCs led to the production of alternative pathway components C3, C5, fB and fD along with C3aR and C5aR1 expression by each of the cognate cell types. Furthermore, C3a and C5a were detected in the supernatant in the presence but not absence of OVA peptide, implying activation dependence. Upon disabling of anaphylatoxin receptor signalling *in vitro* by pharmacological antagonism and/or receptor knockdown, the effector functions of both cell types was blunted as evidenced by reductions of T cell IFN-γ and DC IL-12 expression. It was also shown that anaphylatoxin receptor signalling increased costimulatory molecule expression (B7-CD28 or CD40-CD154) on both cell types. Moreover, anaphylatoxin receptors and the co-stimulatory axes appeared to be mechanistically linked, as loss of T cell responsiveness in the absence of

costimulatory-molecule signalling was reversed by addition of C3a and C5a (Strainic et al, 2008; **Figure 1-3**).

However, it should be noted that Karsten and colleagues were unable to detect C5aR1 on murine T cells (Karsten et al., 2015). Upon development of a novel floxed GFP-C5aR1 reporter knock-in mouse, $C5aR1^+$ cells were tracked *in vivo* and *in vitro*. Whilst GFP expression was detected in most neutrophil, macrophage and DC populations (including monocyte-derived DCs) at steady state, naïve splenic CD4+ T cells failed to show GFP expression at steady state (Karsten et al., 2015). Moreover, upon stimulation with anti-CD3/CD28 mAbs, C5aR1 surface staining or mRNA expression was not detected in C57BL/6 wild type mice (Karsten et al., 2015). Hence the role of autocrine surface anaphylatoxin receptor engagement in murine T cells remains contentious.

Furthermore, additional work by Strainic and colleagues showed that disabling of C3aR and C5aR1 signalling in murine $CD4^+$ T cells not only blunted Th1 effector responses, but also promoted a regulatory (T_{REG}) phenotype as demonstrated by increased FoxP3 and TGFβ-1 expression (Strainic et al., 2013). More specifically, $CD4^+$ T cells were either treated with C3aR/C5aR1 pharmacological antagonists or co-cultured with C3- and C5-null DCs. Whilst $CD4^+$ T cell FoxP3 surface expression increased in both treatment conditions, it was greater in $CD4^+$ T cells co-cultured with complement-deficient DCs. The authors subsequently speculated that DC-derived complement proteins, specifically anaphylatoxins are required for T_H1 polarisation. Hence, the absence of this anaphylatoxin 'signal' prevents T_H1 polarisation, and in turn promotes a 'default' regulatory phenotype (Strainic et al., 2013).

Additionally, assessment of downstream signalling events following genetic ablation of C3aR and C5aR1 in $CD4^+$ T cells showed increases of adenylyl cyclase activity (as measured by cAMP levels) and thus up-regulation of downstream Protein Kinase A (PKA) activity.

Moreover, C3aR- C5aR1-null CD4+ T cells expressed phosphorylated SMAD2, a transcription factor which induces TGFβ-1 and FoxP3 expression. Interestingly, TGFβ-1 was also shown to upregulate C5aR2 expression which has previously been described as a decoy receptor which sequesters C5a (Li et al., 2019). Moreover, C3aR- C5aR-null FoxP3+ Treg cells also showed suppressive potential *in vivo* through inhibiting antigen-specific T effector cell responses (Strainic et al., 2013; **Figure 1-3**).

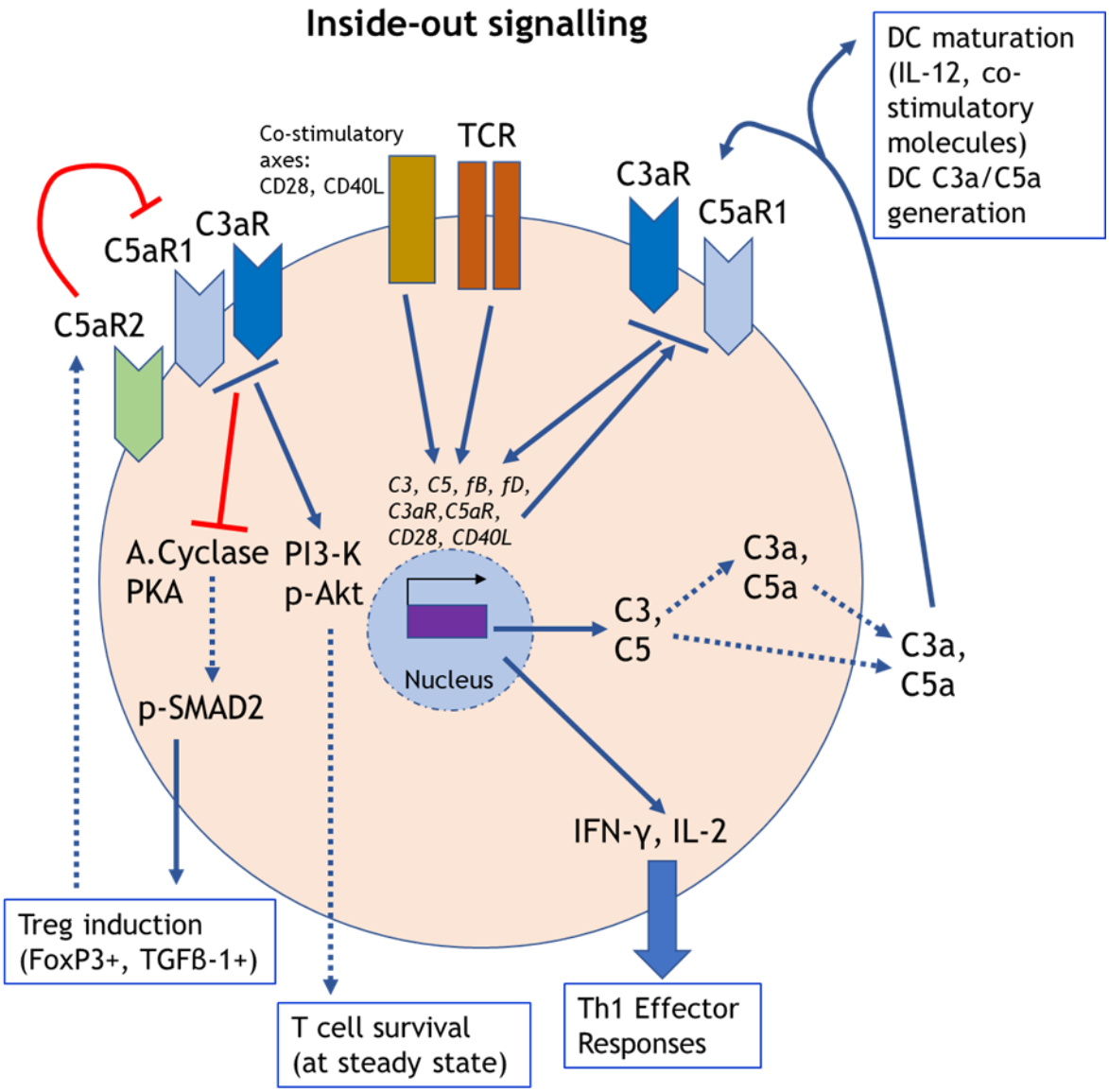


Figure 1-3 Overview of 'inside-out' complement signalling

TCR ligation in combination with the co-stimulatory axes positively modulates native complement, anaphylatoxin receptor and co-stimulatory molecule gene expression. Upon synthesis of native C3 and C5; cleavage (through an undefined mechanism) occurs and the anaphylatoxins C3a and C5a are detected in the extracellular space. C3a and C5a bind cognate receptors in an autocrine or paracrine manner to positively modulate Th1 function and dendritic cell maturation. Anaphylatoxin receptors also positively modulate their own expression and up-regulate Akt expression which is indispensible for naïve T cell survival. Disabling of anaphylatoxin receptor signalling (potentially through C5aR2 which sequesters C5a and possibly C3a) promotes a Treg phenotype, through dis-inhibiting Protein Kinase A and pSMAD2 activation. SMAD2 drives FoxP3 and TGFβ-1 expression. Blue arrows indicate 'direct' positive modulation. Dotted blue arrows indicate positive modulation, through an undefined mechanism. Red blunted arrows indicate inhibition. Italicised text indicate genes, whereas non-italicised text indicates protein.

TCR: T-cell receptor, A. Cyclase: Adenylyl Cyclase, PKA: Protein Kinase A, PI3-K: Phosphoinositide 3-kinase, Akt: also called PKB (Protein Kinase B), p-: phosphorylated, Th1: T helper 1 cell, Treg: regulatory T cell.

In conclusion, work by Strainic and colleagues has demonstrated a previously undefined role of anaphylatoxins in enhancing cognate APC-T cell interactions (Strainic et al., 2008; Strainic et al., 2013). However, a large amount of uncertainty remains with respect to the where these 'locally-derived' anaphylatoxins are generated – a question which was not addressed in this work. From a theoretical perspective, multiple scenarios leading to C3a and C5a generation may occur which are not necessarily mutually exclusive. For example:

1) Native C3 and C5 may be secreted in the extracellular space by both T cells and APCs, prior to cleavage by serum-derived i.e. fluid phase convertases.
2) Native C3, fB and fD may be secreted into the extracellular space prior to generation of plasma-membrane bound convertases, ultimately leading to extracellular 'local' cleavage.
3) Native C3 and C5 may be cleaved into C3a and C5a inside of the cell through an undefined mechanism. Following intracellular cleavage, anaphylatoxins may be remain inside or be secreted into the extracellular space where they act 'locally' in an autocrine or paracrine manner.

Whilst Strainic and colleagues have previously eluded to secretion of native complement followed by extracellular 'local' cleavage (i.e. Points 1 and 2 described above), perhaps the issue with this narrative is that it does not demonstrate a physiological advantage of cell-derived 'local' complement versus liver-derived extracellular complement. Therefore, the anaphylatoxins will by default be generated 'locally' in the extracellular space, irrespective of the mechanism of cleavage. However, more recent work by the Kemper laboratory has demonstrated an elaborate intracellular panoply of complement cleavage events (i.e. Point 3 described above), along with the physiological advantages gained through leveraging intracellular anaphylatoxin signalling, as described next.

1.2.3.2 Intracellular C3a generation and signalling

Initial findings by Liszewski and colleagues demonstrated that human CD4+ T cells rapidly generate functionally active C3a and C3b in a C3 convertase-independent but cathepsin L (CTSL)-dependent manner (Liszewski et al., 2013).

Physiologically:

- In non-activated $CD4^+$ T cells, C3 and C3a were shown to co-localise with CTSL in the endoplasmic reticulum (ER) and lysosomal compartments at steady state, suggesting CTSL generates 'tonic' C3a from existing C3 reserves in resting T cells. Furthermore, C3aR was detected within intracellular compartments (endosomal and lysosomal), but notably absent from the cell surface at steady state.
- Upon activation of CD4+ T cells by both anti-CD3 antibody and anti-CD46 (which mimics physiological engagement of this receptor by its ligand C3b), C3a and C3aR were detected on the cell surface. The authors speculated that both C3a and C3aR had translocated from the inside of the cell to the plasma membrane.
- Finally, this 'new' phenotype correlated with T_H1 polarisation as evidenced by increases in IFN-γ secretion.

Upon pharmacological inhibition of CTSL:

- Non-activated $CD4^+$ T cells were treated with increasing concentrations of a commercially available CTSL inhibitor (CTSLi). As CTSL concentration increased, both cellular viability and phosphorylation of mTOR (mammalian target of rapamycin) decreased. The authors subsequently suggested that steady state intracellular C3a-C3aR are necessary for cell survival.

- Moreover, addition of CTSLi to activated CD4+ T cells at a concentration which was sufficient to reduce C3a (but not affect cell viability) correlated with down-regulation of IFN-γ secretion.
- Furthermore, concomitant addition of C3a in the presence of CTSLi, partially rescued the T_H1 response i.e. increased IFN-γ secretion. The authors suggested that 'local' extracellular C3a-C3aR interactions are required for successful T cell activation; a model which was also proposed by Strainic and colleagues.

How does intracellular C3/C3a modulate CD4+ T cell activation?

Subsequent work by the Kemper laboratory detailed the metabolic effects of intracellular complement, which occur downstream of CTSL-mediated cleavage of C3 into C3a (Kolev et al., 2015). Specifically:

- $CD4^+$ T cells isolated from CD46-deficient patients exhibited diminished T_H1 but not T_H2 response upon TCR engagement when compared to healthy controls. Moreover, CD4+ T cells isolated from CD46-deficient patients exhibited reduced mitochondrial respiration and aerobic glycolysis relative to cells from healthy controls.
- Subsequent gene set enrichment analysis (GSEA) showed that genes associated with metabolic processes were less enriched in CD46-deficient patients, when compared to healthy controls.
- The authors then performed a set of *in vitro* assays and showed that CD46 co-stimulation (in combination with TCR engagement) up-regulates the following proteins:
    1. Glucose transporter 1 (or GLUT1), which is required for glucose and amino acid uptake by cells,
    2. L-type amino acid transporter LAT1 (SLC7A5), which is responsible for uptake of essential amino acids (Scalise et al., 2018),

3. LAMTOR (part of the Ragulator-Rag Complex which is a regulator of lysosomal signalling and mTORC assembly).

Moreover, pharmacological inhibition of mTORC1 negatively regulated GLUT1 and LAT1 expression (Kolev at al., 2015), suggesting that CD46 behaves as a T cell costimulatory molecule in addition to CD28. Additional work by the same laboratory demonstrated upstream mechanisms which increase intracellular C3 protein to drive successful T_H1 induction (Kolev et al., 2020).

- T cell expressed integrin leukocyte function antigen 1 (LFA-1) is the major cognate ligand for Intercellular Adhesion Molecule 1 (ICAM-1). LFA-1-ICAM-1 engagement occurs during T cell transmigration into tissues.
- More specifically, LFA-1-ICAM-1 engagement *in vitro* induced C3 mRNA (via the transcription factor AP-1) and protein expression during cognate APC-T cell interactions but was unable to initiate T_H1 polarisation.
- Confirming that LFA-1 indeed drives C3 expression, LAD (leukocyte adhesion deficiency) patients which lack LFA-1 were unable to upregulate C3 expression and displayed impaired T_H1 responses. Finally, reconstitution of intracellular C3 (through electroporation) or intracellular C3a (through adenoviral vector delivery) restored T_H1 response in these patients, confirming the role of LFA-1 in driving C3 expression and T_H1 responses in CD4+ T cells (Kolev et al., 2020; **Figure 1-4**).

In conclusion, the Kemper laboratory suggests that crosstalk between CD46 co-engagement, intracellular C3 cleavage into C3a and downstream mTOR promotes metabolic reprogramming of $CD4^+$ T cells to ultimately 'drive' a T_H1 response. Subsequent work by Kemper and colleagues has also suggested a similar role for intracellular cleavage of C5 into C5a generation in driving T cell effector responses – as discussed next.

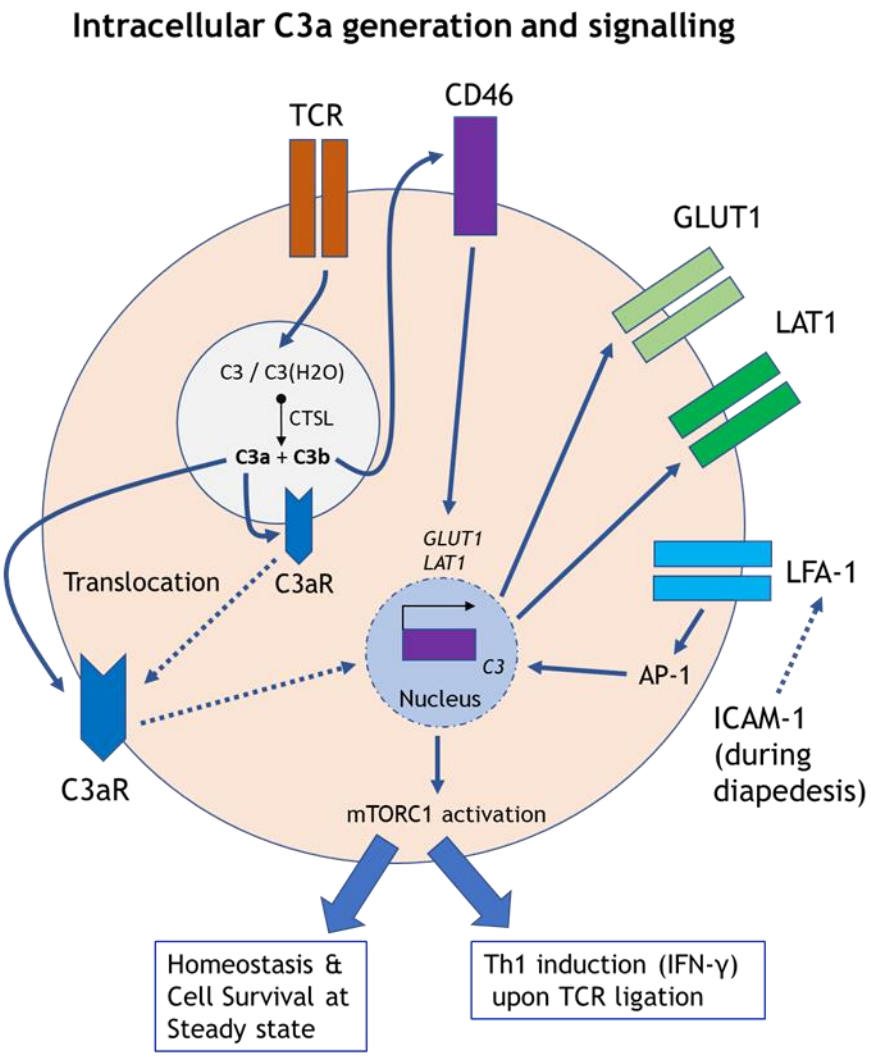


Figure 1-4 Overview of intracellular C3a generation and signalling

At steady state, C3aR is expressed on intracellular compartments. Low levels of C3a are also present. TCR engagement positively modulates intracellular cleavage of C3 into C3a and C3b by CTSL. C3a binds C3aR which is expressed intracellularly but also translocates to the plasma membrane upon cellular activation. C3b binds plasma membrane-bound CD46. CD46 co-stimulation positively modulates expression of GLUT1 and LAT1. Metabolic reprogramming of T cells drives downstream mTORC1 formation and subsequent Th1 induction. C3aR engagement synergises with CD46-mediated T cell metabolic reprogramming through an undefined mechanism. During T cell diapedesis, LFA-1-ICAM-1 interactions positively modulate *de novo* C3 generation through AP-1; C3 is subsequently cleaved into C3a and C3b.

Blue arrows indicate 'direct' positive modulation. Dotted blue arrows indicate positive modulation, through an undefined mechanism. Italicised text indicate genes, whereas non-italicised text indicates protein.

TCR: T-cell receptor, CTSL: Cathepsin L, GLUT1: Glucose transporter 1, LAT1: L-Type Amino Acid Transporter 1, LFA-1: Lymphocyte function-associated antigen 1, ICAM-1: Intercellular Adhesion Molecule 1, mTORC1: mammalian target of rapamycin complex 1, AP-1: Activator protein 1, T_H1: T helper 1 cell.

1.2.3.3 Intracellular C5a generation and signalling

Arbore and colleagues have demonstrated a role for intracellular C5a in the modulation of $CD4^+$ T cell activation (Arbore et al., 2016) and in driving $CD8^+$ T cell cytotoxic responses (Arbore et al., 2018).

Physiologically:

- In non-activated and activated $CD4^+$ T cells, the pro-inflammatory anaphylatoxin receptor C5aR1 was shown to be located exclusively in the intracellular space whereas its anti-inflammatory counterpart C5aR2 was detected on the cell surface.
- Moreover, intracellular stores of C5 along with low levels of C5a were detected in non-activated CD4+ T cells. Upon activation (i.e. TCR engagement plus CD46 co-stimulation), levels of intracellular C5a increased. This correlated with increased C5a at the cell surface as well. The mechanism by which intracellular C5 was cleaved into C5a remains undefined.

Upon pharmacological agonism/antagonism:

The authors used three different commercially available pharmacological treatments on activated $CD4^+$ T cells, to understand the role of intracellular C5a in the modulation of $CD4^+$ T cell effector function:

1) **C5aR1/C5aR2 double receptor antagonist** – which is unable to cross the plasma membrane, so therefore can only inhibit cell surface C5aR2. However, it should be noted that the authors did not experimentally test this for the possibility that the inhibitor may be taken up by cells (via endocytosis or pinocytosis).

2) **C5aR1 antagonist** – which is shown to cross the plasma membrane and inhibit the intracellular receptor.

3) **C5aR2 agonist.**

The authors showed that antagonism of intracellular C5aR1 blunted T_H1 functional response i.e. IFN-γ secretion. Moreover, extracellular agonism of C5aR2 also promoted this phenotype, which suggests an opposing relationship between intracellular C5aR1, and plasma membrane bound C5aR2. These findings were also observed upon siRNA mediated genetic ablation of C5aR1. Autocrine intracellular engagement of C5aR1 (by C5a) and/or pharmacological antagonism of plasma membrane bound C5aR2 promoted reactive oxygen species (ROS) generation. Additional transcriptome analysis revealed enrichment of NLRP3 and IL1β genes, upon C5aR1 engagement. Caspase-1 was recruited by the canonical NLR family pyrin domain containing 3 (NLRP3) inflammasome and cleaved pro-IL-1β to generate functional IL-1β (Arbore et al., 2016).

In a similar manner to C5aR1 antagonism, pharmacological blockade of NLRP3 inflammasome activity also reduced $CD4^+$ IFN-γ secretion. It is noteworthy that NLRP3 was also detected in the nucleus, suggesting direct regulation of T_H1 transcriptomic profiles, independent of IL-1β generation. The inverse relationship was observed upon inhibition of plasma membrane bound C5aR2 whereby T_H1 response was increased. The authors concluded that C5aR1 positively modulates T_H1 effector function via NLRP3 inflammasome activation (and IL-1β generation) and C5aR2 is a negative regulator of this process. (Arbore et al., 2016; **Figure 1-5**).

In $CD8^+$ T cells:

At steady state, CD8+ T cells expressed C5aR1 and C5aR2 at levels and locations comparable to CD4+ T cells. Also, intracellular stores of C5 and C5a were observed. Upon activation (via polyclonal TCR stimulation and CD46 co-stimulation), increased IFN-γ and TNF protein expression was observed. In addition, cytotoxic activity was observed as evidenced by upregulation of CD107a and granzyme B expression. In a manner like $CD4^+$ T cells, NLRP3

activation was detected in cytotoxic T lymphocytes (CTLs). But unlike $CD4^+$ T cells, caspase-1 or downstream IL-1β gene expression were not observed suggesting a different mechanism by which intracellular C5a modulates CTL function.

Subsequent RNA-sequencing analysis revealed up-regulation of multiple genes involved in metabolic re-programming of $CD8^+$ T cells including FASN (fatty-acid synthase), FABP5 (fatty-acid binding protein 5), and SLC7A5 (coding for the L-type large neutral amino acid transporter LAT1). Consequently, LAT1 surface protein expression was also upregulated upon $CD8^+$ T cell activation. Moreover, pharmacological blockade of FASN reduced IFN-γ protein expression and the degranulation potential of CTLs (Arbore et al., 2018; **Figure 1-5**).

The authors concluded that like C3a and CD4+ T cells – C5a modulates the metabolic reprogramming of $CD8^+$ T cells, via cognate intracellular C5aR1 engagement. However, it must be noted that a clear mechanistic link between C5a-C5aR1 engagement, NLRP3 activation and changes in transcriptomic profiles of metabolism-related genes which drive CTL effector function remains unclear.

In conclusion, whilst the Kemper laboratory has provided new insights into mechanisms of intracellular complement cleavage, multiple controversies surrounding this phenomenon remain unsolved and are detailed next.

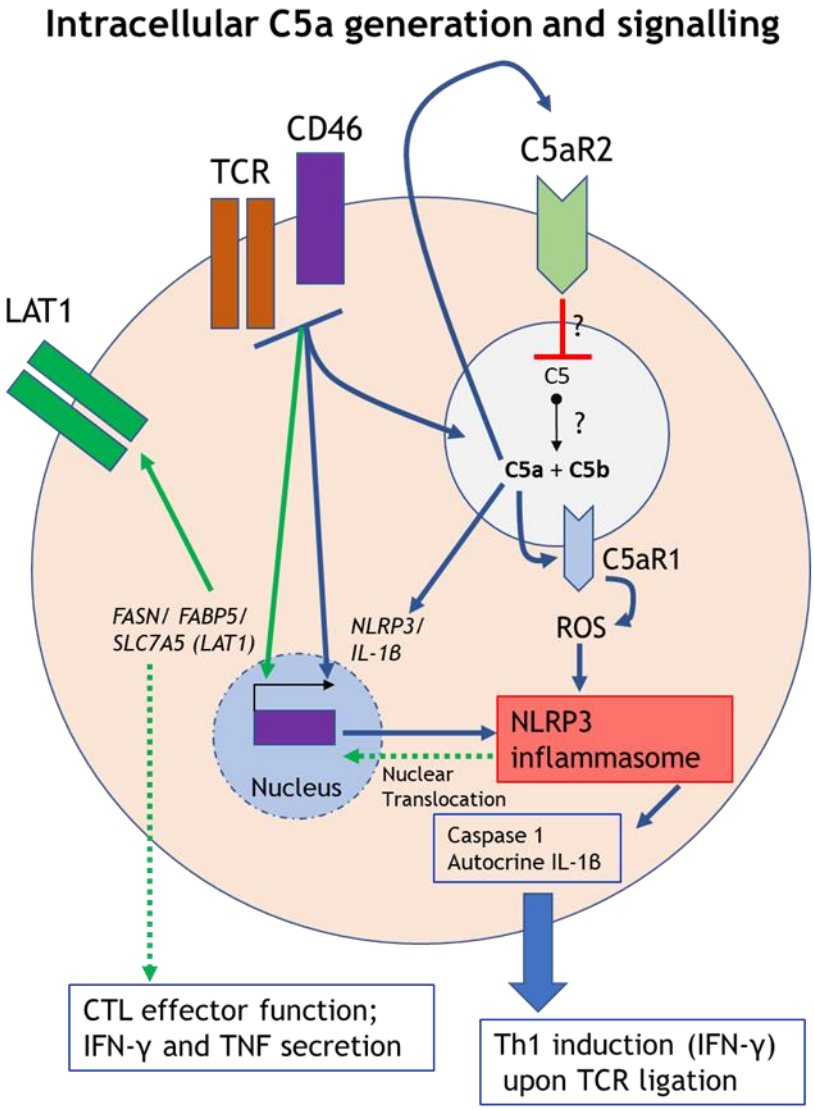


Figure 1-5 Overview of intracellular C5a signalling and generation

CD4+: TCR engagement in combination with CD46 ligation (by C3b; most likely generated by upstream intracellular C3 cleavage) positively modulates cleavage of C5 into C5a and C5b by an undefined mechanism. C5a binds intracellular C5aR1 and plasma membrane bound C5aR2. C5aR1 positively modulates NLRP3 inflammasome activation through a) positive modulation of upstream ROS or b) positive modulation of gene expression. NLRP3 inflammasome recruits caspase-1 which cleaves pro-IL-1β to functional IL-1β. Autocrine IL-1β positively modulates IFN-γ secretion and hence T_H1 polarisation

CD8+: TCR engagement in combination with CD46 ligation positively modulates C5a generation and NLRP3 inflammasome activation. However, downstream signalling of NLRP3 remains unclear. Additional up-regulation of genes implicated in metabolic re-programming such as LAT1 were shown to positively correlate with CTL polarisation.

Blue arrows indicate 'direct' positive modulation in CD4+ T cells. Dotted blue arrows indicate positive modulation, through an undefined mechanism in CD4+ T cells. Red blunted arrows indicate inhibition in CD4+ T cells. Green arrows represent CD8+ T cells. Italicised text indicate genes, whereas non-italicised text indicates protein.

TCR: T-cell receptor, LAT1: L-Type Amino Acid Transporter 1, T_H1: T helper 1 cell, CTL: Cytotoxic T-lymphocyte.

1.3 CONTROVERSIAL ASPECTS OF INTRACELLULAR COMPLEMENT GENERATION AND SIGNALLING

The discovery of intracellular complement generation and signalling is still relatively recent with many controversial aspects, and as such many questions remain unanswered. Some of these questions are discussed below and shown in **Figure 1-6**.

1) The 'source' of C3:

Liszewski and colleagues showed that in conventional $CD4^+$ T cells, C3a is generated at steady state, independent of TCR engagement (Liszewski et al., 2013). However, C3 mRNA and protein are only up regulated when T cells are activated (Strainic et al., 2008).

The discrepancy between lack of de novo C3 generation, but consistent detection of C3a at steady state suggested that there may be another 'source' of native C3 which is cleaved into C3a in non-activated cells. This hypothesis was tested by Elvington et al. who compared intracellular C3 between peripheral blood mononuclear cells (PBMCs) and cell lines by Western blot (WB) (Elvington et al., 2017). Elvington et al., observed the following at steady state:

- C3 protein was detected in $CD4^+$ T cells and B cells but was absent in the respective B and T cell lines, Farage and Jurkat.
- Kinetic analysis revealed that exposure to 10% normal human serum (NHS), plasma or whole blood positively correlated with subsequent detection of C3 in the Farage and Jurkat cell lines. More specifically, the hydrolysed component of C3 termed C3(H_2O) (Bexborn et al., 2009) was observed at the plasma membrane at 1 minute, and within endosomes at 15 minutes post-culture. However, the mechanism of loading remained unclear, as inhibition of multiple cell surface complement receptors had no effect on C3 uptake.

- Subsequent analysis of supernatant from multiple cell lines, but also $CD4^+$ T cells revealed that up to 80% of internalised C3(H_2O) was secreted into the extracellular milieu, whereas ~20% was retained. Further analysis of retained C3(H_2O) showed that it was degraded intracellularly by the soluble complement regulators FI and FH in the Farage cell line.
- Moreover, activated Farage and $CD4^+$ T cells cultured in NHS showed increased intracellular C3a generation when compared to cells cultured in serum-free medium, suggesting uptake of C3(H_2O) is indispensable for sufficient anaphylatoxin generation and hence downstream effector responses (Elvington et al., 2017, Liszewski et al., 2013).

The authors concluded that as the major difference between PBMCs and cell lines is the amount of time absent from a fluid-phase complement source. Hence, exposure of cell lines to exogenous complement promoted 'loading' of complement from the extracellular to intracellular milieu. Moreover, this process is considered dynamic and 'loaded' complement is subsequently able to 'leave' the cells at steady state (Elvington et al., 2017).

A similar observation of C3 uptake by primary B cells and the B cell lines Raji and Namalwa was reported by Kremlitzka et al., (2019). Internalisation of C3 was investigated in EDTA-GVB buffer in which activation of all complement pathways are blocked. When cells were cultured in this buffer:

- C3 was detected in cytoplasmic but not the membrane fraction of all cell types. C3a was also detected in total cell lysate which suggests complement activation.
- C3a generation was reduced when cells were cultured in Factor B depleted serum, but this was not observed following depletion of C1q (part of the classical pathway) or MBL (part of the lectin pathway).

The authors concluded that C3a was generated by a serum-derived C3-convertase on the surface of B cells and not by intracellular proteases as reported by Elvington and colleagues.

However, this conclusion may be slightly premature as uptake of Factor B by B cells was not assessed. Moreover, C3a was assessed in total cell lysate rather than the cytoplasmic or membrane fractions.

In conclusion, both primary cells and multiple cell lines 'load' C3 from the extracellular milieu, and subsequently 'release' it at steady state. It is thus tempting to speculate that 'loaded' C3 is leveraged by unstimulated cells to generate 'tonic' C3a (in the absence of *de novo* C3 generation). Tonic C3a generation is implicated in homeostatic T cell survival (Liszewski et al., 2013), and may have a similar role in other cell types.

However, what remains unclear is if the phenomenon of C3 'loading' also occurs in stimulated cells, and to what extent. As TCR activation has been shown to promote *de novo* C3 generation (Strainic et al., 2018), one may speculate that C3 'loading' is reduced so as not to overwhelm cells with disproportionately high levels of C3. Moreover, as the mechanism by which C3 'loading' occurs is currently undefined, one may speculate that potential cross-talk between the TCR (or other cell surface receptors) and the 'receptors' responsible for C3 'loading' in activated cells may influence intracellular levels of C3.

2) <u>Location of C3a (and C5a) generation:</u>

Liszewski and colleagues have previously shown that multiple cell types of myeloid, lymphoid and non-myeloid non-lymphoid lineage express intracellular C3 and C3a (Liszewski et al., 2013). However, what remains unclear is the location of where cleavage of C3 into C3a takes place i.e. in the cytoplasm or within cytoplasmic organelles and vesicles.

As shown in Figure 1-6, *de novo* generation of C3 follows the secretory pathway:

- The protein is translated as a 180,000 dalton single-chain molecule called pro-C3 (Morris et al., 1982) and is detected in the rough endoplasmic reticulum. It is subsequently cleaved

to generate mature C3 which traverses the golgi network and is detected in endosmomal compartments (Kulkarni et al., 2019).

- As C3a is also detected in endosomal compartments (Liszewski et al., 2013), one may speculate that *de novo* generated C3 is cleaved into C3a within endosomes. However, the actual intracellular location of cleavage remains unclear. Therefore, future work should attempt to further ascertain where cleavage occurs.
- Additionally, it also remains unclear what happens in cells following 'loading' of C3(H_2O) from the extracellular milieu. One may speculate that C3(H_2O) would remain in early endosomes post-endocytosis and subsequently be cleaved into C3a. However, this also remains undetermined.

3) <u>Mechanism by which intracellular anaphylatoxin receptor engagement occurs:</u>

As previously described, the Kemper laboratory suggests C3a (and C5a) are secreted from intracellular compartments and subsequently interact with their intracellular cognate receptors (Liszewski et al., 2013; Arbore et al., 2016). However, the mechanism by which this happens in not made clear. As shown in **Figure 1-6**, two hypotheses have been postulated:

- Hypothesis 1 suggests that C3a is cleaved within an intracellular compartment and then binds to its cognate receptor – the ligand binding motif of the receptor is luminal facing. This suggests that C3a always remains exclusively inside of the compartment.
- Hypothesis 2 has also been implied whereby C3a is generated inside of the intracellular compartment and is then secreted into the cytosol. Cytosolic C3a binds its cognate receptor, which is expressed on the surface of the intracellular compartment. This suggests that the ligand binding motif of the receptor is cytosol facing.

4) <u>Complement proteins in the nucleus:</u>

Kremlitzka and colleagues have suggested a previously undefined role for C3 and C3a in the regulation of DNA transcription via chromatin remodelling (Kremlitzka et al., 2019). Both proteins were detected in the nuclear fraction and chromatin-associated cellular fraction of the Raji B cell line. Subsequent ChIP sequencing analysis showed genomic DNA binding by C3, which in turn correlated with increased interactions with histone proteins involved in chromatin remodelling (Kremlitzka et al., 2019). Moreover, Arbore and colleagues detected NLRP3 in the nucleus, upon intracellular C5aR1 engagement in $CD4^+$ T cells (Arbore et al., 2016).

The role of complement in the nucleus remains unclear. It was postulated that complement proteins may behave as transcription factors – however, a literature search of interactions between complement proteins and DNA revealed no significant findings. In conclusion, a lack of clarity remains with regards to both the cell biological concepts which underscore intracellular anaphylatoxin receptor engagement along with the physiological implications of this phenomenon on cell effector function.

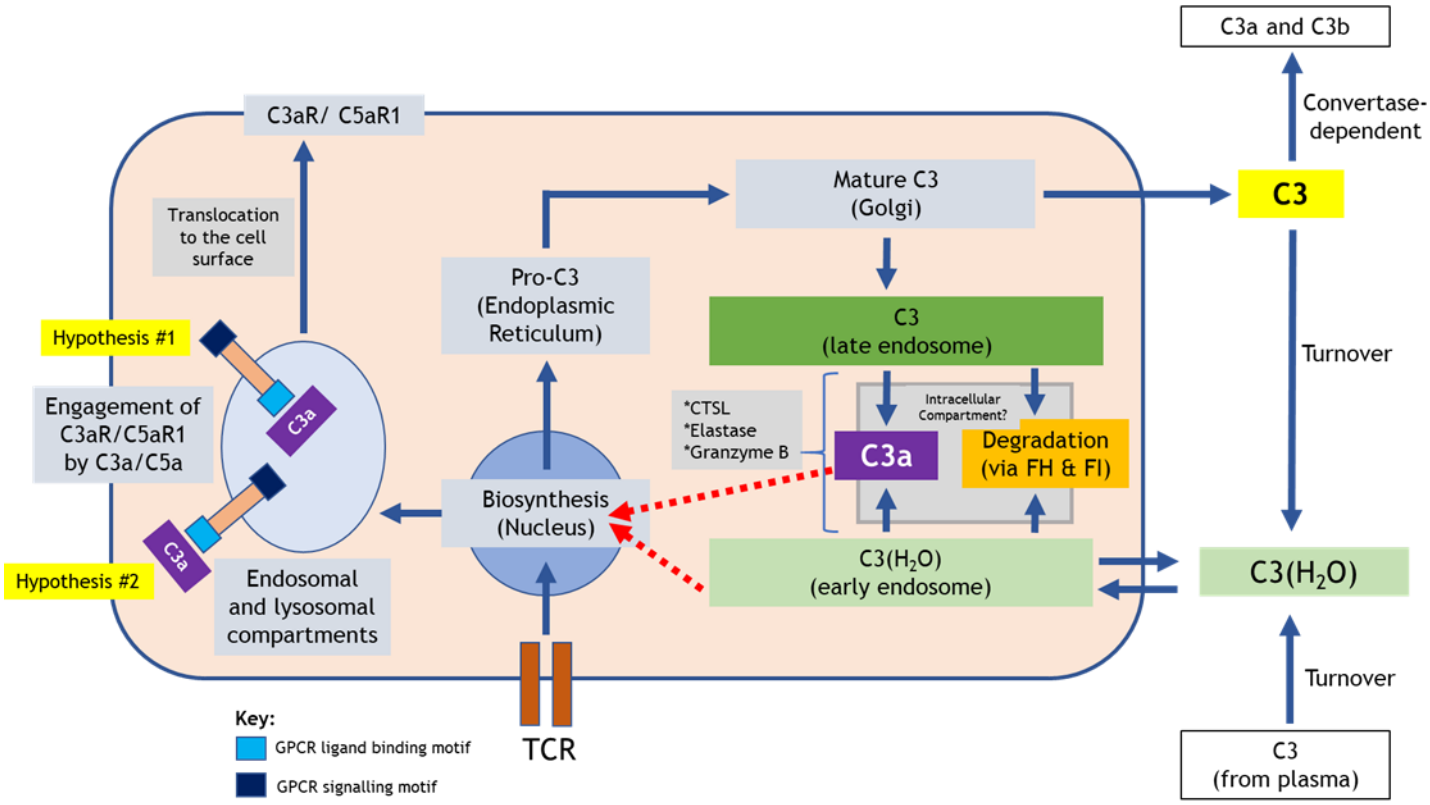


Figure 1-6 Controversial aspects of intracellular complement generation and signalling

- At steady state, the hydrolysed counterpart of C3 called C3(H_2O) is taken up by primary cells and cell lines from the extracellular milieu i.e. C3 'loading'. Loaded C3 is subsequently secreted back in to the extracellular space during complement deficit e.g. serum-free medium. Retained C3 is degraded by the AP negative regulators FH and FI.
- In activated CD4+ T cells, *De novo* generation of C3 occurs. The proteases CTSL, Elastase and Granzyme B then cleaves C3 into generate C3a. However, the location of cleavage remains unclear. Both C3 and C3a have been observed in nuclear fractions interacting with genomic DNA, suggesting potential translocation from the cytoplasm to nucleus.
- *De novo* generation of C3aR and C5aR1 mRNA and protein is also observed upon TCR engagement in T cells. C3a (and C5a) have been shown to interact with their cognate receptors intracellularly. However, it is unclear how C3a interacts with C3aR:
    - C3a and C3aR interact inside of intracellular compartments (Hypothesis #1).
    - Cytosolic C3a may interact with C3aR (Hypothesis #2).

TCR: T-cell receptor, CTSL: Cathepsin L, FI: Complement Factor I, FH: Complement Factor H.

1.4 NON-CONVENTIONAL T CELLS

Several non-conventional α/β T cells exist, and the two major subsets comprise those restricted by the monomorphic MHC-I like molecules cluster of differentiation 1 (CD1) and MHC Class I related protein (MR1). Whereas mucosal associated invariant T cells (MAITs) recognise vitamin metabolites in the context of MR1 (Howson et al., 2015), all CD1 restricted T cells recognise lipid antigens (Vincent et al., 2003). Humans express four CD1 isoforms: CD1a, CD1b, CD1c and CD1d. Group I CD1 molecules (i.e. CD1a, CD1b and CD1c) are expressed by professional antigen-presenting cells (APCs) such as dendritic cells (DCs), expression of the Group II molecule CD1d is more diverse, encompassing monocytes and epithelial cells as well (Vincent et al., 2003). The best characterised innate-like T cell subset which recognise lipids in the context of CD1d molecules are invariant Natural Killer T (iNKT) cells (Wolf et al., 2018).

1.4.1 Invariant Natural Killer T (iNKT) cells

Invariant Natural Killer T (iNKT) cells comprise a subset of lymphocytes expressing a highly restricted T-cell receptor (TCR) repertoire and markers of NK cells (Mao et al., 2016; Krovi and Gapin, 2018), and respond to lipid antigens in a CD1d-dependent manner (Kjer-Nielsen et al., 2006). They express an invariant TCR α-chain (Vα14-Jα18 in mice and Vα24-Jα18 in humans) which pairs with Vβ11 in humans and Vβ2, Vβ7 or Vβ8.2 in mice. $CD4^+$ and double-negative iNKT cells are present in humans and mice whereas humans also possess $CD8^+$ iNKT cells (Godfrey et al., 2004). The iNKT cell TCR is conserved across species (Zajonc and Girardi, 2015), leading to cross-species conservation of the molecular mechanism of antigen recognition by iNKT cells (Kjer-Nielsen et al., 2006). It was previously shown that the human iNKT TCR α-chain has 54% sequence homology with its murine counterpart, and human Vβ11 and mouse Vβ8.2 have 65% sequence homology (Kjer-Nielsen et al., 2006). Moreover, the human iNKT TCR has been shown to bind murine CD1d complexes (Kjer-Nielsen et al., 2006)

and the murine iNKT TCR can bind human CD1d complexes (Borg et al., 2007; Yu et al., 2019). Furthermore, Kjer-Nielsen and colleagues showed that the CDR3α and CDR1α loops of the human and mouse semi-invariant NKT TCRs plays are indispensable for antigen specificity and cross-species reactivity via CD1d (Kjer-Nielsen et al., 2006).

Invariant NKT cells originate in the thymus from $CD4^+$ $CD8^+$ double and are positively selected by self-lipids presented by CD1d-expressing DP thymocytes (Krovi and Gapin, 2018). Homotypic co-stimulatory interactions between members of the signalling lymphocytic activated molecules (SLAM) family are also required, as iNKT cells are not present in SLAM-signalling deficient mice (Griewank et al., 2007). TCR and SLAM engagement promotes high expression of the transcription factor *Egr2* which induces transcription of *Zbtb16*, the gene encoding the master transcription factor promyelotic leukaemia zinc finger (PLZF) which is indispensable for iNKT cell development (Krovi and Gapin., 2018). More specifically, PLZF has been shown to directly bind multiple immune effector genes which have critical functions in the uNKT cell effector program (Savage et al., 2008; Mao et al., 2016).

Invariant NKT cells progress through three developmental stages in the mouse (Klibi et al., 2020). Stage 1 cells are $CD44^-NK1.1^-$, and transition to stage 2 upon acquisition of the activation marker CD44 generating $CD44^+NK1.1^-$ cells. Both stage 1 and stage 2 iNKT cells require IL-7 to enable intrathymic proliferation. Subsequent acquisition of NK1.1 in the thymus or after migration into the periphery generates stage 3 iNKT cells (i.e. $CD44^+NK1.1^+$); this transition requires IL-15. Whilst stage 1 cells secrete mainly T_H2 cytokines, stage 3 iNKT cells secrete T_H1 cytokines (Klibi et al., 2020). Through a combination of ChiP-seq and microarray analysis in Vα14-Jα18 stage 1 NKT thymocytes from WT and PLZF-deficient C57BL/6 mice, Mao et al. showed that PLZF binds and subsequently down-regulates the gene *Sell*, which encodes CD62L and is required for recirculation to lymph nodes. PLZF was also shown to bind and increase expression of the adhesion molecule CD44, thereby reinforcing the

$CD44^{hi}CD62L^{lo}$ nonrecirculating effector phenotype of iNKT cells (Mao et al., 2016). Moreover, PLZF was also shown to directly bind and up-regulate *Il12rb1* and *Il18r1* genes but repressed the *Il21r* gene, therefore enabling iNKT cells to quickly respond to antigen-presenting cell-derived cytokines at the iNKT-APC interface (Mao et al., 2016).

Unlike conventional T cells which differentiate in the periphery, iNKT cells differentiate in the thymus. In the mouse, distinct iNKT functional subsets referred to as iNKT1, iNKT2 and iNKT17 have been observed in the periphery which express the canonical transcription factors *T-bet*, *GATA-3* and *RORγt*, respectively (Kim et al., 2017). Upon stimulation *in vitro*, iNKT1 cells secreted high concentrations of IFN-γ and little IL-4, iNKT2 cells secreted mainly IL-4, and iNKT17 secreted mainly IL-17, when stimulated with PMA/ionomycin (Lee et al., 2013; Krovi and Gapin., 2018). iNKT1 cells make up most of the stage 3 $CD44^{+}NK1.1^{+}$ iNKT cells in mice (Buechel et al., 2015) and are particularly enriched in the liver (Lee et al., 2015). On the other hand, iNKT2 cells are mainly detected in the lymph nodes (Lee et al., 2015), whereas iNKT17 cells mainly reside in the lymph nodes along with the skin and in the lung (Buechel et al., 2015). Unlike conventional T cells, iNKT cells possess a 'memory' phenotype and are functionally poised to rapidly secrete cytokines upon activation, despite no previous encounter with antigen (Krovi and Gapin, 2018).

Finally, a PLZF-negative iNKT cell population was observed in the adipose tissue of C57/BL6 mice. This population of iNKT cells expressed the transcription factor e*4bp4*, which increased IL-10 secretion and downstream transactivation of conventional regulatory T cells (Lynch et al., 2014). Moreover, follicular helper iNKT cells ($iNKT_{FH}$) which express the transcriptional repressor *Bcl6* have also been observed in secondary (peripheral) lymphoid organs (Chang et al., 2011; **Figure 1-7**).

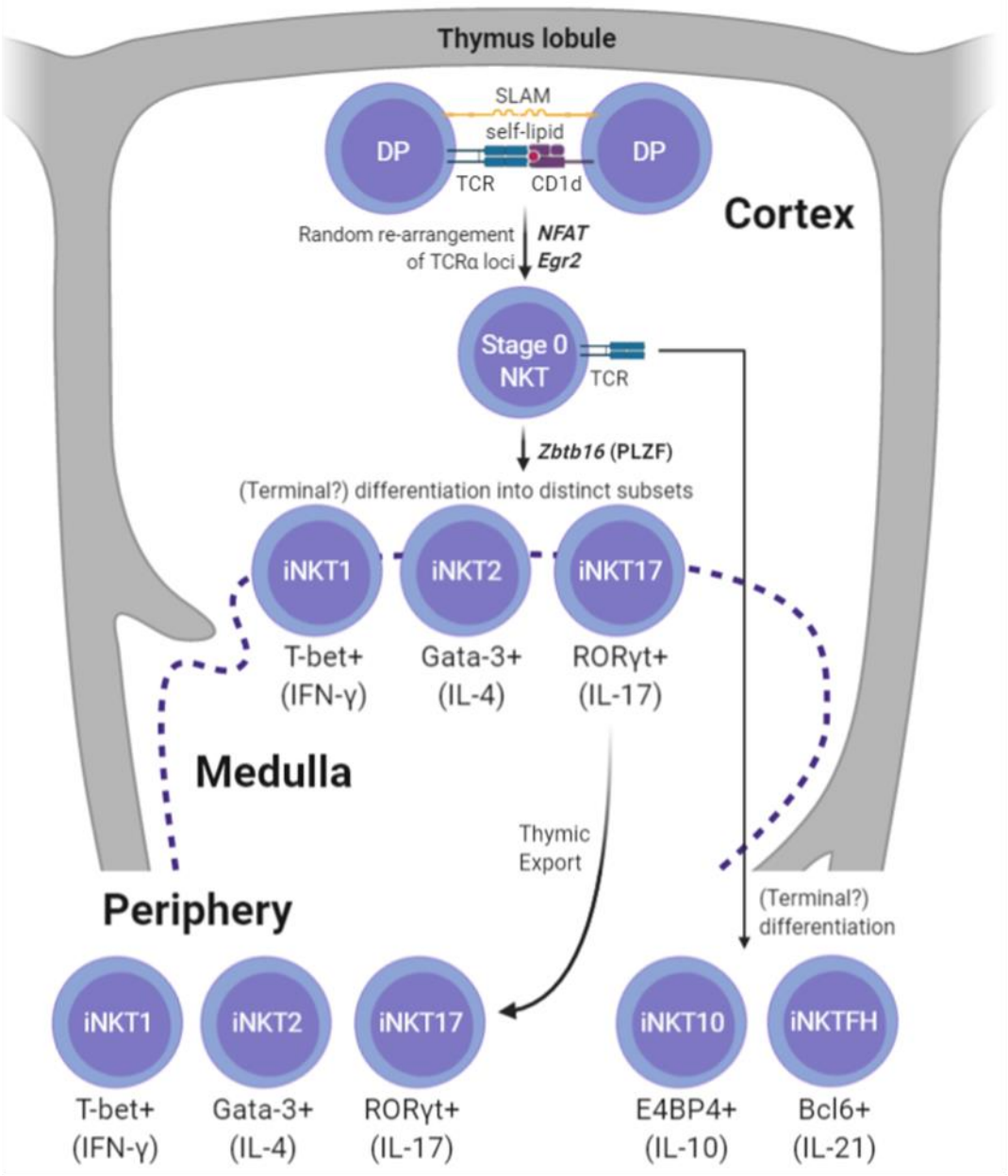


Figure 1-7 Overview of iNKT cell development and differentiation

Homotypic interactions between double positive (CD4+/ CD8+) cortical thymocytes in the presence of self-lipid, the SLAM co-stimulatory axis and the NFAT-modulated transcription factor EgR2 drives Stage 0 iNKT cell development. Stage 0 iNKT cells express the master transcription factor *Zbtb16* which encodes for PLZF. In the mouse, cortical PLZF+ iNKT cells differentiate into distinct subsets, termed iNKT1, iNKT2 and iNKT17 and subsequently migrate to the medulla before entering the periphery. iNKT cell subsets are defined by both canonical transcription factor and cytokine expression. However, it remains unclear if canonical transcription factor expression is a pre-requisite for terminal differentiation, or is simply a consequence i.e. downstream of lineage commitment. Additional iNKT cell subsets have also been observed in peripheral tissues, however the location of their differentiation remains unclear.

DP: Double positive, TCR: T-cell receptor, SLAM: signalling lymphocytic activation molecule, PLZF: promyelotic leukemia zinc finger, T-bet: T-box transcription factor (TBX21), RORγt: RAR-related orphan receptor gamma (2) FH: follicular helper, E4BP4: E4 promoter–binding protein 4, Bcl6: B-cell lymphoma 6 protein. Figure developed using biorender.com/ image template designed by Dr Nabil Zeidan (McGill University).

1.4.2 CD1d Structure and Function

The CD1 gene families have been identified in nearly every mammalian genome that has been sequenced (Yu et al., 2019). The CD1 gene is located on chromosome 1 whilst the MHC locus is on chromosome 6 (Reinink and Rhijn, 2016). Allelic variants are observed for human CD1a and CD1d, but not human CD1b and CD1c. However, the single nucleotide polymorphisms in CD1d are not located in the antigen-binding cleft or the TCR-binding surface – hence unlike MHC, CD1d is considered non-polymorphic (Reinink and Rhijn, 2016).

Invariant NKT cells respond to endogenous glycosphingolipids (GSL), exogenous microbial ligands and several synthetic agonists such as alpha-galactosylceramide (α-GalCer) presented by the monomorphic major histocompatibility complex (MHC) class-I like molecule CD1d (McEwen-Smith et al., 2015). The CD1d binding groove consists of two channels termed A' and F' which accommodate the alkyl chains of the glycolipid allowing the polar sugar head group to protrude and interact with the iNKT TCR (Koch et al., 2004). CD1d assembly and association with β-2 microglobulin occurs in the endoplasmic reticulum (ER), where multiple glycosylation events along with interactions with chaperone proteins influence the repertoire of self-lipid loading and egress to the plasma membrane (Girardi et al., 2012).

1.4.3 CD1d-dependent and independent iNKT cell activation

In humans, the repertoire of cytokine secretion is modulated by iNKT cell TCR signal strength, with the canonical ligand α-GalCer possessing a very high affinity and thus polarising towards a T_H1 response, whereas the synthetic analogue OCH promotes T_H2 polarisation (McCarthy et al., 2007). Specifically, modifications to the acyl or sphingosine chains of α-GalCer such as unsaturation of carbon-carbon bonds or truncation, alter occupancy of the CD1d binding groove (McCarthy et al., 2007).

Whilst the α-anomericity of the lipid is an important requisite for CD1d-specific activation of iNKT cells (Ilan et al., 2009), mammals lack α-anomeric glycolipids such as α-GalCer (McEwen-Smith et al., 2015). Therefore, the search for iNKT endogenous ligands has focused on β-anomers (McEwen-Smith et al., 2015). Whilst the β-anomeric self-antigen isoglobotryhexosylceramide (iGb3) was initially thought to be the major selecting ligand during iNKT cell development, it was later demonstrated by Gadola et al. that defects in glycosphingolipids (GSL) storage impairs antigen presentation and hence thymic selection of iNKT cells (Gadola et al., 2006). More specifically, iNKT cell numbers were reduced in mice with GSL storage diseases, even though CD1d expression and the total number of $CD1d^+$ APCs remained unchanged. However, the absolute numbers of α-GalCer/CD1d–specific thymocytes were reduced in these mice when compared to wild-type controls. Moreover, APCs from these mice were shown to have a reduced capacity to process and present a lysosome-dependent analogue of α-GalCer (named galactosyl galactosylceramide; Prgozy et al., 2001), suggesting that defects in GSL storage also compromises downstream antigen presentation (Gadola et al., 2006).

However, a more prolonged interaction has been observed between the iNKT TCR and CD1d, when CD1d molecules are occupied by non-glycosidic compounds such as threitol ceramide 6 (ThrCer 6) which possesses a non-glycosidic polar head group (Jukes et al., 2016; Silk et al., 2008). More specifically, human CD1d (hCD1d) molecules were refolded *in vitro* with ThrCer 6 or α–GalCer and coupled to BIAcore chips over which refolded human iNKT cell TCR was injected at different concentrations (Jukes et al., 2016). The human iNKT cell TCR showed a more prolonged interaction (i.e. a longer off-rate) with hCD1d/ThrCer 6 than with hCD1d/α–GalCer. The more prolonged interaction in turn correlated with a higher affinity of binding i.e. the dissociation constant (K_D) of hCD1d/ThrCer 6 was 0.61 ± 0.10 μM whereas the K_D of hCD1d/α–GalCer was 1.12 ± 0.13 μM, for the human iNKT cell TCR (Jukes et al., 2016).

Furthermore, it has been demonstrated that full iNKT cell activation requires cytokine signalling (Brigl et al., 2011). More specifically, activation can be achieved by a weak TCR-mediated signal (i.e. self-lipid) in association with interleukin-12 (IL-12), IL-18 and type I interferon. Furthermore, under certain physiological conditions, IL-12 and IL-18 signalling alone is sufficient to drive cell activation thus bypassing the requirement for direct recognition of lipid antigen (Brigl et al., 2011). This intriguing finding sheds new light on how iNKT cells can respond to a disparate number of lipid antigens and hence become activated, even though the diversity of their TCR is quite limited.

1.4.4 The CD40-CD40L Signalling Axis

The CD40 receptor is a 48-kDa type I transmembrane protein and a member of the TNF-receptor superfamily, primarily expressed on professional antigen-presenting cells including macrophages and DCs, but also on B cells (Elgueta et al., 2009). The cognate ligand of CD40 is the ~35-kDa type II transmembrane protein CD40L (CD154). CD40L is up-regulated upon activation of conventional T and B lymphocytes, along with activated iNKT cells (Elgueta et al., 2009). The CD40-CD40L cognate interaction is a critical co-stimulatory axis at the T cell-APC interface, producing an array of effects including B cell germinal centre (GC) formation, fine-tuning of effector T cell responses and modulation of APC cytokine secretion profiles (Grewal and Flavell, 1998).

The CD40-CD40L co-stimulatory axis also plays a critical role at the iNKT-DC interface. Specifically, iNKT cells license DCs maturation through promoting up-regulation of co-stimulatory molecules such as CD80 and CD86 along with increased IL-12 secretion in a CD40L-dependent manner (Hermans et al., 2003 and 2007). Invariant NKT cell-induced DC maturation in turn correlated with enhanced conventional T-helper and cytotoxic effector function *in vivo*; an effect which was abrogated in mice lacking iNKT cells or CD1d molecules (Hermans et al., 2003).

1.4.5 iNKT Cell Effector Functions

iNKT cells exist in a poised effector state and possess a unique capacity to bridge the innate and adaptive immune systems, by directly modulating NK cell transactivation (via IFN-γ) and inducing DC and B cell maturation (Cerundolo et al., 2009). More specifically, iNKT cells have been shown to boost antibody responses through cognate interactions with B cells presenting glycolipid antigen, an effect which was positively modulated by the T_H2 cytokine IL-4 (Doherty et al., 2018). Furthermore, iNKT crosstalk may also modulate the polarisation state of suppressive IL-10-secreting neutrophils and myeloid-derived suppressor cells (MDSCs) (DeSanto et al, 2008; DeSanto et al., 2010). More specifically, iNKT cells were shown to down-regulate IL-10 but promoted IL-12 secretion in neutrophils from melanoma patients – an effect which was CD40, CD1d and IFN-γ dependent (DeSanto et al., 2010).

Additionally, iNKT cells also release cytolytic mediators such as perforin and granzyme B thereby promoting cytotoxicity which is a necessary component of antitumor responses (Lam et al., 2017). More specifically, Bassiri et al. used NOD-SCID IL2Rγ$^{-/-}$ (NSG) mice which lack endogenous T, B and NK cells (Bassiri et al., 2014). NSG mice were reconstituted with either wild-type (WT) or perforin-deficient (*Prf1*$^{-/-}$) iNKT cells and subsequently challenged with luciferase-expressing EL4 T-lymphoma cells which express CD1d. NSG mice reconstituted with WT iNKT cells showed a significantly lower tumour burden (as evidenced by lower bioluminescence) when compared to NSG mice reconstituted with *Prf1*$^{-/-}$ iNKT cells, thus confirming an indispensable role for iNKT cells in antitumour responses (**Figure 1-8**).

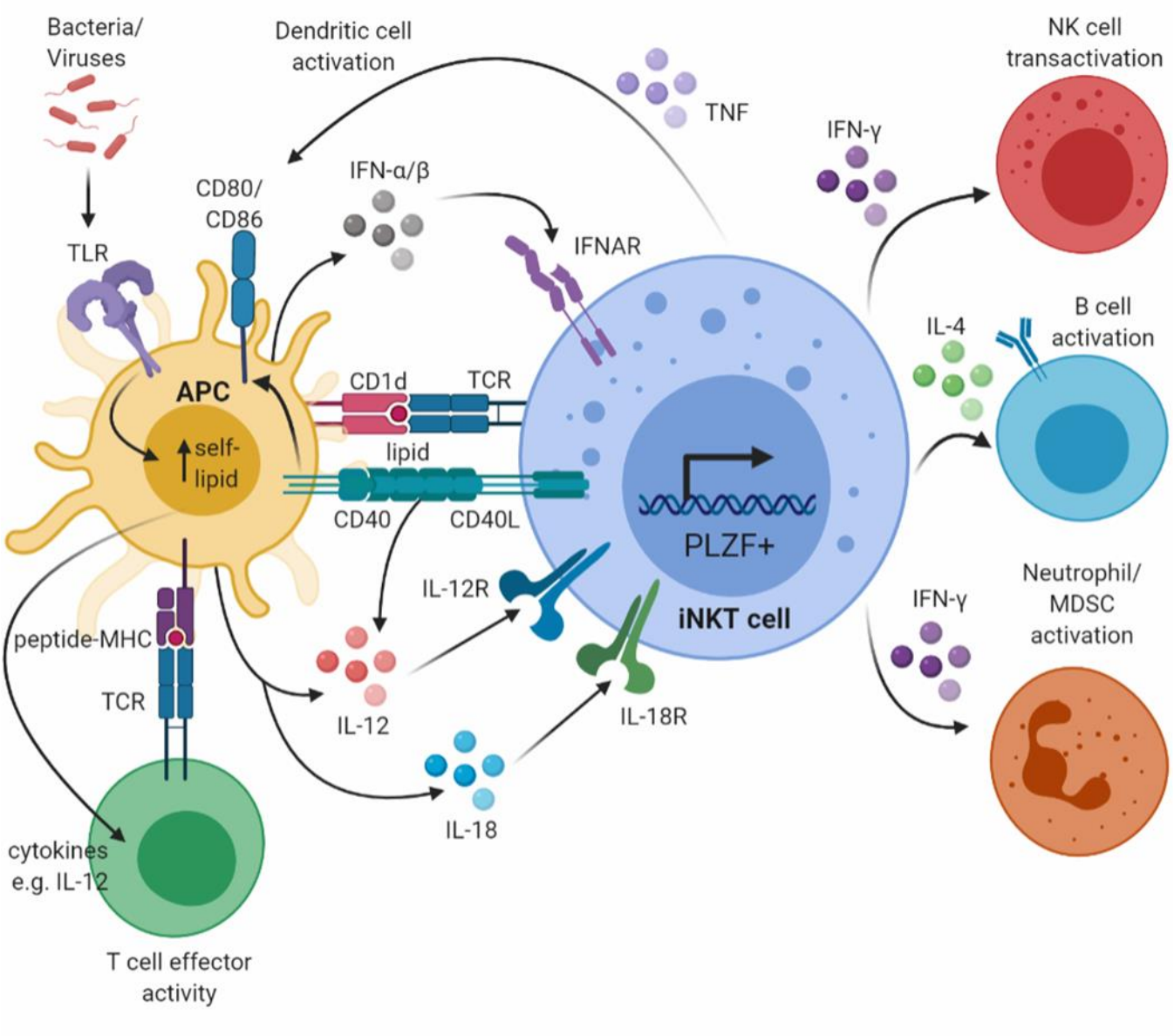


Figure 1-8 Overview of iNKT cell effector function

Invariant NKT cells respond to microbial and self-lipid antigens in a CD1d-dependent manner, and rapidly secrete multiple T_H1 and T_H2 cytokines including IFN-γ and IL-4. In addition to the CD1d-TCR interaction, there are multiple co-stimulatory axes including the CD40-CD40L axis which positively modulate APC cytokine secretion (e.g. IL-12). Moreover, bacterial/viral antigen recognition by TLRs also promotes iNKT cell autoreactivity, as evidenced by increased cytokine secretion and agonistic self-lipid generation. Downstream effector functions of iNKT cells include modulation of conventional αβ T cell effector function, NK cell transactivation, B cell activation and promoting a pro-inflammatory phenotype in neutrophils and MDSCs.

TCR: T-cell receptor, APC: antigen presenting cell, MDSC: myeloid-derived suppressor cell, TLR: toll-like receptor, PLZF: promyelocytic leukaemia zinc finger, MHC: major histocompatibility complex.

1.4.6 iNKT cells and complement

As iNKT cells form a nexus between innate and adaptive immune responses, it was speculated by Fusakio et al., (2011) that complement, specifically anaphylatoxins may modulate iNKT cell effector function in a manner analogous to DC effector cytokines. More specifically, murine iNKT cells were shown to express high levels of C5aR1 and lower levels of C5aR2 mRNA, but no protein at steady state. Upon *Escherichia coli*-induced sepsis, C5aR1 mRNA was rapidly translated to functional protein and the receptor was detected on the cell surface. Moreover, genetic ablation of C5aR1 in iNKT cells blocked IFN-γ and TNF secretion, which in turn promoted longer survival of C57/BL6 mice following bacterial encounter (Fusakio et al., 2011).

As Fusakio et al., (2011) did not determine downstream mechanisms by which anaphylatoxin receptor engagement positively modulates iNKT cell activation, one may speculate on a potential role of intracellular complement generation and 'inside-out' signalling as described for conventional T cells (Liszewski et al., 2013; Strainic et al., 2008). To date, the role of intracellular complement generation in iNKT cells remains unexplored.

1.5 COMPLEMENT PATHOLOGY AND THERAPEUTIC POTENTIAL

Disrupted complement signalling is implicated in several autoimmune and immune complex (antibody-dependent) diseases (Holers and Thurman, 2004), with clinical manifestations localised to certain organs including the eyes and kidneys (Ricklin et al., 2016). Genetic defects have been observed in multiple early, late, and terminal components of the complement cascade. Diseases associated with aberrations in alternative pathway components are described below.

1.5.1 Kidney Disease

C3 glomerulopathies comprise a rare group of kidney diseases, characterised by C3 deposition in the glomeruli and usually associated with dysregulation of alternative pathway complement activation (Smith et al., 2019). More specifically, autoantibodies known as C3 or C5 nephritic factors i.e. C3NeF or C5NeF stabilise the alternative pathway C3 and C5 convertases thereby increasing their usually short half-lives (Paixão-Cavalcante et al., 2014; Corvillo et al., 2019). This in turn drives uncontrolled activation and consumption of complement in the fluid phase. As terminal complement pathway inhibitors such as the anti-C5 monoclonal antibody, Eculizumab (AstraZeneca) showed limited efficacy in the clinic (Ricklin et al., 2016), clinical trials targeting early components of the alternative pathway are currently underway (Smith et al., 2019). These therapies currently being tested include:

- an oral Factor D inhibitor (ACH0144471) in trials NCT03369236, NCT03459443 and NCT03124368
- an oral Factor B inhibitor (Iptapocan [LPN023]) in trials NCT04154787 and NCT03955445
- a subcutaneously administered C3 inhibitor called AMY101 in trial NCT03316521 (Smith et al., 2019).

1.5.2 Age-related Macular Degeneration (AMD)

AMD is the most common cause of blindness worldwide (Morgan and Harris, 2015). The aetiology of the disease is complex and multi-faceted (Handa et al., 2019). For example, polymorphisms in several lipid-related genes have been observed which are subsequently associated with drusenogenesis i.e. the development of yellow lipid droplets in the eye called drusen. Moreover, double stranded RNA (which is also a component of drusen) binds its cognate receptor TLR3 which promotes an acute inflammatory response and downstream cell death of photoreceptors (Handa et al., 2019). In addition, AMD is also associated with genetic polymorphisms in the alternative pathway inhibitor Factor H (Morgan and Harris, 2015). Hageman et al., (2005) showed that changes in a single amino acid in the middle of the molecule (Y402H) tripled the risk of developing AMD. Additional polymorphisms which promote disease susceptibility have also been observed in C3 and Factor B (Morgan and Harris, 2015). Current therapeutic interventions for AMD include the C3 Convertase inhibitor Compstatin (Wu et al., 2019) along with other non-complement treatments such as anti-VEGF (vascular endothelial growth factor) therapy (Wu et al., 2019). Additionally, intravital administration of a monoclonal antibody antigen-binding fragment (Fab) targeting the rate-limiting alternative pathway enzyme Factor D (FD) called Lampalizumab reached Phase III clinical trials but failed to meet its primary endpoints in AMD patients (Holz et al., 2018).

1.5.3 Systemic Lupus Erythematosus (SLE)

Classical pathway deficiency, specifically C1 and C4 is associated with the autoimmune condition SLE (Morgan and Harris, 2015). This is because C1q/ C4-mediated opsonisation of immune complexes does not occur, thus leading to the deposition of insoluble aggregates which promote inflammation (Thurman et al., 2019). Downstream tissue injury, as observed in lupus nephritis is paradoxically associated with alternative pathway (AP) activation – as deficiency of AP proteins including Factor B and C3 is protective, but the exact mechanism remains

unclear (Thurman et al., 2019). As such, Apellis Pharmaceuticals is currently conducting a phase II clinical trial of a novel pegylated cyclic peptide inhibitor of C3 termed pegcetacoplan (APL-2) in lupus nephritis patients (Zipfel et al., 2019; clinical trial reference NCT03453619).

1.5.4 Haematological Disorders

There is a strong link between complement and coagulation pathways, as many coagulation enzymes such as thrombin and kallikrein can activate C3 and C5 (Ricklin et al., 2016). Paroxysmal nocturnal haemoglobinuria (PNH) is a rare disease in which erythrocytes lack the surface complement regulators CD55 (DAF) and CD59, caused by a mutation in the X-linked phosphatidylinositol glycan class A (PIG-A) gene (Risitano et al., 2012). CD55 disrupts C3 convertase formation, whereas CD59 inhibits terminal MAC formation – thus, making PNH erythrocytes more susceptible to complement-mediated haemolysis (Risitano et al., 2010).

Atypical haemolytic uraemic syndrome (aHUS) is a disease caused by mutations in the C-terminus of Factor H (a central regulator of AP) and the C3d-domain of C3 (Rodriguez et al., 2014). Clinical manifestations include damage to the endothelium and thrombus formation which are treated using the anti-C5 monoclonal antibody Eculizumab (Morgan and Harris., 2015; Ricklin et al., 2016). Additional treatments currently being assessed in clinical trials include:

- The MASP-2 inhibitor Narsoplimab (OMS-721) in trial NCT03205995
- The anti-C5 monoclonal antibodies Ravulizumab (ALXN121) in trials NCT02949128 and NCT02949128 and Crovalimab in trial NCT04861259
- The RNAi therapeutic which targets C5, Cemdisiran (ALN-CC5) in trial NCT03303313
- The Factor B inhibitor Iptacopan (LNP023) in trial NCT04889430
- A biosomilar of Eculizumab called Elizaria in trial NCT04749810

- Empaveli™ (systemic pegcetacoplan), which targets C3 has recently been approved in the United States

1.5.5 Transplant Rejection

Complement is strongly implicated in cell-mediated and antibody-mediated transplant rejection (Ricklin et al., 2016). Notably, transplantation of kidneys from C3-knockout mice transplanted into wildtype mice survived up to 100 days without immunosuppression whereas wild-type kidneys were swiftly rejected with mean allograft survival of only 12 days (Pratt et al., 2002).

Cell-mediated transplant rejection is modulated by interactions between APCs and alloreactive T cells. More specifically, locally derived anaphylatoxins (C3a and C5a) promote an acute inflammatory response but also bind their cognate receptors (C3aR and C5aR1) on allogeneic T cells, driving T helper 1 polarisation in the mouse (Strainic et al., 2013). Moreover, complement activation fragments, specifically C3dg also prime the adaptive immune response by opsonising donor antigens. Presentation of opsonised antigens reduces the threshold for B cell activation and promotes the generation of donor-specific antibodies (DSA), specifically up-regulation of the complement fixing anti-donor IgG2a isotype (Marsh et al., 2001). Clinical trials assessing the therapeutic potential of the C5 blocking antibody Eculizumab and the classical pathway inhibitor (C1-INH) in treating antibody-mediated rejection are currently underway (Grafals and Thurman., 2019).

1.5.6 Ischaemia-reperfusion injury (IRI)

Ischemia-reperfusion injury (IRI) is characterised by limited tissue perfusion, where tissues do not receive sufficient oxygen and nutrients to maintain successful energy homeostasis (Danobeitia et al., 2014). Tissues become necrotic and activate incoming innate immune cells, including neutrophils and macrophages to the ischaemic site. The release of pro-inflammatory

cytokines, reactive oxygen species (ROS) and complement in turn promote further necrosis and apoptosis (Danobeitia et al., 2014). Anti-complement therapeutics used in IRI patients include anti-C5 antibodies, C1 esterase inhibitors (C1INH) or treatment with a soluble form of complement receptor type 1 (CR1) called Mirococept (APT-070) which inhibits all pathways of complement activation (Vogel et al., 2020). Souza et al. investigated the effect of APT-070 on intestinal ischaemia and reperfusion in the male Wistar rats (Souza et al., 2009). Prior administration of APT-070 was shown to significantly reduce neutrophil infiltration into the gut and associated vascular leakage. Moreover, levels of the proinflammatory cytokines, TNF-α and IL-6 were reduced but concentrations of protective IL-10 remained unchanged. The authors concluded that inhibition of complement activation by APT-070 was effective in reducing inflammatory responses and downstream tissue damage (Souza et al., 2009).

1.5.7 Leveraging iNKT cells as a therapeutic strategy

As discussed in Section 1.4, invariant NKT cells extensively crosstalk with other immune cell types, further increasing their therapeutic potential (Van Kaer and Wu, 2018). For example, iNKT cells increase cytokine secretion by DCs and macrophages following TCR engagement and transactivate NK cells by promoting IFN-γ production and cytotoxicity. Additional modulation of adaptive immunity, including effects on T cell and B cell antibody responses have also been described (Van Kaer and Wu, 2018).

Therefore, it is perhaps unsurprising that the immunomodulatory potential of iNKT cells has been exploited in several preclinical models of inflammatory and autoimmune diseases, including EAE and SLE (Van Kaer, 2005). Yang et al. previously demonstrated that α-GalCer treatment of BWF1 mice which develop autoantibody-mediated lupus nephritis, led to improved renal function and reduced IgG anti-DNA autoantibody production (Yang et al., 2012). Subsequent assessment of cytokine production showed that IL-10 production was lower in splenic cultures of αGalCer-treated BWF1 mice, when compared to their vehicle-treated

counterparts (Yang et al., 2012). The authors concluded iNKT cells may protect against lupus by suppressing IL-10 production, but the exact mechanism of cytokine suppression remains undetermined.

Thus, it is tempting to speculate that leveraging the immunomodulatory potential of iNKT cells in combination with anti-complement therapeutics may provide enhanced efficacy in multiple autoimmune diseases such as SLE and C3 glomerulopathies.

1.6 MAIN HYPOTHESIS & PROJECT AIMS

Extrahepatic complement generation, cleavage and signalling has been extensively described in multiple cell types (Strainic et al, 2008; Strainic et al., 2013; Liszewski et al., 2013; Arbore et al., 2016; Arbore et al., 2018; Kolev et al., 2020). However, knowledge of complement signalling in the context of invariant Natural Killer T (iNKT) cell effector function is unexplored.

The main hypothesis of this project is that locally derived complement, most likely anaphylatoxins modulate iNKT cell effector function via their cognate receptors through autocrine or paracrine signalling by neighbouring antigen-presenting cells. This hypothesis will be addressed, as follows:

1) Characterise the complement expression profiles in iNKT cells, at steady state and during activation.
2) Examine complement expression profiles in antigen presenting cells (MdDC) at steady state and during activation.
3) Inhibit complement e.g. through pharmacological blockade and assess changes in complement expression profiles, with a focus on anaphylatoxin generation.
4) Assess autocrine or paracrine engagement of anaphylatoxin receptors, and downstream changes in cellular effector response.
5) Interrogate a mechanistic link between complement (specifically anaphylatoxin receptor engagement), in iNKT-MdDC co-cultures and assess downstream effector responses.

2 MATERIALS AND METHODS

2.1 CELL CULTURE MEDIA

Cells (iNKT, MdDC, THP-1) were either cultured in complete medium (CM) or serum-free medium (SFM). CM was Roswell Park Memorial Institute (RPMI)-1640 (Life Technologies, Paisley UK) supplemented with 2 mM L-glutamine (Gibco, A2916801), 1% v/v non-essential amino acids (Gibco, 11140035), 1% v/v Sodium Pyruvate (Gibco, 11360070), 1% v/v Penicillin-Streptomycin (Gibco, 15070063), 1% v/v HEPES (Gibco, 15630056), 0.1% v/v 2-Mercaptoethanol (Gibco, 31350010) and 10% v/v heat-inactivated Foetal Calf Serum (FCS) (Sigma). SFM was X-Vivo 15^{TM} formulated with L-glutamine and gentamicin (Lonza, BE02-060F). The medium used for culture and stimulation of each cell type (in each experiment) is mentioned within the respective figure legends.

2.2 SAMPLE PROCESSING

Leukocyte cones were purchased from National Health Service (NHS) blood and transplant service (NHSBT). The human biological samples were sourced ethically and their research use was in accord with the terms of the informed consents under an IRB/EC approved protocol. Apheresis enriched blood (approximately 8 mL) from the leukocyte cones was diluted in 112 mL RPMI-1640 medium (plus 5% v/v HEPES [Gibco] or PBS (LifeTechnologies). Up to 30 mL of diluted blood was overlaid onto 15 mL of Lymphoprep (AxisShield) in a 50mL Falcon® tube or a 50 mL Leucosep™ tube (Greiner Bio-One; 227288). The tubes were centrifuged for 30 min at 2000 rpm with slow acceleration and no brake. The peripheral blood mononuclear cell (PBMC) layer was collected using a transfer pipette and transferred into a new Falcon® tube containing CM plus 1% v/v HEPES. The tubes were centrifuged at 1500 rpm for 15 minutes at RT. The supernatant was removed, and the cells were once again resuspended in

CM plus 1% v/v HEPES. The tubes were centrifuged at 1000 rpm for 10 minutes at RT. The supernatant was removed, and the cells were prepared for their respective assays (as described below)

2.3 GENERATION OF MONOCYTE-DERIVED DENDRITIC CELLS (MDDCS)

CD14+ monocytes were positively selected by magnetic bead separation using either the MACS® CD14 MicroBeads (Miltenyi Biotec; 130-050-201) or EasySep™ Human CD14 Positive Selection Kit II (STEMCELL; 17858), according to the manufacturer's instructions (as described below).

2.3.1 Separation using the MACS® MicroBeads (Miltenyi Biotec):

- PBMCs were re-suspended with 3 mL MACS buffer plus 200 µL CD14 human MicroBeads for 16 min at 4°C.
- An LS column (with plunger removed; 130-042-401) was placed on to a MACS magnet and a cell strainer was placed on top of the column.
- 3 mL MACS buffer was added to the LS column. Once the buffer was eluted out, the sample prepared in Step 1 was added to the column.
- CD14 negative cells were eluted out, and 3 wash steps (i.e. addition of 3 x 3 mL MACS buffer) were performed to ensure successful elution.
- The LS column was removed from the MACS magnet and placed on top of a 15 mL Falcon tube. 3 mL MACS buffer was added to the LS column
- The plunger (removed in Step 2) was re-attached to the column and pushed down to elute the CD14+ cells.

2.3.2 Separation using the EasySep™ Human CD14 Positive Selection Kit II (STEMCELL):

- 300 million PBMCs were diluted in 3 mL MACS buffer (PBS plus 2% FCS). The cells were transferred to a 14 mL polystyrene round bottom tube (Falcon).
- 300 µL of EasySep™ Human CD14 Positive Selection Cocktail II was added to the samples, mixed and incubated for 10 min at RT.
- 300 µL of EasySep™ Dextran RapidSpheres™ were then added to the samples, mixed and incubated for 3 min at RT.
- Additional MACS buffer was added to the sample tubes, giving a final volume of 10 mL. The sample tubes were placed into the "The Big Easy" Magnet (STEMCELL; 18001) for 3 min at RT.
- The supernatant was discarded, and the tubes were removed from the magnet. Steps 4 and 5 were repeated twice more, before the isolated CD14+ cells were ready for use.

The CD14+ cells were differentiated into MdDCs using 50 ng/ml GM-CSF (Peprotech [300-03] or R&D Systems [215-GM/CF]) and 1000 units/ml IL-4 (generated in house; Traunecker) or 30 ng/mL IL-4 (R&D Systems; 204-IL/CF) in CM for 4 or 5 days prior to being phenotyped for CD1a surface expression by flow cytometry. CD1a surface expression was observed to be between 10^3 and 10^4 on a typical x-axis logarithmic scale of a histogram.

2.4 GENERATION OF iNKT CELLS

Human MdDCs were co-cultured with autologous CD14- cells in the presence of 100 ng/ml α-GalCer (Enzo Life Sciences; BML-SL232-0100) in CM. After 14 days, human CD3, CD4 double-positive iNKT cells were sorted using biotinylated CD1d-α-GalCer tetramers (generated in house by Dawn Shepherd; MRC Human Immunology Unit, University of Oxford, UK) conjugated to Brilliant Violet® 421-Streptavidin (Biolegend; 405226). The ratio of CD1d-

tetramer positive iNKT cells within the total co-culture was between 1 and 5%. The sorted iNKT cells were re-suspended in Iscove's Modified Dulbecco's Medium (IMDM) (Gibco) supplemented with recombinant IL-2 (1000 U/mL; generated in house by Prathiba Kurupati; MRC Human Immunology Unit), 5% human serum (Sigma; H4522), 1% penicillin/streptomycin, 2 mM L-glutamine (Gibco), 1 mM sodium pyruvate (Gibco), 1X MEM nonessential amino acids (Gibco), 10 mM HEPES buffer solution (Gibco), 50 μM 2-mercaptoethanol (Gibco). 500 μl each was dispensed into each well of a 48-well plate (Corning; 3548).

Allogeneic peripheral blood mononuclear cells (PBMCs) from 2 donors were generated as described in Section 1.2, pooled and irradiated (5000 rad) for 22 minutes. The irradiated allogeneic PBMCs were resuspended in supplemented IMDM (as described in the above paragraph) at a concentration of $5x10^6$ cells/ml. This was followed by the addition of 2 μg/ml Phytohemagglutinin (PHA) (Thermo Scientific Oxoid; R30852801). 500 μl of allogeneic irradiated PBMCs were dispensed on top of the sorted iNKT cells (500 μl) giving a final volume of 1 ml in each well of a 48-well plate and a final concentration of 1 μg/ml PHA. Every three or four days, the medium was replenished in order to maintain iNKT cells at 37°C/ 5% CO_2.

2.5 STIMULATION AND INHIBITION ASSAYS

2.5.1 CD40L (CD154) Blockade

APCs were plated at a density of 50,000 in a 96 well plate (Corning; U-bottom for THP-1 and flat-bottom for MdDCs) in 100 μl CM or SFM and pulsed with α-GalCer (Enzo Life Sciences; ALX-850-064-KI01; 1-30 ng/ml) for 2 hours at 37°C. LEAF™ Purified anti-human CD154 (CD40L) blocking antibody (Clone 24.31; Biolegend [310811]) or LEAF™ Purified Mouse IgG1, κ isotype control (Clone MOPC-21; Biolegend [400123]) were added at 10 μg/mL,

followed directly by the addition 20,000 iNKT cells/ 100 µl CM or SFM. The co-culture was left overnight at 37°C/ 5% CO_2. The medium in which the cells were stimulated i.e. CM or SFM is mentioned within each figure legend.

2.5.2 CD40L-induced MdDC maturation

MdDCs were plated at a density of 50,000/ 200 µl CM or SFM in a 96 well flat-bottom plate and stimulated with the recombinant soluble human CD40L set (Enzo Life Sciences; ALX-850-064-KI01), consisting of the following three reagents: 10 µg of CD40L (ALX-522-015) and 2 x 50 µg (1 mg/ml) of Enhancer for Ligands (ALX-804-034), which increases the biological activity of CD40L.

More specifically, one vial of lyophilised CD40L was reconstituted with 100 µl sterile water to give a stock concentration of 100 µg/ml. CD40L was subsequently diluted by a factor of 1.25 in CM or SFM to give a concentration of 80 µg/ml. Enhancer was diluted by a factor of 12.5 in CM or SFM to also give a concentration of 80 µg/ml. CD40L (80 µg/ml) was incubated with Enhancer (80 µg/ml) at 1:1 (v/v) for 30 mins at RT to induce multimerization. As the reaction volume had doubled upon incubation, respective concentrations of both components were halved to 40 µg/ml. 10 µl CD40L multimer was added to the cells, giving a final working concentration of 2 µg/ml. The plate was left overnight at 37°C/ 5% CO_2.

2.5.3 CD1d plate-bound assay

On day 1, biotinylated CD1d monomers (generated in house by Claudia Gonzalez-Lopez; MRC Human Immunology Unit) were diluted in 1x PBS to a final concentration of 10 µg/ml. 50 µl of monomer was immobilised in each well of a 96-well flat bottom streptavidin-coated plate (Pierce™; 15124) overnight at 4°C.

On day 2, the 96-well plate was washed twice in 1x PBS (50 µl). This was followed by the temporary addition of 50 mM citrate-phosphate buffer (pH ~5), prior to the addition of 0.1-5 µg/ml α-GalCer (Enzo Life Sciences; BML-SL232-0100) diluted in 1x PBS.

50 mM citrate-phosphate buffer was made in house by dissolving 7.1 g anhydrous sodium phosphate dibasic [Na_2HPO_4] (Sigma; S3264) and 11.5 g citric acid (Sigma; 251275) in 1000 ml of distilled water.

On day 3, the 96-well plate was washed three times in 1x PBS (50 µl). 50,000 iNKT cells were added in SFM or CM, in the presence of 0.05 ng/ml IL-12p70 (Peprotech; 200-12) and left overnight at 37°C/ 5% CO_2.

On day 4, the supernatant was collected and frozen at -20°C for further analysis. The cells were subsequently harvested and stained for flow cytometry (as described in section 1.6).

2.5.4 Small-molecule or antibody-mediated inhibition of AP

MdDCs were plated in a 96-well flat-bottom plate (Costar) at a density of $2.5x10^5$ in 200 µl of CM or SFM. Cells were pre-treated with the small-molecule Factor B inhibitors named 'FB Inhibitor 1' and 'FB Inhibitor 2'or the vehicle control DMSO, Factor B blocking antibodies named 'FB blocking antibody 1' and 'FB blocking antibody 2' or the isotype control (IgG1, kappa) for 20 mins at RT. Cells were subsequently stimulated with 2 µg/ ml CD40L (Enzo Life Sciences; ALX-850-064-KI01), Lipopolysaccharide [LPS] (Invitrogen; 00-4976-93) and/ or R-848 [Resiquimod] (Sigma-Aldrich; SML0196) overnight at 37°C/ 5% CO_2.

2.6 Flow Cytometry and Cell Sorting

2.6.1 Cell Viability and Surface Staining

Cells were resuspended in 150 µl PBS and transferred from a 96-well flat-bottom plate (Costar) to a 96-well v-bottom plate (Costar). LIVE/DEAD® Fixable Aqua Dead Cell Stain Kit (Life Technologies; L34957) was initially reconstituted with 50 µl DMSO and subsequently diluted

1:50 in PBS. 10 µl of diluted Aqua Dead Cell Stain was added to each well (containing up to $1x10^6$ cells) for 10 mins at RT.

MdDCs were blocked using Human Fc Receptor Binding Inhibitor (starting concentration: 1 mg/ml [eBioscience; 14-9161-73]) diluted 1:5 v/v for 20 min at 4°C, in accordance with the manufacturer's instructions. Cells were surface stained with antibodies (as described below in Section 2.6.3) for 20 min at 4°C. Cells were then washed twice in FACS buffer (PBS with 10% FCS).

2.6.2 Intracellular Staining

Cells were fixed and permeabilised using the BD Cytofix/ Cytoperm™ Fixation/ Permeablization Kit (BD; 554714). More specifically, cells were fixed with 100 µl BD Cytofix for 20 mins at 4°C. The plate was centrifuged at 1200 rpm for 5 mins and the supernatant was discarded. The cells were subsequently washed in 150 µl Perm/Wash™ Buffer which had been diluted 1:10 in distilled water. Cells were then stained with 10 µl antibody cocktail (also diluted in Perm/Wash™ Buffer) for 20 mins at 4°C. After this time, the cells were resuspended in 150 µl diluted Perm/Wash™ Buffer and the plate was centrifuged at 1200 rpm for 5 minutes. Once the supernatant was discarded, the plate was washed a further two times with 150 µl diluted Perm/Wash™ Buffer.

2.6.3 Flow Cytometry Antibodies

Target (human)	Clone	Supplier	Catalogue Number	Dilution Factor
PerCP-Cyanine 5.5 CD3 (Mouse IgG1, κ)	SK7	Biolegend	344808	1:50
APC CD4 (Mouse IgG2b, κ)	OKT-4	Biolegend	317416	1:100
APC-Cyanine7 CD4 (Mouse IgG2b, κ)	OKT-4	Biolegend	317418	1:100
PE-Dazzle ™ 594 CD25	M-A251	Biolegend	356126	1:100

(Mouse IgG1, κ)				
Brilliant Violet 421™ CD69 (Mouse IgG1, κ)	FN50	Biolegend	310930	1:100
PE C3aR (Mouse IgG2b)	hC3aRZ8	Biolegend	345804	1:100
FITC C5aR (Mouse IgG2a, κ)	S5/1	Biolegend	344306	1:50
APC CD1a (Mouse IgG1, κ)	HI149	Biolegend	300110	1:100
PE CD40 (Mouse IgG1, κ)	5C3	Biolegend	334308	1:100
PerCP-Cy5.5 CD86 (Mouse IgG2b, κ)	IT2.2	Biolegend	305420	1:50
Alexa Fluor® 647 C3 (Rabbit IgG)	EPR2988	Abcam	ab196639	1:100
FITC C3c (Rabbit Ig fraction)	Polyclonal	Dako	F0201	1:50
Factor B (unconjugated)	JC1	In house	-	1:50
PE HLA ABC	W6/32	Biolegend	311406	1:100
Alexa Fluor® 488 F(ab')2-Goat anti-mouse IgG (H+L) Cross-adsorbed Secondary antibody	Polyclonal	Invitrogen	A117017	1:50
UltraComp eBeads™ Compensation Beads	n/a	eBioscience (ThermoFisher)	01-2222-42	n/a

2.6.4 Analysers and Cell Sorters

Flow cytometry was performed on the BD LSRFortessa™, BD LSRFortessa™ X20 or BD Canto™ II. Cell sorting was performed on BD FACSAria™ III cell sorter. The cytometers were calibrated using the BD™ CS&T (cytometer setup and tracking) beads prior to starting each experiment, according to the manufacturer's instructions. Then, the relevant antibody-stained single colour controls (either cells or compensation beads) were recorded and compensation was performed.

Data was analysed using FlowJo™ cell analysis software (FlowJo, LLC) in the following manner:

- The cells were first gated on for viability (FSC-A vs Viability), followed by single cells (FSC-A vs FSC-H).
- The gated single cells were assessed for surface expression or total expression (if permeabilisation was performed during sample preparation) of the marker of interest in each treatment condition, using the 'Histogram' function. The histograms for each condition were overlaid, so that a direct comparison could be made. A representative gating strategy is shown in Figure 3.1.
- In addition, the mean fluorescent intensity (MFI) for the marker of interest in each condition was calculated using the following command functions: 'Σ' followed by 'Add Statistic' followed 'Geometric Mean'. The MFI values were tabulated in FlowJo, exported as a Microsoft Excel file and visualised thereafter in GraphPad Prism.

2.7 Enzyme-Linked Immunosorbent Assay (ELISA) of IFN-gamma and IL-12p40/70

Enhanced binding polystyrene 96-well clear flat bottom assay plates (Corning; 3690) were coated with 2 µg/ml capture monoclonal antibody (see table 2.7.1 below; 25 µl per well), diluted in coating buffer overnight at 4°C. Coating buffer was generated by dissolving sodium bicarbonate [$NaHCO_3$] (Honeywell Fluka; S6014) in distilled water to a final working concentration of 0.1 M and kept at RT thereafter.

The following day, the plates were washed six times with PBS/ 0.5% Tween-20 and blocked in PBS/ 10% FCS (200 µl per well) for 20 mins at 4°C. The blocking solution was removed and the samples along with cytokine standards were added (see table 2.7.2 below; 25 µl per well) and left overnight at 4°C. The cytokine standards were serially diluted by a factor of two in PBS/ 10% FCS eleven times, whereas one well contained only PBS/ 10% FCS i.e. the 'blank' well. The following day, the plates were washed six times in PBS/ 0.5% Tween-20 and 1 µg/ml

biotinylated detection antibody (see table 2.7.1 below; 25 µl per well), diluted in PBS/ 10% FCS was added for 1-2h at RT. The plate was then washed eight times in PBS/ 0.5% Tween-20.

Avidin-peroxidase (Sigma; A3151) was diluted in PBS/ 10% FCS to a final concentration of 2.5 µg/ml and 25 µl was added to each well for 30 min at RT. The plate was then washed eight times in PBS/ 0.5% Tween-20. This was followed by the addition of 25 µl per well of substrate solution (containing phenylenediamine dihydrochloride [Sigma; P3084-50TAB] and hydrogen peroxide [Sigma; H1009] for assay development. Sulfuric acid (Honeywell Fluka; 35276) was then added (25 µl per well) to stop the reaction.

Absorption (OD) at 560 nm was determined using a spectrophotometric plate reader (BMG LABTECH). A 4-parameter standard curve was generated (using the machines software) to determine the concentration of the cytokine of interest. Background fluorescence was determined from the 'blank' well and subsequently removed by the machine's software before the raw data points were exported to Microsoft Excel and visualised in GraphPad Prism thereafter.

2.7.1 Capture and Detection Antibodies

Target (human)	**Clone**	**Supplier**	**Catalogue Number**	**Assay concentration**
Capture				
IFN-γ (Mouse IgG1, κ)	NIB42	BD Pharmingen™	#551221	2 µg/ ml
IL-12p40 (Mouse IgG1, κ)	C8.3	BD Pharmingen™	#551227	2 µg/ ml
IL-12p70 (Rat IgG1, κ)	20C2	BD Pharmingen™	#555065	2 µg/ ml
Detection (biotinylated)				
IFN- γ (Mouse BALB/c IgG1, κ)	4S.B3	BD Pharmingen™	#554550	1 µg/ ml
IL-12 (p40/ p70) (Mouse IgG1, κ)	C8.6	BD Pharmingen™	#554660	1 µg/ ml

2.7.2 Cytokine Standards

Target (human)	Supplier	Catalogue Number	Starting Concentration
IFN- γ	Peprotech	300-02	20 ng/ml
IL-12p40	Peprotech	200-12P40	50 ng/ml
IL-12p70	Peprotech	200-12	10 ng/ml

2.8 COMPLEMENT C3 AND FACTOR B DETECTION (ELISA KITS)

The samples were prepared according to the manufacturer's instructions (Abcam; see table below for catalogue numbers). More specifically, cell culture supernatants were thawed and centrifuged at 1500 rpm for 10 minutes at 4°C. The standards were diluted in 1X Assay Diluent N (provided as part of the kit; diluted in distilled water) to the recommended starting concentrations described in the table below. This was followed by seven consecutive 1 in 2 serial dilutions of the standards in 1X Assay Diluent N, whereas one well contained 1X Diluent N only i.e. the 'blank' well. 50 µl of standard or sample (also diluted in 1X Diluent N) were added to each well of the pre-coated 96-well plate (provided as part of the kit) and incubated for two hours at RT. The plate was then washed five times with 200 µl of 1X Wash Buffer (provided as part of the kit; diluted from 20X to 1X in distilled water). 50 µl of 1X Biotinylated detection antibody (diluted in 1X Assay Diluent N) was then added to each well for one hour at RT. The plate was once again washed five times with 200 µl of 1X Wash Buffer. This was followed by the addition of 50 µl of 1X SP (streptavidin) Conjugate (diluted in 1X Assay Diluent N) to each well and the plate was incubated for 30 minutes at RT. Once again, the plate was washed five times with 200 µl of 1X Wash Buffer. 50 µl of Chromogen Substrate was added to each well and the plate was incubated in ambient light until the optimal blue colour

density developed. 50 µl of Stop Solution was then added to each well and a colour change from blue to yellow was observed.

Absorption (OD) at 450 nm was determined using a spectrophotometric plate reader (BMG LABTECH). A 4-parameter standard curve was generated (using the machines software) to determine the concentration of the cytokine of interest. Background fluorescence was determined from the 'blank' well and subsequently removed by the machine's software before the raw data points were exported to Microsoft Excel and visualised in GraphPad Prism thereafter.

Target (human)	Supplier	Catalogue Number	Target Specificity	Standard concentrations
C3 ELISA Kit	Abcam	ab108823	No information on epitope binding sequences (ELISA detects C3a and C3b in the context of native C3).	0.625 – 40 ng/ml
Factor B ELISA Kit	Abcam	ab137973	No information on epitope binding sequences (ELISA detects Ba and Bb in the context of native Factor B).	4.375 – 140 ng/ml

2.9 MESOSCALE DISCOVERY (MSD) FOR ANAPHYLATOXIN DETECTION

2.9.1 Sample Generation i.e. Alternative Pathway activation in plasma

600 µl pooled human plasma (generated in house) was diluted in 1000 µl solid Zymosan (generated in house) and 8400 µl Alternative Pathway Buffer (APB; generated in house – see table below) to give a final concentration of 6% (v/v) activated human plasma in a total volume of 10 ml. In a 96-well flat bottom plate (NUNC), multiple concentrations of Factor B Inhibitor 1, Factor B Inhibitor 2, DMSO, Factor B blocking antibody 2 and the isotype (mIgG1, kappa)

were diluted into APB to the required concentrations and dispensed (3 technical replicates/ condition). This was followed by the addition of 200 µl final reaction volume of 6% (v/v) activated human plasma in to each well. The plate was shaken at 750 rpm for 90 mins at a constant temperature of 27°C. The samples were either used immediately for analysis (see below) or frozen at -80°C until required.

APB	Supplier	Catalogue Number	Final assay concentration (millimolar)
1 ml 1 M HEPES	Gibco Life Technologies	15-630-080	4.2 mM
176.55 ml MQ Water	In house	n/a	n/a
36 ml 1 M NaCl	In house	n/a	150 mM
1.7 ml 1 M $MgCl_2$	In house	n/a	7.1 mM
24 ml 100 mM EGTA	In house	n/a	0.1 mM

2.9.2 Analysis of anaphylatoxin (C3a and C5a) generation

The biotinylated capture antibodies (see table below) were diluted in Diluent 100 (MSD; R50AA-2) to a final concentration of 1 µg/ml and 25 µl was dispensed in to each well of a 96-well MSD GOLD 96-Well Streptavidin SECTOR Plate (MSD; L15SA-1). The plates were incubated for 1 hour at room temperature with shaking at 600 rpm. The plates were washed three times using a plate washer (BioTek™) in 0.05% Tween-20 (diluted in 1x PBS). The plates were subsequently blocked with 30% BSA (Sigma; A9576) diluted 1: 15 (v/v) in 0.05% Tween-20 to 2%, overnight at 4°C. The following day, the plates were washed using a plate washer (BioTek™) in 0.05% Tween-20 (diluted in 1x PBS). 50 µl of the samples generated in section 2.9.1 were dispensed in to each well of the MSD plates. The plates were incubated for 90 mins at room temperature with shaking at 600 rpm. The plates were subsequently washed using a plate washer (BioTek™) in 0.05% Tween-20 (diluted in 1x PBS). The detection antibodies (see table below) were diluted in Diluent 100 (MSD; R50AA-2) to 1 µg/ml and 25 µl was dispensed in to each well of a 96-well MSD GOLD 96-Well Streptavidin SECTOR

Plate (MSD; L15SA-1). The plates were incubated for 1 hour at room temperature with shaking at 600 rpm. The plates were washed using a plate washer in 0.05% Tween-20 (diluted in 1x PBS). 4X Read Buffer T (MSD) was diluted to 2X in deionised water and 150 µl was dispensed in to each well. The plates were immediately read for electrochemiluminescence using a MSD Sector 6000 Plate Reader.

Target (human)	**Clone**	**Supplier**	**Catalogue Number**
Capture			
Biotinylated anti-C3a (Stock: 1.74 mg/ml)	2991	Hycult	HM2074BT-B
Biotinylated anti-C5a (Stock: 0.42 mg/ml)	C17/5	Biolegend	518202
Detection			
Ruthenylated anti-C3a (Stock: 187 µg/ml)	474	In house	n/a
Ruthenylated anti-C5a (Stock: 300 µg/ml)	G25/2	In house	n/a

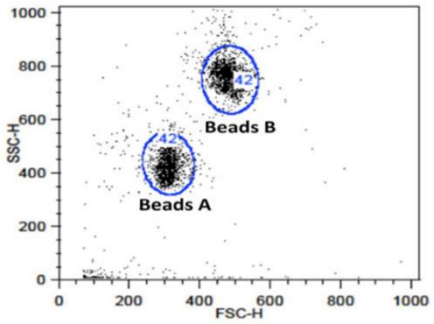
2.10 CYTOKINE BEAD ARRAY

MdDC cell supernatants generated in Section 2.5 were analysed using the LEGENDPLEX Macrophage/Microglia 8-plex Kit (Biolegend; 740505) according to the manufacturer's instructions. More specifically, lyophilised Human Macrophage/ Microglia Panel Standard Cocktail (containing eight different cytokines) was reconstituted with 250 µl Assay Buffer and incubated for 10 minutes at RT, giving a starting concentration of 10,000 pg/ml. This was followed by seven consecutive 1 in 4 dilutions in Assay Buffer, of which 50 µl was dispensed into each well of a 96-well v-bottom plate (Greiner; 651180). One well contained 50 µl Assay Buffer alone i.e. the 'blank' well. Cell culture supernatants were also diluted in Assay Buffer and 50 µl was dispensed into each well of a 96-well v-bottom plate.

The 13X concentrated beads (one vial for each cytokine of interest) were sonicated for 1 minute and vortexed for a further 30 seconds. The 13X beads were combined and diluted to a final concentration of 1X in Assay Buffer. 25 µl of 1X mixed beads were added to each well of a 96-well v-bottom plate, giving a final volume of 75 µl in each well. The plate was sealed with a plate sealer and shaken at 600 rpm for 2 hours. 150 µl of 1X Wash Buffer (diluted in distilled water) was added and the plate was centrifuged at 1500 rpm for 5 minutes prior to the supernatant being discarded. This was followed by the addition of 25 µl of detection antibodies (biotinylated) and the plate was sealed and shaken at 600 rpm for 1 hour. 25 µl Streptavidin-PE was then added to each well, and the plate was shaken at 600 rpm for a further 30 minutes. Once again, 150 µl of 1X Wash Buffer (diluted in distilled water) was added and the plate was centrifuged at 1500 rpm for 5 minutes prior to the supernatant being discarded.

The beads were re-suspended in 110 µl of 1X Wash Buffer and the samples were acquired on the BD Canto™ II and analysed using the LEGENDPLEX platform (Biolegend) in the following way:

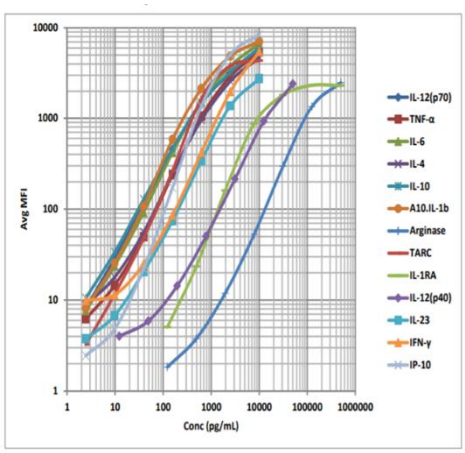
- The panel uses two sets of beads. Each set has a unique size that can be identified based on their forward scatter (FSC) and side scatter (SSC) profiles (Beads A and Beads B). The bead sets are further resolved by their internal fluorescence intensities and are detected using the APC channel.
- The smaller beads (Beads A) consist of 4 bead (i.e. cytokine) populations and the larger beads (Beads B) consist of 4 different bead (i.e. cytokine) populations (see image below).



Beads A = smaller beads

Beads B = larger beads

- Following acquisition, the FCS files were exported to the LEGENDPLEX v8.0 software (Vigenetech) and a 5-parameter curve was generated for each bead i.e. cytokine of interest (see image below of a representative standard curve for a 13-plex assay).



- This was followed by the determination of individual cytokine concentrations within each sample i.e. a total of 8 pre-selected cytokine concentrations by the manufacturer (IL-12p70, TNF-α, IL-6, IL-1β, IL-12p40, IL-23, IFN-γ, CXCL10) were given for each sample. As this assay was used to determine MdDC maturation upon stimulation with either CD40L or different TLR ligands, the DC cytokines IL-12p40 and IL-12p70 were of particular interest.
- The numerical data values were exported into Microsoft Excel File and visualised thereafter in GraphPad Prism.

2.11 Quantitative Reverse Transcription (RT-qPCR)

RNA was extracted from cells using the RNeasy Mini Kit (Qiagen; 74104) according to the manufacturer's instructions. More specifically, a maximum of 1 x 10^7 cells per sample was treated with 350 µl of Buffer RLT. This was followed by the addition of 350 µl 70% ethanol to each sample, giving a total volume of 700 µl. The samples were subsequently transferred to a RNeasy Mini spin column placed in a 2 ml collection tube. The columns were centrifuged at ≥8000 x g for 1 minute. The flow-through was then discarded. 350 µl Buffer RW1 was then

added to each column and centrifuged ≥8000 x g for 1 minute. The flow-through was then discarded.

In column DNase treatment was performed using the RNase-free DNase Set (Qiagen; 79254). More specifically, lyophilised DNase I stock solution was prepared by injecting by 550 µl RNase-free water into the DNase I vial using a RNase-free needle and syringe. DNase I stock solution was combined with Buffer RDD at a ratio of 1:7 (v/v), of which 80 µl was added directly to each column and incubated for 15 min at RT. 350 µl Buffer RW1 was subsequently added and the columns were centrifuged at ≥ 8000 x g for 1 minute. The flow-through was then discarded. 700 µl Buffer RW1 was then added and the columns were centrifuged at ≥ 8000 x g for 1 minute. The flow-through was discarded. This was followed by the addition of 500 µl Buffer RPE and the columns were centrifuged at ≥ 8000 x g for 1 minute. The flow-through was discarded. 500 µl Buffer RPE was added once again and the columns were centrifuged at ≥ 8000 x g for 1 minute. The flow-through was discarded. The columns were placed into new 2 ml collection tube and centrifuged at full speed for 1 min to dry the membrane. The columns were then placed into new 1.5 ml collection tubes and 30 µl RNase-free water was added. The columns were centrifuged at ≥ 8000 x g for 1 min to elute the RNA.

RNA was quantified using the Nanodrop (Thermo) or Tapestation 4200 (Agilent), according to the manufacturer's instructions.

Samples were tested using the **Nanodrop** in the following way:

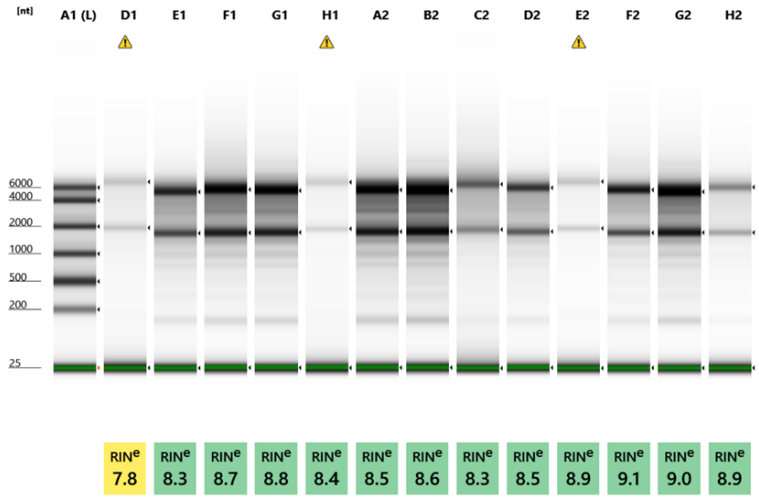
- The Nanodrop software was launched and the 'RNA' assay mode was selected.
- 1 µL RNAse-free water was initially loaded to set a 'blank' value. This was followed by the addition of 1 µL of the RNA samples of interest. The loading dock was cleaned in between applications.

- The sample purity was determined by the A260/280 ratio and the quantity of RNA was provided in ng/ µL. The numerical values were recorded and exported to a Microsoft Excel file for further analysis.

Samples were tested using the **TapeStation 4200** in the following way:

- RNA Sample Buffer (Agilent; 5067-5577) was equilibrated at RT for 30 minutes and the RNA ladder (Agilent; 5067-5578) along with the samples of interest were thawed on ice.
- The Agilent 4200 TapeStation Controller Software was launched and the 'RNA assay mode' was selected.
- The RNA ScreenTape device (Agilent; 5067- 5576) and the loading tips (Agilent; 5067-5598) were loaded into the 4200 TapeStation instrument.
- 5 µL RNA Sample Buffer was combined with either 1 µL RNA Ladder or 1 µL RNA sample of interest in an optical tube strip (Agilent; 401428). The strips were sealed with the appropriate caps (Agilent; 401425) and vortexed at 2000 rpm for 1 min.
- The samples were briefly centrifuged, heated at 72°C (162°F) for 3 min and then placed on ice for a further 2 min.
- The optical tube strip containing the RNA samples was placed into the Agilent 4200 TapeStation instrument, ensuring the tube containing RNA Sample Buffer was placed in position A1. The RNA integrity number (RIN) score and the amount of RNA (~200 ng/ µL) was determined for each sample and exported to a Microsoft Excel file for further analysis.

Below is an example plot from the TapeStation which shows the RIN scores of multiple RNA samples:



cDNA was synthesised by High-Capacity cDNA Reverse Transcription Kit (Applied Biosystems; 4368814) following the manufacturer's instructions. Specifically, all kit components were thawed on ice. Two µl 10× RT Buffer, 0.8 µl 25× dNTP Mix, 2 µl 10× RT Random Primers, 1 µl MultiScribe™ Reverse Transcriptase, 4.2 µl Nuclease-free water were combined in an eppendorf tube (these numbers are for one reaction and can be increased proportionally, depending on the total number of reactions). 10 µl reaction mixture and 10 µl RNA (maximum total concentration of 2 µg) were added to each tube within a 0.2 ml MicroAmp™ Optical 8-Tube Strip (Thermo; 4316567), giving a total reaction volume of 20 µl. The thermal cycler (Applied Biosystems) was programmed, and the following conditions were used for reverse transcription:

- 25°C for 10 min
- 37°C for 120 min
- 85°C for 5 min
- 4°C until samples were removed from thermal cycler

A quantitative PCR was performed in a 384-well plate (4titude; 4ti-0384), as described below. Each 10 µl reaction volume contained:

- 5 µl 2X TaqMan® Fast Advanced Mastermix (Applied Biosystems; 4444557)
- 0.5 µl 20X TaqMan® probe (Applied Biosystems; listed below in Section 2.11.1)
- Varying volume and concentration of cDNA (up to 200 ng)
- Varying volume of nuclease-free water (Ambion; AM9937).

Samples were run in duplicate or triplicate on the QuantStudio 7 RealTime PCR System (LifeTechnologies). Following initial denaturation of the template strand at 95°C for 10 min, a total of 40 amplification cycles were repeated in which the following steps were performed:

- Denaturation at 95°C for 15 sec
- Annealing at 60°C for 60 sec

This was followed by a final incubation at 72°C for 10 minutes to allow for the completion of partial extension products. The C_T (cycle threshold) values for each gene of interest were exported to a Microsoft Excel file and analysed using either the ΔC_T or $\Delta\Delta C_T$ method, dependent on the type of experiment performed. For each condition, transcript levels were normalised to the housekeeping gene HPRT to account for variations in total RNA between samples i.e. mRNA for gene of interest (GOI) = 2^ [C_T (HPRT) – C_T (GOI)]. The fold-difference of the GOI transcript levels in stimulated conditions compared to the unstimulated negative control was subsequently determined using the following formula: Fold change of GOI relative to unstimulated control = 2^ [ΔC_T (GOI_stimulated) – ΔC_T (GOI_unstimulated)] (Schmittgen et al., 2008).

2.11.1 Probes used for RT-qPCR

Target (human)	ID	Supplier

HPRT	Hs99999909_m1	Applied Biosystems
C3	Hs00163811_m1	Applied Biosystems
C5	Hs00156197_m1	Applied Biosystems
fB	Hs00156060_m1	Applied Biosystems
fD	Hs00157263_m1	Applied Biosystems
C3aR	Hs00377780_m1	Applied Biosystems
C5aR	Hs00383718_m1	Applied Biosystems
Beta2Microglobulin	Hs00984230_m1	Applied Biosystems

2.12 CONFOCAL MICROSCOPY

iNKT cells were fixed and permeabilised in 100 µl Fixation/Permeabilization solution (BD Cytofix/Cytoperm™ kit; 554714). Specifically, cells were fixed with 100 µl BD Cytofix in a 96 well u-bottom plate (Corning® Costar®; CLS3799) for 20 mins at 4°C. The plate was centrifuged at 1200 rpm for 5 mins and the supernatant was discarded. The cells were subsequently washed in 150 µl 1x Perm/Wash™ Buffer which had been diluted 1:10 in distilled water.

The cells were stained with primary unconjugated antibodies listed below (diluted in PBS with 10% FCS) for 20 mins at 4°C. The cells were then washed with 150 µl Perm/Wash™ Buffer (diluted 1:10 in distilled water). The cells were subsequently stained with fluorophore-conjugated secondary antibodies (listed below) for 20 mins at 4°C. The cells were washed once again in washed in 150 µl Perm/Wash™ Buffer (diluted 1:10 in distilled water).

The cells were resuspended in 10 µl PBS with 10% FCS and transferred to a frosted microscope slide (VWR; 631-1551) containing 10 µl VECTASHIELD with DAPI (Vector Laboratories; H-2000). Cover slips were placed in a 24-well plate, washed with 500 µl EtOH and subsequently coated with 500 µl 0.1 mg/ml Poly-D-lysine [Sigma; P6407]) for 30 mins at RT. After this time, the Poly-D-lysine was removed, and the cover slips were left to air dry for 1-2 h at RT. The cover slips were then carefully placed on top of the glass slide and left to set for

20 mins at RT in the dark. Finally, the cover slips were immobilised with clear nail varnish, which was left to dry at RT in the dark. The glass slides were kept at 4°C until acquisition.

Images were acquired on a Confocal Laser Scanning Microscope (Zeiss LSM 880) using the following objectives: Plan-Apochromat 63x/1.4 Oil DIC M27 and Plan-Apochromat 20x/0.8 M27 at the Wolfson Imaging Centre, Oxford. 10-13 μm Z-stack images of single cells were taken and are presented as either a selected individual single plane (of the Z-stack) or a maximum intensity projection (i.e. all planes of the Z-stack merged). Analysis was performed on ZEN 2.3 Imaging Software (Zeiss).

2.12.1 Antibodies used for Confocal Microscopy

Target (human)	**Clone**	**Supplier**	**Catalogue Number**	**Dilution Factor**
Primary				
C3a (Mouse IgG1)	2991	Abcam	ab11873	1:50
C5a (Mouse IgG1)	2952	Abcam	ab11878	1:50
C3aR (Mouse IgG2a, k)	hC3aRZ8	Biolegend	345802	1:50
C5aR (Mouse IgG2a, k)	S5/1	Biolegend	344302	1:50
EEA-1 (Rabbit polyclonal IgG)	-	Santa Cruz	sc-33585	1:50
LAMP-1 (Rabbit polyclonal IgG)	-	Abcam	ab24170	1:100
Secondary				
Alexa Fluor 488 (goat anti-mouse, polyclonal)	Polyclonal	Invitrogen	A11001	1:500
Alexa Fluor 568 (goat anti-rabbit, polyclonal)	Polyclonal	Invitrogen	A11036	1:500

2.13 Assessment of Co-Localisation

To assess potential co-localisation between the protein marker of interest and the intracellular compartment of interest, a macro which leveraged Manders Overlap Coefficient (MOC) was developed by Dominic Waithe (Wolfson Imaging Centre, Oxford). The macro was imported into ImageJ (Fiji) and a brief overview of its user functionality is described below:

- One cell was highlighted; two colour channels corresponding to the marker of interest and the intracellular compartment of interest were chosen.

- Analysis was performed for each individual plane of the Z-stack; referred to as a ‘slice’ in the macro.
- A co-localisation co-efficient (for the Z-stack; average for all individual planes) between 0 and 1 was calculated for each cell, whereby 0 suggests no co-localisation and 1 indicates complete co-localisation. This value was multiplied by 100 and plotted as a percentage.

2.14 WESTERN BLOT

Halt™ Protease Inhibitor Cocktail (100X) (Thermo Scientific™; 78430) which consists of six different protease inhibitors at various concentrations was diluted into RIPA buffer (Thermo Scientific™; 89900) at 20 µl/ml and kept on ice.

Samples (cell lysate or purified protein) were collected by centrifugation at 2500 × g for 5 minutes in an eppendorff tube. The cell culture supernatant was discarded, and the cells were washed twice in cold PBS. 1 ml of ice cold RIPA buffer (supplemented with protease inhibitor) was then added to a pellet of up to 5×10^6 cells and left on ice for 15 min. The eppendorff tubes were centrifuged at ∼14,000 × g for 15 min to pellet the cell debris. The supernatant was transferred to a new tube for further analysis.

Protein concentration in the lysates was quantified using a Pierce™ BCA Protein Assay Kit (Thermo Scientific™; 23227), according to the manufacturer’s instructions. Specifically:

- 25 µl of each standard (albumin) or sample of interest were diluted in ice cold RIPA buffer (supplemented with protease inhibitor) and dispensed into a microplate well (working range = 20 to 2000 µg/ml).
- BCA working reagent (WR) was prepared by mixing 50 parts of BCA Reagent A with 1 part of BCA Reagent B.
- 200 µL of the WR was added to each well and the plate was incubated at 37°C for 30 min.

- The plate was cooled at RT and the absorbance was measured at 562 nm on a spectrophotometric plate reader.
- The absorbance measurement of the 'Blank' well was subtracted from all other 'sample' and 'standard' wells. A standard curve was prepared within the adjoining programme of the spectrophotometric plate reader. Finally, the standard curve was used to determine the protein concentration of each unknown sample (provided in µg/ml). These values were exported and saved into a Microsoft Excel spreadsheet.

The lysates (and/ or purified protein) were combined with the loading buffer (NuPAGE™ LDS Sample Buffer (4X) [NP0007] or Novex™ Tricine SDS Sample Buffer (1X; diluted from 2X in distilled water) [LC1676]; Invitrogen™) with or without 10X Bolt™ Sample Reducing Agent which contained 500 mM dithiothreitol (DTT) (Invitrogen™, B0009). The samples were heated at 95°C for 5 min and then allowed to cool at RT. Finally, the samples were loaded onto one of the following pre-cast gels:

- NuPAGE™ 4 to 12%, Bis-Tris, 1.0 mm, 12-well (Invitrogen™, NP0322BOX)
- Novex™ 10 to 20%, Tricine, 1.0 mm, 10-well (Invitrogen™, EC6625BOX),

and subsequently run by electrophoresis in either NuPAGE™ MES SDS Running Buffer (1X; diluted from 20X in distilled water) [Invitrogen™; NP0002], NuPAGE™ MOPS SDS Running Buffer (1X; diluted from 20X in distilled water) [Invitrogen™; NP0001] or Novex™ Tricine SDS Running Buffer (10X) [Invitrogen™; LC1675].

The gels were transferred onto nitrocellulose membranes (PB7320; Invitrogen™) for 7 minutes using the iBlot 2 dry transfer machine (Invitrogen™). The membranes were blocked with 20 µl Odyssey® (TBS) Blocking Buffer (Li-Cor; 927-50000) or Intercept® (TBS) Blocking Buffer (Li-Cor; 927-60001) for 1 h at RT (with shaking). The membranes were subsequently washed ten times in PBS/ 0.05% Tween-20 and stained with 20 µl of the primary antibody

(diluted in blocking buffer; described further in Section 2.14.1) overnight at 4°C (with shaking). The membranes were manually washed by shaking ten times in 20 ml PBS/ 0.05% Tween-20 and stained with 20 µl of the secondary antibody (diluted in PBS/ 0.05% Tween-20; described further in Section 2.14.2) for 1 h at RT (with shaking). Images were acquired on either the FujiFilm LAS-3000 (chemiluminescence) or Li-Cor BioSciences Odyssey CLx (fluorescence) machines.

2.14.1 Primary Antibodies for Western Blot

Target (human)	Clone	Supplier	Catalogue Number	Final concentration
Mouse anti-GAPDH	6C5	Abcam	ab8245	0.2 µg/ml (1:10,000)
Rabbit anti-C3a (antiserum)	Antiserum	Comptech	A218	8 µg/ml (1:5000)
Mouse FB blocking antibody 1	Confidential GSK asset	In-house	n/a	0.95 µg/ml (1:10,000)
Mouse FB blocking antibody 2	Confidential GSK asset	In-house	n/a	0.95 µg/ml (1:5526)

2.14.2 Secondary Antibodies for Western Blot

Target (various)	Clone	Supplier	Catalogue Number	Final concentration
Goat anti-Mouse IgG, HRP	Polyclonal	ThermoFisher	62-6520	0.75 µg/ml (1:2000)
Sheep anti-rabbit IgG, HRP	Polyclonal	Life Technologies	A16172	1 µg/ml (1:1000)
IR-Dye 680RD Donkey anti-Mouse IgG Secondary Antibody	Polyclonal	Li-Cor	926-68072	0.1 µg/ml (1:10,000)
IR-Dye 800W Donkey anti-Rabbit IgG Secondary Antibody	Polyclonal	Li-Cor	926-32213	0.1 µg/ml (1:10,000)

2.15 CELL-FREE ASSAY (SILVER STAIN)

C3b purified from NHS (500 ng/ml; diluted in APB) and Bb (250 ng/ml; diluted in APB) [Complement Technologies; A114] were combined in an eppendorff tube (100 µl total reaction volume) and heated at 21°C for 5 minutes ('Reaction 1'). During this time, purified C3 (2500 ng/ml; diluted in PBS), fB (135 ng/ml; diluted in PBS) and fD (5 ng/ml; diluted in PBS) [Complement Technologies] were combined in an eppendorff tube (300 µl reaction volume i.e. 'Reaction 2') at RT to seed the pro-C3 convertase.

Reaction 1 (4 µl) was mixed with Reaction 2 (36 µl) in an eppendorff tube i.e. at a ratio of 1:9 (v/v) in the presence of 10 µM FB Inhibitor 1, DMSO or 10 mM EDTA and heated at 21°C for either 30 or 60 minutes. The samples were subsequently run through a 3 kDa cut-off Ultra-0.5 Centrifugal Filter Unit (Amicon) and proteins below this molecular weight were discarded. The concentrated samples (24 µl) were diluted at a ratio of 3:4 (v/v) in 8 µl NuPAGE™ LDS Sample Buffer (4X) (Invitrogen™, NP0007) and heated at 95°C for 5 minutes before being allowed to cool at RT. 25 µl of each sample was run on a NuPAGE™ 4 to 12%, Bis-Tris, 1.0 mm, 12-well gel (Invitrogen™, NP0322BOX) by electrophoresis in 1X MES Buffer at 200V.

The gel was visualised using the SilverXpress™ Silver Staining Kit (LC6100; Invitrogen™), according to the manufacturer's instructions. Specifically:

- Fixation: 90 ml Ultra-Pure Water was combined with 100 ml Methanol and 20 ml Acetic Acid (20 ml) and subsequently added to the gel for 10 min, before being discarded.
- Sensitisation: 105 ml Ultra-Pure Water was combined with 100 ml Methanol and 5ml Sensitiser 100 ml and subsequently added to the gel for 30 min, before being discarded. This step was then repeated for a second time.
- Wash: 200 ml Ultra-Pure Water was added to the gel for 10 min and then discarded. This step was then repeated for a second time.

- Staining: 5ml Stainer A (5 ml) was combined with 5 ml Stainer B and 90 ml Ultra-Pure Water and added to the gel for 15 min, before being discarded.
- Wash: 200 ml Ultra-Pure Water was added to the gel for 10 min and then discarded. This step was then repeated for a second time.
- Development: 5 ml Developer was combined with 95 ml Ultra-Pure Water and added to the gel for up to 15 min, before being discarded.
- Stop: 5 ml Stopper was then added to the gel for 10 min before being discarded.
- Wash: 200 ml Ultra-Pure Water was added to the gel for 10 min and then discarded. This step was then repeated a further two times.

2.16 CRISPR/CAS 9

2.16.1 Transfection Protocol

Guide RNA i.e. crRNA sequences were designed using Synthego CRISPR design tool (https://design.synthego.com/#/) and validated on ApE (A plasmid Editor) which is a proprietary sequence editor developed by Wayne Davis from the University of Utah. More specifically, the original gene (nucleotide) sequence was found using ENSEMBL Genome Browser (https://www.ensembl.org/index.html) in which the exons are shown in orange whilst the introns in between were not highlighted. The nucleotide sequence was exported from ENSEMBL into ApE, in which the guide RNA sequences (or their respective reverse complement strands) were localised to one exon of the nucleotide sequence. To further confirm guide RNA specificity, the protospacer adjacent motif (PAM) i.e. 'NGG' motif' specific for *S. pyogenes* Cas9 which must be located downstream of the ~20 nucleotide target sequence was confirmed on ApE. The pooled crRNA sequences were purchased from IDTand are listed below. Together with Alt-R® CRISPR-Cas9 tracrRNA [20 nmol] (IDT; 1072533). they were hybridised in Nuclease Free Duplex Buffer (IDT; 11-05-01-12) at a ratio of 1:1 v/v to form

guide RNA (gRNA) at a final concentration of 50 µM by heating at 95°C for 5 min, followed by cooling at 4°C for 10 min. Guide RNA was mixed with recombinant *Alt-R® S. pyogenes* Cas9 nuclease V3 (IDT; 1081058) at a ratio of 1:1 v/v to form ribonucleoprotein (RNP). 15 µl RNP was directly added to 20 µl wild-type THP-1 cells pre-diluted in P3 Primary Cell Nucleofector™ Solution (component of the P3 Primary Cell 4D-NucleofectorTM X Kit [Lonza; V4XP-3032]). 20 µl of the total 35 µl volume was transferred to a 16-well Nucleocuvette™ cassette (also a component of the P3 Primary Cell 4D-Nucleofector™ X Kit [Lonza; V4XP-3032]) and the cells underwent electroporation in the Amaxa 4D Nucleofector™ Core Unit (Lonza; AAF-1002B) using the pulse codes DP-148 or EH-115. The following pulse codes were chosen, based on the manufacturer's recommendations for efficient transfection of THP-1 and $CD4^+$ T cells, respectively. The cells were harvested post-transfection from the cassette and transferred to a pre-warmed 12-well plate (CoStar) containing 1 ml pre-warmed complete medium (CM) and maintained at 37°C/ 5% CO_2.

2.16.2 Guide RNA (gRNA) Sequences

crRNA ID	Sequence	Supplier
β2M	**GCAGAGAATGGAAAGTCAAA**	IDT
β2M	**TCCGACATTGAAGTTGACTT**	IDT
β2M	**CCACTGAAAAAGATGAGTAT**	IDT
C3_exon 2	**GGAGGCCCACGACGCGCAAG**	IDT
C3_exon 13	**GCGTGTAGTACGCCACCAGG**	IDT
C3_exon 10	**GGTAGGGAGAGGTCACGATG**	IDT
Factor B	**GACCACCACTCCATGGTCTT**	IDT
Factor B	**GGCCCCAGGGATCCTGCTCT**	IDT

2.16.3 Assessment of gene and protein expression post-CRISPR

After a minimum of 5 days post-nucleofection, cells were removed from the incubator and viability was assessed using Vi-Cell Automated Cell Counter (Beckman). More specifically, cells from each nucleofection condition were stained using trypan blue and the percentage of live cells was determined by the Vi-Cell. If viability was determined to be below ~50%, then

the cells were discarded. THP-1 protein marker expression was assessed by flow cytometry (as previously described in Section 2.6) and THP-1 gene expression profiles were assessed by RT-qPCR (as previously described in Section 2.11).

2.17 Statistical Data Analysis (Implementation Strategy)

2.17.1 Assessment of normality

Assessment of normality was performed in Prism software (GraphPad) as follows, to determine if data points in each sub-group of an experiment follow a Gaussian (normal) distribution:

a. Normality was tested (by default) using 4 different tests: Anderson-Darling, D'Agostino Pearson, Shapiro-Wilk and Kolmogorov-Smirnov.
b. Normality testing was performed on all the values in each sub-column (condition) e.g. Unstimulated, Stimulated with Ligand X, Stimulated with Ligand Y etc.
c. In accordance with published work, the significance level (alpha) was set at 0.05.
d. Normality testing was only performed if the data points of each sub-column met the required criteria i.e.
    i. Kolmogorov-Smirnov test required 5 or more data points per sub-column i.e. condition.
    ii. Shapiro-Wilk test required 3 or more data points per sub-column i.e. condition.
    iii. D'Agostino Pearson and Anderson-Darling tests required 8 or more data points per sub-column i.e. condition.
e. If the abovementioned criteria are met for one test e.g. Shapiro-Wilk but not others, then decision regarding normality is based solely on one test (rather than all 4).
f. Prism calculated a P-value for each sub-column. If $P>0.05$, normality was assumed for each condition within the total experiment. If $P<0.05$, the assumption of normality was not met so non-parametric testing (see below) will be undertaken.

2.17.2 Statistical analysis (on normally distributed data):

Statistical analysis was performed using Prism software (GraphPad). As the type of statistical test used is dependent on the type of experiment performed, specific details regarding the type of test along with post-hoc analysis is described in detail in each figure legend. In brief, Student's t-test (paired or unpaired) was used when assessing two treatment groups. One- or Two-way analysis of variance (ANOVA) along with a post-hoc multiple comparisons test (recommended by Prism) was used when assessing statistical significance between three or more treatment groups. A result was considered statistically significant (i.e. the null hypothesis was rejected) if *$p < 0.05$, **$p < 0.01$, ***$p < 0.001$ or ****$p < 0.0001$.

2.17.3 Statistical analysis (on data which was NOT normally distributed):

A non-parametric Kruskal-Wallis was also performed in Prism software (GraphPad). Prism first ranked all the values from low to high, where the smallest number was given a rank of one and the largest number was given a rank of N, where N is the total number of values. This was followed by Dunn's multiple comparison's test which compared the difference in the sum of ranks. Once again, a result was considered statistically significant (i.e. the null hypothesis was rejected) if *$p < 0.05$, **$p < 0.01$, ***$p < 0.001$ or ****$p < 0.0001$.

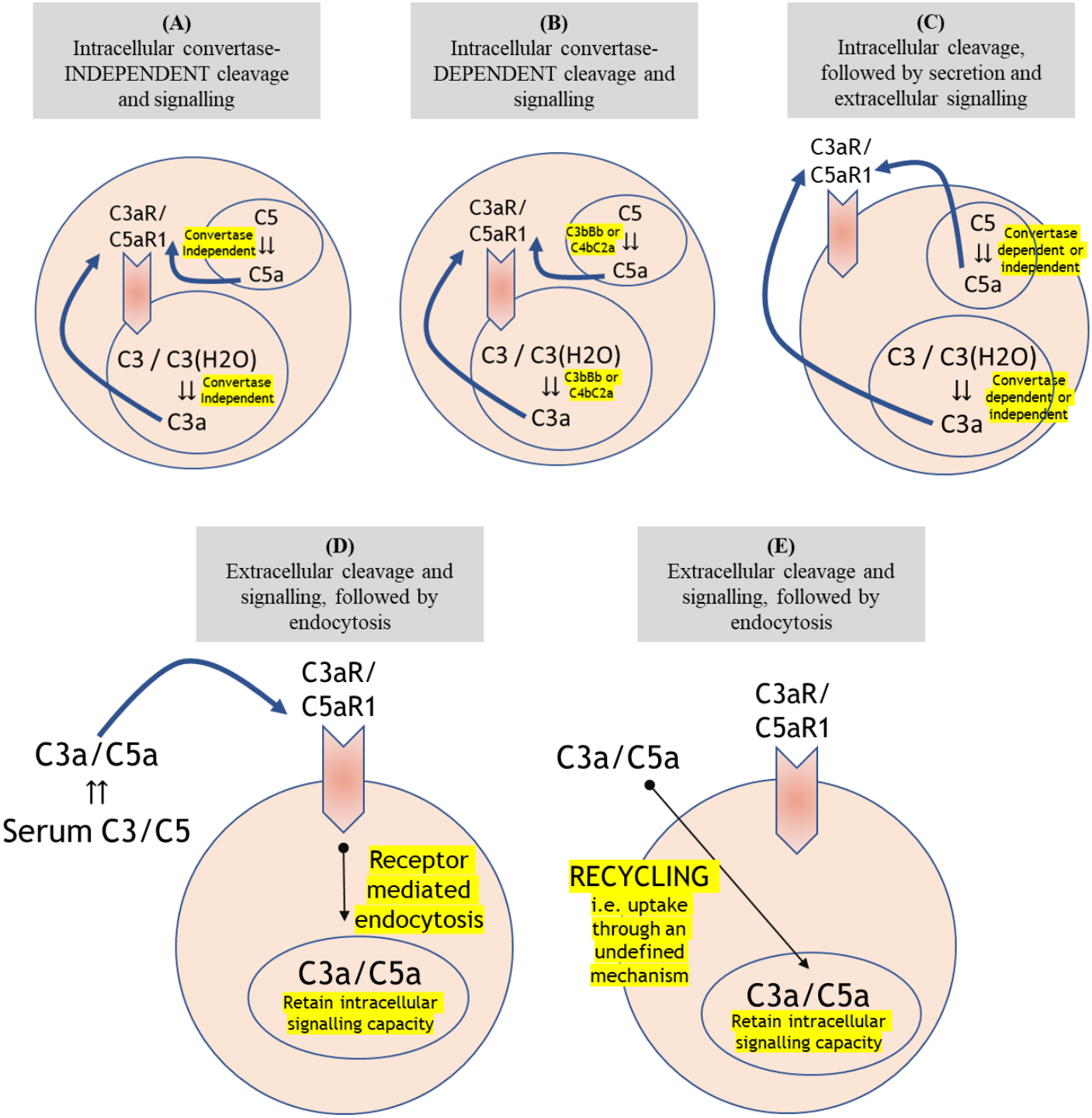
3 CHARACTERISATION OF iNKT CELL AND DENDRITIC CELL COMPLEMENT EXPRESSION PROFILES

In conventional α/β T cells, C3 and C5 have been shown to be cleaved intracellularly to generate the anaphylatoxins C3a and C5a (Liszewski et al., 2013; Arbore et al., 2016). The generation of anaphylatoxins has been shown to positively correlate with and modulate T cell responses e.g. T_H1 effector function, specifically through cognate interactions with their respective receptors C3aR and C5aR1/2 (Liszewski et al., 2013; Arbore et al., 2016). It should also be noted that co-stimulation of anti-CD46 in combination with TCR engagement plays a crucial role in anaphylatoxin receptor engagement and hence the modulation of T cell effector function (Liszewski et al., 2013; Arbore et al., 2016).

Notably, intracellular 'stores' of C3a and C5a have also been detected at steady state suggesting a mechanism of intracellular cleavage (Liszewski et al., 2013; Arbore et al., 2016). Furthermore, ligand-receptor interactions were observed at the level of the plasma membrane but also intracellularly (Liszewski et al., 2013; Arbore et al., 2016). Moreover, Fusakio et al. demonstrated high levels of C5aR1 on murine iNKT cells upon *E. coli*-induced sepsis induction which once again positively correlated with modulation of T_H1 effector responses – potentially through cognate ligand-receptor interaction with C5a, although this was not addressed (Fusakio et al., 2011).

The complex interplay of cleavage events along with autocrine/ paracrine ligand-receptor interactions is unknown and may function under multiple mutually inclusive guises, such as the following:

a. C3a/C5a are generated inside of the cell through a convertase-independent mechanism e.g. via Cathepsin L and remain exclusively intracellular, where they bind and activate their intracellular receptors.
b. C3a/C5a are generated inside of the cell through a convertase-dependent mechanism i.e. through C3bBb or C4bC2a and remain exclusively intracellular (postulated by West et al., 2018), where they bind and activate their intracellular receptors.
c. C3a/C5a are generated inside of the cell and are secreted into the extracellular space where they bind and activate their cognate receptors at the level of the plasma membrane in an autocrine manner.
d. C3a/C5a are generated outside of the cell and enter the cell, following cognate-ligand receptor interactions at the level of the plasma membrane e.g. via endocytosis. Upon entry, they bind to and activate their cognate receptors located intracellularly.
e. C3a/C5a are generated outside of the cell and enter the cell, independent of their cognate plasma-membrane bound receptors. Upon entry, they bind to and activate their cognate receptors located intracellularly **(see schematic on next page**).



Schematic showing the potential mechanisms by which a cell may generate intracellular C3a and C5a, or take up C3a and C5a from the extracellular space.

Knowledge of the modulation of human iNKT cell function by complement, specifically anaphylatoxin generation and cognate ligand receptor engagement is lacking. Therefore, through the optimisation of multiple assays and readouts, anaphylatoxin receptor signalling in either an autocrine or paracrine manner will be assessed, which may potentially be exploited (e.g. pharmacologically) to modulate effector function. Specifically:

1) The expression of key complement proteins, including anaphylatoxins and their cognate receptors will be assessed in multiple iNKT cell donors at steady state and upon activation.
2) Different culture and activation conditions will be leveraged to further understand the 'source' of complement e.g. *de novo* versus recycled from the extracellular milieu.
3) The modulation of cellular effector function by anaphylatoxins and potential crosstalk with T-cell receptor mediated responses and the CD40-CD40L axis will be assessed.
4) Paracrine signalling mechanisms i.e. anaphylatoxins secreted from neighbouring antigen-presenting cells will be investigated

3.1 SURFACE ANAPHYLATOXIN RECEPTOR EXPRESSION IN iNKT CELLS

Fusakio et al., (2011) previously observed up-regulation of cell surface C5aR1 on murine iNKT cells post-sepsis induction, by flow cytometry. Given this observation was seen *in vivo* following intraperitoneal administration of *E.coli* bacteria, I investigated whether human iNKT cells also expressed C5aR1, along with C3aR.

Currently, the only commercially available antibodies which recognise human C3aR and C5aR1 are derived from the hybridomas *C3aRZ8* and *S5/1*, respectively. These antibodies have previously been used by to assess anaphylatoxin receptor expression by Kemper and colleagues (Liszewski et al., 2013). C5aR2 expression was not assessed as part of this project, given its role in the modulation of cellular effector function remains controversial. More specifically, as C5aR2 lacks G-protein coupling motifs, it was initially considered to have immune-suppressing functions through sequestering C5a and being internalised by β-arrestin, thus preventing C5aR1 signalling (Li et al., 2019). However, additional reports have shown that C5aR2 can crosstalk with TLR4 and is thus implicated in immune-activating functions (Li et al., 2019). In summary, as C3aR/C5aR1 have shown overlapping and potentially synergistic activity in the modulation of $CD4^+$ T cell responses i.e. promotion of IFN-γ secretion (Strainic et al., 2008, Strainic et al., 2013), they will be the main focus of this project.

To assess the reactivity of these antibodies, unstimulated PBMC populations were initially phenotyped for anaphylatoxin receptor expression. As indicated in **Figure 3-1**, only a $CD3^-$ $CD14^+$ myeloid population (most likely monocytes and potentially macrophages) showed steady state expression of both receptors (red histograms) and thus served as a positive control for future experiments. Both CD3+CD4+ and CD3+CD4- T cell populations along with the CD3-CD14- population showed no expression of either receptor at steady state, when compared to the negative FMO controls (grey filled histograms). This finding was consistent with previously published data in conventional α/β T cells by Liszewski et al. 2013 and Arbore

et al. 2016. As both antibodies showed strong reactivity in the context of the myeloid cell population, the same antibodies were used to assess human iNKT cell anaphylatoxin receptor expression.

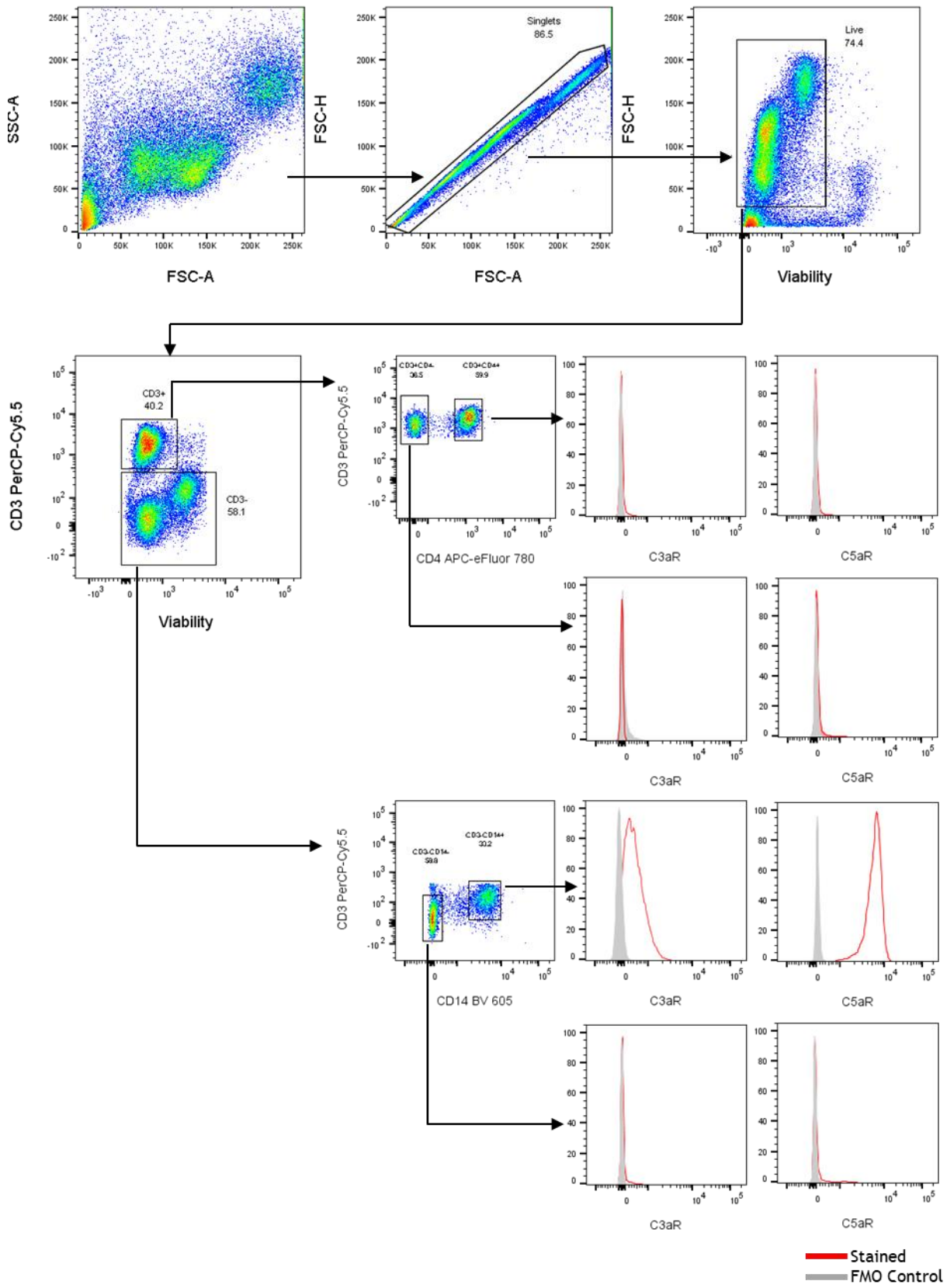


Figure 3-1 Assessment of surface anaphylatoxin receptor expression by flow cytometry
Assessment of antibody clone specificity for the anaphylatoxin receptors C3aR and C5aR1. PBMCs were isolated from whole blood and stained with the anti-C3aR antibody (Clone C3aRZ8) and the anti-C5aR1 antibody (Clone S5/1). Different cell types were gated on and surface anaphylatoxin expression was compared to the relevant FMO control. CD3-CD14+ cells were the only cell type which expressed surface C3aR and C5aR1 when compared to the negative control, as observed by the histograms. FMO: fluorescence minus one.

As described in Methods (Section 2.4), iNKT cells were FACS sorted from PBMCs using biotinylated CD1d-α-GalCer tetramers, expanded *in vitro* using PHA and irradiated allogeneic PBMCs and subsequently kept in long-term culture in IMDM + 5% Human Serum. **Figure 3-2A** shows the gating strategy used to identify $CD3^{+}CD4^{+}$CD1d tetramer^{+} iNKT cells.

Invariant NKT cells were subsequently stimulated overnight using THP-1 cells as APCs pulsed with their canonical ligand α-GalCer, to ensure there was sufficient time for activation and mobilisation of a quantifiable effector response. Moreover, stimulation was performed in two different culture media: complete medium i.e. RPMI plus 10% FCS or serum-free medium, with the purpose of assessing if proteins present in RPMI with heat-inactivated FCS modulate effector function when compared to SFM conditions.

As demonstrated in **Figure 3-2B**, viability as determined by the percentage of cells in the 'FSC-A, Live' gate relative to the total cells acquired was also confirmed to be above ~60% for all tested donors. There was a slight reduction in cell viability upon activation, but this was expected given the cytolytic activity of iNKT cells and hence death of neighbouring antigen-presenting cells.

Representative histograms of one experiment are shown in **Figure 3-2C**. iNKT cells up-regulated cell surface expression of the activation marker CD25, with increasing concentrations of α-GalCer (1-30 ng/ml), relative to the non-stimulated and the unpulsed (i.e. THP1 cells present, but absence of ligand) negative controls (**Figure 3-2C**, first histogram plot). A similar expression profile was also observed for the activation marker CD69 (**Figure 3-2C**, second histogram plot), but the extent of up-regulation was less conspicuous than CD25. Up-regulation in C3aR and C5aR1 were also observed (**Figure 3-2C**, third and fourth histogram plots). Notably, C3aR but not C5aR1 surface expression was observed at steady state i.e. in resting cells.

Subsequent analysis of the surface expression of CD25, CD69, C3aR and C5aR1 in each tested donor activated in either CM or SFM is shown in **Figure 3-2D** and **Figure 3-2E**, respectively. Surface expression was determined using the Mean Fluorescent Intensity (MFI) of each antibody-conjugated fluorophore used to stain the respective cell surface marker of interest (as described in Methods section 2.6.4). As these experiments were performed on different days and using different flow cytometers, the MFI values varied significantly between experiments, thus making it challenging to combine the results and perform a statistical test. Therefore, each donor is shown individually.

As shown in **Figure 3-2D**, stimulation with α-GalCer (10 and 30 ng/ml) in complete medium positively correlated with increased surface expression of CD25 and CD69 in both tested donors. Moreover, surface expression of C3aR and C5aR1 was also increased in both tested donors (**Figure 3-2D** (i) and (ii)). It should also be noted that C3aR surface expression was observed at steady state i.e. in resting cells, but C5aR1 was not. Furthermore, fold change increases in both C3aR and C5aR1 surface expression upon activation (relative to the unpulsed negative control) were observed in both donors but were greater in Donor 1. This in turn correlated with higher levels of CD25 and CD69 fold change increases in Donor 1 (**Figure 3-2D** (iii)).

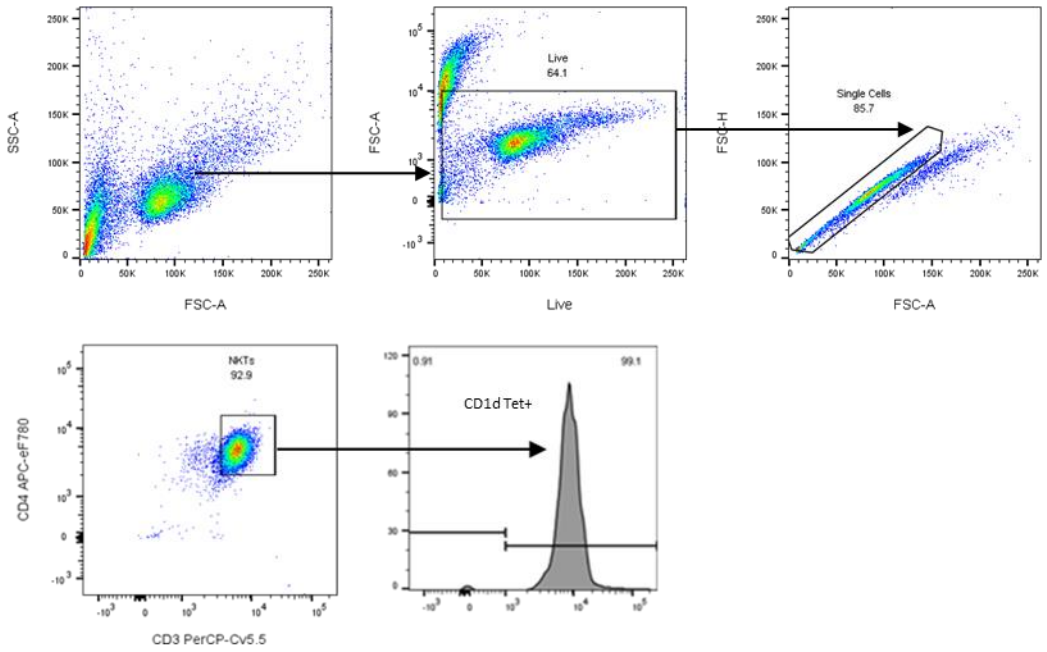
Subsequent analysis of iNKT cells activated with α-GalCer in SFM is shown in **Figure 3-2E**. As previously observed in complete medium, all tested iNKT cell donors up-regulated CD25 and CD69 surface expression upon stimulation with α-GalCer (1, 3, 10 and 30 ng/ml). However, except for iNKT cell donor 3 (**Figure 3-2E** (iii)), all tested donors failed to show noticeable changes in surface expression of both C3aR and C5aR1 when activated with α-GalCer in SFM (Figure **Figure 3-2E** (i), (ii) and (iv)). Moreover, there was a fold change increase in both C3aR and C5aR1 surface expression in all tested donors upon activation

(relative to the unpulsed negative control) (**Figure 3-2E** (v)). However, statistical significance was only achieved at certain concentration of α-GalCer.

In conclusion, all iNKT cell donors were sufficiently activated by α-GalCer as demonstrated by up-regulation of the activation markers CD25 and CD69. However, modulation of anaphylatoxin receptor expression seems to be heavily influenced by the medium in which the cells were activated. More specifically, when cells were activated in complete medium, a greater level of up-regulation was observed when compared to cells activated in SFM. Moreover, cell viability specifically at steady state was also greater in complete medium. In turn, increased cell viability may positively correlate with increased surface receptor expression. However, the loss of an external complement source in SFM may also correlate with and potentially promote anaphylatoxin receptor down-regulation at steady state and during activation. This hypothesis can be further tested using commercially available media or more specifically sera which are deficient in only a single complement protein such C3 or C5 (Kremlitzka et al., 2019).

As iNKT cells showed steady state surface expression of C3aR, but not C5aR1 with potential up-regulation in certain donors upon activation – I speculated that these cells may also express anaphylatoxin receptors in intracellular compartments with the potential to translocate to the cell surface as previously observed in $CD4^+$ T cells (Liszewski et al., 2013; Arbore et al., 2016). This hypothesis will be explored next.

A

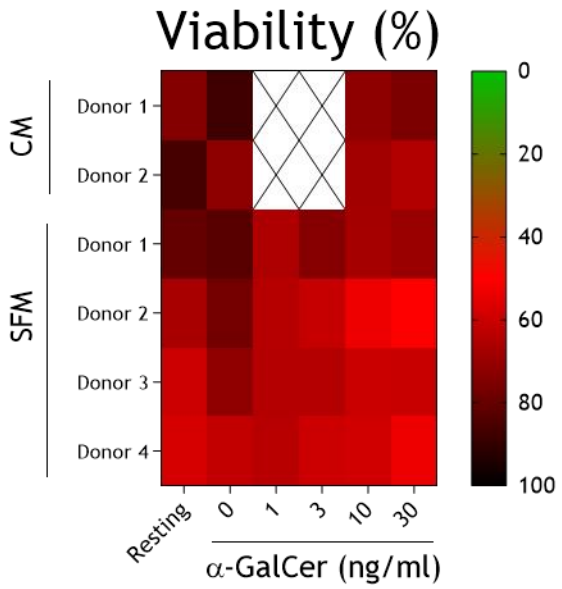


B

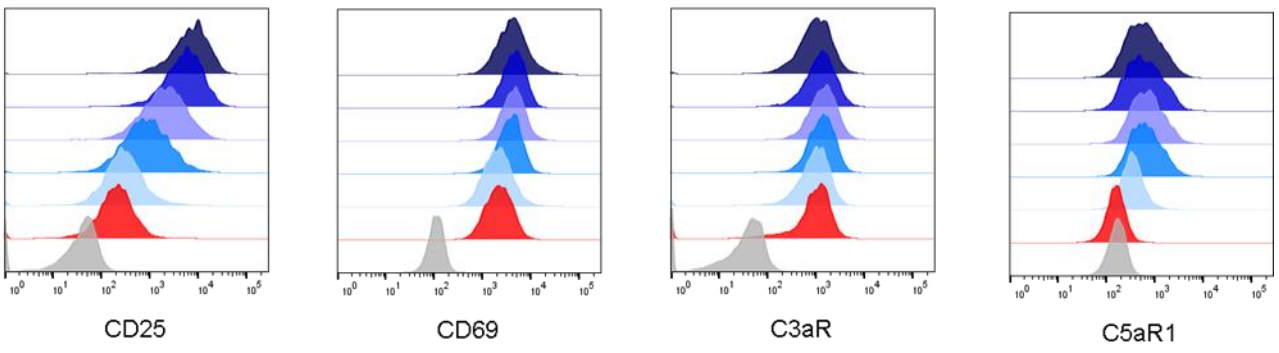
iNKT Donor ID	Complete Medium (CM)	Serum Free Medium (SFM)
D1	plus THP* *(15 Feb 2017)*	plus THP *(17 Oct 2017)*
D2	plus THP* *(22 Feb 2017)*	plus THP *(30 Oct 2017)*
D3	not tested	plus THP *(09 Nov 2017)*
D4	not tested	plus THP *(16 Nov 2017)*

*1 and 3 ng/ml α-GalCer concentrations not tested in these experiments

+ THP-1



C



30ng/mL α-GC
10ng/mL α-GC
3ng/mL α-GC
1ng/mL α-GC
Unpulsed
Resting
Unstained

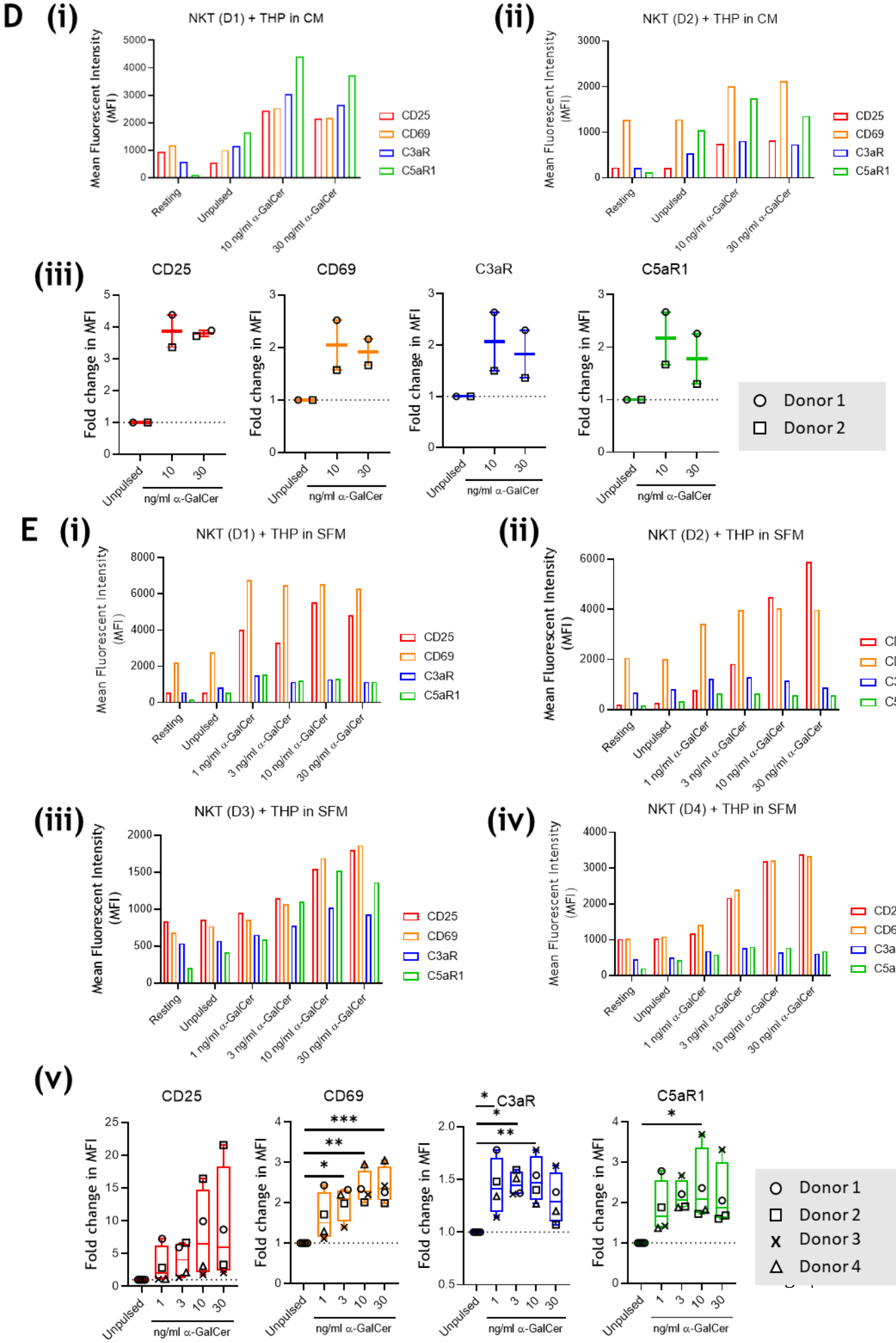

D
(i)
NKT (D1) + THP in CM
Mean Fluorescent Intensity (MFI)
5000
4000
3000
2000
1000
0
Resting
Unpulsed
10 ng/ml α-GalCer
30 ng/ml α-GalCer
CD25
CD69
C3aR
C5aR1
(ii)
NKT (D2) + THP in CM
Mean Fluorescent Intensity (MFI)
3000
2000
1000
0
Resting
Unpulsed
10 ng/ml α-GalCer
30 ng/ml α-GalCer
CD25
CD69
C3aR
C5aR1
(iii)
CD25
CD69
C3aR
C5aR1
Fold change in MFI
Unpulsed
10
30
ng/ml α-GalCer
Donor 1
Donor 2
E
(i)
NKT (D1) + THP in SFM
Mean Fluorescent Intensity (MFI)
8000
6000
4000
2000
0
Resting
Unpulsed
1 ng/ml α-GalCer
3 ng/ml α-GalCer
10 ng/ml α-GalCer
30 ng/ml α-GalCer
CD25
CD69
C3aR
C5aR1
(ii)
NKT (D2) + THP in SFM
Mean Fluorescent Intensity (MFI)
6000
4000
2000
0
Resting
Unpulsed
1 ng/ml α-GalCer
3 ng/ml α-GalCer
10 ng/ml α-GalCer
30 ng/ml α-GalCer
CD25
CD69
C3aR
C5aR1
(iii)
NKT (D3) + THP in SFM
Mean Fluorescent Intensity (MFI)
2000
1500
1000
500
0
Resting
Unpulsed
1 ng/ml α-GalCer
3 ng/ml α-GalCer
10 ng/ml α-GalCer
30 ng/ml α-GalCer
CD25
CD69
C3aR
C5aR1
(iv)
NKT (D4) + THP in SFM
Mean Fluorescent Intensity (MFI)
4000
3000
2000
1000
0
Resting
Unpulsed
1 ng/ml α-GalCer
3 ng/ml α-GalCer
10 ng/ml α-GalCer
30 ng/ml α-GalCer
CD25
CD69
C3aR
C5aR1
(v)
CD25
CD69
C3aR
C5aR1
Fold change in MFI
Unpulsed
1
3
10
30
ng/ml α-GalCer
Donor 1
Donor 2
Donor 3
Donor 4

Figure 3-2 Assessment of surface anaphylatoxin receptor expression by flow cytometry
(A) Gating strategy used to identify CD3+CD4+ CD1d tetramer positive iNKT cells.
(B) Left panel: Table showing the different experimental conditions in which multiple iNKT cell donors were assessed for C3aR/C5aR1 surface expression at steady state and upon activation, and dates when experiments were performed. Right panel: Assessment of iNKT cell viability in each experiment i.e. % of cells in the 'FSC-H vs Live' gate vs total number of cells acquired. X on heatmap: condition not tested in that experiment.
(C) Representative histogram plots from a typical experiment in which iNKT cells were activated with increasing concentrations of α-GC (1-30 ng/ml) in the presence of THP-1 cells. Activation was confirmed by CD25 (plot #1) and CD69 (plot #2) up-regulation. C3aR (plot #3) and C5aR1 (plot #4) surface expression was also assessed.
(D) Assessment of changes in CD25, CD69, C3aR and C5aR1 surface expression in iNKT cells stimulated in CM. (i) Donor 1 and (ii) Donor 2. (iii) Calculation of fold change values i.e. MFI activation condition / MFI unpulsed condition, to normalise absolute MFI values which varied between experiments. The fold change values were then collated for each donor: Donor 1 (open circles) and Donor 2 (open squares). Statistical analysis could not be performed as n=2.
(E) Assessment of changes in CD25, CD69, C3aR and C5aR1 surface expression in iNKT cells stimulated in SFM. (i) Donor 1, (ii) Donor 2, (iii) Donor 3 and (iv) Donor 4. (v) Calculation of fold change values i.e. MFI activation condition / MFI unpulsed condition, to normalise absolute MFI values which varied between experiments. The fold change values were then collated for each donor: Donor 1 (open circles) and Donor 2 (open squares), Donor 3 (crosses), Donor 4 (open triangles). Statistical significance was calculated using one-way analysis of variance (ANOVA) followed by Dunnett's multiple comparisons test, where *$p<0.05$, **$p<0.01$, ***$p<0.001$ and ****$p<0.0001$
Mean Fluorescent Intensity (MFI) raw data values were calculated as described in the 'Materials & Methods' section.
FSC: forward scatter, SSC: side scatter, α-GC: alpha-galactosylceramide, CM: complete medium i.e. RPMI-1640 plus 10% FCS, SFM: serum-free medium.

3.2 iNKT Anaphylatoxin Receptors and their Cognate Ligands

Previous work from the Kemper laboratory has demonstrated that the anaphylatoxin receptors C3aR and C5aR1 are expressed in intracellular compartments, including endosomes in $CD4^+$ T cells (Liszewski et al., 2013; Arbore et al., 2016). As such, the intracellular presence of C3aR and C5aR1, along with their cognate ligands C3a and C5a was assessed by confocal microscopy. Specifically, iNKT cells were removed from their culture medium i.e. IMDM plus 5% Human Serum and were immediately fixed and permeabilised before being stained with primary unconjugated antibodies. The same antibodies used for flow cytometric assessment of the anaphylatoxin receptors were also used for microscopy. Moreover, the antibodies used to assess the anaphylatoxins (clone *2991* for C3a (Liszewski et al., 2013) and clone *2952* for C5a (Arbore et al., 2016)) recognised neo-epitopes which are exposed upon cleavage thus preventing cross-reactivity with native protein. This was followed by staining with fluorophore-conjugated secondary antibodies, transfer to a microscope slide containing DAPI and coverage with a poly-D-lysine coated cover slip.

As shown in **Figure 3-3**, iNKT cells (right panels) along with $CD4^+$ T cells were stained for the receptor or ligand of interest (shown in green) and the intracellular compartment of interest (shown in red). Co-localisation with the endosomal compartment (detected using an anti-EEA-1 antibody (Liszewski et al., 2013)) or the lysosomal compartment (detected using an anti-LAMP-1 antibody (Liszewski et al., 2013)) was subsequently assessed by Mander's algorithm and plotted as a percentage of total staining (left panels).

C3aR was localised to both intracellular compartments but was greater i.e., increased fluorescent staining in lysosomes (~60% in both cell types; **Figure 3-3B**) than endosomes (~40% in both cell types; **Figure 3-3A**). C5aR1 followed a similar trend (**Figure 3-3C** and **Figure 3-3D**). However, variability was observed between the two iNKT cell donors, with increased levels of anaphylatoxin receptor expression in Donor B relative to Donor A.

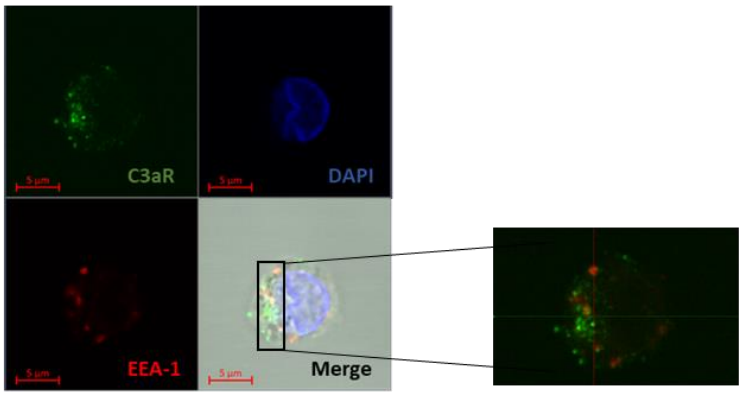
C3a was present in both compartments but was slightly greater i.e., increased fluorescent staining in lysosomes (~50% in both cell types; **Figure 3-3F**) than endosomes (~40% in both cell types; **Figure 3-3E**). C5a expression followed a similar trend, with particularly high expression in lysosomes (~70% for both cell types; **Figure 3-3H**) compared to endosomes (~40% for both cell types; **Figure 3-3G**). Intracellular C3a co-localisation and C5a co-localisation with the endosomal compartment was lower i.e., less fluorescent staining in iNKT cells relative to $CD4^+$ T cells. The reverse trend was observed for the co-localisation of anaphylatoxins with the lysosomal compartment.

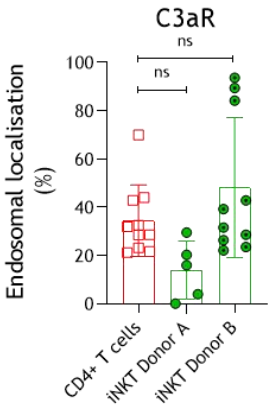
In conclusion, confocal microscopy was performed on iNKT cells to determine if the anaphylatoxin receptors C3aR and C5aR1 along with their cognate ligands C3a and C5a were expressed intracellularly. Increased localisation i.e., increased fluorescent staining was observed within the lysosomal compartment relative to the endosomal compartment for both the receptors and ligands in iNKT cells. Whilst this experiment has provided initial insight into iNKT complement expression at steady state, subsequent experiments are required to assess:

1) the effect of different culture conditions on steady state complement expression. In this experiment, cells had been cultured in IMDM + 5% Human Serum prior to analysis by microscopy. Thus, one may speculate that following culture in serum-free medium or FCS, intracellular complement expression profiles may change i.e. loss of an external human complement source i.e. Human Serum may promote a compensatory increase in *de novo* complement generation.
2) The effect of stimulation by α-GalCer on complement expression. As surface anaphylatoxin receptor expression was shown to be increased in activated cells (**Figure 3-2**) by flow cytometry – one may speculate that a similar response is observed intracellularly. Moreover, co-localisation assessment of each anaphylatoxin with its cognate receptor in an intracellular compartment (as previously performed by Liszewski et al., 2013 in activated

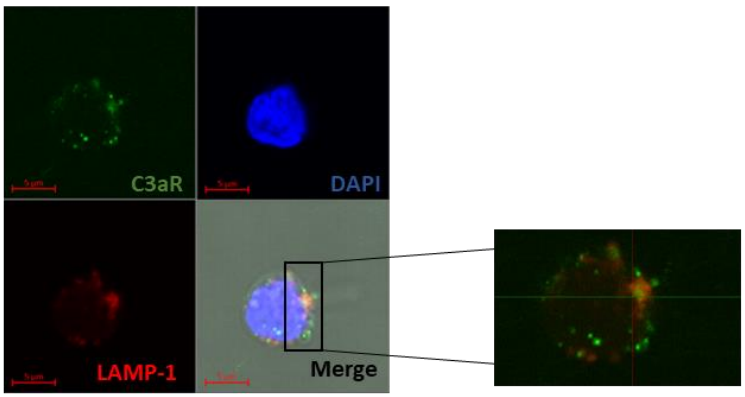
CD4+ T cells) may provide insight into potential intracellular anaphylatoxin signalling as postulated by the Kemper laboratory.

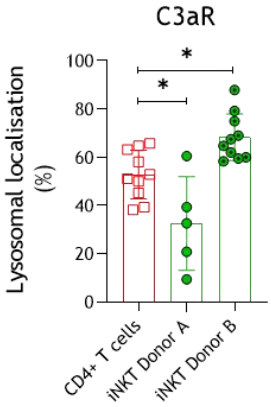
A **C3aR and EEA-1**



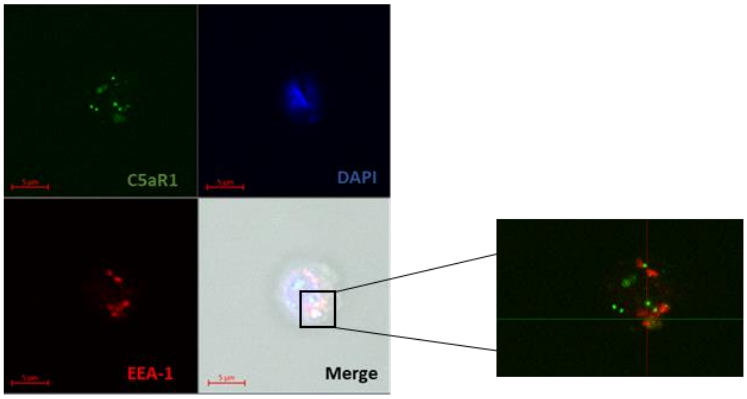


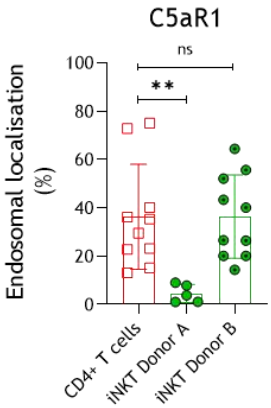
B **C3aR and LAMP-1**



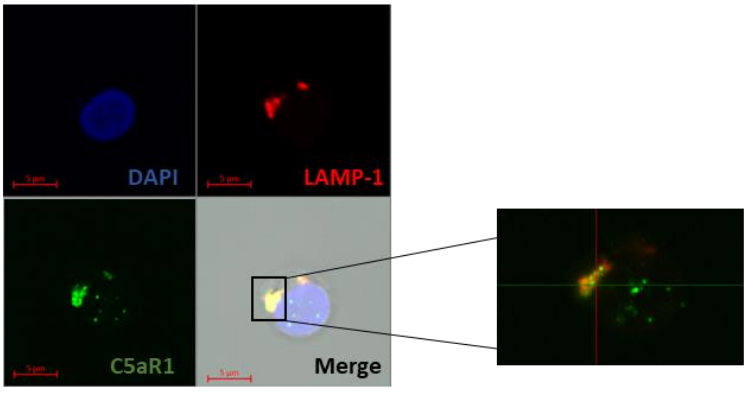


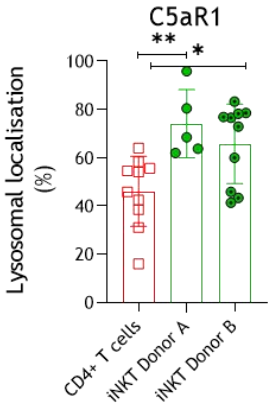
C **C5aR1 and EEA-1**





D **C5aR1 and LAMP-1**





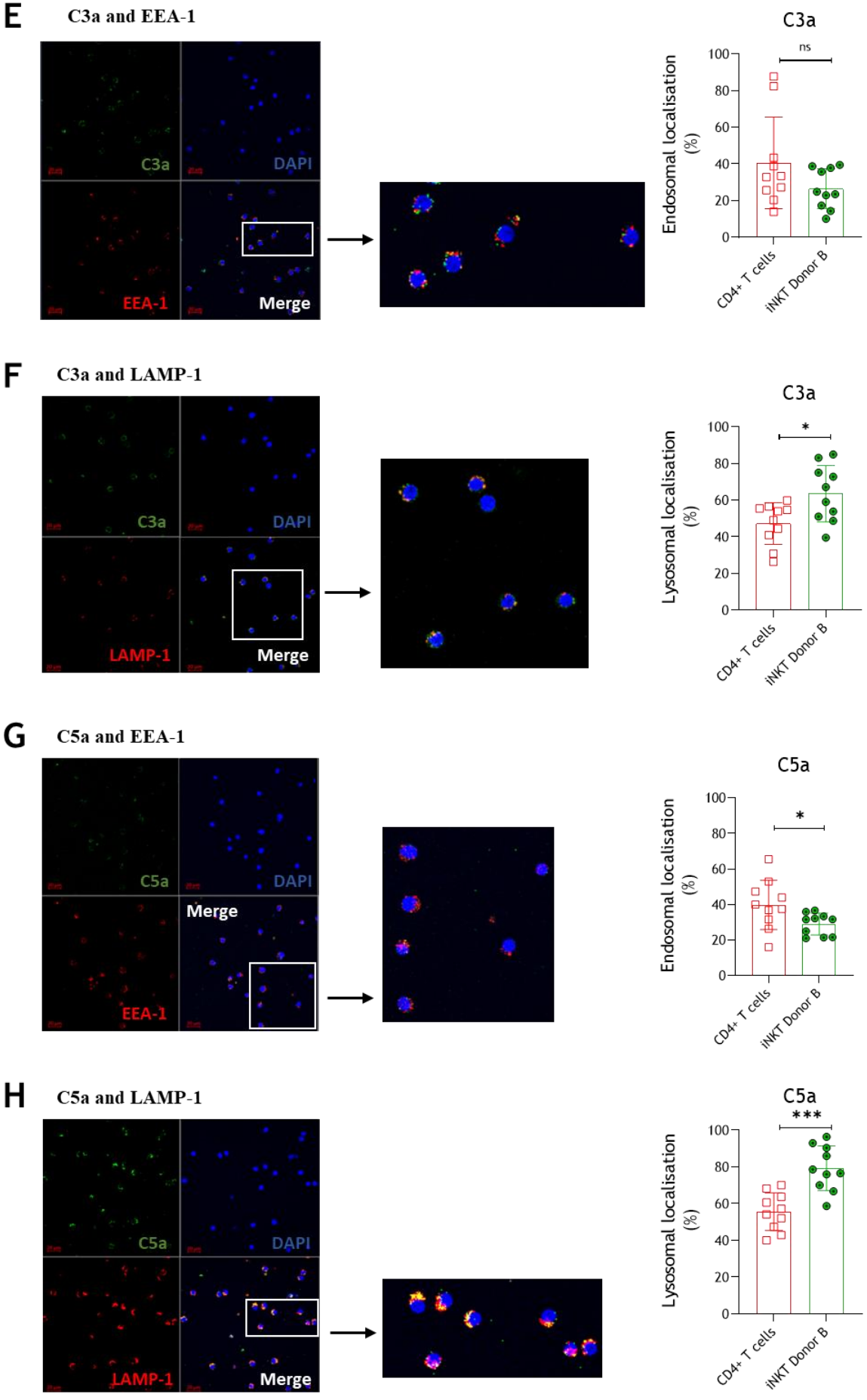

E
C3a and EEA-1
C3a
DAPI
EEA-1
Merge
C3a
ns
Endosomal localisation (%)
100
80
60
40
20
0
CD4+ T cells
iNKT Donor B
F
C3a and LAMP-1
C3a
DAPI
LAMP-1
Merge
C3a
*
Lysosomal localisation (%)
100
80
60
40
20
0
CD4+ T cells
iNKT Donor B
G
C5a and EEA-1
C5a
DAPI
Merge
EEA-1
C5a
*
Endosomal localisation (%)
100
80
60
40
20
0
CD4+ T cells
iNKT Donor B
H
C5a and LAMP-1
C5a
DAPI
LAMP-1
Merge
C5a
***
Lysosomal localisation (%)
100
80
60
40
20
0
CD4+ T cells
iNKT Donor B

Figure 3-3 Assessment of iNKT intracellular anaphylatoxins and their cognate receptors at steady state

Left panels: Representative image of one iNKT cell [Donor A for Figure A, B, C, D and Donor B for Figure E, F, G, H] (single plane of a Z-stack maximum intensity projection) where blue represents nucleus, green represents anaphylatoxin receptor or anaphylatoxin and red represents intracellular compartment. Zoom in of merged colour image shows co-localisation of receptor with intracellular compartment.

Right panels: Assessment of co-localisation of C3a, C3aR, C5a and C5aR with the endosomal compartment (EEA-1) or the lysosomal compartment (LAMP-1). A detailed description of the Manders measure algorithm used to assess for co-localisation is described in the 'Materials & Methods' section. Error bars represent mean ± SD. Statistical significance was calculated using either an unpaired t-test or a one-way analysis of variance (ANOVA) followed by Dunnett's multiple comparisons test, where *p <0.05, **p<0.01, ***p<0.001 and ****p<0.0001. EEA-1: Early Endosome Antigen 1, LAMP-1: Lysosomal-associated membrane protein 1.

(A) Staining shows C3aR and endosomal compartment (EEA-1).
(B) Staining shows C3aR and lysosomal compartment (LAMP-1).
(C) Staining shows C5aR1 and endosomal compartment (EEA-1).
(D) Staining shows C5aR1 and lysosomal compartment (LAMP-1).
(E) Staining shows C3 and endosomal compartment (EEA-1).
(F) Staining shows C3 and lysosomal compartment (LAMP-1).
(G) Staining shows C5a and endosomal compartment (EEA-1).
(H) Staining shows C5a and lysosomal compartment (LAMP-1).

3.3 iNKT Native Complement Expression

The presence of intracellular C3a and C5a in iNKT cells at steady state indicates that these proteins had recently been generated from their native counterparts C3 and C5. However, what remains unclear is whether the anaphylatoxins were generated intracellularly or had entered the cell following extracellular cleavage. To address this question, *de novo* mRNA expression of C3 and C5 at steady state and upon activation was assessed by RT-qPCR. The additional proteins involved in alternative pathway activation i.e. Factor D and Factor B were also assessed by RT-qPCR, given their potential role in the 'local' generation of C3a and C5a as previously described by Strainic et al. 2008. As an iNKT-APC co-culture would confound downstream analysis following RNA isolation, a reductionist approach was employed whereby iNKT cells were stimulated independent of antigen-presenting cells in a CD1d-plate bound assay. Activation was performed in serum-free medium to ensure that native complement proteins present in human serum or FCS did not promote further complement up-regulation i.e. via positive signalling feedback loop.

As shown in **Figure 3-4A**, C3 mRNA was up-regulated in all iNKT cell donors upon stimulation with α-GalCer relative to the unstimulated negative control. However, large variation between donors was observed. Statistical significance ($p<0.05$) was achieved at the two highest concentrations of α-GalCer used (1 and 5 µg/ml). C5 mRNA levels were down-regulated in all donors, and statistical significance was observed in four stimulation conditions (**Figure 3-4B**). Although *de novo* Factor B expression was not observed by RT-qPCR, upstream Factor D (**Figure 3-4C**) was detected at steady state. Factor D mRNA expression was slightly down-regulated upon activation, and statistical significance ($p<0.05$) was achieved at the highest concentration of α-GalCer tested. Finally, to confirm a concentration-dependent effect of stimulation by α-GalCer, *de novo* mRNA expression of the positive control IFN-γ was

assessed (**Figure 3-4D**). Up-regulation of IFN-γ reached statistical significance ($p<0.05$) at 0.5, 1 and 5 µg/ml α-GalCer.

In conclusion, *de novo* complement mRNA expression was assessed in non-activated and activated iNKT cells by RT-qPCR. The variation in C3 mRNA up-regulation between donors correlated with up-regulation of IFN-γ mRNA levels, suggesting that the activation status of the cells positively modulates *de novo* C3 expression. However, Factor B mRNA was not detected and both C5 and fD mRNA levels were reduced upon stimulation. This was surprising, given that both the anaphylatoxins C3a and C5a had been detected by confocal microscopy (**Figure 3-3**). The discrepancy between *de novo* native complement generation and downstream anaphylatoxin detection may suggest that:

- local autocrine alternative pathway is unlikely to be responsible for C3a and C5a generation.
- Or that iNKT cells take up anaphylatoxins from the extracellular milieu e.g. by recycling or receptor-mediated endocytosis.

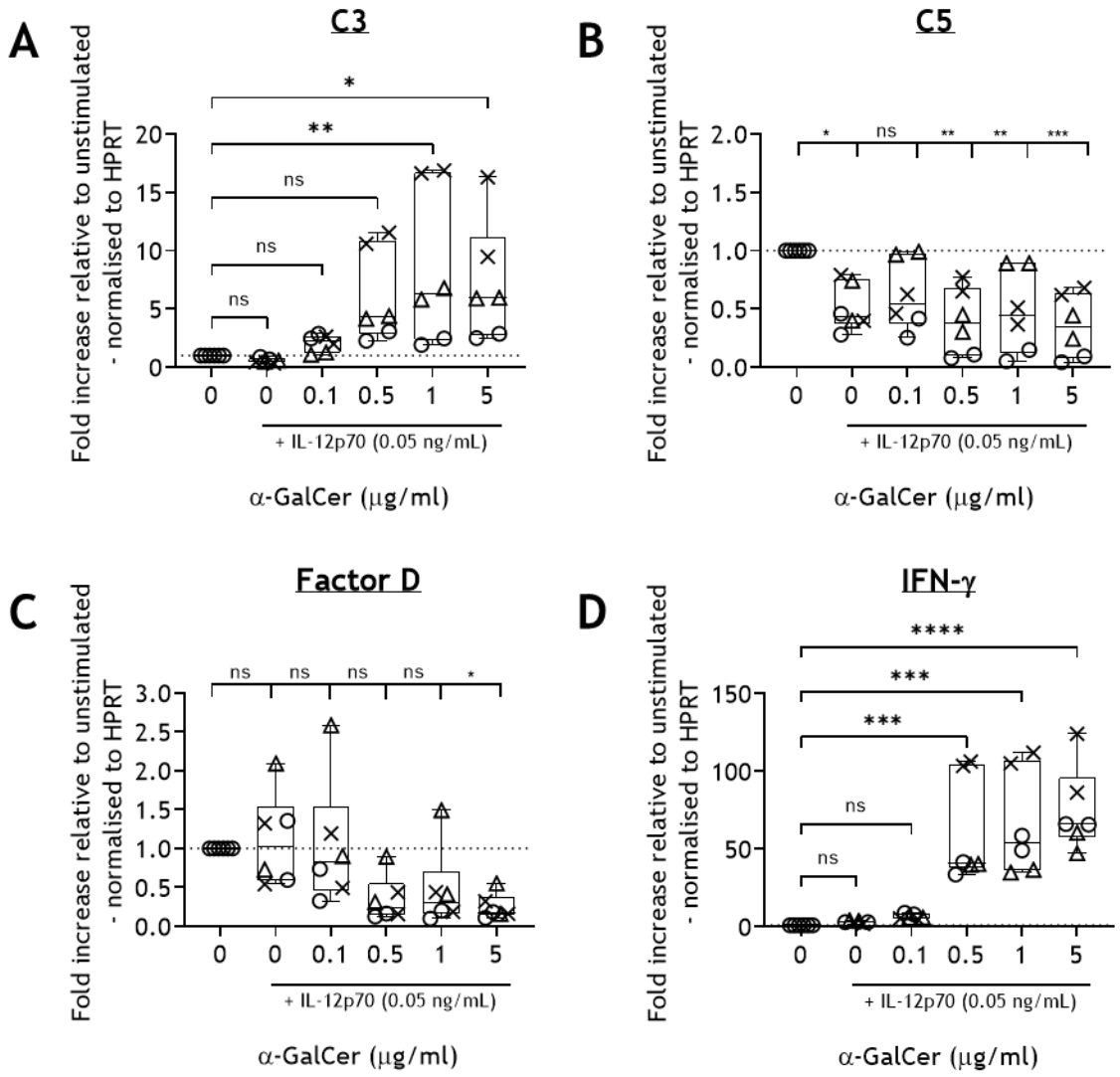


Figure 3-4 Assessment of iNKT native complement protein expression by RT-qPCR
iNKT cells were stimulated with immobolised CD1d monomers and α-GalCer (0-5μg/ml) in the presence of 0.05ng/mL IL-12p70 (in SFM). Fold gene expression changes in native C3 (A), C5 (B), Factor D (C) and the positive control IFN-γ (D) relative to the unstimulated negative control (normalised to the housekeeping control HPRT) were determined by RT-qPCR. Each symbol represents a different donor (two technical replicates per donor). Dotted line at n=1 represents no change in fold expression, when compared to the unstimulated negative control. Data is visualised using a box and whisker plot where the box includes the upper quartile, median and lower quartile of the data set. The whiskers (error bars) represent the lowest and highest values. Statistical significance was calculated using one-way analysis of variance (ANOVA) followed by Dunnett's multiple comparisons test, where *p<0.05, **p<0.05, ***p<0.001, ****p<0.0001. α-GalCer: alpha-galactosylceramide.
Donor ID – Circles (C_T values): HPRT (between 24 and 26), C3 (between 25 and 29), IFN-γ (between 20 and 28), C5 (between 32 and 34), Factor D (between 28 and 30).
Donor ID – Crosses (C_T values): HPRT (between 25 and 26), C3 (between 26 and 32), IFN- γ (between 19 and 28), C5 (between 32 and 34), Factor D (between 27 and 28).
Donor ID – Triangles (C_T values): HPRT (between 24 and 25), C3 (between 23 and 27), IFN- γ (between 20 and 27), C5 (between 31 and 33), Factor D (between 25 and 28).

3.4 COMPLEMENT RECYCLING PATHWAYS IN iNKT CELLS

Although C3 mRNA levels were low at steady state, anaphylatoxins were detected inside of the cell by microscopy. Therefore, one may speculate that steady state C3a (and downstream C5a) generation may be a consequence of taking up and storing complement from the extracellular milieu during culture or potentially were 'loaded' with complement prior to isolation from PBMCs. More specifically, Elvington and colleagues showed that certain human cell types recycle complement, specifically C3(H_2O) – the hydrolytic product of C3 between the intra- and extra-cellular space. Furthermore, different phenotypes are observed between cell lines and primary cells, which may reflect the amount of time absent from a fluid-phase complement source (Elvington et al., 2017).

To address this hypothesis, iNKT cells were cultured in two different media conditions which replicated the study published by Elvington et al., (2017). Specifically, iNKT cells were cultured for one week in their standard culture medium i.e. IMDM (Iscove's Modified Dulbecco's Medium) plus 5% heat-inactivated Human Serum or in RPMI plus 10% heat-inactivated FCS. As serum-free medium (SFM) had previously caused high levels of cell death (personal observation, unpublished), the second medium condition (RPMI plus 10% heat-inactivated FCS) was used as a surrogate for SFM i.e. a human complement-deficient culture system. However, it should be noted that there is a high degree of conservation between C3 in both types of serum, which may confound downstream data analysis (as further described in Section 3.10 – Discussion).

Following a one-week culture in their respective media, iNKT cells were stimulated overnight with α-GalCer (independent of antigen-presenting cells) in serum-free medium. As shown in **Figure 3-5A** (left panel), *de novo* C3 expression as determined by RT-qPCR was up-regulated in all tested donors following stimulation with α-GalCer. However, up-regulation of C3 mRNA was greater in iNKT cells cultured in RPMI plus 10% heat-inactivated FCS relative to cells

cultured in IMDM + 5% heat-inactivated HS. The differences in *de novo* C3 expression between culture conditions reached statistical significance ($p<0.05$) at 0.5, 1 and 5 μg/ml α-GalCer. This may suggest that the absence of a fluid-phase C3 complement source promotes a compensatory increase in *de novo* iNKT C3 generation, which is only partially modulated by TCR engagement. However, peak up-regulation of *de novo* mRNA encoding C3 was observed at 0.5 μg/ml α-GalCer suggesting an all or none response. In future experiments, multiple concentrations of α-GalCer specifically between 0.1 and 0.5 μg/ml can be used to determine if a concentration-dependent increase in *de novo* C3 mRNA generation occurs.

However, subsequent analysis of the serum-free medium by ELISA in which the cells were activated overnight (**Figure 3-5A**; right panel) showed that C3 was present in the activation medium of cells cultured in IMDM + 5% heat-inactivated Human Serum, but not in the activation medium of cells cultured in RPMI + 10% heat-inactivated FCS. Moreover, the presence of C3 in the activation medium of cells cultured in Human Serum was high (~1500 ng/ml) in both non-activated and activated cells. As the cells were stimulated in SFM, this suggests that iNKT cells take up C3 from human serum (during culture) and subsequently release it into serum-free medium. Moreover, this process does not seem to be modulated by iNKT TCR dependence.

In addition to the assessment of C3, *de novo* expression of the positive control IFN-γ along with its subsequent secretion was also assessed (**Figure 3-5B**). As expected, IFN-γ mRNA profiles (left panel) and secretion (right panel) positively correlated with the addition of α-GalCer. However, up-regulation of IFN-γ was greater in cells cultured in IMDM + 5% heat-inactivated HS relative to RPMI plus 10% heat-inactivated FCS, suggesting human serum (and potentially complement C3 along with additional protein components) positively modulate iNKT cell effector function.

Finally, as shown in **Figure 3-5C**, levels of C3 were assessed in the different types of culture media used in this experiment. As expected, C3 was detected in IMDM plus 5% heat-inactivated Human Serum, but not in RPMI plus 10% heat-inactivated FCS or in Serum-Free Medium. Moreover, human serum which had not been heat-inactivated was also tested and levels of C3 seemed to be comparable to that of its heat-inactivated counterpart. This is in line with previous reports which have showed that C3 is heat stable (Elvington et al., 2017).

In conclusion, C3 recycling in iNKT cells was investigated to determine if the extracellular milieu can influence intracellular C3 levels and potentially downstream C3a generation, as previously demonstrated by Elvington et al. (2017). Whilst this experimental protocol in which cells were initially cultured in a complement-sufficient source followed by their activation in a complement-deficient source has provided insights into a potential mechanism of C3 recycling in iNKT cells – further work is required as described below:

- Prior to assessment of recycling, ensure that the 'health' of iNKT cells in their respective culture media is equivalent. For example, use flow cytometry to compare viability, along with levels of CD3 (as a readout for TCR levels) in cells cultured in either heat-inactivated FCS or HS.
- When cells have been activated in serum-free medium (following culture in a complement sufficient environment), assess C3 levels in both the supernatant and in cell lysates e.g. by Western Blot. If the hypothesis of C3 recycling hold true, then the lysates from cultured cells will have high intracellular C3, whereas cells that have been in SFM will have low intracellular C3 because it has been secreted into the extracellular milieu.
- Finally, consider the use of inhibitors in this assay such as
    - Brefeldin A which is a protein transport inhibitor. Addition of Brefeldin A should prevent the release of *de novo* generated C3 (which is part of the secretory pathway) but should not have any effect on C3 which was taken up by cells during culture.

One may speculate that addition Brefeldin A will correlate with a partial reduction in C3 levels in the supernatant, as secretion of *de novo* but not 'loaded' C3 has been prevented.

- Inhibitors of endosomal recycling – which can be added to cells during or after culture in a complement sufficient source but before stimulation in serum-free medium. If the hypothesis of C3 recycling holds true, then addition of such inhibitors should prevent 'release' of C3 and hence the levels of C3 detected in cell supernatants should be lower than supernatants from their non-treated counterparts.

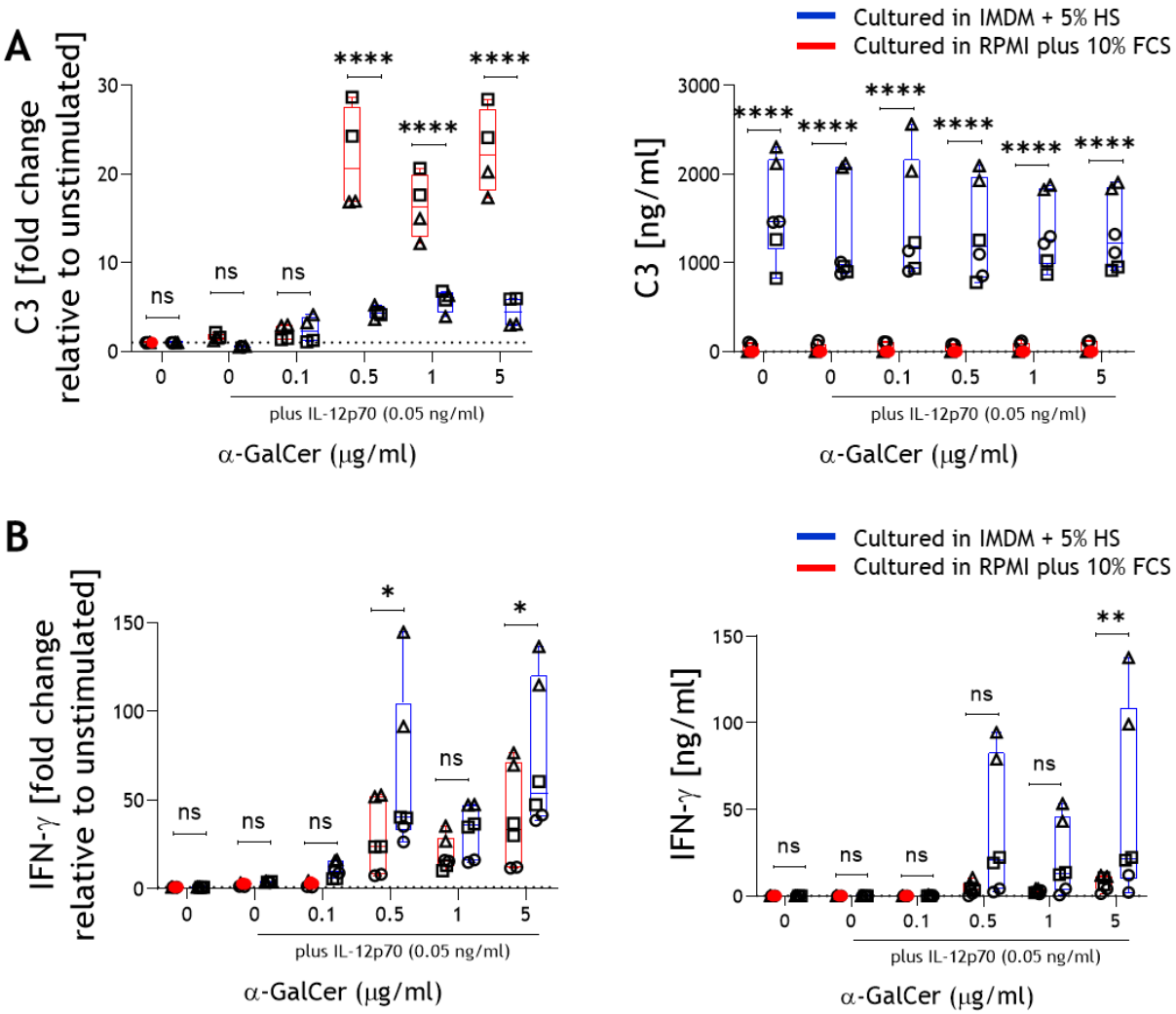

A
C3 [fold change relative to unstimulated]
C3 [ng/ml]
Cultured in IMDM + 5% HS
Cultured in RPMI plus 10% FCS
plus IL-12p70 (0.05 ng/ml)
α-GalCer (μg/ml)
B
IFN-γ [fold change relative to unstimulated]
IFN-γ [ng/ml]
C
C3 in media
C3 [AU]
Serum-Free Medium
RPMI plus 10% FCS (heat inactiv.)
IMDM plus 5% HS (heat inactiv.)
IMDM plus 5% HS

Figure 3-5 Assessment of iNKT cell activation profiles following week-long culture in different media

(A, B) iNKT cells were cultured for one week in in RPMI plus 10% FCS (blue) or IMDM plus 5% heat-inactivated HS (red). The cells were then removed from their respective media and stimulated with immobilised CD1d monomers and α-GalCer (0-5µg/ml) in the presence of 0.05ng/mL IL-12p70, in serum-free medium.

Left panels: Fold gene expression changes in native C3 and IFN-γ relative to the unstimulated negative control (normalised to the housekeeping control HPRT) were determined by RT-qPCR. Dotted line at 1 indicates no fold change relative to the unstimulated negative control. *Right panels:* Assessment of changes in native C3 and IFN-γ secretion, determined by ELISA. Dotted line at 0.625ng/ml (C3) and 0.625ng/ml (IFN-γ) represents LLOD (lower limit of detection) of this assay. Each symbol represents a different donor (2 technical replicates per donor). Data is visualised using a box and whisker plot where the box includes the upper quartile, median and lower quartile of the data set. The whiskers (error bars) represent the lowest and highest values. Statistical significance was calculated using a two-way analysis of variance (ANOVA), followed by Sidak's multiple comparisons test where *$p<0.05$, **$p<0.01$, ***$p<0.001$ and ****$p<0.0001$. α-GalCer:

(C) Assessment of C3 levels in different media. Error bars represent mean ± SD (2 technical replicates/ condition). AU: arbitrary units.

alpha-galactosylceramide, FCS: foetal calf serum, HS: human serum, heat inactiv.: heat-inactivated.

3.5 MODULATION OF iNKT CELL EFFECTOR FUNCTION BY ANAPHYLATOXINS

As iNKT *de novo* C3 expression was positively modulated by α-GalCer, I hypothesised that C3 cleavage products such as the anaphylatoxin C3a may modulate iNKT cell effector function. This hypothesis is based on previous observations by Strainic et al, (2008), who demonstrated synergy between TCR engagement and anaphylatoxins in murine T cell functional responses. Purified anaphylatoxins were added to iNKT cells at a concentration of 10 or 100 ng/ml concomitantly with 1 μg/ml α-GalCer. These concentrations were previously used by Liszewski et al., (2013) in combination with immobilised anti-CD3 antibodies to assess the activation potential of conventional CD4+ T cells. The addition of anaphylatoxins did not further increase IFN-γ levels when compared to anti-CD3 alone.

As demonstrated in **Figure 3-6A**, the addition of purified C3a at 10 or 100 ng/ml did not have a statistically significant effect on iNKT cell effector function, as determined by IFN-γ secretion ($p>0.05$). This may be a consequence of the variability observed between donor responses. However, a statistically significant reduction in IFN-γ secretion ($p<0.05$) was observed upon addition of 10 or 100 ng/ml C5a (**Figure 3-6B**). However, it should be noted that the data points were not normally distributed, and a non-parametric test was used to analyse this data set.

In conclusion, the down regulation of iNKT cell effector function in the presence of both C3a and C5a contradicts previously published reports in both human and murine $CD4^+$ T cells. More specifically, C3a and C5a were shown to increase IFN-γ production in transgenic OT-II T cells which had been stimulated with OVA peptide (Strainic et al., 2008). Furthermore, in human $CD4^+$ T cells which had been stimulated with anti-CD3/CD46 mAbs, the concomitant addition of C3a either had no effect or was able to 'partially rescue' the cytokine response upon addition of a commercially available CTSL inhibitor (Liszewski et al., 2013).

As this was only a single preliminary experiment, multiple optimisations can be made as described below:

- As the physiological concentrations of anaphylatoxins in the local cellular microenvironment are difficult to determine given their short-half life and rapid inactivation to their des-arginated counterpart, the des-arginated counterparts of C3a and C5a (which are commercially available) on iNKT cell effector function can be tested. It has previously been reported that the affinity of the des-arginated proteins for their respective receptors is lower than their non-des-arginated counterparts, thus one may speculate that changes in receptor affinity may correlate with an altered effector response i.e. cytokine secretion.
- In addition, only two concentrations of C3a and C5a were used in this experiment, and a titratable effect on cell effector response was not observed. Therefore, concentrations of anaphylatoxins should be lowered in future experiments.
- Also, cells can be assessed by flow cytometry to
    a. Specifically quantify viability.
    b. Assess expression of surface activation markers such as CD25, in the absence and presence of C3a and C5a. As cytokine secretion is decreased in the presence of C3a and C5a, one may speculate that the expression of CD25 is also reduced, when compared to activated cells (in the absence of anaphylatoxins).
    c. Assess cognate C3aR and C5aR1 expression, in the absence and presence of C3a and C5a. Also assess the expression of C5aR2 which is postulated to have anti-inflammatory potential (Li et al., 2019).
    d. Assess the phosphorylation of intracellular signalling proteins which are downstream of G-protein receptor coupling and hence implicated in C3aR/C5aR1 effector function (as extensively described in the Introduction).

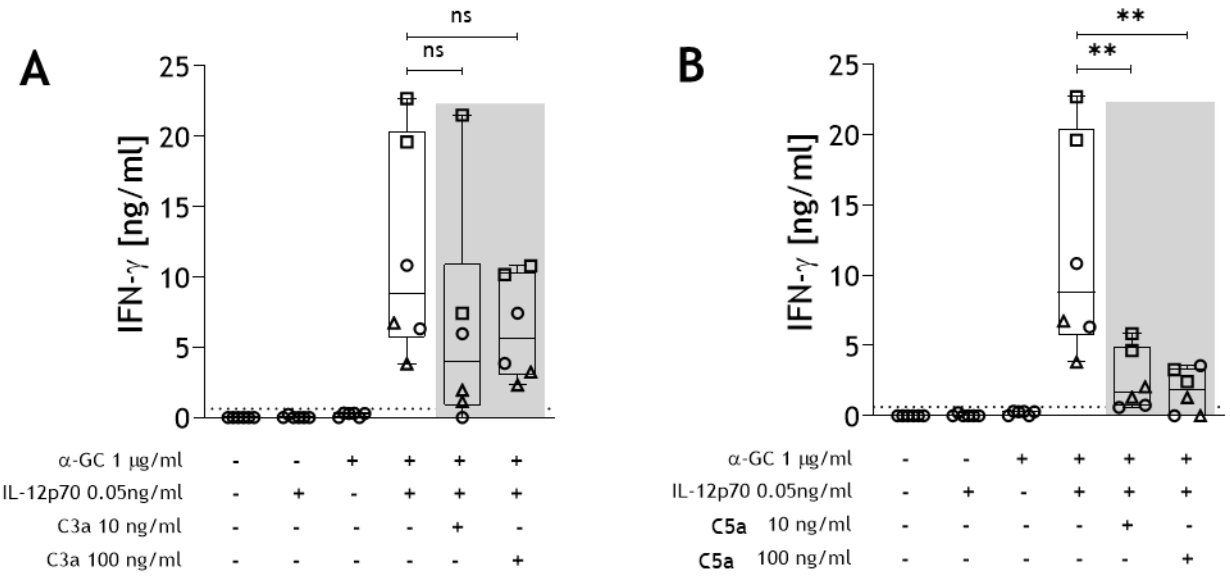


Figure 3-6 Assessment of iNKT cell activation in the presence of C3a and C5a
(A, B) iNKT cells were stimulated with immobolised CD1d monomers and α-GalCer (1μg/ml) in the presence of 0.05ng/mL IL-12p70, in SFM. This was followed by concomitant addition of 10 or 100ng/ml C3a (A) or (C5a). Dotted line at 0.625ng/ml represents LLOD (lower limit of detection) of this assay. Each symbol represents a different donor (2 technical replicates per donor). Data is visualised using a box and whisker plot where the box includes the upper quartile, median and lower quartile of the data set. The whiskers (error bars) represent the lowest and highest values. For A) Statistical significance was calculated using one-way analysis of variance (ANOVA) followed by Dunnett's multiple comparisons test. For B) Statistical significance was calculated using a Mann-Whitney Test (as the data points were not normally distributed). α-GC: alpha-galactosylceramide,

3.6 THE CD40-CD40L AXIS AND POTENTIAL IMPLICATIONS FOR COMPLEMENT SIGNALLING PATHWAYS

Strainic et al., (2008) previously reported that murine T cells positively modulate DC complement expression profiles through exploiting the CD40-CD40L co-stimulatory axis upon TCR engagement with peptide-loaded MHC. Moreover, DC-derived anaphylatoxins were shown to positively modulate T cell effector function through paracrine signalling (Strainic et al., 2008).

In view of this, anti-CD40L mAbs were employed to inhibit this co-stimulatory axis and subsequently assess iNKT and DC functional responses. As CD40L expressed by iNKT cells interacts with CD40 on DC to induce production of IL-12, inhibition of this co-stimulatory axis negatively regulated IL-12p40 secretion (**Figure 3-7B**). Specifically, a statistically significant reduction in IL-12p40 ($p<0.05$) secretion was observed at all stimulating concentrations of α-GalCer tested when compared to the isotype control. As secreted IL-12 positively modulates iNKT cell activation through paracrine signalling, down-regulation of IL-12 secretion positively correlated with reduced secretion of iNKT cell generated IFN-γ (**Figure 3-7A**). Once again, a statistically significant reduction in IFN-γ secretion ($p<0.05$) was observed at all tested concentrations of α-GalCer tested relative to the isotype control.

In conclusion, inhibition of the CD40-CD40L axis negatively regulates dendritic cell maturation and in turn iNKT cell effector function, in line with previously published reports. What remains unclear is whether anaphylatoxin generation through alternative pathway activation may be partially responsible for driving this effect, and so will be explored next.

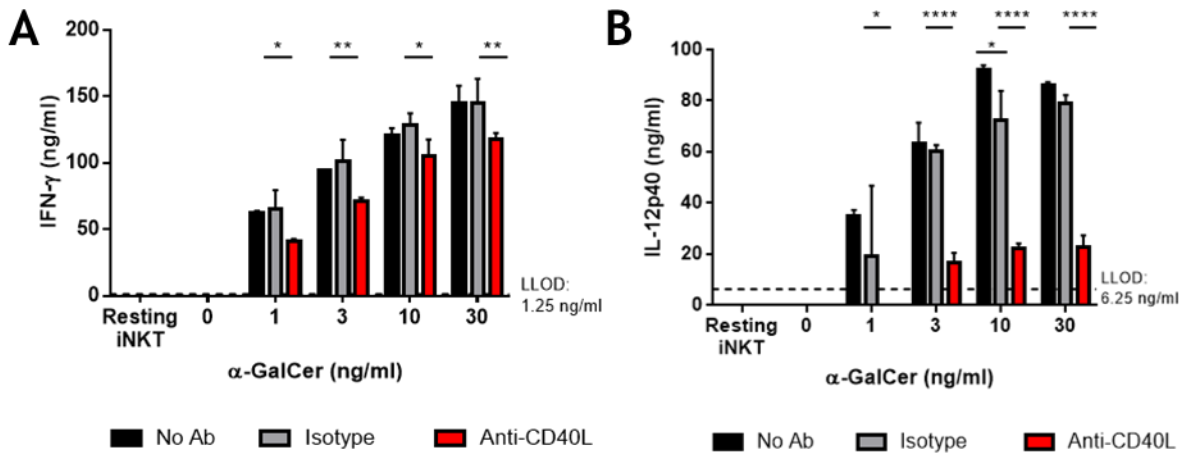


Figure 3-7 Modulation of iNKT cell activation by the CD40-CD40L axis

iNKT cells were stimulated by MdDCs and α-GalCer (1-30 ng/ml) in SFM, followed by concomitant addition of anti-human CD40L blocking antibody (Clone 24.31) or mouse IgG1, κ isotype control (Clone MOPC-21). The following day, IFN-γ (A) and IL-12p40 (B) secretion within cell supernatant was assessed by ELISA. Dotted line at 1.25ng/ml (IFN- γ) and 6.25ng/ml (IL-12p40) represents LLOD (lower limit of detection) of this assay. Error bars represent mean ± SD (2 technical replicates/ condition). This figure shows data from one experiment, which is representative of the following five experimental conditions:

- iNKT Donor 2/ MdDC Donor A
- iNKT Donor 2/ MdDC Donor B
- iNKT Donor 1/ MdDC Donor C
- iNKT Donor 2/ MdDC Donor C
- iNKT Donor 1/ MdDC Donor F

Statistical significance was calculated using a two-way ANOVA followed by Dunnett's multiple comparisons test where *p<0.05, **p<0.01, ***p<0.001 and ****p<0.0001 (when compared to isotype for each activated condition). α-GalCer: alpha-galactosylceramide.

3.7 CD40L-INDUCED MDDC COMPLEMENT EXPRESSION PROFILES

As *de novo* Factor B mRNA expression was not detected in iNKT cells, it is unlikely that autocrine derived AP convertase generation, downstream anaphylatoxin generation and subsequent autocrine signalling modulates their effector function.

However, Strainic et al., (2008) also showed that $CD4^+$ T cell effector function can be modulated via paracrine signalling. More specifically, C3a and C5a secreted from neighbouring APCs were shown to bind their cognate receptors (C3aR and C5aR1, respectively) on $CD4^+$ T cells and upregulate their cytokine secretion. Moreover, antibody-mediated inhibition of CD40 signalling on APCs negatively regulated the alternative pathway components C3 and fB, which in turn correlated with dampened $CD4^+$ T cell cytokine responses. This suggests that local and potentially intracellular generation of the AP convertase and downstream anaphylatoxin generation may be modulated by the CD40-CD40L axis.

Although Strainic et al., (2008) fluorescently tagged and sorted the respective cell types post-stimulation and prior to performing qPCR analysis, this approach was not feasible with iNKT cells as they are cytolytic upon activation (Bassiri et al., 2013). Therefore, a reductionist approach was employed whereby CD40L multimers were used to activate MdDCs overnight (independent of iNKT cells) in serum-free medium. Assessment of *de novo* native complement expression profiles was subsequently performed by RT-qPCR.

As shown in **Figure 3-8A** and **Figure 3-8B**, both C3 (~3.7-mean fold change, upon activation) and Factor B (~65.4-mean fold change, upon activation) were up-regulated upon addition of 2 µg/ml CD40L, relative to the unstimulated negative control. Moreover, up-regulation of Factor B by CD40L was greater in all donors tested, when compared to that induced by the toll-like receptor (TLR) 7/8 ligand R-848 (~10.2-mean fold change) used as a positive control for activation (Hatterman et al., 2007) (**Figure 3-8B**). R-848 (also referred to as Resiquimod) was

chosen as a positive control for activation, as it has always provided a robust and reproducible stimulatory response when compared to other TLR ligands such as LPS (personal observation, unpublished). CD40L but not R-848-induced up-regulation of Factor B did reach statistical significance ($p<0.05$).

As expected, IL-12p40 secretion was also upregulated with the addition 2 µg/ml CD40L or 10 µg/ml R-848. However, statistical significance ($p<0.05$) was only achieved when both ligands were combined, where synergy was observed in two out of 3 donors tested (**Figure 3-8C**), i.e. the mean fold change in IL-12p40 gene expression in the presence of both ligands was ~4 times greater than with either ligand alone. However, this synergy was not observed for either *de novo* C3 (**Figure 3-8A**) or Factor B mRNA expression (**Figure 3-8B**), suggesting that the intracellular signalling pathways which modulate the *de novo* generation of IL-12p40 and complement do not wholly overlap. Finally, *de novo* C5 (**Figure 3-8D**) and Factor D (**Figure 3-8E**) expression either remained unchanged or was down-regulated upon addition of 2 µg/ml CD40L, 10 µg/ml R-848 or a combination of both ligands i.e. mean-fold change was <1 for all but one of the tested donors. Statistical significance ($p<0.05$) was observed for both C5 and Factor D, in all tested ligand conditions.

In conclusion, CD40 ligation by CD40L positively modulates *de novo* generation of the *cfb* gene in MdDCs, as demonstrated by RT-qPCR. This finding aligns with previously published work by Strainic et al. (2008). Moreover, down-regulation of both the *C5* and *cfd* genes is also observed. Subsequent work will now determine if these mRNA profiles positively correlate with protein expression and potential generation of an active AP C3 convertase and downstream anaphylatoxin generation.

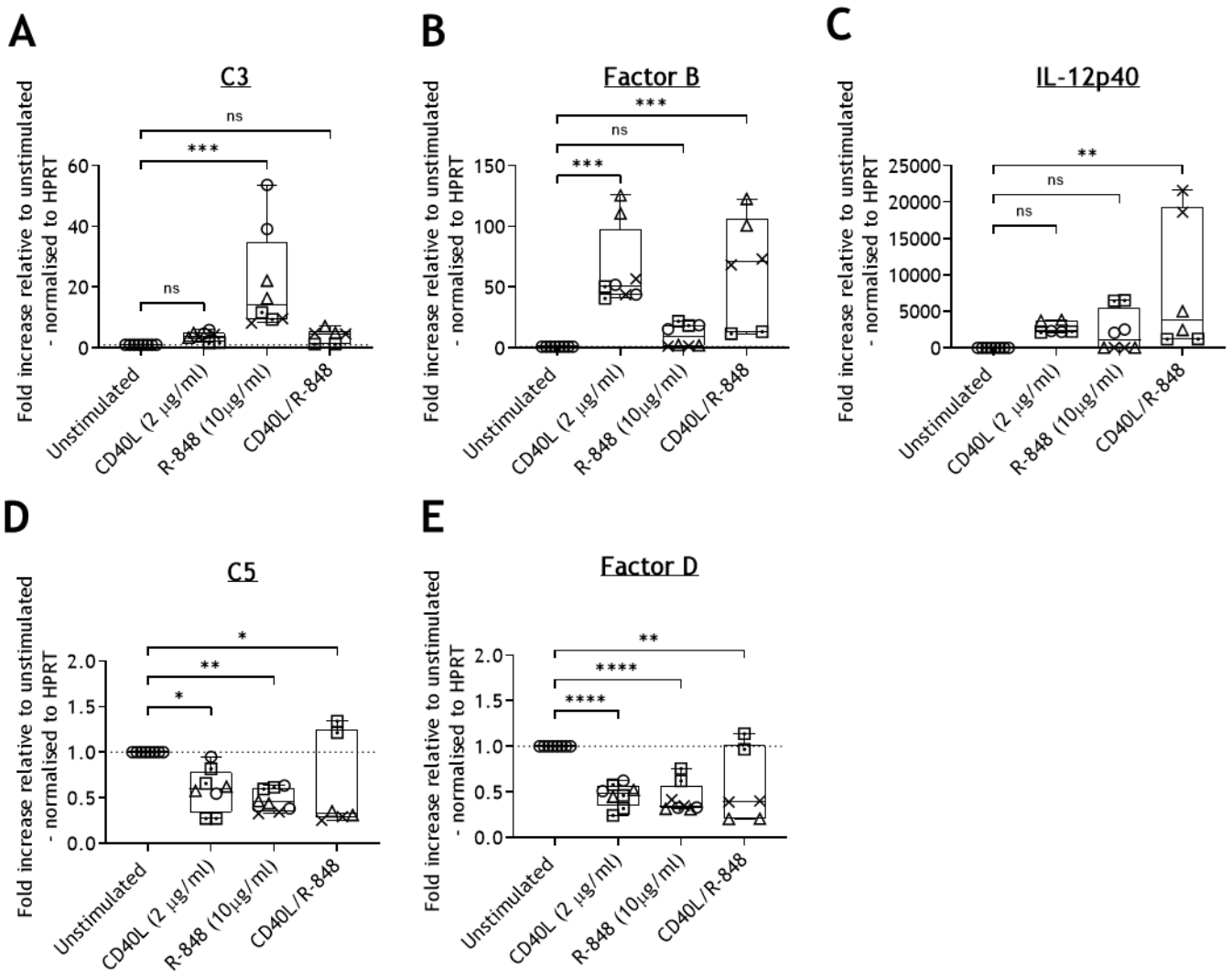


Figure 3-8 Assessment of CD40L-induced MdDC complement protein expression by RT-qPCR

MdDCs were stimulated with CD40L (2µg/ml), R-848 (10µg/ml) or a combination of both ligands overnight, in SFM. Fold gene expression changes in native C3 (A), Factor B (B), the positive control IL-12p40 (C), C5 (D) and Factor D (E) relative to the unstimulated negative control (normalised to the housekeeping control HPRT) were determined by RT-qPCR. Each symbol represents a different donor (2 technical replicates per donor). A total of 3 or 4 donors/ condition. Dotted line at n=1 represents no change in fold expression, when compared to the unstimulated negative control. Data is visualised using a box and whisker plot where the box includes the upper quartile, median and lower quartile of the data set. The whiskers (error bars) represent the lowest and highest values. Statistical significance was calculated using one-way analysis of variance (ANOVA) followed by Dunnett's multiple comparisons test, where *$p<0.05$ and**$p<0.01$. SFM: serum-free medium.

3.8 CD40L-INDUCTION OF MDDC COMPLEMENT SECRETION PROFILES

As described in **Section 3.7**, ligation of CD40 by CD40L positively modulated *de novo* generation of the alternative pathway protein Factor B in MdDCs. It was thus tempting to speculate that *de novo* generated Factor B may be secreted in to the extracellular milieu, where it would be cleaved to Bb and form active C3 convertase within the local microenvironment. Another possibility may be that Factor B is retained, cleaved and hence activated intracellularly. Accordingly, to explore the first possibility, the secretion of native complement into the extracellular space was assessed to further ascertain the potential 'source' of downstream anaphylatoxins.

As demonstrated in **Figure 3-9A** and **Figure 3-9B**, C3 and Factor B were both secreted by activated MdDCs into the extracellular space. There was a statistically significant increase ($p<0.05$) in C3 secretion upon stimulation with 2 µg/ml CD40L (~1.3 ng/ml) and the positive control 10 µg/ml R-848 (~2.6 ng/ml), when compared to the unstimulated negative control. Moreover, statistical significance ($p<0.05$) was also observed when both ligands were combined, although synergy was not observed (**Figure 3-9A**). Moreover, a statistically significant up-regulation ($p<0.05$) in Factor B was also observed following stimulation with 2 µg/ml CD40L (~20 ng/ml), but not 10 µg/ml R-848 (~10 ng/ml). Once again, a statistically significant increase ($p<0.05$) in Factor B secretion was also seen upon combination of the activating conditions, yet a clear synergistic effect could not be determined (**Figure 3-9B**). Finally, secretion of the positive control for cellular activation, IL-12p40 was also increased in the presence of 2 µg/ml CD40L and 10 µg/ml R-848 (**Figure 3-9C**). However, statistical significance ($p<0.05$) and potential synergy was only observed upon ligand combination.

Finally, it should be noted that the symbols used in **Figure 3-9** correspond to the same donor and experiment as described in **Figure 3-8**, enabling a direct comparison between *de novo* complement gene expression and subsequent secretion to be made. The mRNA profiles for C3,

Factor B and IL-12p40 correlated with their respective secretion profiles. More specifically, C3 up-regulation at both the mRNA and protein levels was greater with R-848 than CD40L, whereas the reverse trend was observed for Factor B. Once again, potential synergy between the two ligands was observed for both IL-12p40 secretion and mRNA profiles but was not observed for the complement proteins. As described previously, this may be a consequence of different intracellular signalling pathways which are employed to modulate IL-12 and complement expression.

In conclusion, secretion of C3 and fB into the extracellular milieu by activated MdDCs was positively modulated by CD40 ligation. Although this does not completely rule out intracellular retention and potential cleavage, it is perhaps more likely that antigen-presenting cell-derived C3 and fB function within the extracellular microenvironment to form a 'local' AP C3 convertase.

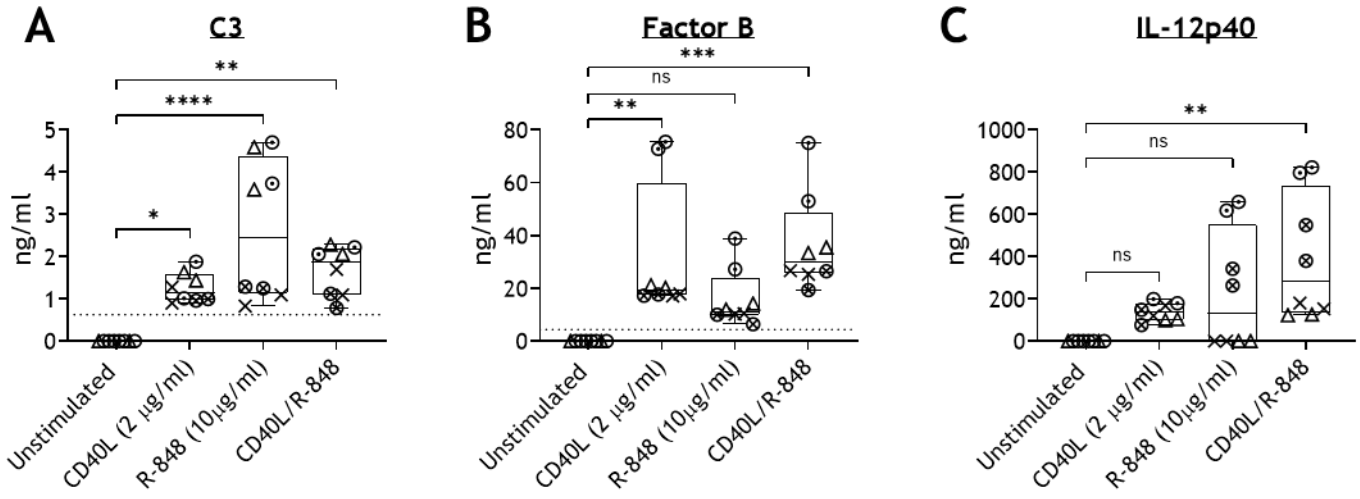


Figure 3-9 Assessment of CD40L-induced MdDC complement protein secretion by ELISA

MdDCs were stimulated with CD40L (2µg/ml), R-848 (10µg/ml) or a combination of both ligands overnight, in SFM. Assessment of secretion for native C3 (A), Factor B (B) and the positive control IL-12p40 was assessed by ELISA. Each symbol represents a different donor (2 technical replicates per donor); total of 4 donors. Dotted line at 0.625ng/ml (C3), 4.375ng/ml (Factor B) and 1.5625ng/ml (IL-12p40) represents LLOD (lower limit of detection) of this assay. Data is visualised using a box and whisker plot where the box includes the upper quartile, median and lower quartile of the data set. The whiskers (error bars) represent the lowest and highest values. Statistical significance was calculated using one-way analysis of variance (ANOVA) followed by Dunnett's multiple comparisons test, where *p<0.05, **p<0.01, ***p<0.001 and ****p<0.0001. SFM: serum-free medium.

3.9 CD40L-INDUCED COMPLEMENT CLEAVAGE

The alternative pathway (AP) protein Factor B was positively modulated by the CD40-CD40L axis at both the mRNA (**Figure 3-8**) and the secreted protein level (**Figure 3-9**). However, the ELISA used (**Figure 3-9**) does not differentiate between native Factor B and its cleavage components Ba and Bb. Therefore, flow cytometric assessment of Factor B protein expression was performed using antibodies which detect either Factor B or its activated form Bb which is part of AP C3 convertase.

To examine this, MdDCs were permeabilised and stained, following stimulation with CD40L, R-848 or a combination of both ligands. As demonstrated in **Figure 3-10B**, total (i.e. surface and intracellular) Factor B expression showed a trend towards an increase upon stimulation with 2 µg/ml CD40L and 10 µg/ml R-848 in all tested donors, but statistical significance was not reached ($p>0.05$) when compared to the negative unstimulated control. Factor B expression levels positively correlated with the surface activation marker CD86 (**Figure 3-10A**), which was also up-regulated upon stimulation 2 µg/ml CD40L and 10 µg/ml R-848 in all tested donors. This was followed by the assessment of total Factor Bb expression, using a neo-epitope specific antibody clone which does not cross-react with Factor B (Hourcade et al., 1998; Jansen van Vuren et al., 2014). Factor Bb expression remained low at steady state and upon stimulation, in all tested donors (**Figure 3-10C**; top panel). Moreover, there was no statistically significant difference ($p>0.05$) in Bb expression upon stimulation with all tested ligands, when compared to the negative unstimulated control (**Figure 3-10C**; bottom panel).

In conclusion, whilst there was a trend in Factor B up-regulation in all tested donors upon treatment with 2 µg/ml CD40L and 10 µg/ml R-848 – statistical significance was only achieved when both ligands were combined ($p<0.05$). This may be due to the intrinsic variability in mean fluorescent intensity (MFI) values between donors which usually occurs between different

experiments and when using different cytometers. Furthermore, Bb levels remained unchanged irrespective of stimulus.

Up-regulation of Factor B but not Bb may suggest that upon CD40 engagement, most of the *de novo* generated Factor B is secreted into the extracellular space where it contributes to 'local' AP C3 convertase generation and downstream DC effector function. This hypothesis will be addressed in the next chapter.

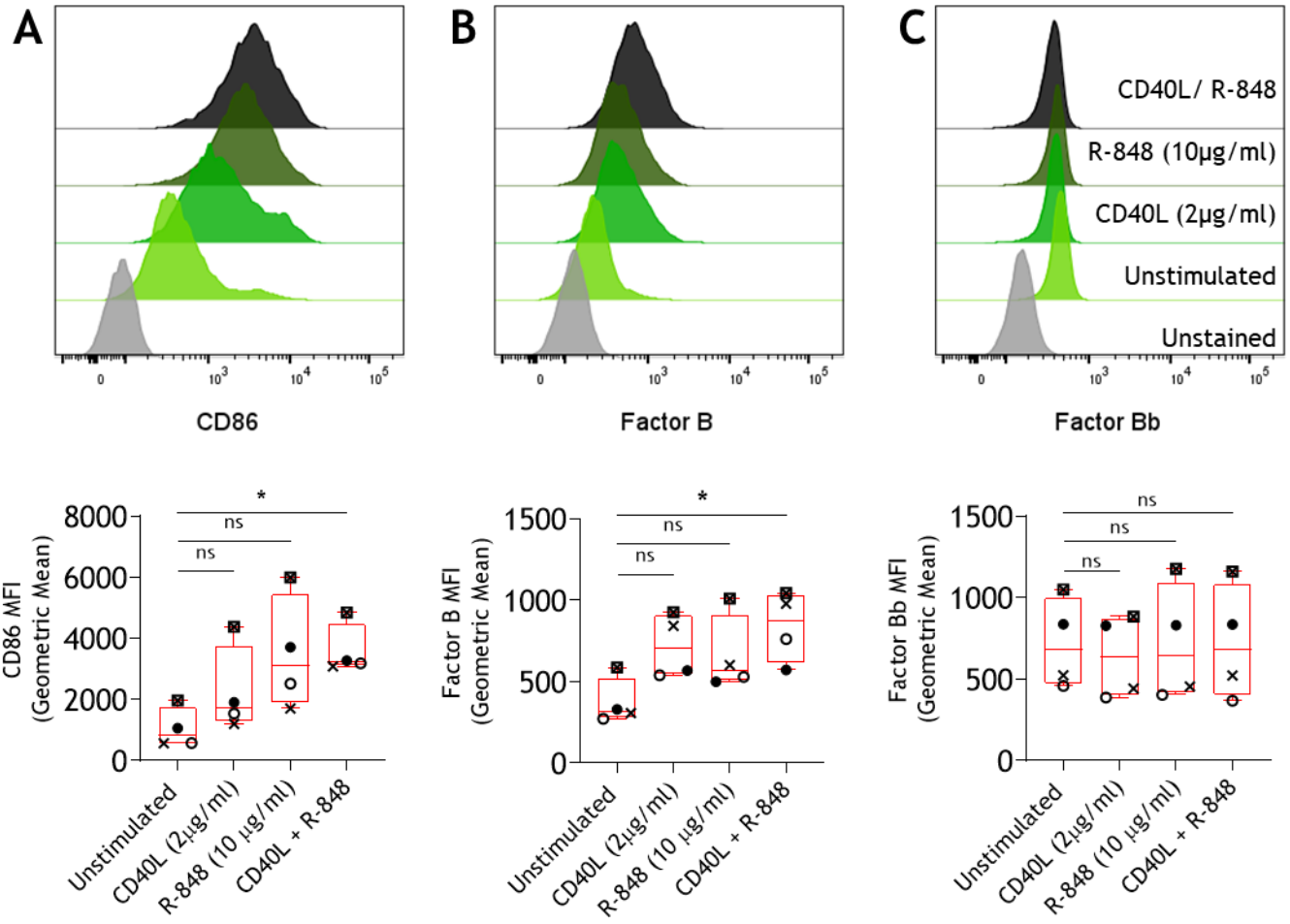


Figure 3-10 Assessment of MdDC complement protein Factor B and Factor Bb complement protein expression, by flow cytometry

MdDCs were stimulated with CD40L (2µg/ml), R-848 (10µg/ml) or a combination of both ligands overnight, in SFM. Assessment of surface CD86 expression (A), total Factor B expression (B) and total Factor Bb expression (C) by flow cytometry. *Top panels:* representative histograms for each marker (from a single experiment). *Bottom panels:* MFI values of each marker, determined by geometric mean. Each symbol represents a different donor (one technical replicate per donor); total of 4 donors. Data is visualised using a box and whisker plot where the box includes the upper quartile, median and lower quartile of the data set. The whiskers (error bars) represent the lowest and highest values. Statistical significance was calculated using one-way analysis of variance (ANOVA) followed by Dunnett's multiple comparisons test, where *p<0.05, **p<0.01, ***p<0.001 and ****p<0.0001. MFI: Mean Fluorescent Intensity.

3.10 DISCUSSION

In this chapter, the role of alternative pathway complement activation and downstream anaphylatoxin generation on iNKT cell and MdDC effector function was investigated. The modulation of iNKT cells or MdDCs by complement can manifest in two ways:

1) Through autocrine generation of and subsequent receptor signalling by anaphylatoxins.
2) Through paracrine generation of anaphylatoxins by antigen-presenting cells, and subsequent iNKT cell receptor signalling.

3.10.1 What complement proteins do iNKT cells express?

- Assessment of iNKT anaphylatoxin receptor expression upon stimulation revealed significant variation between donors and experimental conditions. Whilst cellular viability remained relatively constant across all testing conditions, increased up-regulation of C3aR and C5aR1 was observed when iNKT cells were activated in complete medium versus serum-free medium. The biological significance of these findings is further discussed within the general discussion.
- Subsequent analysis of intracellular C3aR and C5aR1 expression by confocal microscopy was also performed using the same antibody clones as previously used for flow cytometry, thus ensuring consistency across experiments. Moreover, intracellular C3a and C5a were also assessed at steady state using neo-epitope antibodies, thus preventing cross-reactivity with native protein. Whilst both C3a and C5a along with their cognate receptors were detected to varying degrees in either the endosomal or lysosomal compartments of iNKT cells, future work should consider increasing the size of the antibody panel or using another instrument with more lasers. This in turn will enable the assessment of co-localisation of C3a/C5a and C3aR/C5aR1 within a given intracellular compartment. If direct co-

localisation is observed, this may suggest a mechanism whereby intracellular autocrine anaphylatoxin receptor engagement modulates effector function, as described above.

- Finally, donor variability was once again observed when assessing native complement mRNA expression profiles by RT-qPCR. Although *de novo* generation of C3 was observed upon iNKT cell activation, Factor B (fB) expression never reached C_T (cycle threshold) with the standard qPCR set-up of 40 cycles. It should be noted that the qPCR probes used to assess iNKT Factor B expression were also used to successfully detect MdDC Factor B, hence the reason for a lack of detection remains unclear. Moreover, iNKT cells may have the potential to 'recycle' Factor B along with C3 from the extracellular milieu, as previously observed for conventional $CD4^+$ T cells (Elvington et al., 2017).

3.10.2 Is iNKT cell effector function modulated by complement?

During the study of C3 recycling between the intra- and extracellular compartments, iNKT cells were initially cultured in either a human complement-rich source i.e. human serum or a human complement-deficient source i.e. foetal calm serum. FCS was chosen as a surrogate for commercially available serum-free (and hence complement-free) medium, due to previously observed high cell death during long-term culture in serum-free medium (personal observation, unpublished).

However, it was subsequently determined that there was a high degree of conservation between C3 in both types of serum, which may confound downstream data analysis, notably the results obtained from the C3 ELISA. More specifically, the genetic sequence of bovine C3 was obtained from the ENSEMBL genome browser and BLAST analysis i.e. alignment with the human C3 genetic sequence was performed using the NCBI (blastn) algorithm. BLAST analysis revealed 81.9% identical match sequence alignment between bovine and human C3. Subsequent analysis of the protein sequence (obtained from UniProt) revealed 77.1% sequence alignment with human C3, using the NCBI (blastp) algorithm.

Given the high degree of conservation for both the genetic and protein sequences of C3, one may speculate that the ELISA data (**Figure 3-5A**; right panel) only partially shows human C3 secretion. However, when the 'media only' controls were tested using this C3 ELISA kit, no cross-reactivity with FCS was observed i.e. there was no chemiluminescent signal in the FCS control wells. This suggests that only human but not bovine C3 was detected in the cell culture supernatants.

3.10.3 Do neighbouring antigen-presenting cells express and secrete complement AP proteins?

A detailed rationale for exploiting the CD40-CD40L axis and its potential effects on anaphylatoxin generation was previously described in **Section 3.6**. In brief, engagement of CD40 by CD40L was shown to positively modulate anaphylatoxin generation in APCs. APC-derived anaphylatoxins in turn influenced CD4+ T cell effector function via paracrine signalling (Strainic et al., 2008). In this work, it was shown that CD40 engagement in MdDCs positively modulated C3 and Factor B expression. More specifically,

- C3 and Factor B mRNA and ELISA profiles both revealed significant donor variation. However, two important trends were noted. Firstly, the up-regulation of Factor B mRNA and protein expression was always greater in the presence of CD40L versus the toll-like receptor ligand R-848 (resiquimod), whereas the reverse trend was observed for C3. Secondly, whilst synergy in activation i.e. IL-12p40 secretion was observed upon combining the two ligands (CD40L and R-848), a similar trend was not observed in C3 and Factor B expression. This suggests that the molecular pathways which modulate IL-12p40 and complement expression following activation, do not wholly overlap. The biological significance of this divergence in signalling pathways will be further discussed within the General Discussion. Finally, as C5 and fD mRNA levels were down-regulated upon stimulation with all tested ligands, subsequent ELISAs were not performed.

- As *de novo* Factor B mRNA expression in MdDCs was positively modulated upon CD40 engagement by CD40L, assessment of potential complement cleavage products was performed. More specifically, the presence of Bb i.e. the functional component of the AP C3 convertase was assessed in MdDCs by flow cytometry. Once again, a neo-epitope antibody which does not cross-react with native Factor B was used. This antibody was conjugated in-house with a FITC fluorophore and multiple antibody concentrations were used to stain MdDCs. Whilst Bb was detected by flow cytometry at steady state when compared to the negative unstained control, Bb expression was not increased in any tested MdDC donor following stimulation.

Alternative approaches such as a Western Blot, ELISA or MSD may prove more useful when assessing 'local' Bb generation. Successful detection of Bb would strengthen the idea of 'local' Factor B activation and potential C3/C5 convertase formation and hence downstream C3a/C5a generation.

In conclusion, a thorough examination of complement expression profiles in iNKT cells and monocyte-derived dendritic cells (MdDCs) has helped to define a clearer phenotype for both cells, which can be exploited either pharmacologically or through genetic manipulation. One may speculate that dendritic cell-derived complement fragments i.e. C3a/C5a may modulate iNKT cell function through paracrine signalling. This hypothesis will be explored in the next chapter.

4 ALTERNATIVE PATHWAY (AP) INHIBITION IN MONOCYTE-DERIVED DENDRITIC CELLS (MDDCS)

Whilst the generation of fluid-phase C3 convertase from liver-derived complement is extensively described (Merle et al., 2015, Reis et al., 2019), the mechanism of local C3 convertase generation from cell-derived complement remains unclear (Strainic et al., 2008). More specifically, Strainic et al., (2008) positively correlated cell-derived C3 and fB generation with downstream cell-derived anaphylatoxin generation, cognate C3a-C3aR and C5a-C5aR1 interactions and changes in cellular effector function. The authors speculated that cell derived C3 and fB form a 'local' C3 (and C5) convertase, which subsequently cleaves C3 in to C3a and C5 in to C5a (Strainic et al., 2008). Mechanistically, the generation of a 'local convertase' remains unclear and may exist under multiple mutually inclusive guises as described below:

a) Cells may synthesise and secrete Factor B into the extracellular space, where in combination with serum-circulating C3 and/or C3(H_2O), it forms functional fluid-phase C3 and C5 convertases which generate C3a and C5a.
b) Cells may synthesise and secrete Factor B, which in combination with cell-surface bound C3b forms functional cell-surface bound C3/C5 convertases i.e. C3bBb and C3bBbC3b. However, cell-surface AP convertases are quickly inactivated by DAF (CD55) or by CD46 (in the presence of FI) (Merle et al., 2015), thus making their generation difficult to detect experimentally.
c) Cells may synthesise and retain Factor B intracellularly, where in combination with *de novo* generated C3 or recycled C3/ C3(H_2O) forms functional intracellular C3 and C5 convertases.
d) Cells may synthesise and retain C3 and/ or Factor B intracellularly, where the proteins function independently of one another.

In the previous chapter, Factor B was shown to be expressed at low levels at steady state and its expression was subsequently upregulated in monocyte-derived dendritic cells (MdDCs) upon stimulation with 2 µg/ml CD40L, 10 µg/ml R-848 or a combination of both ligands. Therefore, experiments in this chapter will investigate the role of local AP convertase generation in the modulation of DC effector function. Tool small-molecules and antibodies which target Factor B will be employed and the following experiments will be undertaken:

1) The inhibitory potential of these cell permeable and impermeable Factor B inhibitors on AP activation will be assessed in a cell-free assay. The specificity of pharmacological blockade will be confirmed through the assessment of downstream anaphylatoxin generation.
2) This work will then be repeated in cells i.e. MdDCs, where both anaphylatoxin generation and effector function including costimulatory molecule expression and cytokine secretion will be assessed.
3) CRISPR-Cas9 mediated inhibition of C3 production will be leveraged to determine
    a. if loss of complement negatively regulates cellular effector responses
    b. if loss of target protein i.e. C3 and by default C3 convertase negatively regulates the inhibitory potential of small molecule inhibitors described above.

4.1 PROFILING OF FACTOR B INHIBITORS IN THE MODULATION OF ALTERNATIVE PATHWAY ACTIVATION

The following antagonists which target Factor B were assessed for their ability to inhibit AP activation: the small-molecules FB Inhibitor 1 and FB Inhibitor 2 and the antibodies FB blocking antibody 1 and FB blocking antibody 2.

As shown in **Figure 4-1A** and **Figure 4-1B**, normal human plasma (NHP) was activated with zymosan to initiate AP in the absence or presence of increasing concentrations of the small-molecules FB Inhibitor 1 and FB Inhibitor 2 or FB blocking antibody 2. The antibody FB blocking antibody 1 was not available to be tested due to depletion of all existing stocks. Downstream anaphylatoxin (C3a and C5a) generation was subsequently assessed by MSD. Both C3a (**Figure 4-1A**) and C5a (**Figure 4-1B**) were successfully detected in the zymosan-activated plasma. Pre-treatment of activated plasma with FB Inhibitor 1, FB Inhibitor 2 or FB blocking antibody 2 caused a concentration-dependent and statistically significant ($p<0.05$) reduction in C3a and C5a generation when compared to the untreated negative control. Inhibition of anaphylatoxin generation by these FB inhibitors was comparable to the inhibition observed with the positive control for AP blockade, EDTA. Moreover, the respective vehicle control for the small-molecules (DMSO) and the isotype control for antibody FB blocking antibody 2 (mIgG1, κ) had no effect on anaphylatoxin generation. The small inset graphs in **Figure 4-1A** and **Figure 4-1B** represent the respective negative controls of this assay confirming that anaphylatoxin generation is a specific response to zymosan activation i.e. mobilisation of AP. Moreover, zymosan itself is not a 'source' for complement, but rather mobilises complement proteins in the plasma to drive AP and hence anaphylatoxin generation. However, it should be noted that low levels of C3a and C5a were observed in non-activated plasma and are most likely a consequence of the steady state 'tick-over' response or activation of the serum during preparation and/or handling.

Finally, **Figure 4-1C** shows data from an additional experiment in which the antibodies FB blocking antibody 1, FB blocking antibody 2 and the isotype control (mIgG1, κ) were assessed for their capacity to inhibit haemolysis. Normal human serum (NHS) was incubated with rabbit erythrocytes to initiate terminal membrane attack complex (MAC)-induced pore formation and cell lysis (Mollnes et al., 2007). The subsequent release of haemoglobin was measured by ELISA. Both antibodies negatively regulated haemolysis in a concentration-dependent manner, when compared to the isotype control.

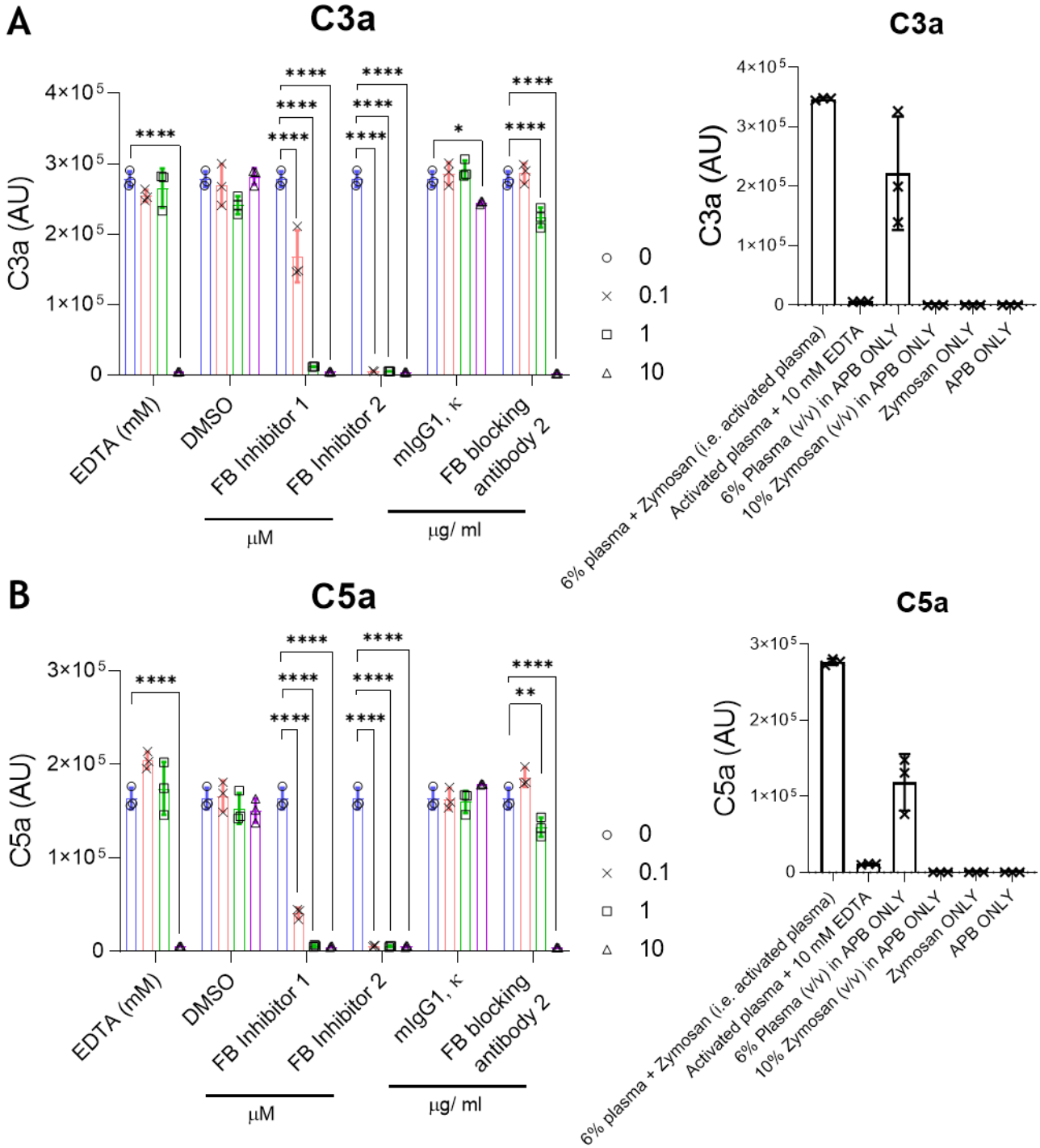

A
C3a
C3a (AU)
4×10^5
3×10^5
2×10^5
1×10^5
0
****
*
EDTA (mM)
DMSO
FB Inhibitor 1
FB Inhibitor 2
mIgG1, κ
FB blocking antibody 2
μM
μg/ ml
0
0.1
1
10
C3a
C3a (AU)
6% plasma + Zymosan (i.e. activated plasma)
Activated plasma + 10 mM EDTA
6% Plasma (v/v) in APB ONLY
10% Zymosan (v/v) in APB ONLY
Zymosan ONLY
APB ONLY
B
C5a
C5a (AU)
3×10^5
2×10^5
1×10^5
0
****
**
EDTA (mM)
DMSO
FB Inhibitor 1
FB Inhibitor 2
mIgG1, κ
FB blocking antibody 2
μM
μg/ ml
0
0.1
1
10
C5a
C5a (AU)
6% plasma + Zymosan (i.e. activated plasma)
Activated plasma + 10 mM EDTA
6% Plasma (v/v) in APB ONLY
10% Zymosan (v/v) in APB ONLY
Zymosan ONLY
APB ONLY
C
Human Serum
Percentage lysis
120
100
80
60
40
20
0
-9
-8
-7
-6
Log10Antibody Concentration (M)
hIgG1, κ (batch #1)
hIgG1, κ (batch #2)
Epofix
FB blocking antibody 5
FB blocking antibody 1
rIgG2a, κ
FB blocking antibody 4
FB blocking antibody 3
mIgG1, κ
FB blocking antibody 2

Figure 4-1 Assessment of the inhibitory potential of the following GSK assets: the small molecules FB Inhibitor 1, FB Inhibitor 2 and the antibodies FB blocking antibody 1 and FB blocking antibody 2 on alternative-pathway derived anaphylatoxins C3a and C5a.
(A) and (B) 6% NHP (pooled from multiple donors) was pre-treated with 0.1, 1 or 10 μM FB Inhibitor 1 or FB Inhibitor 2 and 0.1, 1 or 10 μg/ml FB blocking antibody 2 or the isotype control (mIgG1, κ), prior to activation with zymosan. 0.1, 1 and 10 mM EDTA were used as a positive control for AP inhibition. Samples (n=3 technical replicates per condition) were incubated at 27°C for 90 mins prior to stopping the reaction with EDTA. Samples were diluted 1:50 and run in triplicates. C3a (A) and C5a (B) generation was quantified by MSD. The smaller graphs on the right hand side show steady state anaphylatoxin generation in the negative control samples. Error bars represent mean ± SD. Statistical significance was determined by a two-way ANOVA, followed by Dunnett's post-hoc multiple comparisons test where ****$p<0.0001$, ***$p<0.001$, **$p<0.01$ and $p<0.05$ (when compared to untreated negative control).
(C) This experiment was conceptualised and performed by Isabelle Osuch. NHS was incubated with rabbit erythrocytes at 37°C in APB, initiating membrane attack complex (MAC)-induced pore formation and cell lysis. The subsequent release of haemoglobin was measured at OD 405nm and 540nm. The antibodies FB blocking antibody 1, FB blocking antibody 2, the isotype control (mIgG1, κ) along with additional GSK assets were assessed for their inhibition of NHS-induced haemolysis (via AP) and a concentration-response curve was generated.
NHP: normal human plasma, NHS: normal human serum. ns: non-significant, APB: alternative pathway buffer, AU: arbitrary units, DMSO: dimethyl sulfoxide.

In conclusion, all four inhibitors successfully targeted Factor B to inhibit mobilisation of AP activation and downstream anaphylatoxin generation. Therefore, the inhibitory potential of these assets will subsequently be assessed in MdDCs.

4.2 ANTIBODY-MEDIATED BLOCKADE OF FACTOR B

As it is speculated that the Factor B blocking antibodies do not cross the plasma membrane, they were employed to assess the importance of cell-derived 'extracellular' Factor B and hence extracellular C3 convertase in the modulation of MdDC effector function. The binding specificity of both antibodies was initially validated by Western Blot. As shown in **Figure 4-2A**, FB blocking antibody 1 showed binding specificity for intact Factor B (~93 kDa) and its cleavage component Ba (~30 kDa). Conversely, FB blocking antibody 2 was specific for cleavage component Bb (~61 kDa) along with intact protein (**Figure 4-2B)**. As Bb is the component of the functional AP C3 convertase (C3bBb), FB blocking antibody 2 was predicted to have greater efficacy in the modulation of MdDC functional response, when compared to its counterpart FB blocking antibody 1 which does not bind Bb.

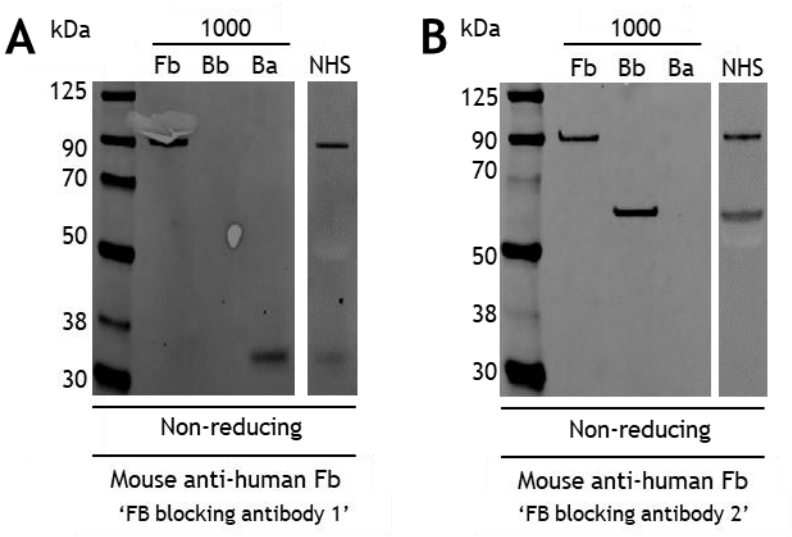


Figure 4-2 Binding of Factor B by 2 Factor B-blocking antibodies.
Target validation by Western Blot of two monoclonal Factor B blocking antibodies named FB blocking antibody 1 (A) and FB blocking antibody 2 (B). Although both antibodies recognise full length Factor B (~93kDa), FB blocking antibody 1 preferentially binds the Ba subunit (~30kDa; left panel), whereas clone FB blocking antibody 2 preferentially binds the Bb subunit (~61kDa; left panel). Purified Fb, Bb and Ba proteins used at 1000ng/ml diluted in 1x PBS. NHS (activated) was used as a positive control for alternative pathway complement activation kDa: kilodalton, NHS: normal human serum.

To assess the modulation of MdDC effector function by these antibodies, cells were pre-treated with 10 µg/ml FB blocking antibody 1 or FB blocking antibody 2 (or the respective isotype control) prior to stimulation with 2 µg/ml CD40L, 10 ng/ml LPS, 10 µg/ml R-848, a combination of both CD40L and LPS or a combination of both CD40L and R-848 overnight in complete medium (RPMI plus 10% FCS). The 10 µg/ml antibody concentration was chosen for this assay, as 100% inhibition of plasma C3a and C5a generation had previously been observed (**Figure 4-1A** and **Figure 4-1B**).

As shown in **Figure 4-3A**, viability as determined by cells negative for aqua fluorescent dye (measured by flow cytometry) was unchanged (between 70-90%) for all but one of the tested donors. Surface expression of the activation marker CD86, visualised by mean fluorescence (**Figure 4-3B**) was up-regulated upon stimulation with all tested ligands when compared to the unstimulated control. However, statistical significance ($p<0.05$) was only observed for two out of five of these activation conditions: 10 ng/ml LPS and CD40L/LPS. Subsequent analysis of the antibodies FB blocking antibody 1 and FB blocking antibody 2 in each stimulation condition had no effect when compared to the isotype control i.e. there was no statistically significant difference ($p>0.05$) in viability (**Figure 4-3A**) or CD86 surface expression (**Figure 4-3B**) when compared to the isotype control (irrespective of the stimulation condition).

Analysis of cytokine secretion revealed an up-regulation in both IL-12p40 (**Figure 4-4A**) and IL-12p70 (**Figure 4-4B**) secretion upon stimulation with all tested ligands, when compared to the unstimulated negative control. Once again, statistical significance ($p<0.05$) was only observed in some, but not all activation conditions. In the case of IL-12p70, significance was observed for both CD40L/LPS and CD40L/R-848, most likely due to the synergistic effects of ligand combination. Pre-treatment with the antibodies FB blocking antibody 1 and FB blocking antibody 2 in each stimulation condition had no statistically significant effect ($p>0.05$) on cytokine secretion when compared to the isotype control. It should also be noted that a

logarithmic y-axis scale was chosen to visualise both data sets due to the high variations between donor responses.

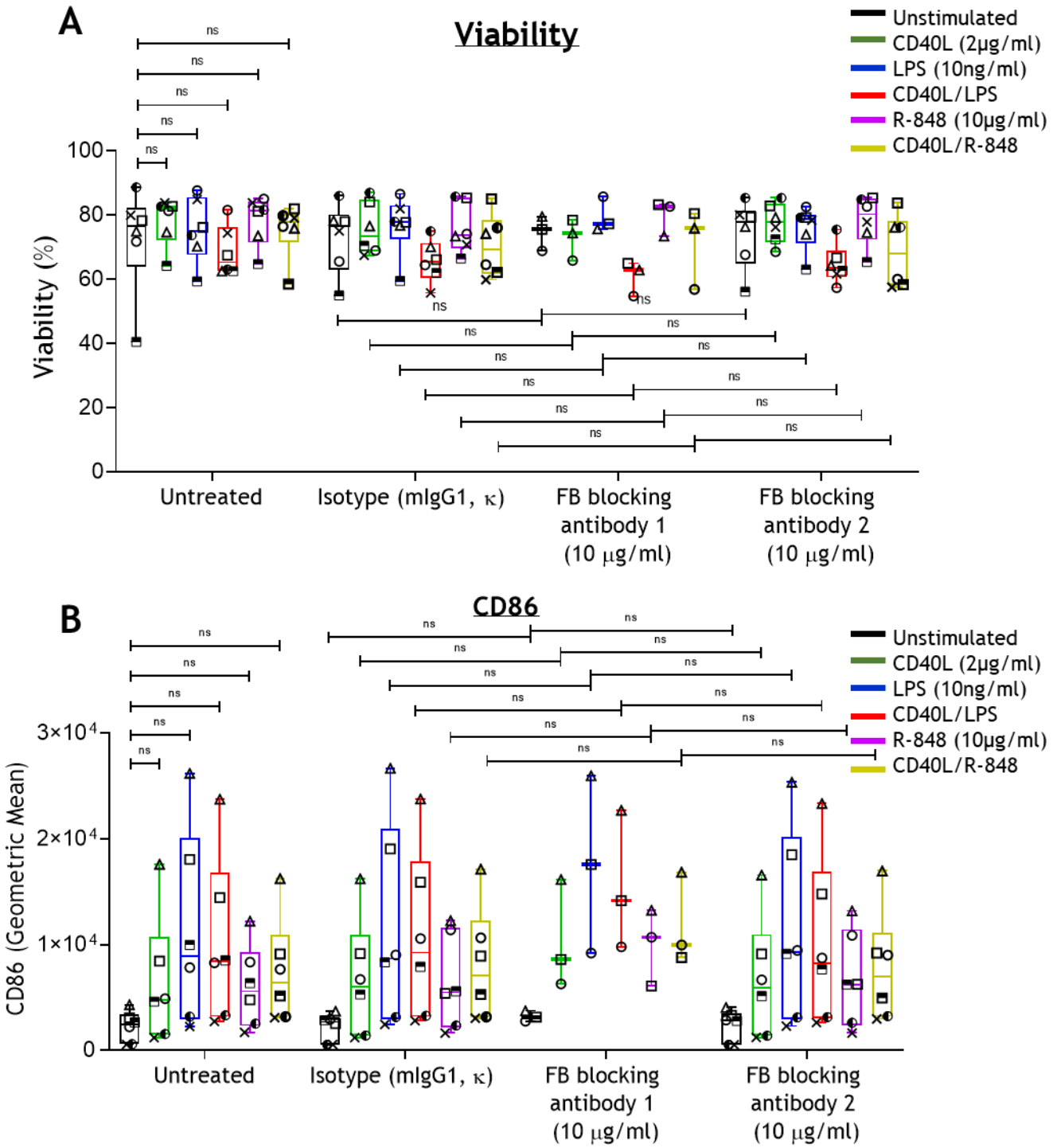


Figure 4-3 Influence of inhibition of (intracellular) Factor B by 2 Factor B-blocking antibodies
MdDCs were stimulated with CD40L (2µg/ml), LPS (10ng/ml), R-848 (10µg/ml) or a combination of both ligands overnight, in Complete Medium (RPMI plus 10% FCS). Cells were pre-treated with the Factor B-blocking antibodies (10µg/ml) or the isotype control (IgG1a, 10µg/ml) for ~20mins before stimulation. Viability (A) and CD86 (B) surface expression profiles, visualised as MFI (mean fluorescent intensity) were assessed by flow cytometry. Each symbol represents a different donor (one technical replicate per donor), with 3 to 6 donors/ condition. Data is visualised using a box and whisker plot where the box includes the upper quartile, median and lower quartile of the data set. The whiskers (error bars) represent the lowest and highest values. Statistical significance was calculated using a two-way analysis of variance (ANOVA), followed by Dunnett's multiple comparisons test where *$p<0.05$, **$p<0.01$, ***$p<0.001$ and ****$p<0.0001$. The first post-test assessed the effect of stimulation, compared to the unstimulated negative control (in the untreated condition); the second post-test compared effect of blocking antibody, compared to the negative isotype control (in each stimulation condition).

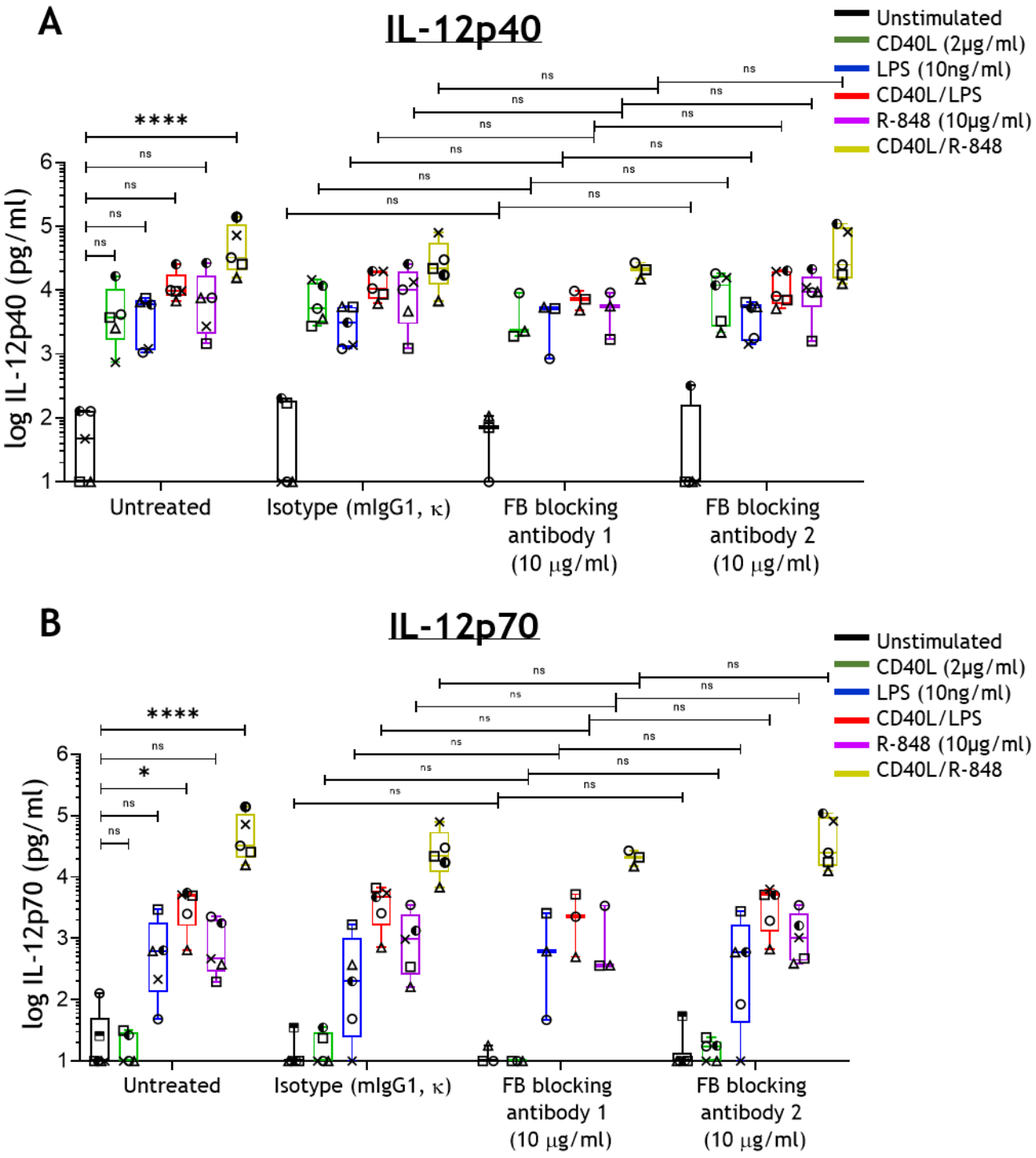


Figure 4-4 Influence of inhibition of (intracellular) Factor B by Factor B-blocking antibodies
MdDCs were stimulated with CD40L (2µg/ml), LPS (10ng/ml), R-848 (10µg/ml) or a combination of both ligands overnight, in Complete Medium (RPMI plus 10% FCS). Cells were pre-treated with the Factor B-blocking antibodies (10 µg/ml) or isotype control (IgG1a, 10 µg/ml) for ~20mins before stimulation. IL-12p40 (A) and IL-12p70 (B) were assessed by a bead-based flow cytometric assay. Each symbol represents a different donor (one technical replicate per donor), with 3 to 6 donors/ condition. Dotted line at 9.9 pg/ml (A) and 1.0 pg/ml (B) represents LLOD (lower limit of detection) of this assay Data is visualised using a box and whisker plot where the box includes the upper quartile, median and lower quartile of the data set. The whiskers (error bars) represent the lowest and highest values. Statistical significance was calculated using two-way analysis of variance (ANOVA), followed by Dunnett's multiple comparisons test where *p<0.05, **p<0.01, ***p<0.001 and ****p<0.0001. The first post-test assessed the effect of stimulation, compared to the unstimulated negative control (in the untreated condition); the second post-test compared effect of blocking antibody, compared to the negative isotype control (in each stimulation condition).

4.3 SMALL MOLECULE-MEDIATED INHIBITION OF FACTOR B

As 'extracellular' antibody-mediated blockade of Factor B had no effect on MdDC effector function, cell permeable small-molecule inhibitors were used to explore potential effects of 'intracellular' Factor B signalling. It was speculated that MdDCs may retain Factor B intracellularly, following *de novo* generation. In turn, MdDC-derived Factor B may form part of a functional C3 convertase inside of the cell, as no difference in functional response was observed with cell impermeable anti-Factor B antibodies.

As shown in **Figure 4-5**, the plasma membrane permeability of FB Inhibitor 1 and FB Inhibitor 2 was confirmed by mass spectrometry. Specifically, monocytes were pre-treated for 15 minutes with 10 µM small-molecule prior to stimulation with LPS over a 2-hour period. Although both small-molecules were detected within the cell lysate; FB Inhibitor 1 (~2 µM, left panel) exhibited ~10-fold greater plasma membrane permeability than FB Inhibitor 2 (~0.2 µM; right panel).

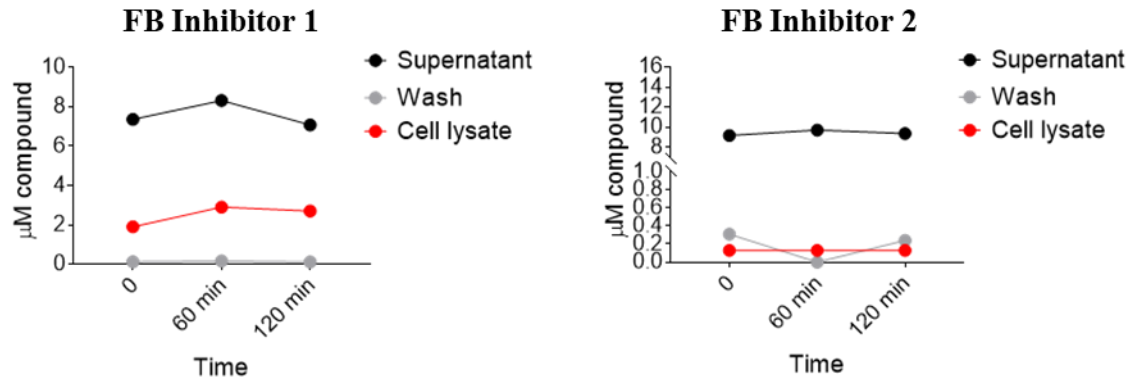


Figure 4-5 Assessment of the plasma membrane permeability of small molecule FB Inhibitor 1 and FB Inhibitor 2 by mass spectrometry
Monocytes were pre-treated with the small-molecule inhibitors for 15 minutes followed by stimulation with 100 ng/ml LPS. Cell lysate, wash and supernatant was collected at 60 and 120 mins following stimulation. Note '0' represents non-activated cells.
Experiment performed by Martin Kolev and members of GSK's Medicinal Chemistry department.

To assess the modulation of MdDC effector function by the small-molecule inhibitors, cells were pre-treated with 10 µM of FB Inhibitor 1, FB Inhibitor 2 or the vehicle control DMSO (which was also diluted in RPMI-1640 at the same v/v ratio as the small molecules) for ~20 minutes at room temperature. Cells were then stimulated with 2 µg/ml CD40L, 10 ng/ml LPS, 10 µg/ml R-848, a combination of both CD40L and LPS or a combination of both CD40L and R-848 overnight in complete medium (RPMI plus 10% FCS).

As shown in **Figure 4-6A**, cell viability determined by cells negative for aqua fluorescent dye (measured by flow cytometry) was relatively constant (>60%) for all but one tested donor. Furthermore, there was no statistically significant difference in viability when comparing the different stimulation conditions to the unstimulated negative control ($p>0.05$). Cell viability was also unchanged upon treatment with the small molecule inhibitors when compared to the vehicle control, in each stimulation condition ($p>0.05$) confirming that the compounds were not cytotoxic at 10 µM (**Figure 4-6A**).

Surface expression of the activation marker CD86, measured as mean fluorescent intensity was up-regulated upon stimulation with all tested ligands, when compared to the negative unstimulated control (**Figure 4-6B**). However, statistical significance was only observed in two out of the five stimulation conditions: LPS and CD40L/ LPS ($p<0.05$). Although a slight decrease in CD86 surface expression was observed in all activation conditions following pre-treatment with 10 µM FB Inhibitor 1 (in all stimulation conditions) when compared to the negative vehicle control, this decrease did not reach statistical significance ($p>0.05$). FB Inhibitor 2 also did not induce statistically significant CD86 down-regulation when compared to the vehicle control ($p>0.05$), irrespective of stimulation condition.

Subsequent analysis of cytokine secretion showed an up-regulation of IL-12p40 (**Figure 4-7A**) and IL-12p70 (**Figure 4-7B**) upon addition of all tested activating ligands, when compared to

the unstimulated negative control. However, statistical significance ($p<0.05$) was only observed in two stimulation conditions: CD40L/LPS and CD40L/R-848, most likely due to the synergistic effects of ligand combination. As shown in **Figure 4-7A**, IL-12p40 was slightly reduced in the presence of FB Inhibitor 1 but not FB Inhibitor 2. Although this trend was observed across all stimulation conditions, statistical significance ($p>0.05$) was never reached in two conditions: CD40L/LPS and 10 µg/ml R-848. Moreover, IL-12p70 secretion (**Figure 4-7B**) was also reduced in the presence of FB Inhibitor 1 but not FB Inhibitor 2. Statistical significance ($p<0.05$) was reached in the following three stimulations: 10 ng/ml LPS, 10 µg/ml R-848 and a combination of both CD40L/R-848.

In conclusion, this work may suggest that small molecule but not antibody-mediated inhibition of Factor B and potentially AP mobilisation negatively regulates dendritic cell (DC) effector function. A reduction in MdDC effector response may be a consequence of loss of cell-derived anaphylatoxin i.e. C3a. This hypothesis will be tested using different molecular biology approaches, as described next. However, a statistically significant down-regulation was only observed in certain experimental conditions (and only for IL-12p70 but not IL-12p40). Therefore, further optimisation of experimental conditions will be required including reducing the concentrations of the respective activating stimuli. Whilst the concentrations of the ligands were titrated down in smaller pilot experiments, the addition of Factor B inhibitors at these lower concentrations was not tested. One may speculate that at lower ligand concentrations, only 50- to 70% of the maximal activation response will be observed versus currently where saturation of response is observed – potentially enabling the role of complement in the modulation effector response to be more conspicuous.

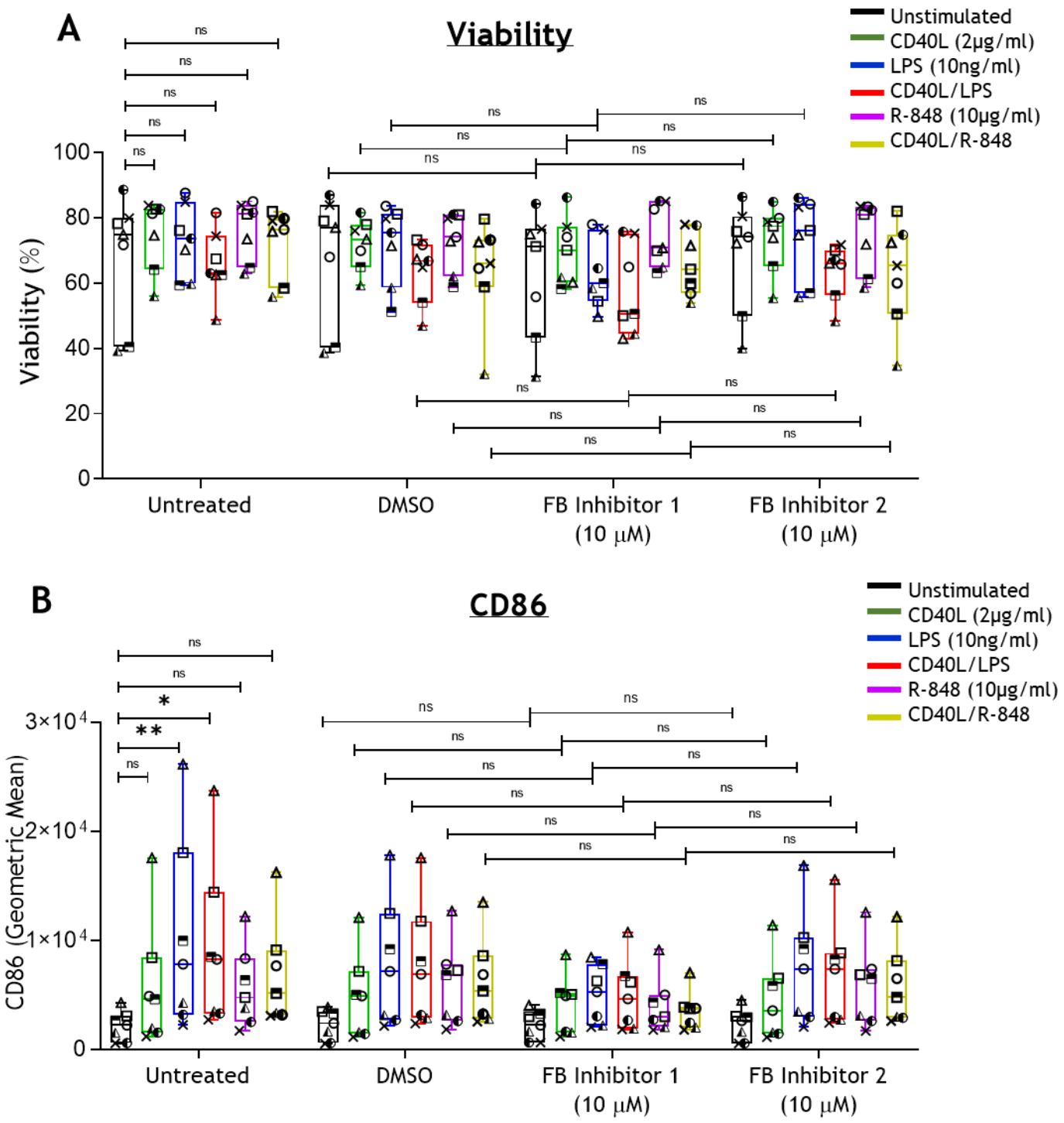


Figure 4-6 Inhibition of Factor B by the small-molecule inhibitors FB Inhibitor 1 and FB Inhibitor 2 in MdDCs

MdDCs were stimulated with CD40L (2µg/ml), LPS (10ng/ml), R-848 (10µg/ml) or a combination of both ligands overnight, in Complete Medium (RPMI plus 10% FCS). Cells were pre-treated with the small-molecule inhibitors (10µM) or vehicle control (DMSO) for ~20mins before stimulation. Viability (A) and CD86 (B) surface expression profiles, visualised as MFI (mean fluorescent intensity) were assessed by flow cytometry. Data is visualised using a box and whisker plot where the box includes the upper quartile, median and lower quartile of the data set. The whiskers (error bars) represent the lowest and highest values. Statistical significance was calculated using a two-way analysis of variance (ANOVA), followed by Dunnett's multiple comparisons test where *p<0.05, **p<0.01, ***p<0.001 and ****p<0.0001. The first post-test assessed the effect of stimulation, compared to the unstimulated negative control (in the untreated condition); the second post-test compared effect of small molecule inhibitor, compared to the negative vehicle control (in each stimulation condition).

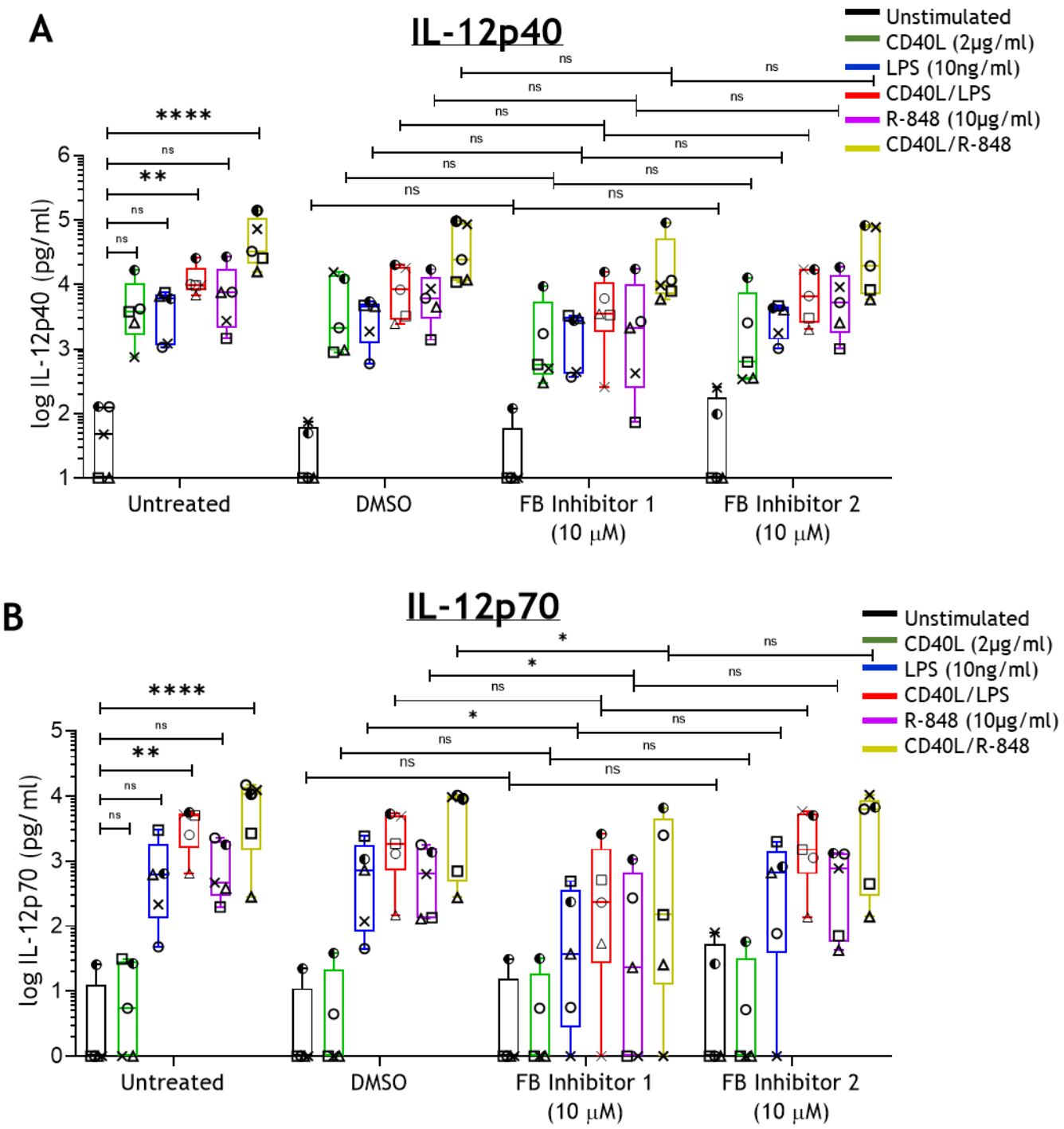


Figure 4-7 Inhibition of Factor B by the small-molecule inhibitors FB Inhibitor 1 and FB Inhibitor 2 in MdDCs

MdDCs were stimulated with CD40L (2µg/ml), LPS (10ng/ml), R-848 (10µg/ml) or a combination of both ligands overnight, in Complete Medium (RPMI plus 10% FCS). Cells were pre-treated with the small-molecule inhibitors (10µM) or vehicle control (DMSO) for ~20mins before stimulation. IL-12p40 (A) and IL-12p70 (B) were assessed by a bead-based flow cytometric assay. Each symbol represents a different donor (one technical replicate per donor), with 5 to 7 donors/ condition. Dotted line at 9.9 pg/ml (C) and 1.0pg/ml (D) represents LLOD (lower limit of detection) of this assay Data is visualised using a box and whisker plot where the box includes the upper quartile, median and lower quartile of the data set. The whiskers (error bars) represent the lowest and highest values. Statistical significance was calculated using a two-way analysis of variance (ANOVA), followed by Dunnett's multiple comparisons test where *p<0.05, **p<0.01, ***p<0.001 and ****p<0.0001. The first post-test assessed the effect of stimulation, compared to the unstimulated negative control (in the untreated condition); the second post-test compared effect of small molecule inhibitor, compared to the negative vehicle control (in each stimulation condition).

4.4 ATTEMPT AT VALIDATION OF SMALL MOLECULE INHIBITION OF FACTOR B BY ASSESSMENT OF ANAPHYLATOXIN GENERATION

4.4.1 Approach 1: Assessment of C3a and C5a secretion by MSD

As previously shown in **Figure 4-1**, FB Inhibitor 1 and FB Inhibitor 2 negatively regulates plasma C3a generation, following mobilisation of AP complement activation by zymosan. It was hypothesised that a similar phenomenon may exist in the context of DC derived C3a and downstream C5a. Therefore, cells were stimulated overnight with the same ligands and at the same concentrations as previously described i.e. 2 µg/ml CD40L, 10 ng/ml LPS, a combination of both CD40L and LPS, 10 µg/ml R-848 or a combination of both CD40L and R-848. This was followed by the assessment of C3a (**Figure 4-8A**) and C5a (**Figure 4-8B**) secretion into the extracellular space by MSD. As shown in **Figure 4-8A**, C3a within the cell culture supernatant samples (red dots) was below the lower limit of detection of the assay. Moreover, C5a within the cell culture supernatant samples was not detected by this assay (**Figure 4-8B**). However, it should be noted that this was not a technical issue associated with the specificity of the assay, as these assays successfully detected both C3a and C5a within activated NHS (**Figure 4-1**).

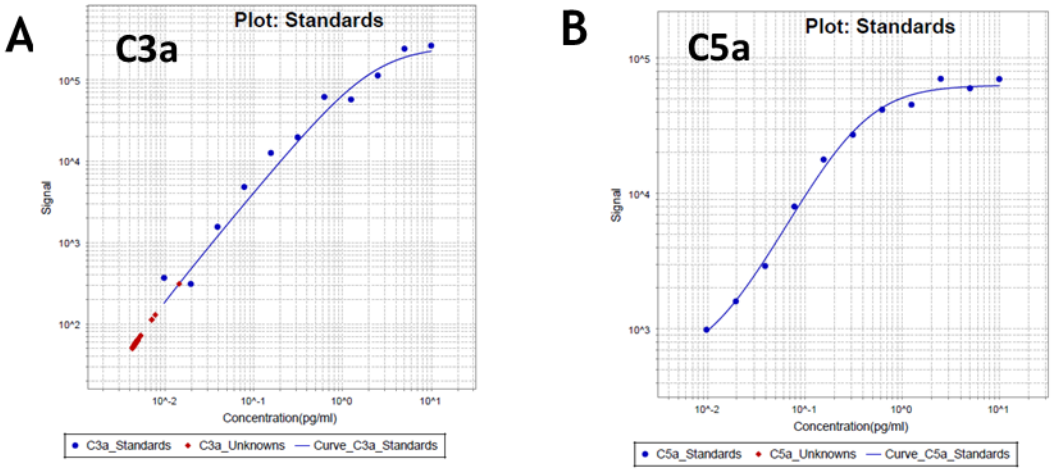


Figure 4-8 Assessment of C3a and C5a secretion by MdDCs into the extracellular space
MdDCs were stimulated with CD40L (2 µg/ml), LPS (10 ng/ml) or a combination of both ligands overnight, in complete medium. Cells were pre-treated with 10 µM FB Inhibitor 1 or DMSO for ~20mins before stimulation. The supernatants (red dots) were collected and plated neat i.e. no prior dilution. The standard curve (blue dots) starts at 10 nM, followed by eleven consecutive 1:2 dilutions. Both C3a (A) and C5a (B) were below the lower limit of detection of the assay. One MSD plot is representative of one donor (total of 2 donors tested for C3a and C5a).

4.4.2 Approach 2: Assessment of C3a generation by Western Blot

As C3a (and C5a) secretion was not detected in cell culture supernatants, it was speculated that C3a may be synthesised and retained inside of the cell. Therefore, C3a generation at steady state, upon activation and in the presence of FB Inhibitor 1 was assessed by Western Blot (**Figure 4-9**).

As shown in **Figure 4-9A**, the binding specificity of a polyclonal rabbit-anti human C3a antibody was initially assessed by Western blot using purified proteins. This antibody detected C3a (~9 kDa) but not C3 (~190 kDa) in non-reducing conditions. However, a faint band was detected at ~110 kDa in Lane 2 (500 ng/ml C3) – this may represent non-specific binding of the C3 α chain. Additional bands were observed in NHS (in both reducing and non-reducing conditions) which may represent non-specific binding of the primary or secondary antibodies. This antibody was chosen for all subsequent analyses of C3a generation in cell lysates.

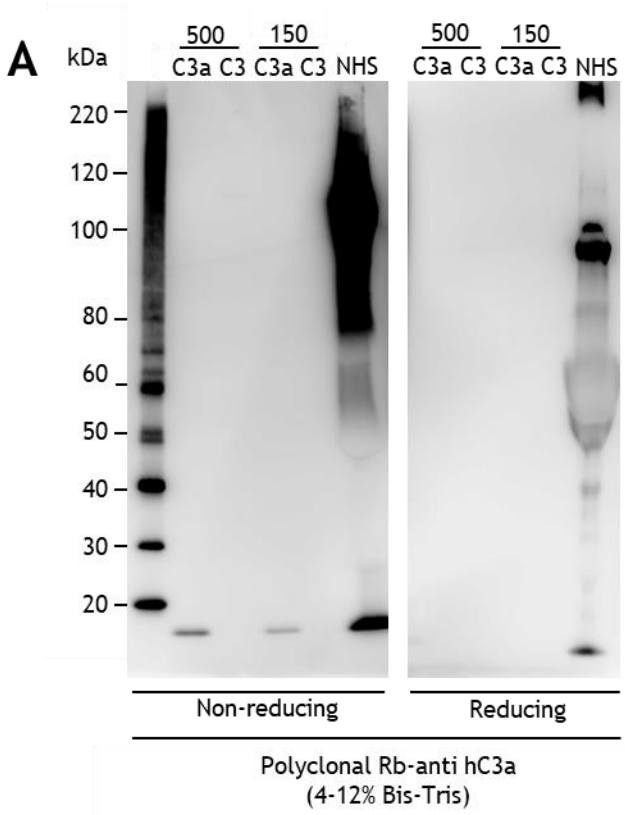
As shown in **Figure 4-9B**, MdDCs were stimulated with CD40L (2 µg/ml) or LPS (5 µg/ml) overnight in complete medium. Cell lysates (3.21 µg total protein/10 µl total reaction volume) were run on a 4-12% Bis-Tris gel in non-reducing conditions. In a similar manner to **Figure 4-9A**, purified C3a protein was once again detected but C3a within cell lysates was not (**Figure 4-9B**). Therefore, the experimental conditions were further optimised, and the experiment was repeated (**Figure 4-9C**). More specifically:

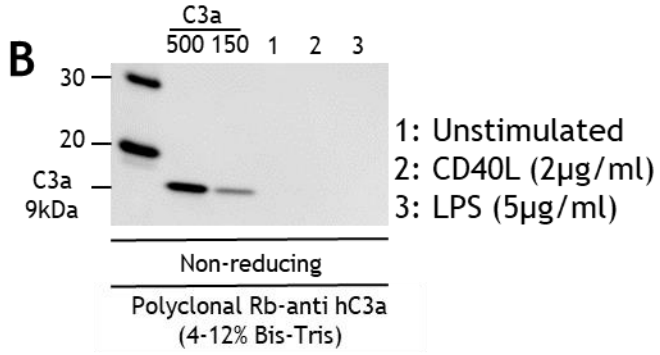
a) Cell lysate concentration was increased (22.2 µg total protein/10 µl total reaction volume) compared to samples used in **Figure 4-9B** (3.21 µg total protein/10 µl total reaction volume).
b) Cell lysates were run on a 10-20% Tricine gel rather than a 4-12% Bis-Tris gel. Features of the Tricine system include increased resolution of proteins with low molecular weights (such as C3a) and minimal protein modification due to the lower pH of the running buffer.

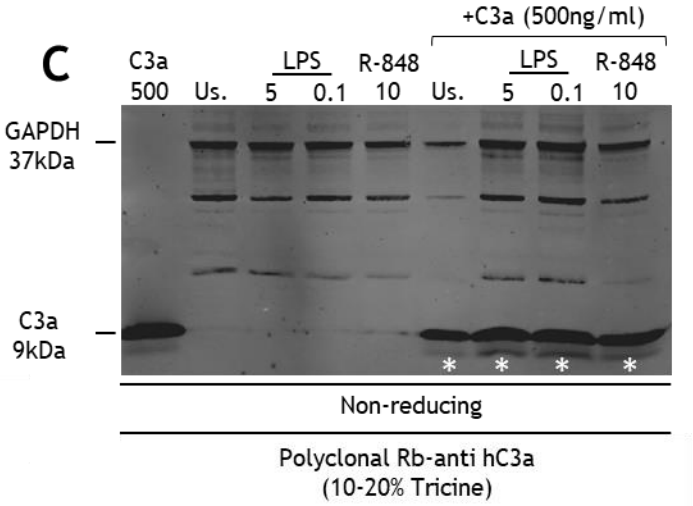
c) Purified C3a was introduced to cell lysates post-lysis to assess if protease inhibition was successful i.e. if 'spiked' C3a was not detected following addition of protease inhibitor, this would suggest the inhibitor was non-functional.

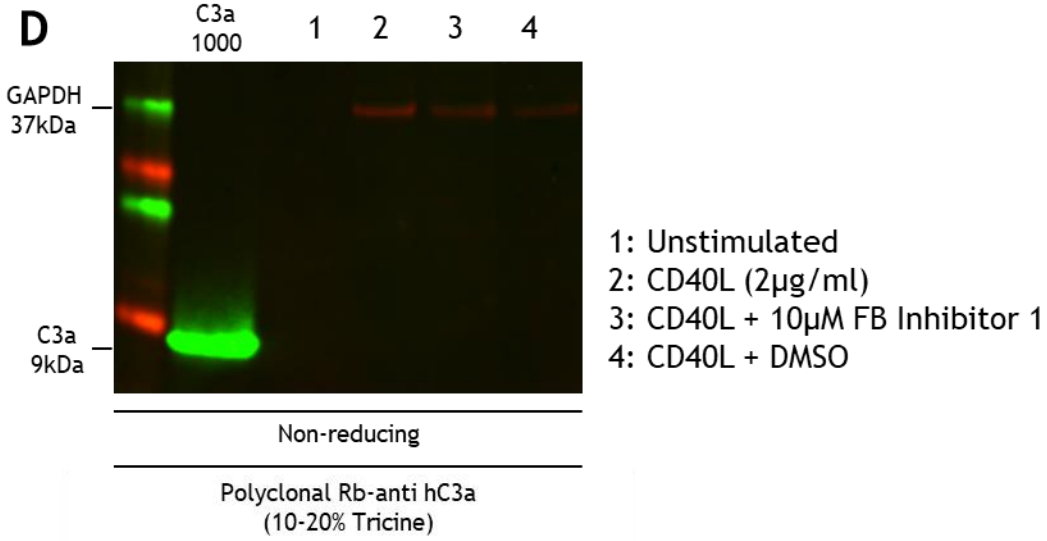
Purified C3a protein (500 ng/ml) and 'spiked' C3a protein (also at 500 ng/ml) were both detected, confirming successful protease inhibition (**Figure 4-9C**). However, C3a (~9 kDa) in cell lysate was only observed at very low levels, thus making this result difficult to interpret (**Figure 4-9C**). Moreover, a 'hybrid' C3a band was also detected (asterisks), suggesting potential protein modifications during cell lysis and Western Blot preparation. Interestingly, non-specific binding of the polyclonal antibody was also observed with 2 bands detected below GAPDH (37 kDa) but above C3a (~9 kDa). The reason for this is unclear but may be a consequence of high lysate concentrations or non-specific binding of the primary or secondary antibodies.

Finally, C3a generation was assessed in MdDCs pre-treated with FB Inhibitor 1 or the respective vehicle control. As successful blockade of MdDC effector function by FB Inhibitor 1 was observed through down-regulation of IL-12p40 (**Figure 4-9E**; left panel), it was speculated that this may be a consequence of decreased anaphylatoxin generation. However, it should be noted that the experiment in **Figure 4-9E** only represents a single donor. As shown in **Figure 4-9D**, purified C3a protein (1000 ng/ml) was detected, but C3a was not detected in cell lysates (41.7 µg total protein/ 25µl total reaction volume). Although native C3 expression was not assessed in this experiment, the up-regulation of C3 mRNA (**Figure 3-8A**) and protein secretion (**Figure 3-9A**) was previously demonstrated, following stimulation with 2 µg/ml CD40L.


A
kDa
500 150
C3a C3 C3a C3 NHS
500 150
C3a C3 C3a C3 NHS
220
120
100
80
60
50
40
30
20
Non-reducing
Reducing
Polyclonal Rb-anti hC3a
(4-12% Bis-Tris)


B
C3a
500 150 1 2 3
30
20
C3a
9kDa
1: Unstimulated
2: CD40L (2µg/ml)
3: LPS (5µg/ml)
Non-reducing
Polyclonal Rb-anti hC3a
(4-12% Bis-Tris)


C
+C3a (500ng/ml)
C3a
500
Us.
LPS
5
0.1
R-848
10
Us.
LPS
5
0.1
R-848
10
GAPDH
37kDa
C3a
9kDa
Non-reducing
Polyclonal Rb-anti hC3a
(10-20% Tricine)


D
C3a
1000
1 2 3 4
GAPDH
37kDa
C3a
9kDa
1: Unstimulated
2: CD40L (2µg/ml)
3: CD40L + 10µM FB Inhibitor 1
4: CD40L + DMSO
Non-reducing
Polyclonal Rb-anti hC3a
(10-20% Tricine)

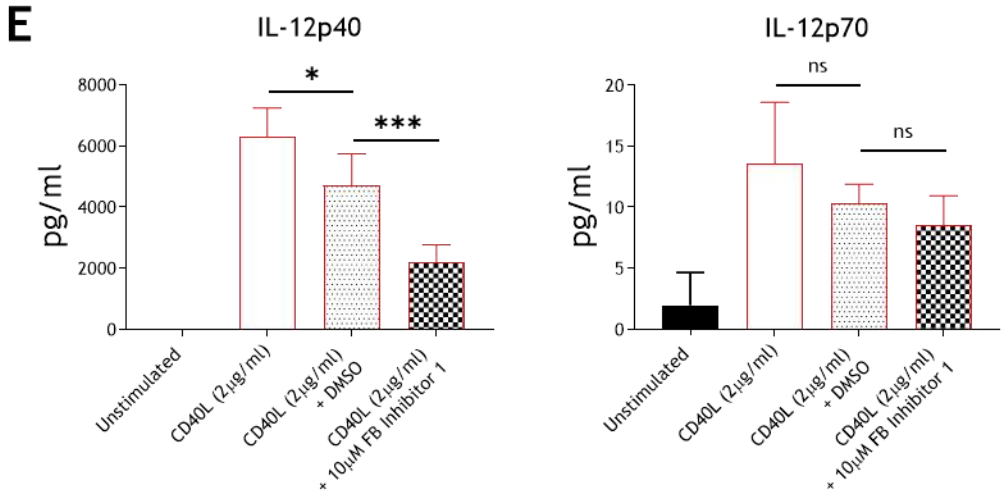

E
IL-12p40
pg/ml
8000
6000
4000
2000
0
*
***
Unstimulated
CD40L (2µg/ml)
CD40L (2µg/ml) + DMSO
CD40L (2µg/ml) + 10µM FB Inhibitor 1
IL-12p70
pg/ml
20
15
10
5
0
ns
ns
Unstimulated
CD40L (2µg/ml)
CD40L (2µg/ml) + DMSO
CD40L (2µg/ml) + 10µM FB Inhibitor 1

Figure 4-9 Assessment of intracellular C3a, as a validation readout for intracellular alternative pathway (AP) inhibition

A) Target validation of polyclonal rabbit anti-human C3a (2 µg/ml), which detects C3a but not C3 in non-reducing conditions. Purified C3a and C3 were diluted in 1x PBS and used at 500 and 150ng/ml; NHS (activated) was used as positive control for alternative pathway complement activation. Proteins were run on a 4-12% Bis-Tris gel.

B) Assessment of intracellular C3a in MdDCs, either unstimulated (Lane 1) or stimulated with 2µg/ml CD40L (Lane 2) or 5µg/ml LPS (Lane 3). Purified C3a (500 and 150 ng/ml) was used as a positive control for detection. Protein and lysates were run on a 4-12% Bis-Tris gel.

C) Assessment of intracellular C3a in MdDCs, either unstimulated or stimulated with LPS (0.1 and 5 µg/ml) and R-848 (10 µg/ml). 500 ng/ml purified C3a (diluted in 1x PBS) was used as a positive control for detection. Protein and lysates were run on a 10-20% Tricine gel.

D) Assessment of intracellular C3a in MdDCs, either unstimulated (Lane 1) or stimulated with 2 µg/ml CD40L (Lane 2). C3a was also assessed in CD40L-stimulated cells, pre-treated with FB Inhibitor 1 (Lane 3) or DMSO (Lane 4). 1000 ng/ml purified C3a (diluted in 1x PBS) was used as positive control for detection. Protein and lysates were run on a 10-20% Tricine gel.

E) Confirmation of cell activation for lysates shown in Figure 4-3D, as demonstrated by up-regulation of IL-12p40 (left panel) and IL-12p70 (right panel). Error bars represent mean ± SD. Statistical significance was calculated using one-way analysis of variance (ANOVA) followed by Dunnett's multiple comparisons test, where *$p<0.05$, **$p<0.01$ and $p<0.001$.

kDa: kilodalton, NHS: normal human serum, Rb: rabbit.

4.4.3 Approach 3: Attempt at assessment of C3a generation in a Cell-Free Assay

As C3a was only detected at very low levels in cell lysates by Western Blot, an additional approach was employed to assess the inhibitory potential of FB Inhibitor 1 on C3a generation, as a potential proxy for intracellular C3 convertase.

Specifically, AP C3 convertase and downstream anaphylatoxins were generated as demonstrated in **Figure 4-10A**. 'Reaction 1' i.e. C3bBb was incubated with 'Reaction 2' i.e. native C3, Factor B and Factor D at 21°C for either 30 or 60 minutes. The relevant negative controls i.e. absence of C3, Factor B or Factor D in 'Reaction 2' were also included to ensure that C3a observed generation was a consequence of successful mobilisation of AP.

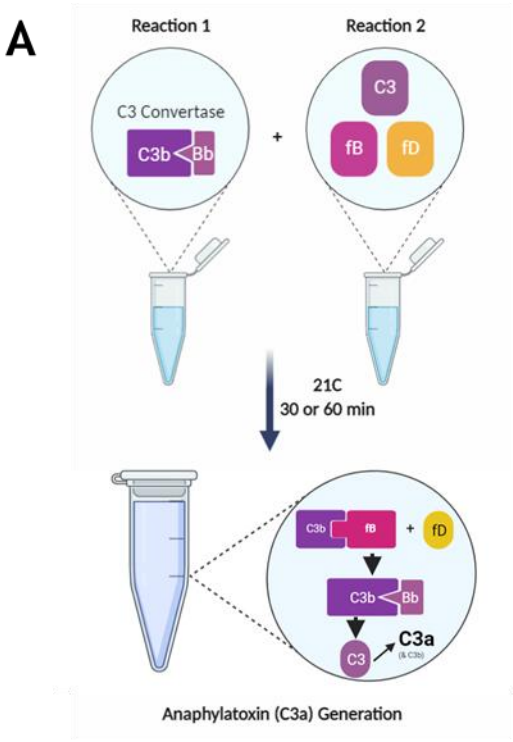
All AP proteins of interest including purified C3a, when run on a 4-12% Bis-Tris gel in non-reducing conditions were detected by silver staining (**Figure 4-10B**). However, C3a generation was not observed following AP activation in the cell-free assay (**Figure 4-10C**). Specifically, C3a detection in Lane 4 (i.e. the positive control) or Lanes 1-3 (the negative controls) was not observed at either 30- or 60-minutes post-heating at 21°C. Therefore, the effect of pre-treatment with the AP inhibitor EDTA (Lane 5), FB Inhibitor 1 (Lane 6) or its vehicle control DMSO (Lane 7) on downstream C3a generation could not be determined.

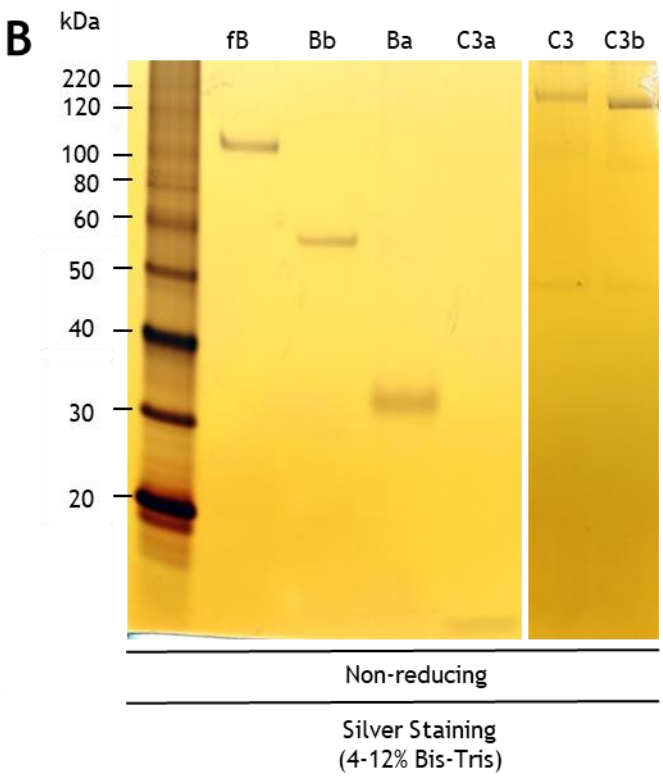
Finally, as shown in **Figure 4-10D** the cell-free assay was optimised further in the following ways to further aid C3a detection:

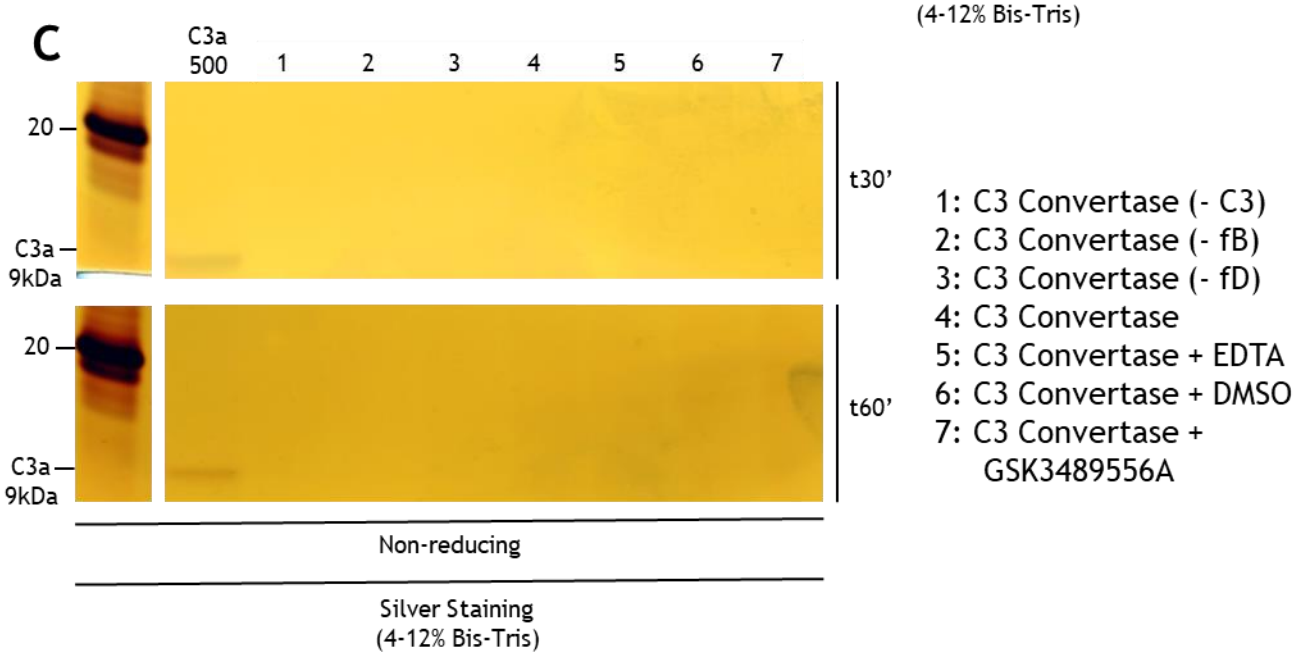
a) The total reaction volume was reduced from 200µl to 100 and 50 µl, with the ratio of individual protein concentrations remaining constant. The rationale for this change was to increase the concentration of the overall reaction, thus increasing the probability of detecting C3a.

b) Samples were run on a 10-20% Tricine gel to increase the resolution of proteins with low molecular weights (such as C3a) and reduce protein modification due to the lower pH of the running buffer.

c) A Western blot (fluorescence readout) with greater sensitivity was employed. Although purified C3a protein (500 ng/ml) was successfully detected by Western blot, C3a generation post-C3 convertase formation was not observed irrespective of the total reaction volume used (**Figure 4-10D**).


A
Reaction 1
Reaction 2
C3 Convertase
C3b
Bb
C3
fB
fD
21C
30 or 60 min
C3b
fB
fD
C3b
Bb
C3a
C3
Anaphylatoxin (C3a) Generation


B
kDa
fB
Bb
Ba
C3a
C3
C3b
220
120
100
80
60
50
40
30
20
Non-reducing
Silver Staining
(4-12% Bis-Tris)


C
C3a
500
1
2
3
4
5
6
7
20
C3a
9kDa
t30'
20
C3a
9kDa
t60'
Non-reducing
Silver Staining
(4-12% Bis-Tris)
1: C3 Convertase (- C3)
2: C3 Convertase (- fB)
3: C3 Convertase (- fD)
4: C3 Convertase
5: C3 Convertase + EDTA
6: C3 Convertase + DMSO
7: C3 Convertase +
GSK3489556A

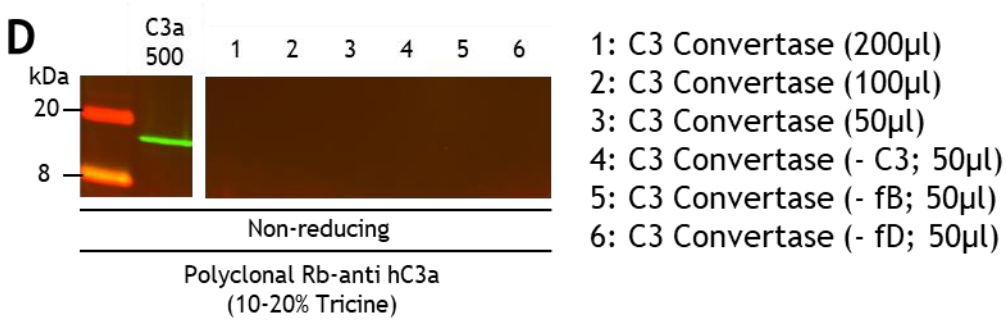

D
C3a
500
1
2
3
4
5
6
kDa
20
8
Non-reducing
Polyclonal Rb-anti hC3a
(10-20% Tricine)
1: C3 Convertase (200µl)
2: C3 Convertase (100µl)
3: C3 Convertase (50µl)
4: C3 Convertase (- C3; 50µl)
5: C3 Convertase (- fB; 50µl)
6: C3 Convertase (- fD; 50µl)

Figure 4-10 Assessment of C3a generation in a cell-free assay
(A) Schematic representation of C3 convertase generation, perpetuation and downstream anaphylatoxin (C3a) generation. (B) Optimisation of silver stain protocol using 500ng/ml purified proteins: fB (93kDa), Bb (61 kDa), Ba (30kDa), C3a (9kDa), C3 (190kDa) and C3b (175kDa). Proteins were run on a 4-12% Bis-Tris gel in non-reducing conditions. (C) Assessment of C3a generation by silver stain, in a cell free assay at 30 and 60 minutes post-combining and heating of 'Reaction 1' and 'Reaction 2' at 21°C; total reaction volume for all samples was 200µl. 500 ng/ml purified C3a was used as a positive control for detection. Protein and samples were run on a 4-12% Bis-Tris gel in non-reducing conditions. (D) Assessment of C3a generation by Western Blot, in a cell free assay at 60 minutes post-combining and heating of 'Reaction 1' and 'Reaction 2' at 21°C; total reaction volume was either 200µl, 100µl or 50µl. 500ng/ml purified C3a was used as a positive control for detection. Protein and samples were run on a 10-20% Tricine gel in non-reducing conditions. kDa: kilodalton, Rb: rabbit.

In conclusion, three different molecular biology approaches (MSD, Western Blot and Silver Staining) were developed and optimised with the sole purpose of detecting C3a at steady state and its hypothesised down-regulation in the presence of FB Inhibitor 1. However, C3a was either not detected or only detected at very low levels and hence the assessment of small-molecule mediated inhibition of C3a generation, via intracellular C3/C5 convertases remains inconclusive.

Next, CRISPR-Cas 9 genome editing will be employed to assess if loss of C3 i.e. the precursor of C3a negatively regulates cellular effector function, in a manner which is similar to previously observed with the small molecule FB Inhibitor 1.

4.5 ASSESSMENT OF COMPLEMENT EXPRESSION PROFILES IN THP-1 CELLS

To overcome the challenges associated with the transfection of primary cells such as DCs, the myelo-monocytic THP-1 cell line was employed as a model for the assessment of native complement and anaphylatoxin expression by myeloid cells. Before performing CRISPR/Cas9 mediated knockdown, THP-1 cells were assessed for complement expression at both steady state and upon activation.

As demonstrated in **Figure 4-11A** (top left panel), THP-1 cells expressed MHC Class I at steady state, which was subsequently up-regulated upon stimulation with the toll-like receptor ligand R-848 (resiquimod) when used at 10 µg/ml. The surface expression of the activation marker CD86 was only slightly up-regulated (**Figure 4-11A**, bottom left panel) following stimulation. Moreover, there was a statistically significant up-regulation in IL-12p40 secretion ($p<0.05$) following stimulation with 10 µg/ml R-848 when compared to the unstimulated negative control (**Figure 4-11B**), but statistically significant ($p<0.05$) was not achieved.

Flow cytometric analysis of total (i.e. surface plus intracellular) Complement C3 **(Figure 4-11A**, top right panel) and Factor B **(Figure 4-11A**, bottom right panel) showed high expression profiles at steady state, with only a slight increase observed upon activation with 10 µg/ml R-848. C3 expression was assessed using an Alexa Fluor™ 647 conjugated rabbit monoclonal antibody (clone: EPR2988) which was shown by the manufacturer i.e. Abcam to detect native C3 in human plasma and serum samples by Western Blot. Moreover, Factor B expression was assessed using FITC-conjugated mouse monoclonal antibody named 'FB blocking antibody 2', which was previously validated for specificity in **Figure 4-2B**.

However, Western Blot analysis of THP-1 cell lysates (25.5 µg total protein/25 µl total reaction volume) failed to detect C3a at steady state or upon activation (**Figure 4-11C**), even though

the loading control GAPDH (~37 kDa) was detected. Once again, the positive control i.e. 500 ng/ml purified C3a protein was also detected.

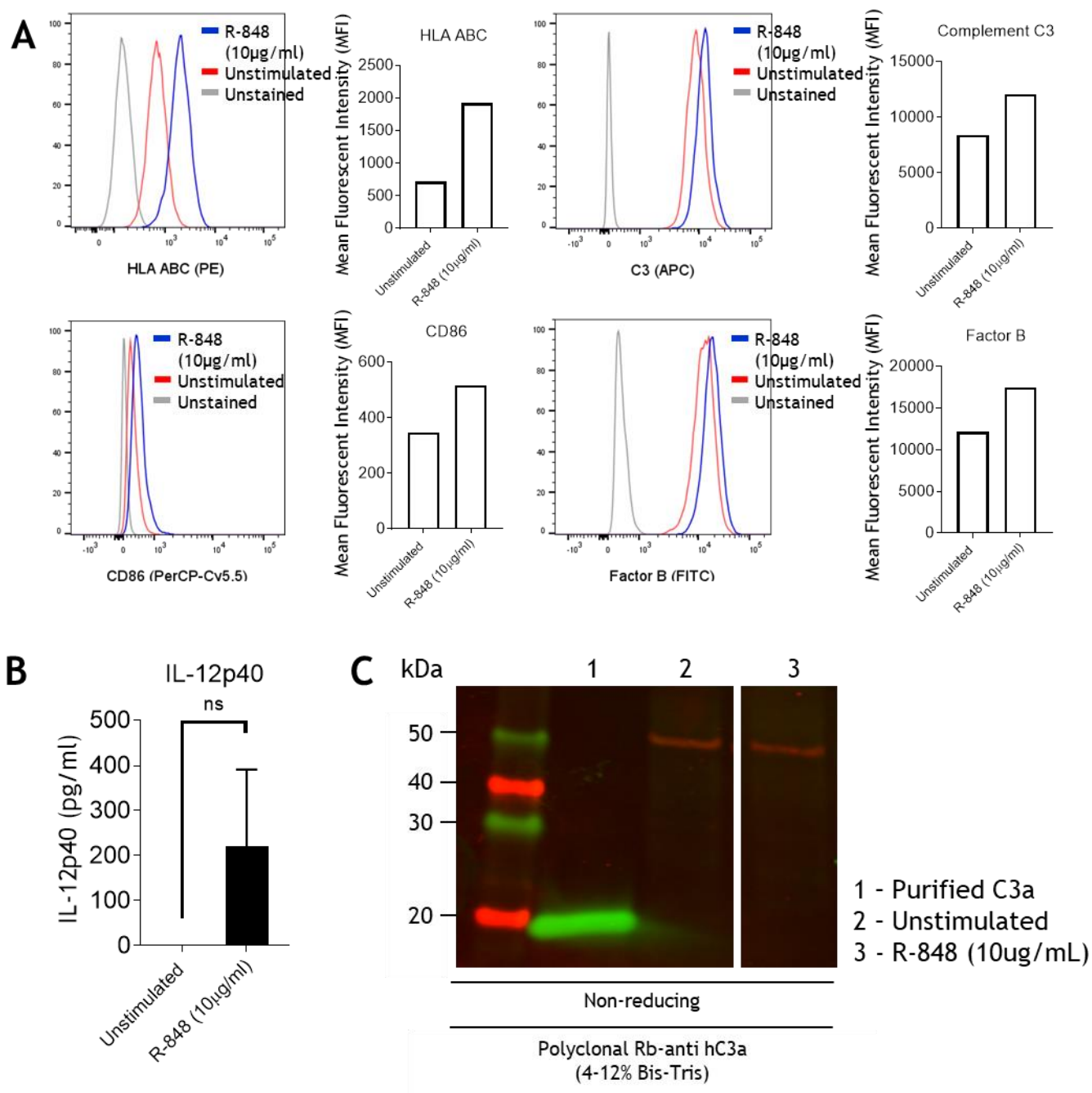


Figure 4-11 Assessment of Complement C3, Factor B and C3a expression in THP-1 cells
THP-1 cells were stimulated overnight with 10µg/ml R-848 in Complete Medium (i.e. RPMI + 10% FCS).

A) Assessment of surface expression of MHC Class I (HLA ABC) and CD86 and total (i.e. intracellular plus surface) C3 and Factor B expression, by flow cytometry. Each condition is representative of 2 technical replicates which were pooled, prior to acquisition.

B) Assessment of IL-12p40 secretion, by a bead based flow cytometric assay. Error bars represent mean ± SD (2 technical replicates/ condition). Statistical significance was calculated using an unpaired t-test between the unstimulated and stimulated conditions, in which *p<0.05, **p<0.01, ***p<0.001 and ****p<0.0001. ns: non-significant.

C) Assessment of C3a generation by Western Blot. Lane 1 shows the positive control: purified C3a (500 ng/ml; green band). The loading control GAPDH is shown in red. Protein and lysates were run on a 4-12% Bis-Tris gel. This data is from the same experiment (with one 'empty' lane spliced out, containing no protein sample).

4.6 CRISPR-CAS9 TARGETING OF COMPLEMENT C3 IN THP-1 CELLS

As C3 were detected in THP-1 cells, CRISPR guide RNAs were employed to determine if loss of C3 may negatively regulate effector function i.e. cytokine secretion.

As described in the Chapter 4 Discussion (specifically section 4.7.3), THP-1 cells were electroporated using pulse codes DP-148 (**Figure 4-12A**) or EH-115 (**Figure 4-12B**), with pooled gRNAs targeting β2 microglobulin, Complement C3 or a combination of both genes. Electroporators have multiple electrical wave form pulse settings with varying voltage, resistance and time intervals. Each cell type has a specific field strength (E) which is dependent on the pulse parameters applied. Application of optimal field strength causes permeability of the plasma membrane enabling guide RNAs to pass through. THP-1 cells were electroporated with two different pulse codes in line with previously developed protocols:

- DP-148 – this code was recommended by the manufacturer of the nucleofector (Lonza), specifically for THP-1 cells.
- EH-115 – this code was used by members of GSK's Functional Genomics department in the successful down-regulation of multiple genes including β2 microglobulin, in conventional CD4+ T cells and THP-1 cells.

As β2 microglobulin forms one of the two polypeptide chains of the widely expressed MHC I molecule, it was chosen as a positive control to measure efficient CRISPR editing. Following electroporation, THP-1 cells were maintained in complete medium (RPMI +10% FCS) for 48 hours. After this time, half of the cells were transferred to serum-free medium (SFM). The rationale for transferring cells to SFM was to assess potential compensatory up-regulation of *de novo* complement upon loss of external sources of complement e.g. from serum. Cells were subsequently maintained in either CM or SFM for a further 5 days.

As shown in **Figure 4-12A and 4-12B** (first left histogram), surface expression of the positive control HLA ABC (surrogate readout for β2 microglobulin) was down-regulated in the β2 microglobulin gRNA-treated condition when compared to the buffer treated control in THP-1 cells cultured in CM. As expected, surface expression of HLA ABC remained unchanged in the C3 gRNA-treated condition (green) and was only partially downregulated in the double β2M and C3-treated condition. A similar result was obtained for THP-1 cells cultured in SFM (**Figure 4-12A** and **4-12B**; first right histogram) except for the double KO condition in which knockdown appeared less efficient.

Total (i.e. surface plus intracellular) Complement C3 expression was also assessed by flow cytometry (**Figure 4-12A** and **4-12B**). Irrespective of the electroporation pulse code chosen, there was no change in total C3 expression in the C3 knockout or the double knockout conditions when compared to the negative buffer control in cells cultured in RPMI plus 10% FCS (Figure **4-12A** and **4-12B**; second left histograms) or serum-free medium (Figure **4-12A** and **4-12B**; second right histograms).

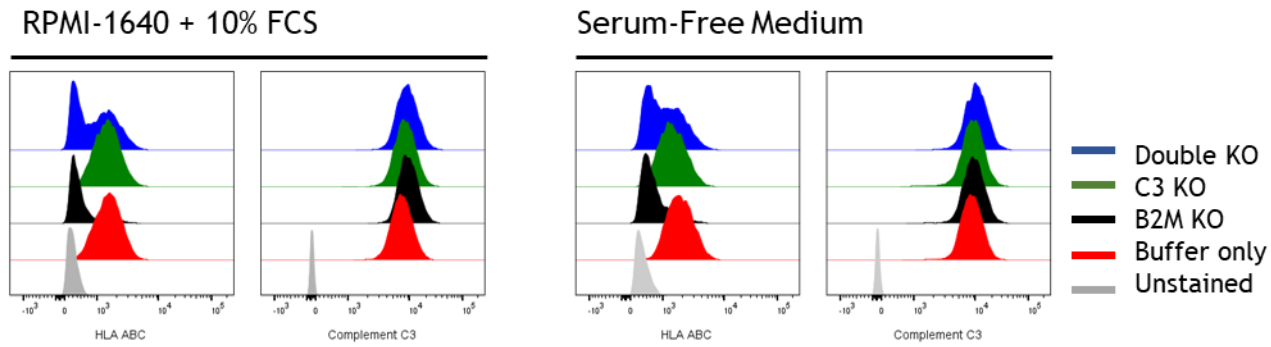
A separate experiment subsequently attempted to perform knockdown of Complement Factor B, along with knockdown of β2 microglobulin and Complement C3 in THP-1 cells (**Figure 4-12C**). It should be noted that the same pooled guide RNAs targeting β2 microglobulin and C3 used in **Figure 4-12A** and **Figure 4-12B** (which had been externally validated) were also used in **Figure 4-12C**. The guide RNAs targeting Factor B were designed using www.synthego.com (as described in the Materials & Methods section) but had not been externally validated.

THP-1 cells were electroporated using pulse code DP-148, as this provided the most robust knockdown of β2-microglobulin in the previous experiment i.e. **Figure 4-12A** and subsequently cultured in complete medium for 5 days post-CRISPR. High cell death was

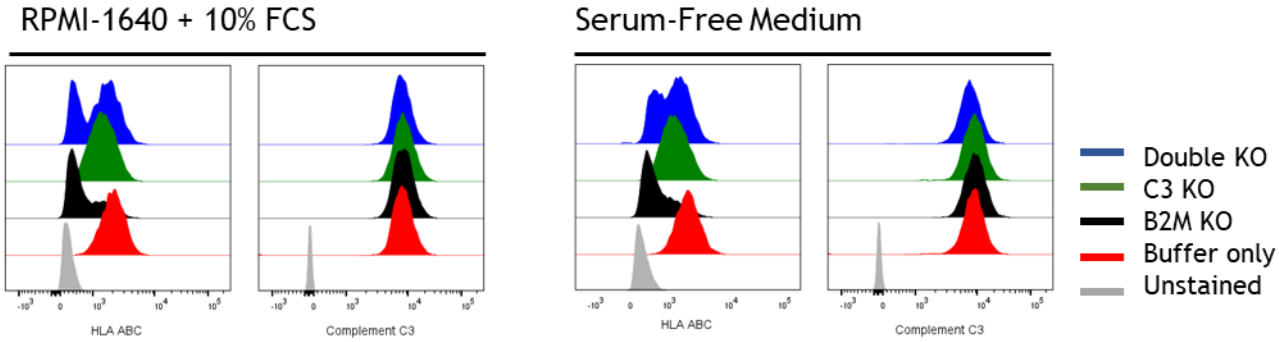
observed in all guide RNA-treated conditions (**Figure 4-12C;** top panel) but not in the buffer-treated negative control (which was also electroporated). The reason for this remains unclear.

Subsequent analysis of protein expression (by flow cytometry) revealed a slight downregulation in MHC Class I expression in the β2 microglobulin guide RNA treated condition, when compared to the negative buffer-treated control (**Figure 4-12C**; bottom left panel). No change was observed in total C3 or FB expression, in their respective guide RNA treated conditions when compared to negative buffer-treated control (**Figure 4-12C**; bottom middle and right panels). However, assessment of protein expression is confounded by the high cell death observed in this experiment.

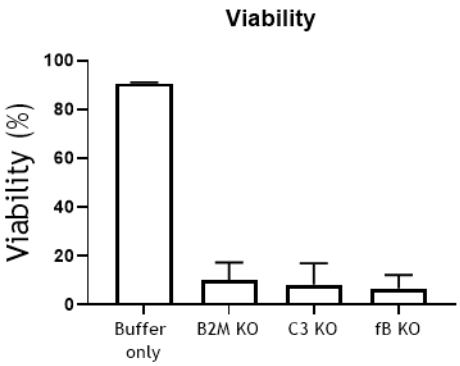
A Electroporation Pulse Code: **DP-148**



B Electroporation Pulse Code: **EH-115**



C



Electroporation Pulse Code: **DP-148** / RPMI-1640 + 10% FCS

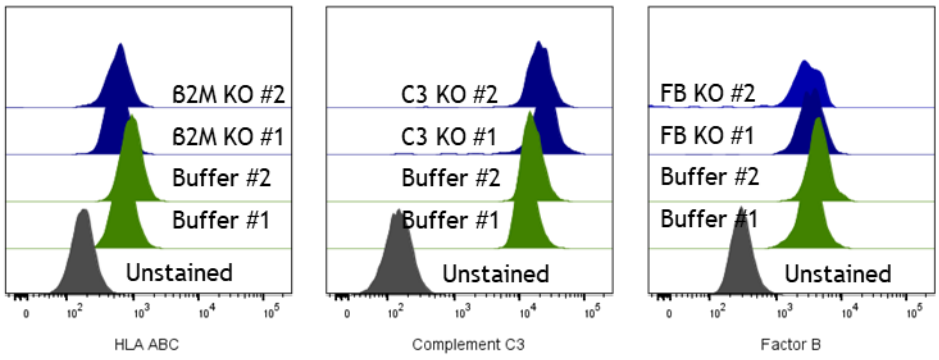


Figure 4-12 Assessment of CRISPR knockdown of the B2M and C3 genes in THP-1 cells
THP-1 cells were electroporated with pulse code DP-148 (A) or EH-115 (B) with pooled guide RNAs and cultured in Complete Medium (i.e. RPMI + 10% FCS) for 48 hours. Half of the cells (from each transfection condition) were then transferred to Serum-Free Medium, for a further 5 days. The other half remained in Complete Medium for an additional 5 days.
(A, B) Surface expression of MHC Class I (HLA ABC) and total (i.e. surface plus intracellular) C3, by flow cytometry in THP-1 cells electroporated with pulse code DP-148 and EH-115, respectively. Data representative of three individual experiments.
(C) THP-1 cells were once again electroporated with pulse code DP-148 (2 technical replicates/ condition) with pooled guide RNAs targeting β2-microglobulin, C3 and Factor B. Cells were cultured in Complete Medium (i.e. RPMI + 10% FCS) for 5 days. Viability (top panel) along with surface MHC Class I, total C3 and total FB expression (bottom panels) was assessed by flow cytometry. Data representative of two individual experiments.

Messenger RNA expression profiles of β2 microglobulin and C3 (from the experiment shown in **Figure 4-12A** and **Figure 4-12B**) were subsequently assessed by RT-qPCR (**Figure 4-13**).

As shown in Figure **4-13A** (left panel), β2 microglobulin mRNA levels were downregulated in the β2 microglobulin knockout and the double knockout conditions, when compared to the negative buffer-treated control in THP-1 cells electroporated using pulse code DP-148 (**Figure 4-13A**; left panel). This down-regulation did reach statistical significance ($p<0.05$), irrespective of the medium used for culture. An unexpected up-regulation in β2 microglobulin mRNA was observed in the C3 knockout/ SFM culture condition (**Figure 4-13A**). β2 microglobulin mRNA levels remained unchanged i.e. there was no statistically significant difference, when compared to the negative buffer treated control in THP-1 cells electroporated with pulse code EH-115 (**Figure 4-13B**; left panel). Once again, β2 microglobulin mRNA was up-regulated in the C3 knockout condition (irrespective of culture medium) – an observation which reached statistical significance (**Figure 4-13B**; left panel).

C3 mRNA levels were downregulated in the C3 knockout (~1.6 fold) and double knockout (~1.25) conditions, when compared to the negative control in THP-1 cells electroporated using pulse code DP-148 (**Figure 4-13A**; right panel). This observation reached statistical significance, irrespective of medium used for cell culture. There was also a slight up-regulation in C3 mRNA in the β2 microglobulin knockout in THP-1 cells cultured in RPMI plus 10% FCS and this observation also reached statistical significance (**Figure 4-13A**; right panel). When THP-1 cells were electroporated with pulse code EH-115, C3 mRNA was downregulated in the C3 knockout/RPMI culture condition but was upregulated in the C3 knockout/ SFM culture condition (**Figure 4-13B**; right panel). Similar results were obtained in the C3 knockout condition (**Figure 4-13B**; right panel). In the double knockout condition, C3 mRNA was upregulated, irrespective of the culture medium used (Figure **4-13B**; right panel).

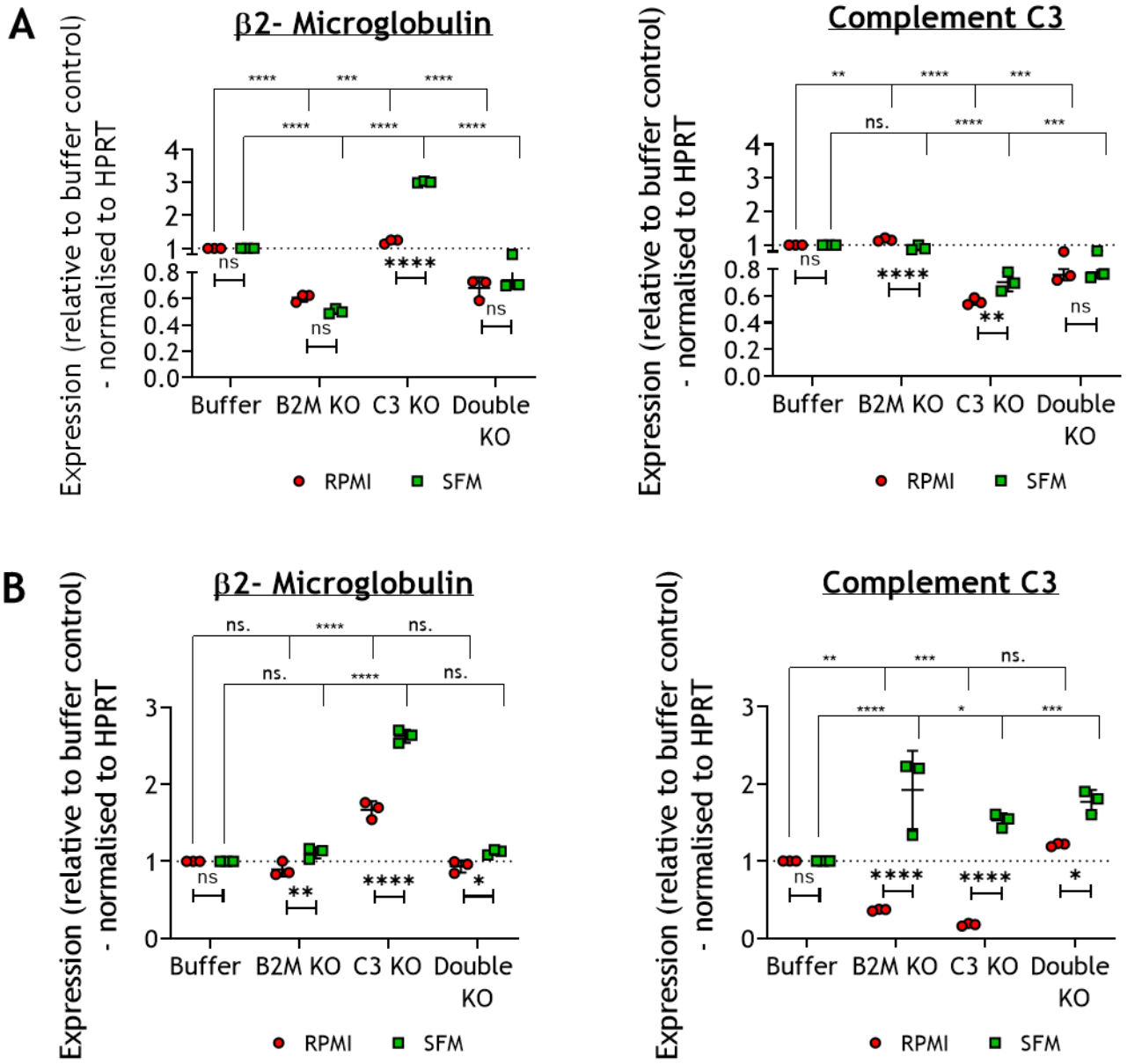


Figure 4-13 Assessment of CRISPR knockdown of the β2-macroglobulin (B2M) and C3 genes in THP-1 cells (by RT-qPCR)

Assessment of fold gene expression changes in B2M (left) and C3 (right) relative to the buffer-treated negative control (normalised to the housekeeping control HPRT) by RT-qPCR; 3 technical replicates per condition, in (A) cells electroporated using pulse code **DP-148** and (B) cells electroporated using pulse code **EH-115**. Dotted line at 1 (on *y-axis*) represents no change in fold expression, when compared to the buffer-treated negative control. Cycle threshold (CT) value ranges: HPRT (22.5 to 23.6), B2M (17.9 to 19.8), C3 (25.5 to 29.9). Error bars represent mean ± SD. Statistical significance was calculated using a two-way analysis of variance (ANOVA) followed by Dunnett's post-hoc multiple comparisons test where *p<0.05, **p<0.01, ***p<0.001,****p<0.0001, ns: not significant (RPMI vs SFM). Data representative of three individual experiments.

Following CRISPR genome editing, the THP-1 functional response was assessed upon activation with the TLR7/8 ligand R-848 (resiquimod). The rationale for assessment of THP-1 functional responses following CRISPR genome editing was to determine whether an effect similar to that observed with small-molecule Factor B inhibitors i.e. reduced cytokine secretion is observed (as demonstrated in **Figure 4-7**). As high cell death was observed in THP-1 cells cultured in SFM following CRISPR, only cells cultured in complete medium i.e. RPMI plus 10% FCS were assessed.

As shown in **Figure 4-14A**, secretion of IL-12p40 was increased upon stimulation with 10 µg/ml R-848, when compared to the negative unstimulated control. This trend was observed in all knockdown conditions, irrespective of the pulse code used. However, there was no difference in the cytokine secretion profiles of the C3 KO condition, when compared to the negative buffer treated control. This may suggest that genetic deletion of C3 does not influence THP-1 effector function. However, this hypothesis cannot be confirmed as the preceding qPCR assessing C3 mRNA levels within the C3 KO remains inconclusive (**Figure 4-13A and B**; left panels). Moreover, secretion of IL-12p40 was superior in the β2 microglobulin KO (specifically cells pulsed with code DP-148), when compared to all other guide RNA treated conditions. The reason for this is unclear. Similar trends were subsequently observed for TNF (**Figure 4-14B**), IL-6 (**Figure 4-14C**) and IL-1β (**Figure 4-14D**).

In conclusion, the effect of CRISPR-mediated deletion of Complement Component C3 on THP-1 cell function remains inconclusive for the following reasons:

1. A dichotomy was observed between C3 protein and mRNA levels. C3 protein levels remained unchanged in the C3 KO condition (irrespective of the electroporation pulse code used) when compared to the negative buffer-treated control, but the qPCR data showed a slight down-regulation in C3 mRNA levels in some of the KO conditions.

2. Moreover, no change in THP-1 effector function i.e. cytokine secretion was observed in the C3 KO condition (irrespective of the electroporation pulse code used) when compared to the negative buffer-treated control.

As discussed in the next section, further optimisation of the CRISPR experiments using a lentiviral delivery system along with additional readouts to assess genetic deletion were in progress.

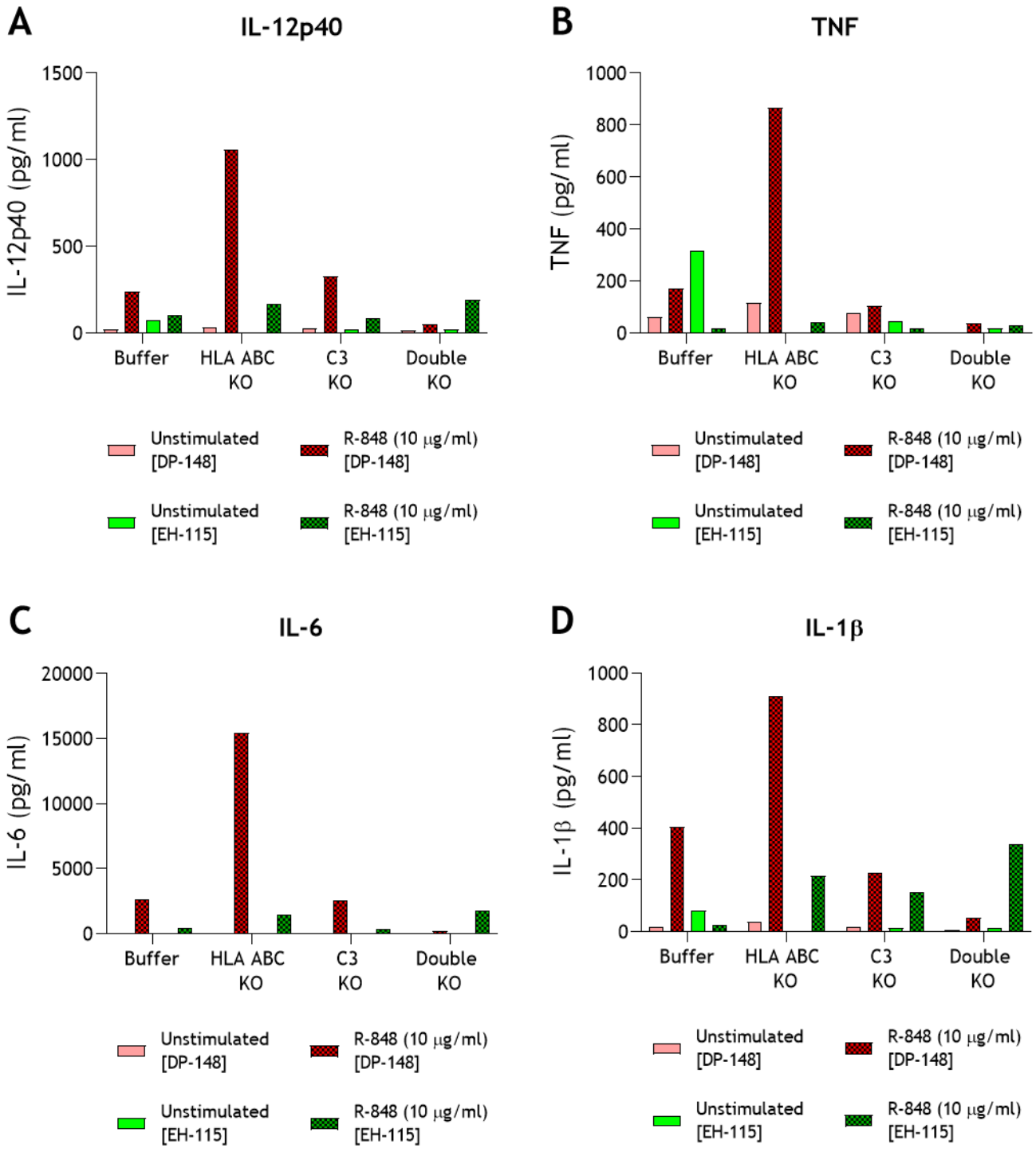


Figure 4-14 Assessment of THP-1 functional response following CRISPR knockdown of the B2M and C3

THP-1 cells were electroporated with pooled guide RNAs, using pulse code DP-148 (red) and EH-115 (green) and subsequently cultured in Complete Medium (i.e. RPMI + 10% FCS) for one week. THP-1 cells were then stimulated overnight with 10 μg/ml R-848 in Complete Medium. Assessment of IL-12p40 (A), TNF (B), IL-6 (C) and IL-1β (D) using a bead-based flow cytometric assay (technical replicate n=1/ condition). Data representative of three individual experiments.

4.7 DISCUSSION

This chapter investigated the presence of a 'locally derived' alternative pathway (AP) C3 convertase, and its downstream modulation of DC effector function. More specifically, tool small-molecules and antibodies which target Factor B were used and the following experiments were performed:

1) The inhibitory potential of these tool antagonists on AP activation was assessed in a cell-free assay. The specificity of pharmacological blockade was confirmed through the assessment of downstream anaphylatoxin generation.
2) This work was then repeated in cells i.e. MdDCs, where both anaphylatoxin generation and effector function including costimulatory molecule expression and cytokine secretion was assessed.
3) CRISPR-Cas9 mediated inhibition of C3 production was leveraged to determine
    a. if loss of complement negatively regulates cellular effector responses
    b. if loss of target protein i.e. C3 and by default C3 convertase negatively regulates the inhibitory potential of tool antagonists described above.

4.7.1 Part 1: Pharmacological blockade of AP

Four tool antagonists were tested for their potential to inhibit mobilisation of the AP and downstream anaphylatoxin generation. A statistically significant down-regulation ($p<0.05$) of both C3a and C5a was observed with all assets, and 100% inhibition was observed at the highest treatment concentrations. Furthermore, the presence of EGTA within the assay buffer inhibited non-specific mobilisation of classical- and lectin-mediated complement activation due to chelation of Ca^{2+} ions thus ensuring specificity of the AP response. The four assets were subsequently tested in DCs, as described below.

4.7.2 Part 2: Assessment of pharmacological blockade of AP in cells

4.7.2.1 Where is the C3 convertase?

It was hypothesised that the constituent proteins of the C3 convertase i.e. C3 and Factor B may be secreted into the extracellular space. Alternatively, the proteins may be retained intracellularly, where they function in combination or independently of one another. Therefore, tool cell-permeable small-molecule inhibitors and non-cell permeable antibodies targeting Factor B were employed. The pharmacological inhibitors were subsequently validated, as described below.

4.7.2.2 Does pharmacological inhibition of Factor B negatively regulate cellular function?

To further understand the functional consequences of pharmacological inhibition of Factor B on MdDC effector function, downstream co-stimulatory molecule expression and cytokine secretion was assessed. A statistically significant down-regulation ($p<0.05$) in cytokine secretion was reached following pre-treatment with FB Inhibitor 1 but not FB Inhibitor 2 or the respective antibodies. This suggests that plasma membrane permeability is a pre-requisite for successful pharmacological inhibition of DC effector function.

4.7.2.3 Does pharmacological inhibition of Factor B negatively regulate downstream convertase-dependent processes?

There are no experimental approaches which test for active AP C3 convertase formation. Therefore, the assessment of downstream anaphylatoxin (C3a) generation was chosen as a surrogate readout for convertase activation. Multiple approaches were utilised to assess C3a generation, all of which failed including:

- Western Blot – multiple optimisations were performed including increasing protein concentration, the modification of gels and running buffers along with using different

secondary antibodies (fluorescent versus chemiluminescent readout). Yet, C3a was not detected.

- MSD – when testing cell supernatant from multiple donors, all undiluted samples were below the lower limit of detection of the assay. The samples could not be concentrated any further, as they had originally been collected from a small 200 µl total volume.
- Cell-free assay – similar approaches as described for the C3a Western Blot were used to optimise this assay. Moreover, samples were concentrated by:
    A. reducing the total reaction volume from 200µL to 100 and 50 µL.
    B. by running samples through Amicon® centrifugal filter units with a 3-kDa cut-off (protein retentate). Yet, C3a (~9 kDa) was not detected in the protein concentrate.

4.7.3 Part 3: Effect of genetic ablation of C3 in cells

As all approaches used to assess anaphylatoxin generation failed, CRISPR-mediated knockdown of the AP protein C3 was employed. As C3-derived C3b is an indispensable component of AP C3 convertase, it was hypothesised that the absence of C3 (and therefore loss of convertase formation upon cellular activation) may correlate with down regulation of effector function.

As primary cells are difficult to transfect, THP-1 cells were chosen as a surrogate cell type for CRISPR given their myelo-monocytic phenotype. THP-1 cells were electroporated with two different pulse codes:

- DP-148 – this code was recommended by the manufacturer of the nucleofector (Lonza), specifically for THP-1 cells.
- EH-115 – this code was used by members of GSK's Functional Genomics department in the successful down-regulation of multiple genes including β2 microglobulin, in conventional CD4+ T cells and THP-1 cells.

The guide RNAs targeting β2 microglobulin had previously been validated by members of the Functional Genomics department at GSK. The guide RNAs targeting C3 had previously been validated by King et al. (2018) and Kulkarni et al. (2019). More specifically:

1) King et al. cloned guide RNAs targeting exons 10 and 13 into the pX330 plasmid from Addgene which also expressed *S. pyogenes* Cas9. DH5a E. coli were transformed with the plasmids and ampicillin-resistant colonies were collected and screened for guideRNA insertion by sequencing using primers which flank the pX330 guideRNA insertion site. Pooled C3-targeting pX330 plasmids were then transfected into INS-1 832/13 cells and single clones were chosen, and genomic DNA was isolated for analysis by both PCR and sequencing. Two homozygous clones were identified which had frameshift mutations and subsequent premature stop codons in exons 12 and 13 respectively.
2) Kulkarni et al., leveraged a similar approach to target exon 2 of the C3 gene. Two clones of C3 deficient BEAS-2B cells were generated named C3KO1 and C3KO2. Clone C3KO1 had two disrupted alleles, one with a 4-bp deletion and the another with a 1-bp deletion whereas clone C3KO2 had an identical 2-bp deletion in both alleles which were identified using targeted deep sequencing.

CRISPR-targeting of C3 was unsuccessful even though the positive control β2-microglobulin was down-regulated. However, it should be noted that there was a 5-day lag between performing the CRISPR experiment and subsequent assessment of gene/protein expression. During this time, the non-CRISPR'ed cells may have proliferated at a faster rate compared to their CRISPR'ed counterparts, leading to a false negative result when assessing C3.

The C3 protein levels remained unchanged, as did downstream cytokine responses in the C3 and double knockout conditions when compared to the negative buffer-treated control. However, it was subsequently noted that the commercially available mRNA probes used to

assess C3 post-transfection (by RT-qPCR) targeted the boundary between exons 19 and 20 of the 41-exon C3 gene. But the guide RNAs used during transfection were complimentary to exons 2, 10 and 13 of the C3 gene, as described above. Hence, this readout may be incorrect or inadequate in the assessment of genetic knockdown following CRISPR, and more relevant readouts of knockdown are required. Moreover, CRISPR knockdown of Factor B was also undertaken. However, high cell death was observed in this experiment thus confounding any downstream analysis of Factor B expression gene/protein expression.

Subsequent work attempted to leverage lentiviral transduction of guide RNAs targeting the B2M, C3 and fB genes in THP-1 cells. As shown in **Supplementary Figure 1**, guide RNAs with high on-target and low-off target specificity were designed using www.benchling.com and subsequently cloned by the manufacturer GENEWIZ (**Figure S1A**). Subsequent analysis of B2M surface expression showed successful down-regulation in two of the three single gRNA-treated conditions and in the pooled gRNA treated condition, when compared to the negative non-transfected control (**Figure S1B**). However, subsequent planned work targeting C3 and Factor B was halted due to the pandemic.

If lentiviral-mediated knockdown of C3 and fB is successful, the small-molecules could be employed to assess their inhibitory potential both at steady state i.e. non-transfected cells and following knockdown i.e. loss of target protein would preclude the small molecules from exerting their inhibitory effect. This would also be followed by the assessment of cytokine secretion.

In conclusion, this chapter has provided insights into the possible role of 'locally derived' alternative pathway (AP) C3 convertase activity in the context of dendritic cell (MdDC) anaphylatoxin generation and downstream effector function. The modulation of cellular C3a

generation and its potential crosstalk with cytokine responses by tool inhibitors of Factor B remains inconclusive, as all assays were unsuccessful.

5 GENERAL DISCUSSION

The discovery of intracellular complement by Liszewski and colleagues, specifically C3a generation and downstream signalling via CD46 and C3aR conventional CD4+ T cells has provided new insights into mechanisms of both T cell activation, polarisation and homeostatic survival in an autocrine fashion (Liszewski et al., 2013; Arbore et al., 2016; Kolev et al., 2020). Moreover, previous work by Strainic and colleagues demonstrated expression of AP complement protein in antigen-presenting cells, whereby cognate peptide-MHC-TCR interactions were shown to regulate DC anaphylatoxin generation and downstream paracrine signalling to T cells (Strainic et al., 2008; Strainic et al., 2013).

5.1 iNKT CELLS AND COMPLEMENT

However, the role of complement signalling in the context of human iNKT cell function is unknown, whether this be through conventional liver-derived complement activation fragments (C3a, C5a) acting extracellularly or potentially through autonomous cell-derived complement. Therefore, the purpose of this study was to determine if iNKT cell effector function was influenced by complement, specifically signalling by cell-derived anaphylatoxins in an autocrine or paracrine manner.

Assessment of iNKT anaphylatoxin receptor expression by flow cytometry revealed that receptor up-regulation was greater in cells activated in foetal calf serum relative to cells activated in serum-free medium. As loss of serum most likely promotes compensatory *de novo* complement generation and subsequent secretion into the extracellular milieu (Elvington et al., 2017), it was speculated that increased cognate ligand-receptor interactions in serum-free medium) were responsible for inducing receptor down-regulation as previously observed in C3a-stimulated keratinocytes (Purwar et al., 2006).

It is noteworthy that surface C3aR but not C5aR1 was detected at steady state in all tested iNKT cell donors, which contrasts with conventional $CD4^+$ T cells where neither receptor is expressed at steady state and C3aR is only transiently up-regulated upon activation whilst C5aR1 remains inside of the cell (Liszewski et al., 2013; Arbore et al., 2016). This suggests that C3aR up-regulation in iNKT cells is not necessarily a pre-requisite for modulation of iNKT cell effector function. Given that C3aR and C5aR1 usually behave in an additive manner as previously demonstrated by Strainic et al., (2008) in which a reduction in $CD4^+$ T cell effector responses (i.e. IFN-γ secretion) was twice as high in cells isolated from C3aR-$C5aR1^{-/-}$ mice when compared to cells isolated from either $C3aR^{-/-}$ or $C5aR1^{-/-}$ mice (Strainic et al., 2008; Verschoor et al., 2016), one may speculate that C3a-C3aR cognate-interactions enhance C5aR1 activity, either at the cell surface but also intracellularly.

Furthermore, confocal microscopy revealed intracellular localisation of anaphylatoxin receptors and their cognate ligands at steady state. However, what currently remains unknown is the following:

a) the 'source' of the anaphylatoxins i.e. are native C3 and C5 cleaved intracellularly into C3a and C5a? If so, the potential mechanisms by which cleavage occurs can be assessed as described in Section 5.3.
b) Are anaphylatoxins co-localised with and potentially engage their cognate receptors inside of intracellular compartments as previously reported in conventional $CD4^+$ T cells (Liszewski et al., 2013, Arbore et al., 2016).
c) Is intracellular engagement of anaphylatoxin receptors associated with mTOR activation and homeostatic survival as previously observed for conventional $CD4^+$ T cells (Liszewski et al., 2013).

The presence of anaphylatoxin receptors on the iNKT cell surface prompted the question of whether iNKT cells themselves are a source of complement. More specifically, it was hypothesised that iNKT cells may synthesise and secrete anaphylatoxins, following activation with their canonical ligand α-GalCer. Subsequent cognate ligand-receptor interactions may suggest that an autocrine feedback loop exists as previously demonstrated in murine T cells (Lalli et al., 2008; Strainic et al., 2008; Strainic et al., 2013). As alternative pathway (AP) complement activation i.e. up-regulation of C3 and fB is independent of pathogen but is induced by TCR engagement (Strainic et al., 2008), initial investigations focused on the presence of intracellular iNKT AP. Although increased *de novo* C3 generation was observed upon iNKT cell activation, Factor B (fB) remained absent suggesting that C3 may be cleaved into C3a independently of AP (Liszewski et al., 2013). Moreover, C3 was 'recycled' between the intra- and extracellular milieu, as previously observed in conventional T cells (Elvington et al., 2017). Future work may involve the assessment of recycling of other native (e.g. Factor B) or cleaved complement proteins such as anaphylatoxins. Although the physiological significance of C3 'recycling' remains unclear, secretion of cell derived C3 into the extracellular space may contribute to or promote increased local anaphylatoxin generation by extracellular i.e. conventional serum complement cleavage pathways during inflammation, such as alternative pathway activation.

Previous work by Strainic and colleagues demonstrated a mechanistic link between TCR engagement and anaphylatoxin receptor (C3aR and C5aR1) ligation, whereby anaphylatoxins enhance Th1 effector responses (Strainic et al., 2008 & 2013). However, in my experiments iNKT cell activation profiles in serum-free medium were reduced upon addition of purified C3a and C5a. It should be noted that a clear extrapolation cannot be made between cell-derived anaphylatoxins and purified proteins regarding structural differences post-cleavage, receptor binding specificity (i.e. intra- vs extracellular) or local concentrations (due to rapid inactivation

of C3a and C5a to C3a-desArg and C5a-desArg respectively by carboxypepidase B) (Bajic et al., 2013). Hence, addition of purified proteins may be inadequate when assessing potential cross-talk between iNKT TCR engagement and anaphylatoxin receptor engagement. Furthermore, previous work by Kemper and colleagues showed that antibody-mediated engagement of CD46 positively modulated intracellular generation of C3a in conventional CD4+ T cells (Liszewski et al., 2013). Therefore, further experiments are required to better understand the role of anaphylatoxins on iNKT cell effector function, as described below in Section 5.3.

5.2 DENDRITIC CELLS AND COMPLEMENT

As autocrine-mediated activation of iNKT cells via alternative pathway activation proved unlikely due to the absence of cell-derived fB and hence 'local' AP convertase generation, paracrine signalling by APC-derived anaphylatoxins was assessed. As iNKT cells are cytolytic upon activation, sorting of APCs post-culturing with iNKT cells as previously described by Strainic et al. (2008) for APC/CD4+ T cell co-cultures could not be performed. Therefore, MdDCs were stimulated independently of iNKT cells, using immobilised CD40L multimers. In agreement with previous work in the mouse, DC CD40 engagement induced transcription of the AP proteins C3 and fB along with IL-12 (Lalli et al., 2008; Strainic et al., 2008). Transcript profiles were consistent with increased secretion of C3 and fB into the extracellular space. Notably, upstream Factor D (fD) required for generation of extracellular AP C3 convertase (by cleaving fB into Bb) was down regulated.

The dichotomy in fD and fB expression profiles in response to CD40 ligation by CD40L was explored further by assessing downstream Bb generation. To ensure Bb was detected post-cleavage and not as native fB, an antibody recognising neo-epitopes exposed only upon cleavage was used. Flow cytometric analysis of Bb showed it to be absent at steady state, with

little to no change in expression upon activation. However, the following questions remain unclear:

a) The specificity of the neo-epitope antibody for Bb. Potential experimental approaches to address this issue are discussed in Section 5.3.
b) The mechanism by which Factor B is cleaved, given that Factor D expression (specifically mRNA) was downregulated. It has previously been reported that other serine proteins such as kallikreins cleave Factor B (Hiemstra et al., 1985), hence further work (as discussed in Section 5.3) is required to understand if intracellular Factor B is cleaved to generate Bb.

Subsequent work leveraged pharmacological inhibitors of Factor B to determine if potential crosstalk mechanisms between the CD40-CD40L axis and alternative pathway mobilisation modulates DC effector function, and by default downstream iNKT cell effector responses. The small molecules FB Inhibitor 1 and FB Inhibitor 2 were shown to cross the plasma membrane in monocytes, by mass spectrometry. Pre-treatment with FB Inhibitor 1 but not FB Inhibitor 2 reduced DC cytokine secretion. As the intracellular localisation of FB Inhibitor 1 was shown to be 10-fold greater than FB Inhibitor 2, it is possible that FB Inhibitor 1's inhibitory potential is a direct consequence of higher plasma membrane permeability. Moreover, pre-treatment with Factor B blocking antibody 1 and Factor B blocking antibody 2 which do not cross the plasma membrane had no effect on DC activation profiles. This suggests that mobilisation of intracellular Factor B is partially responsible for modulating DC effector function.

As activated Factor B is a component of the alternative pathway C3 convertase i.e. C3bBb (Freeley et al., 2016), one may speculate that pharmacological inhibition of Factor B negatively regulates convertase mobilisation and downstream anaphylatoxin generation. Moreover, as inhibition of effector function was only observed with plasma membrane-permeable small molecules, the presence of an unreported functional intracellular C3 convertase enzyme in DCs

was postulated. However, as convertases are extremely unstable and dissociate irreversibly with a half-life of 60-90 seconds at 37°C (Rooijakkers et al., 2009), it was experimentally challenging to detect its presence inside of the cell. Potential future experiments to assess for the presence of (intracellular) convertases are discussed in Section 5.3.

Given that convertase enzymes are inherently unstable, downstream C3a generation was assessed as a readout for potential convertase mobilisation. As extensively described in Chapter 4, C3a generation was not observed irrespective of the molecular biology technique employed. However, it remains unclear if the inability to detect C3a is a consequence of the limitations of the assays or if it is absent. As a further matter, Factor B must be cleaved into Bb (Freeley et al., 2016) prior to active convertase mobilisation. Moreover, Factor B must be engaged to C3 to enable upstream Factor D to cleave it into Bb (Rooijakkers et al., 2009). However, as previously mentioned, Factor D mRNA levels were not detected in MdDCs. This may suggest that:

b) Factor B may be cleaved into Bb by a protease other than Factor D e.g. kallikreins (as described above). Cleaved Bb may form part of an intracellular C3 convertase and in turn modulate downstream DC effector function.
c) Factor D may be 'recycled' from the extracellular milieu into the cell, as previously reported for C3(H_2O) (Elvington et al., 2017). Recycled Factor D may function in a manner analogous to fluid-phase Factor D, thereby cleaving intracellular Factor B into BB (in the presence of C3) to form an intracellular C3 convertase. Potential experiments to address this hypothesis are discussed in Section 5.3.
d) Factor B functions independently of Factor D (and C3) to modulate DC effector function i.e. intracellular convertases do not exist.

5.3 POTENTIAL FUTURE EXPERIMENTS

1) As anaphylatoxins were detected inside of iNKT cells by microscopy, it will be important to understand both how and where they were generated. Initial experiments may leverage the plasma membrane permeable inhibitors to inhibit Factor B. Cells can subsequently be fixed and stained at multiple time points following addition of inhibitors, and intracellular localisation of anaphylatoxins can be assessed and quantified by microscopy. If anaphylatoxin presence is reduced in the presence of these inhibitors, this may suggest that Factor B and potentially a convertase-mediated mechanism drives C3a/C5a generation. Alternatively, if anaphylatoxin presence is unchanged in the presence of these inhibitors, this may suggest another mechanism of intracellular cleavage as previously reported by Liszewski et al., (2013) in which the protease cathepsin L (CTSL) was shown to cleave C3 into C3a in $CD4^+$ T cells. As the CTSL inhibitor used by Liszewski et al. is commercially available, it can be leveraged in this work to assess iNKT cell anaphylatoxin generation. However, if anaphylatoxin generation is still unchanged, this may suggest a previously undefined mechanism of intracellular cleavage.
2) Secondly, as anaphylatoxins were located in the same intracellular compartments as their cognate receptors, one may speculate that C3a/C5a may bind and signal through their intracellular receptors as previously reported by Kemper and colleagues in both conventional CD4+ and CD8+ T cells (Liszewski et al., 2013, Arbore et al., 2016; Arbore et al., 2018). This hypothesis may be tested using a combination of different commercially available anaphylatoxin receptor inhibitors, either membrane permeable or impermeable as previously reported by Arbore et al., 2016. If iNKT cell functional response i.e. cytokine secretion is reduced in the presence of cell permeable inhibitors but remains intact with cell impermeable inhibitors, this would suggest that exclusively intracellular anaphylatoxin receptor ligation modulates iNKT cell activation. Moreover, an additional approach may

leverage genetic disruption of C3aR/C5aR1 as previously reported by Strainic et al., (2008) followed by the addition of exogenous C3a/C5a. Functional responses can subsequently be compared between 'wild-type' cells and genetically disrupted cells to determine if autocrine anaphylatoxin receptor engagement modulates iNKT cell activation profiles.

3) If iNKT cell activation profiles remain unchanged following blockade of anaphylatoxin receptors, it will important to assess the presence of additional complement receptors implicated in conventional α/β T cell activation. For example, antibody-mediated ligation of CD46 has previously been shown to modulate T cell effector responses (Liszewski et al., 2013; Arbore et al., 2016). As shown in **Supplementary Figure 2**, a single iNKT cell donor was shown to express CD46 at steady state with an increase in surface, but not total expression upon activation. This may suggest that CD46 is located intracellularly and subsequently traffics to the cell surface upon activation. Future experiments may include increasing the number of donors and inhibition of this receptor followed by the assessment of effector function i.e. cytokine secretion by ELISA or multiplex array.
4) It will also be intriguing to understand what happens downstream of anaphylatoxin receptor ligation, both in iNKT cells and in dendritic cells. Previous work by the Kemper laboratory has shown that activation i.e. phosphorylation of mTOR occurs post-C3aR engagement in CD4+ T cells. Moreover, inhibition of mTOR phosphorylation was shown to negatively correlate with T cell survival, suggesting a role for complement in homeostatic T cell survival. Similar experiments can be performed in iNKT cells. Moreover, the following gene array technology (Qiagen QuantiNova LNA PCR Focus Panel Human GPCR Signaling PathwayFinder [Catalog No. 249950]) was going to be employed to assess the expression profiles of 96 different genes of interest associated with G-protein coupling. However, these experiments were halted during the pandemic, and have not been re-started. If a particular gene(s) of interest were shown to be up regulated, and pharmacological

inhibition/ genetic disruption of its protein counterpart correlated with abrogation of effector responses this may implicate the protein as a downstream effector of anaphylatoxin receptor engagement.

5) Also, a major issue with the current work is an inability to detect the hypothesised cleavage of fB into Bb in monocyte-derived dendritic cells. Moreover, an unsuccessful attempt was made to assess cleaved Bb at steady state and upon activation by Western Blot in these cells (**Supplementary Figure 3**). Therefore, future work may involve further optimisation of this Western Blot to detect intracellular Bb.
6) Additional experiments may also assess the recycling of Factor B (and potentially Factor D) between the intra- and extracellular space. As previously discussed in Chapter 3, high sequence homology is observed between human and foetal complement proteins, when using FCS as a proxy for a non-human complement source. Therefore, one approach may be to culture cells in commercially available complement protein-deficient medium, before performing Western Blot analysis of cell lysates, as previously reported by Elvington et al., (2017). A subsequent comparison can then be made between cells cultured in human complement-sufficient and human complement-deficient medium. For example, if a protein band is detected in cell lysates cultured in human complement-sufficient but not detected in human complement-deficient medium, this may suggest complement uptake i.e. recycling from the extracellular space. However, if protein bands are still detected in serum-deficient medium, this would suggest *de novo* generation, independent of recycling from the extracellular milieu.
7) Finally, an intracellular convertase has been hypothesised, but has not been shown. Potential experimental approaches to assess for convertase may involve:
    a. Using antibodies which detect exposed epitopes present in convertase enzymes, but absent in native/cleaved protein. Cells can be activated at time 0 followed by

staining with such antibodies at multiple time points post-activation to determine if there is an increase in fluorescence over time. Moreover, if fluorescence is reduced in the presence of cell-permeable Factor B inhibitors, this may suggest that these inhibitors negatively regulate convertase generation.

b. An additional approach may be to leverage commercially available Factor D inhibitors. As Factor D cleaves Fb into Bb, one may speculate that inhibition of Factor D will provide a more 'upstream' form of convertase inhibition. It would be interesting to see if the reduction in cytokine secretion in dendritic cells observed with Factor B inhibitors is also seen with Factor D inhibitors. If a similar phenotype is observed, this may suggest that Fb is cleaved by Factor D to generate (intracellular) convertase. However, if Factor D inhibition has no effect on dendritic cell effector responses, this may suggest that Fb functions independently of Factor D and most likely does not form (intracellular) convertase. Additionally, the plasma membrane permeability of these Factor D inhibitors should also be validated beforehand e.g. by mass spectrometry.

5.4 POTENTIAL THERAPEUTIC IMPLICATIONS OF THIS WORK

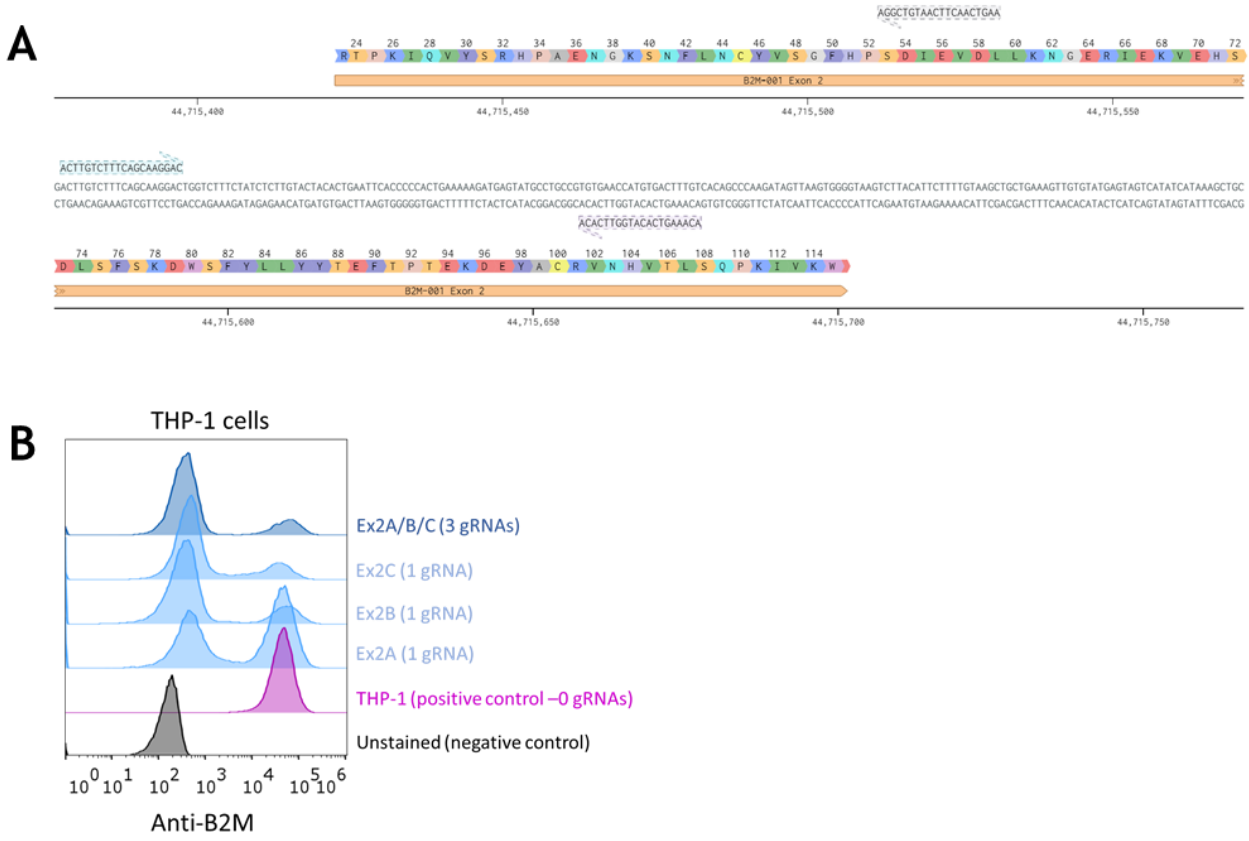
In conclusion, this work has sought to determine if iNKT cell effector function is modulated by local, cell-derived anaphylatoxins. Moreover, it was hypothesised that the mechanism by which iNKT cells or neighbouring DCs generate anaphylatoxins is through Factor B and potentially intracellular alternative pathway (AP) convertase. Whilst the mechanism which underscores molecular crosstalk between Factor B and DC effector responses remains unanswered, this crosstalk may have potential therapeutic implications in disease. As described in Section 1.5, many pharmaceutical companies are currently investing in clinical trials for multiple anti-complement therapeutics, including inhibitors of the AP proteins Factor D, Factor B and C3 (Morgan and Harris, 2015). However, inhibition of Factor B is usually associated with serum complement and downstream convertase generation. This work attempted to assess inhibition of cellular Factor B.

However, unlike this project where only *in vitro* assays were performed, one may assume that in a physiological setting, plasma membrane permeable small-molecule Factor B inhibitors would hold 'dual capability' by inhibiting both conventional (i.e. fluid-phase) and cellular complement activation. This may in turn lead to greater clinical efficacy when compared to current 'non-cell permeable' biological therapies such as the anti-C5 antibody, Eculizumab. In addition, as Factor B is one of the most upstream complement proteins, its pharmacological inhibition may show greater clinical response, as opposed to the inhibition of late stage complement proteins such as C5.

Moreover, like anti-complement therapies, iNKT cells have also shown efficacy in pre-clinical models of inflammatory diseases such as SLE and EAE (as described in Section 1.5). Thus, leveraging the immunomodulatory potential of iNKT cells in combination with anti-complement therapeutics may provide enhanced efficacy in multiple autoimmune diseases such as SLE and C3 glomerulopathies.

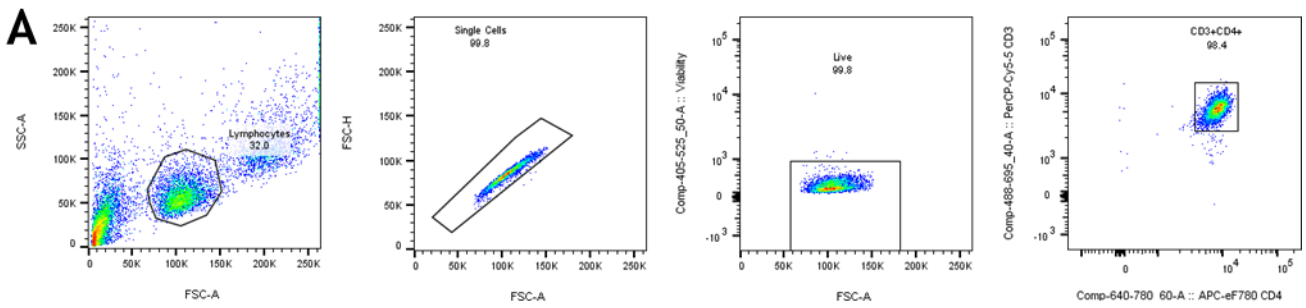
6 APPENDIX

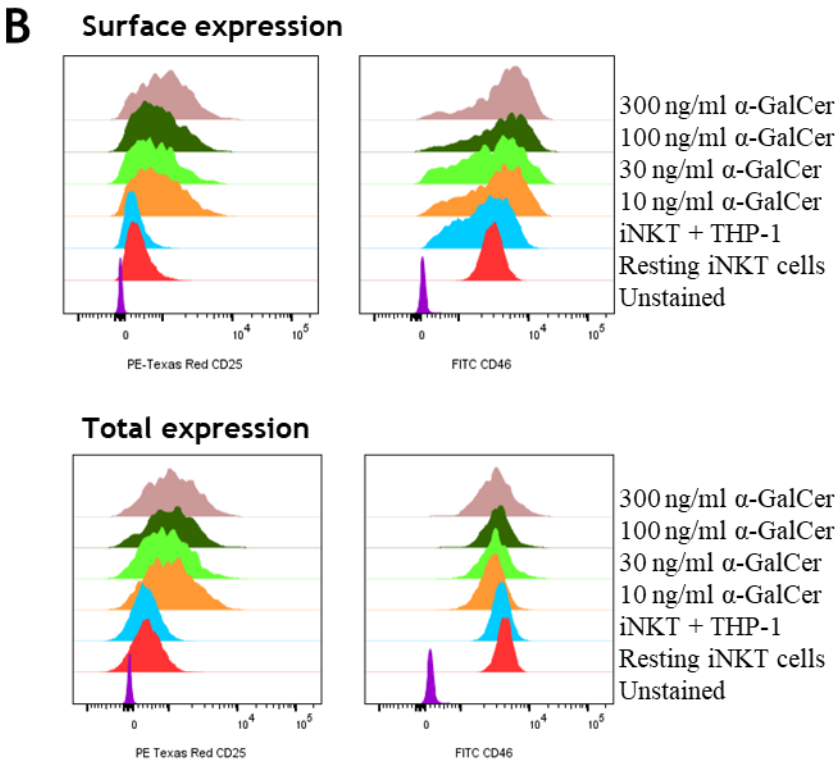
Supplementary Figure 1



Preliminary experiment showing lenti-CRISPR knockdown of B2M in THP-1 cells
The B2M gene sequence (*ensembl* ID: ENSG0000016671) was copied to www.benchling.com and guide RNA sequences were chosen based on the following parameters: high on-target and low off-target specificity. The guide RNA sequences were synthesised and cloned as cDNA. One Shot™ TOP10 Chemically Competent E. coli bacteria were transformed using the Lenti-CRISPR constructs (GeneWiz) and cloned. Ampicillin resistant bacterial monocultures were grown and collected. DNA was isolated using the PureLink HiPure Plasmid DNA Purification Kit (ThermoFisher) and quantified using the Nanodrop. HEK cells (re-suspended in DMEM plus GeneJuice) were transfected with the isolated DNA along with the packaging plasmids (P89.1 and PMD2.G) overnight. The supernatant (containing the lenti-CRISPR construct) was collected and added to THP-1 cells (either as a single guide or pooled together, in RPMI + 10% FCS). This was followed by the addition of blasticidin to enrich for cells where Cas9 was present.
(A) Schematic showing Exon 2 of the B2M gene. 20 bp gRNAs are shown above the dsDNA (downstream of the 'NGG), targeting the forward or reverse strand.
(B) Experiment performed by Ed Jenkins. Assessment of surface β2-microglobulin expression in THP-1 cells, by flow cytometry. Efficient down-regulation of β2-microglobulin was observed in two of the three single guide-RNA treated conditions (light blue) and in the pooled guide-RNA treated condition (dark blue) when compared to the negative control i.e. non-transfected THP-1 cells (purple).

Supplementary Figure 2



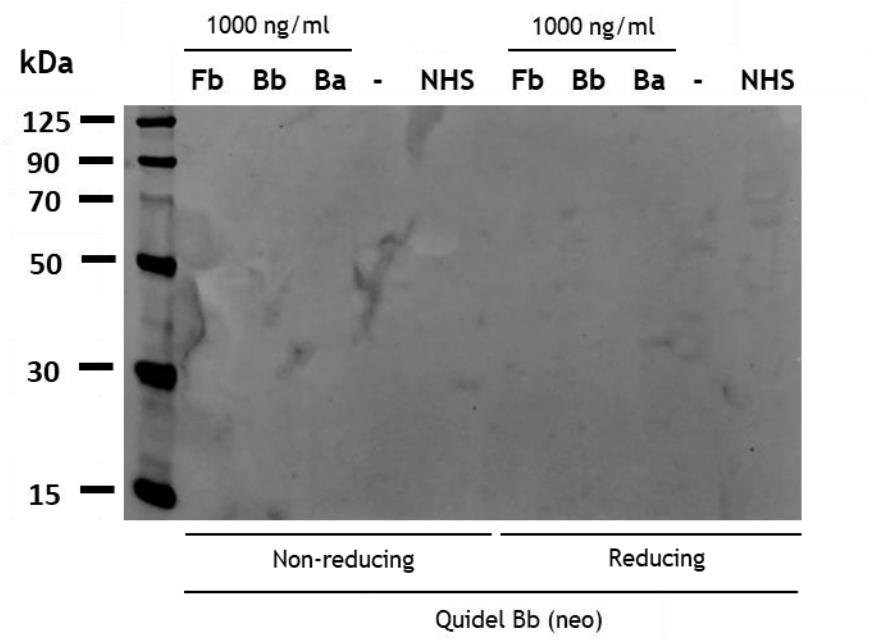


Preliminary experiment assessing CD46 expression in one iNKT cell donor

iNKT cells were cultured with THP-1 cells (in the absence or presence of increasing concentrations of α-GalCer) overnight in complete medium. (A) Gating strategy: Lymphocytes, followed by single cells (FSC-A vs FSC-H) followed by live cells (Aqua negative) followed by CD3+CD4+ cells. (B) Assessment of the activation marker CD25 (left) and the complement receptor CD46 (right, using FITC anti-human CD46; Mouse IgG1,κ; Clone MEM-258 [Biolegend]) in non-permeabilised cells i.e. surface expression (top) and permeabilised cells i.e. total (surface plus intracellular) expression.

α-GalCer: α-galactosylceramide; FSC: forward scatter; SSC: side scatter.

Supplementary Figure 3



Preliminary experiment which attempted to assess the specificity of the Quidel Bb (neo) antibody.

Attempted target validation by Western Blot of the monoclonal Factor B blocking antibody developed by Quidel, claiming to detect cleaved Bb, but not Bb in the context of native Fb (or Fb alone). Purified Fb (~93kDa), Bb (~61kDa) and Ba (~30kDa) proteins were used at 1000 ng/ml diluted in 1x PBS. NHS (activated) was used as a positive control for alternative pathway complement activation. kDa: kilodalton, NHS: normal human serum.

7 REFERENCES

Akkaya, M., Kwak, K., & Pierce, SK. (2020). B cell memory: building two walls of protection against pathogens. Nat Rev Immunol., 20(4), 229-38.

Ando, T., Ito, H., Ohtaki, H., & Seishima, M. (2013). Toll-like receptor agonists and alpha-galactosylceramide synergistically enhance the production of interferon-gamma in murine splenocytes. Scientific reports, 3, 2559.

Arbore, G., Kemper, C., & Kolev, M. (2017). Intracellular complement− the complosome− in immune cell regulation. Molecular immunology, 89, 2-9.

Arbore, G., West, E. E., Rahman, J., Le Friec, G., Niyonzima, N., Pirooznia, M., . . . Kemper, C. (2018). Complement receptor CD46 co-stimulates optimal human CD8(+) T cell effector function via fatty acid metabolism. Nat Commun, 9(1), 4186.

Arbore, G., West, E. E., Spolski, R., Robertson, A. A. B., Klos, A., Rheinheimer, C., . . . Kemper, C. (2016). T helper 1 immunity requires complement-driven NLRP3 inflammasome activity in CD4(+) T cells. Science (New York, N.Y.), 352(6292).

Bae, D. S., & Lee, J. K. (2014). Development of NK cell expansion methods using feeder cells from human myelogenous leukemia cell line. Blood Res, 49(3), 154-161.

Bajic, G., Yatime, L., Klos, A., & Andersen, G. R. (2013). Human C3a and C3a desArg anaphylatoxins have conserved structures, in contrast to C5a and C5a desArg. Protein Sci, 22(2), 204-212.

Barratt, J., & Weitz, I., (2021). Complement Factor D as a Strategic Target for Regulating the Alternative Complement Pathway. Front Immunol., 12:712572.

Bassiri, H., Das, R., Guan, P., Barrett, D. M., Brennan, P. J., Banerjee, P. P., . . . Nichols, K. E. (2014). iNKT cell cytotoxic responses control T-lymphoma growth in vitro and in vivo. Cancer Immunol Res, 2(1), 59-69.

Bassiri, H., Das, R., & Nichols, K. E. (2013). Invariant NKT cells: Killers and conspirators against cancer. Oncoimmunology, 2(12), e27440.

Bayly-Jones, C., Bubeck, D., & Dunstone, M. A. (2017). The mystery behind membrane insertion: a review of the complement membrane attack complex. Philosophical transactions of the Royal Society of London. Series B, Biological sciences, 372(1726).

Benlagha, K., Weiss, A., Beavis, A., Teyton, L., & Bendelac, A. (2000). In vivo identification of glycolipid antigen-specific T cells using fluorescent CD1d tetramers. The Journal of experimental medicine, 191(11), 1895-1903.

Bexborn, F., Andersson, P. O., Chen, H., Nilsson, B., & Ekdahl, K. N. (2008). The tick-over theory revisited: formation and regulation of the soluble alternative complement C3 convertase (C3(H2O)Bb). Mol Immunol, 45(8), 2370-2379.

Blom, A. M., Volokhina, E. B., Fransson, V., Stromberg, P., Berghard, L., Viktorelius, M., . . . Okroj, M. (2014). A novel method for direct measurement of complement convertases activity in human serum. Clin Exp Immunol, 178(1), 142-153.

Bonilla, F. A., & Oettgen, H. C. (2010). Adaptive immunity. J Allergy Clin Immunol, 125(2), S33-40.

Borg, N. A., Kjer-Nielsen, L., McCluskey, J., & Rossjohn, J. (2007). Structural insight into natural killer T cell receptor recognition of CD1d. Adv Exp Med Biol, 598, 20-34.

Bradford, E. M., Ryu, S. H., Singh, A. P., Lee, G., Goretsky, T., Sinh, P., . . . Barrett, T. A. (2017). Epithelial TNF Receptor Signaling Promotes Mucosal Repair in Inflammatory Bowel Disease. J Immunol, 199(5), 1886-1897.

Bradley, T., Yang, G., Ilkayeva, O., Holl, T. M., Zhang, R., Zhang, J., . . . Haynes, B. F. (2016). HIV-1 Envelope Mimicry of Host Enzyme Kynureninase Does Not Disrupt Tryptophan Metabolism. J Immunol, 197(12), 4663-4673.

Brigl, M., Tatituri, R. V., Watts, G. F., Bhowruth, V., Leadbetter, E. A., Barton, N., . . . Brenner, M. B. (2011). Innate and cytokine-driven signals, rather than microbial antigens, dominate in natural killer T cell activation during microbial infection. The Journal of experimental medicine, 208(6), 1163-1177.

Buechel, H. S., MH, D'Cruz, LM. (2015). Stages versus subsets: Invariant Natural Killer T cell lineage differentiation. Cytokine. 72(2), 204-9

Byrareddy, S. N., Sidell, N., Arthos, J., Cicala, C., Zhao, C., Little, D. M., . . . Ansari, A. A. (2015). Species-specific differences in the expression and regulation of alpha4beta7 integrin in various nonhuman primates. J Immunol, 194(12), 5968-5979.

Cardone, J., Le Friec, G., Vantourout, P., Roberts, A., Fuchs, A., Jackson, I., . . . Cope, A. (2010). Complement regulator CD46 temporally regulates cytokine production by conventional and unconventional T cells. Nature immunology, 11(9), 862-871.

Cerundolo, V., Silk, J. D., Masri, S. H., & Salio, M. (2009). Harnessing invariant NKT cells in vaccination strategies. Nature Reviews Immunology, 9(1), 28-38.

Chang, J. Y., Lin, C. C., Salamanca, S., Pangburn, M. K., & Wetsel, R. A. (2008). Denaturation and unfolding of human anaphylatoxin C3a: an unusually low covalent stability of its native disulfide bonds. Arch Biochem Biophys, 480(2), 104-110.

Chang, P. P., Barral, P., Fitch, J., Pratama, A., Ma, C. S., Kallies, A., . . . Vinuesa, C. G. (2011). Identification of Bcl-6-dependent follicular helper NKT cells that provide cognate help for B cell responses. Nat Immunol, 13(1), 35-43.

Cho, M. S., Vasquez, H. G., Rupaimoole, R., Pradeep, S., Wu, S., Zand, B., . . . Huang, J. (2014). Autocrine effects of tumor-derived complement. Cell reports, 6(6), 1085-1095.

Coates, M., Blanchard, S., & MacLeod, A. S. (2018). Innate antimicrobial immunity in the skin: A protective barrier against bacteria, viruses, and fungi. PLoS Pathog, 14(12), e1007353.

Coquet, J. M., Chakravarti, S., Kyparissoudis, K., McNab, F. W., Pitt, L. A., McKenzie, B. S., . . . Godfrey, D. I. (2008). Diverse cytokine production by NKT cell subsets and identification of an IL-17-producing CD4-NK1.1- NKT cell population. Proceedings of the National Academy of Sciences of the United States of America, 105(32), 11287-11292.

Corvillo, F., Okroj, M., Nozal, P., Melgosa, M., Sanchez-Corral, P., & Lopez-Trascasa, M. (2019). Nephritic Factors: An Overview of Classification, Diagnostic Tools and Clinical Associations. Front Immunol, 10, 886.

Cravedi, P., Leventhal, J., Lakhani, P., Ward, S. C., Donovan, M. J., & Heeger, P. S. (2013). Immune cell-derived c3a and c5a costimulate human T cell alloimmunity. American Journal of Transplantation, 13(10), 2530-2539.

Crowe, N. Y., Smyth, M. J., & Godfrey, D. I. (2002). A critical role for natural killer T cells in immunosurveillance of methylcholanthrene-induced sarcomas. The Journal of experimental medicine, 196(1), 119-127.

D, A. V., Demir, M., Chun, N., Fribourg, M., Cravedi, P., Llaudo, I., . . . Heeger, P. S. (2018). T Cell Expression of C5a Receptor 2 Augments Murine Regulatory T Cell (TREG) Generation and TREG-Dependent Cardiac Allograft Survival. J Immunol, 200(6), 2186-2198.

Danobeitia, J. S., Djamali, A., & Fernandez, L. A. (2014). The role of complement in the pathogenesis of renal ischemia-reperfusion injury and fibrosis. Fibrogenesis Tissue Repair, 7, 16.

Das, R., Bassiri, H., Guan, P., Wiener, S., Banerjee, P. P., Zhong, M. C., . . . Nichols, K. E. (2013). The adaptor molecule SAP plays essential roles during invariant NKT cell cytotoxicity and lytic synapse formation. Blood, 121(17), 3386-3395.

De Santo, C., Salio, M., Masri, S. H., Lee, L. Y., Dong, T., Speak, A. O., . . . Cerundolo, V. (2008). Invariant NKT cells reduce the immunosuppressive activity of influenza A virus-induced myeloid-derived suppressor cells in mice and humans. The Journal of clinical investigation, 118(12), 4036-4048.

Derer, S., Cossham, M., Rosner, T., Kellner, C., Beurskens, F. J., Schwanbeck, R., . . . Valerius, T. (2015). A Complement-Optimized EGFR Antibody Improves Cytotoxic Functions of Polymorphonuclear Cells against Tumor Cells. Journal of immunology (Baltimore, Md.: 1950), 195(10), 5077-5087.

Doherty, D. G., Melo, A. M., Moreno-Olivera, A., & Solomos, A. C. (2018). Activation and Regulation of B Cell Responses by Invariant Natural Killer T Cells. Front Immunol, 9, 1360.

Dudek, A. M., Martin, S., Garg, A. D., & Agostinis, P. (2013). Immature, Semi-Mature, and Fully Mature Dendritic Cells: Toward a DC-Cancer Cells Interface That Augments Anticancer Immunity. Front Immunol, 4, 438.

Elgueta, R., Benson, M. J., De Vries, V. C., Wasiuk, A., Guo, Y., & Noelle, R. J. (2009). Molecular mechanism and function of CD40/CD40L engagement in the immune system. Immunological reviews, 229(1), 152-172.

Elvington, M., Liszewski, M. K., Bertram, P., Kulkarni, H. S., & Atkinson, J. P. (2017). A C3(H20) recycling pathway is a component of the intracellular complement system. J Clin Invest, 127(3), 970-981.

Filippi, B. M., Bassiri, A., Abraham, M. A., Duca, F. A., Yue, J. T., & Lam, T. K. (2014). Insulin signals through the dorsal vagal complex to regulate energy balance. Diabetes, 63(3), 892-899.

Freeley, S., Kemper, C., & Le Friec, G. (2016). The “ins and outs” of complement-driven immune responses. Immunological reviews, 274(1), 16-32.

Fusakio, M. E., Mohammed, J. P., Laumonnier, Y., Hoebe, K., Kohl, J., & Mattner, J. (2011). C5a regulates NKT and NK cell functions in sepsis. Journal of immunology (Baltimore, Md.: 1950), 187(11), 5805-5812.

Gadola, S. D., Silk, J. D., Jeans, A., Illarionov, P. A., Salio, M., Besra, G. S., . . . Cerundolo, V. (2006). Impaired selection of invariant natural killer T cells in diverse mouse models of glycosphingolipid lysosomal storage diseases. J Exp Med, 203(10), 2293-2303.

Gaya, M., Barral, P., Burbage, M., Aggarwal, S., Montaner, B., Navia, A. W., . . . Nair, U. (2017). Initiation of Antiviral B Cell Immunity Relies on Innate Signals from Spatially Positioned NKT Cells. Cell, 172(3), 517-533.

Ghannam, A., Pernollet, M., Fauquert, J. L., Monnier, N., Ponard, D., Villiers, M. B., . . . Drouet, C. (2008). Human C3 deficiency associated with impairments in dendritic cell differentiation, memory B cells, and regulatory T cells. J Immunol, 181(7), 5158-5166.

Girardi, E., & Zajonc, D. M. (2012). Molecular basis of lipid antigen presentation by CD1d and recognition by natural killer T cells. Immunological reviews, 250(1), 167-179.

Godfrey, D. I., MacDonald, H. R., Kronenberg, M., Smyth, M. J., & Van Kaer, L. (2004). NKT cells: what's in a name? Nature Reviews Immunology, 4(3), 231-237.

Godfrey, D. I., Stankovic, S., & Baxter, A. G. (2010). Raising the NKT cell family. Nature immunology, 11(3), 197-206.

Grafals, M., & Thurman, J. M. (2019). The Role of Complement in Organ Transplantation. Front Immunol, 10, 2380.

Grewal, I. S., & Flavell, R. A. (1998). CD40 and CD154 in cell-mediated immunity. Annual Review of Immunology, 16(1), 111-135.

Griewank, K., Borowski, C., Rietdijk, S., Wang, N., Julien, A., Wei, D. G., . . . Bendelac, A. (2007). Homotypic interactions mediated by Slamf1 and Slamf6 receptors control NKT cell lineage development. Immunity, 27(5), 751-762.

Gros, P., Milder, F. J., & Janssen, B. J. C. (2008). Complement driven by conformational changes. Nature Reviews Immunology, 8(1), 48-58.

Hageman, G. S., Anderson, D. H., Johnson, L. V., Hancox, L. S., Taiber, A. J., Hardisty, L. I., . . . Allikmets, R. (2005). A common haplotype in the complement regulatory gene factor H (HF1/CFH) predisposes individuals to age-related macular degeneration. Proc Natl Acad Sci U S A, 102(20), 7227-7232.

Hajishengallis, G., Reis, E. S., Mastellos, D. C., Ricklin, D., & Lambris, J. D. (2017). Novel mechanisms and functions of complement. Nature immunology, 18(12), 1288-1298.

Handa, J. T., Bowes Rickman, C., Dick, A. D., Gorin, M. B., Miller, J. W., Toth, C. A., . . . Farrer, L. A. (2019). A systems biology approach towards understanding and treating non-neovascular age-related macular degeneration. Nat Commun, 10(1), 3347. 1

Hansen, C. B., Willer, A., Bayarri-Olmos, R., Kemper, C., & Garred, P. (2018). Expression of complement C3, C5, C3aR and C5aR1 genes in resting and activated CD4(+) T cells. Immunobiology, 224(2), 307-315.

Harboe, M., Garred, P., Lindstad, J. K., Pharo, A., Muller, F., Stahl, G. L., . . . Mollnes, T. E. (2012). The role of properdin in zymosan- and Escherichia coli-induced complement activation. J Immunol, 189(5), 2606-2613.

Hattermann, K., Picard, S., Borgeat, M., Leclerc, P., Pouliot, M., & Borgeat, P. (2007). The Toll-like receptor 7/8-ligand resiquimod (R-848) primes human neutrophils for leukotriene B4, prostaglandin E2 and platelet-activating factor biosynthesis. FASEB J, 21(7), 1575-1585.

Hawlisch, H., Belkaid, Y., Baelder, R., Hildeman, D., Gerard, C., & Köhl, J. (2005). C5a negatively regulates toll-like receptor 4-induced immune responses. Immunity, 22(4), 415-426.

Hermans, I. F., Silk, J. D., Gileadi, U., Masri, S. H., Shepherd, D., Farrand, K. J., . . . Cerundolo, V. (2007). Dendritic cell function can be modulated through cooperative actions of TLR ligands and invariant NKT cells. Journal of immunology (Baltimore, Md.: 1950), 178(5), 2721-2729.

Hermans, I. F., Silk, J. D., Gileadi, U., Salio, M., Mathew, B., Ritter, G., . . . Cerundolo, V. (2003). NKT cells enhance CD4+ and CD8+ T cell responses to soluble antigen in vivo through direct interaction with dendritic cells. Journal of immunology (Baltimore, Md.: 1950), 171(10), 5140-5147.

Hiemstra, P. S., Daha, M. R., & Bouma, B. N. (1985). Activation of factor B of the complement system by kallikrein and its light chain. Thromb Res, 38(5), 491-503.

Holcroft, C. E., Jackson, W. D., Lin, W. H., Bassiri, K., Baines, R. A., & Phelan, P. (2013). Innexins Ogre and Inx2 are required in glial cells for normal postembryonic development of the Drosophila central nervous system. J Cell Sci, 126(Pt 17), 3823-3834.

Holers, V. M., & Thurman, J. M. (2004). The alternative pathway of complement in disease: opportunities for therapeutic targeting. Mol Immunol, 41(2-3), 147-152.

Holl, T. M., Yang, G., Kuraoka, M., Verkoczy, L., Alam, S. M., Moody, M. A., . . . Kelsoe, G. (2014). Enhanced antibody responses to an HIV-1 membrane-proximal external region antigen in mice reconstituted with cultured lymphocytes. J Immunol, 192(7), 3269-3279.

Holz, F. G., Sadda, S. R., Busbee, B., Chew, E. Y., Mitchell, P., Tufail, A., . . . Spectri Study, I. (2018). Efficacy and Safety of Lampalizumab for Geographic Atrophy Due to Age-Related Macular Degeneration: Chroma and Spectri Phase 3 Randomized Clinical Trials. JAMA Ophthalmol, 136(6), 666-677.

Hourcade, D. E. (2006). The role of properdin in the assembly of the alternative pathway C3 convertases of complement. J Biol Chem, 281(4), 2128-2132.

Hourcade, D. E., Mitchell, L. M., & Oglesby, T. J. (1998). A conserved element in the serine protease domain of complement factor B. J Biol Chem, 273(40), 25996-26000.

Ilan, Y. (2009). Alpha versus beta: are we on the way to resolve the mystery as to which is the endogenous ligand for natural killer T cells? Clin Exp Immunol, 158(3), 300-307.

Janeway, C. A., Jr. (2001). How the immune system protects the host from infection. Microbes Infect, 3(13), 1167-1171.

Jukes, J. P., Gileadi, U., Ghadbane, H., Yu, T. F., Shepherd, D., Cox, L. R., . . . Cerundolo, V. (2016). Non-glycosidic compounds can stimulate both human and mouse iNKT cells. European journal of immunology, 46(5), 1224-1234.

Karsten, C. M., Laumonnier, Y., Eurich, B., Ender, F., Broker, K., Roy, S., . . . Kohl, J. (2015). Monitoring and cell-specific deletion of C5aR1 using a novel floxed GFP-C5aR1 reporter knock-in mouse. J Immunol, 194(4), 1841-1855.

Kemper, C., & Atkinson, J. P. (2007). T-cell regulation: with complements from innate immunity. Nature Reviews Immunology, 7(1), 9-18.

Kemper, C., & Köhl, J. (2013). Novel roles for complement receptors in T cell regulation and beyond. Molecular immunology, 56(3), 181-190.

Kim, J. H., Oh, S. J., Ahn, S., & Chung, D. H. (2014). IFN-γ-producing NKT cells exacerbate sepsis by enhancing C5a generation via IL-10-mediated inhibition of CD55 expression on neutrophils. European journal of immunology, 44(7), 2025-2035.

Kim, Y., Pyaram, K., Kumar, A., & Chang, C.-H. (2017). Reactive oxygen species regulate the inflammatory function of NKT cells through Promyelocytic Leukaemia Zinc Finger (PLZF) protein. Journal of immunology, 199(10), 3478-3487.

Kim, Y. H., Kumar, A., Chang, C. H., & Pyaram, K. (2017). Reactive Oxygen Species Regulate the Inflammatory Function of NKT Cells through Promyelocytic Leukemia Zinc Finger. Journal of immunology, 199(10), 3478-3487.

Kjer-Nielsen, L., Borg, N. A., Pellicci, D. G., Beddoe, T., Kostenko, L., Clements, C. S., . . . McCluskey, J. (2006). A structural basis for selection and cross-species reactivity of the semi-invariant NKT cell receptor in CD1d/glycolipid recognition. J Exp Med, 203(3), 661-673.

Klibi, J., Amable, L., & Benlagha, K. (2020). A focus on natural killer T-cell subset characterization and developmental stages. Immunol Cell Biol, 98(5), 358-368.

Klos, A., Tenner, A. J., Johswich, K.-O., Ager, R. R., Reis, E. S., & Köhl, J. (2009). The role of the anaphylatoxins in health and disease. Molecular immunology, 46(14), 2753-2766.

Kolev, M., Dimeloe, S., Le Friec, G., Navarini, A., Arbore, G., Povoleri, G. A., . . . Develioglu, L. (2015). Complement regulates nutrient influx and metabolic reprogramming during Th1 cell responses. Immunity, 42(6), 1033-1047.

Kolev, M., & Kemper, C. (2017). Keeping It All Going—Complement Meets Metabolism. Frontiers in Immunology, 8.

Kolev, M., Le Friec, G., & Kemper, C. (2014). Complement--tapping into new sites and effector systems. Nature Reviews Immunology, 14(12), 811-20.

Kolev, M., West, E. E., Kunz, N., Chauss, D., Moseman, E. A., Rahman, J., . . . Kemper, C. (2020). Diapedesis-Induced Integrin Signaling via LFA-1 Facilitates Tissue Immunity by Inducing Intrinsic Complement C3 Expression in Immune Cells. Immunity, 52(3), 513-527.

Kremlitzka, M., Nowacka, A. A., Mohlin, F. C., Bompada, P., De Marinis, Y., & Blom, A. M. (2019). Interaction of Serum-Derived and Internalized C3 With DNA in Human B Cells-A Potential Involvement in Regulation of Gene Transcription. Front Immunol, 10, 493.

Kronenberg, M. (2005). Toward an understanding of NKT cell biology: progress and paradoxes. Annu.Rev.Immunol., 26, 877-900.

Krovi, S. H., & Gapin, L. (2018). Invariant Natural Killer T Cell Subsets-More Than Just Developmental Intermediates. Front Immunol, 9, 1393.

Kulkarni, H. S., Elvington, M. L., Perng, Y. C., Liszewski, M. K., Byers, D. E., Farkouh, C., . . . Atkinson, J. P. (2019). Intracellular C3 Protects Human Airway Epithelial Cells from Stress-associated Cell Death. Am J Respir Cell Mol Biol, 60(2), 144-157.

Kumar, A., Suryadevara, N., Hill, T. M., Bezbradica, J. S., Van Kaer, L., & Joyce, S. (2017). Natural Killer T Cells: An Ecological Evolutionary Developmental Biology Perspective. Front Immunol, 8, 1858.

Kumar, B. V., Connors, T. J., & Farber, D. L. (2018). Human T Cell Development, Localization, and Function throughout Life. Immunity, 48(2), 202-213.

Kurosaki, T., Kometani, K., & Ise, W. (2015). Memory B cells. Nat Rev Immunol., 15(3), 149-59.

Kwan, W.-h., van der Touw, W., & Heeger, P. S. (2012). Complement regulation of T cell immunity. Immunologic research, 54(1-3), 247-253.

Lalli, P. N., Strainic, M. G., Yang, M., Lin, F., Medof, M. E., & Heeger, P. S. (2008). Locally produced C5a binds to T cell-expressed C5aR to enhance effector T-cell expansion by limiting antigen-induced apoptosis. Blood, 112(5), 1759-1766.

Lam, P. Y., Nissen, M. D., & Mattarollo, S. R. (2017). Invariant Natural Killer T Cells in Immune Regulation of Blood Cancers: Harnessing Their Potential in Immunotherapies. Front Immunol, 8, 1355.

Laudisi, F., Spreafico, R., Evrard, M., Hughes, T. R., Mandriani, B., Kandasamy, M., . . . Mortellaro, A. (2013). Cutting edge: the NLRP3 inflammasome links complement-mediated inflammation and IL-1beta release. Journal of immunology (Baltimore, Md.: 1950), 191(3), 1006-1010.

Lee, C.-H., Romain, G., Yan, W., Watanabe, M., Charab, W., Todorova, B., . . . Lungu, O. I. (2017). IgG Fc domains that bind C1q but not effector Fc [gamma] receptors delineate the importance of complement-mediated effector functions. Nature immunology. 18(8), 889-898.

Lee, H., Whitfeld, P. L., & Mackay, C. R. (2008). Receptors for complement C5a. The importance of C5aR and the enigmatic role of C5L2. Immunology and cell biology, 86(2), 153-160.

Lee, Y. J., Holzapfel, K. L., Zhu, J., Jameson, S. C., & Hogquist, K. A. (2013). Steady-state production of IL-4 modulates immunity in mouse strains and is determined by lineage diversity of iNKT cells. Nat Immunol, 14(11), 1146-1154.

Lee, Y. J., Wang, H., Starrett, G. J., Phuong, V., Jameson, S. C., & Hogquist, K. A. (2015). Tissue-Specific Distribution of iNKT Cells Impacts Their Cytokine Response. Immunity, 43(3), 566-578.

Lenz, P., Bacot, S. M., Frazier-Jessen, M. R., & Feldman, G. M. (2003). Nucleoporation of dendritic cells: efficient gene transfer by electroporation into human monocyte-derived dendritic cells. FEBS Lett, 538(1-3), 149-154.

Li, K., Anderson, K. J., Peng, Q., Noble, A., Lu, B., Kelly, A. P., . . . Zhou, W. (2008). Cyclic AMP plays a critical role in C3a-receptor-mediated regulation of dendritic cells in antigen uptake and T-cell stimulation. Blood, 112(13), 5084-5094.

Li, K., Fazekasova, H., Wang, N., Peng, Q., Sacks, S. H., Lombardi, G., & Zhou, W. (2012). Functional modulation of human monocytes derived DCs by anaphylatoxins C3a and C5a. Immunobiology, 217(1), 65-73.

Li, K., Fazekasova, H., Wang, N., Sagoo, P., Peng, Q., Khamri, W., . . . Zhou, W. (2011). Expression of complement components, receptors and regulators by human dendritic cells. Mol Immunol, 48(9-10), 1121-1127.

Li, X. X., Lee, J. D., Kemper, C., & Woodruff, T. M. (2019). The Complement Receptor C5aR2: A Powerful Modulator of Innate and Adaptive Immunity. J Immunol, 202(12), 3339-3348.

Li, Z., Li, D., Tsun, A., & Li, B. (2015). FOXP3+ regulatory T cells and their functional regulation. Cell Mol Immunol, 12(5), 558-565.

Lian, Z. X., Kikuchi, K., Yang, G. X., Ansari, A. A., Ikehara, S., & Gershwin, M. E. (2004). Expansion of bone marrow IFN-alpha-producing dendritic cells in New Zealand Black (NZB) mice: high level expression of TLR9 and secretion of IFN-alpha in NZB bone marrow. J Immunol, 173(8), 5283-5289.

Lin, X., Chen, M., Liu, Y., Guo, Z., He, X., Brand, D., & Zheng, S. G. (2013). Advances in distinguishing natural from induced Foxp3 ( ) regulatory T cells. Int J Clin Exp Pathol, 6(2), 116-123.

Liszewski, M. K., Kolev, M., Le Friec, G., Leung, M., Bertram, P. G., Fara, A. F., . . . Meri, S. (2013). Intracellular complement activation sustains T cell homeostasis and mediates effector differentiation. Immunity, 39(6), 1143-1157.

Liu, J., Miwa, T., Hilliard, B., Chen, Y., Lambris, J. D., Wells, A. D., & Song, W. C. (2005). The complement inhibitory protein DAF (CD55) suppresses T cell immunity in vivo. The Journal of experimental medicine, 201(4), 567-577.

Liu, Y., Mei, J., Gonzales, L., Yang, G., Dai, N., Wang, P., . . . Worthen, G. S. (2011). IL-17A and TNF-alpha exert synergistic effects on expression of CXCL5 by alveolar type II cells in vivo and in vitro. J Immunol, 186(5), 3197-3205.

Lu, A., Li, H., Niu, J., Wu, S., Xue, G., Yao, X., . . . Meng, G. (2017). Hyperactivation of the NLRP3 Inflammasome in Myeloid Cells Leads to Severe Organ Damage in Experimental Lupus. J Immunol, 198(3), 1119-1129.

Lubbers, R., van Essen, M. F., van Kooten, C., & Trouw, L. A. (2017). Production of complement components by cells of the immune system. Clin Exp Immunol, 188(2), 183-194.

Lynch, L., Michelet, X., Zhang, S., Brennan, P. J., Moseman, A., Lester, C., . . . Brenner, M. B. (2015). Regulatory iNKT cells lack expression of the transcription factor PLZF and control the homeostasis of T(reg) cells and macrophages in adipose tissue. Nat Immunol, 16(1), 85-95.

Maibaum, J., Liao, S. M., Vulpetti, A., Ostermann, N., Randl, S., Rudisser, S., . . . Anderson, K. (2016). Small-molecule factor D inhibitors targeting the alternative complement pathway. Nat Chem Biol, 12(12), 1105-1110.

Mao, A. P., Constantinides, M. G., Mathew, R., Zuo, Z., Chen, X., Weirauch, M. T., & Bendelac, A. (2016). Multiple layers of transcriptional regulation by PLZF in NKT-cell development. Proc Natl Acad Sci U S A, 113(27), 7602-7607.

Markiewski, M. M., DeAngelis, R. A., Benencia, F., Ricklin-Lichtsteiner, S. K., Koutoulaki, A., Gerard, C., . . . Lambris, J. D. (2008). Modulation of the antitumor immune response by complement. Nature immunology, 9(11), 1225-1235.

Markiewski, M. M., & Lambris, J. D. (2009). Is complement good or bad for cancer patients? A new perspective on an old dilemma. Trends in immunology, 30(6), 286-292.

Marsh, J. E., Farmer, C. K., Jurcevic, S., Wang, Y., Carroll, M. C., & Sacks, S. H. (2001). The allogeneic T and B cell response is strongly dependent on complement components C3 and C4. Transplantation, 72(7), 1310-1318.

May, R. M., Okumura, M., Hsu, C. J., Bassiri, H., Yang, E., Rak, G., . . . Kambayashi, T. (2013). Murine natural killer immunoreceptors use distinct proximal signaling complexes to direct cell function. Blood, 121(16), 3135-3146.

McCarthy, C., Shepherd, D., Fleire, S., Stronge, V. S., Koch, M., Illarionov, P. A., . . . Cerundolo, V. (2007). The length of lipids bound to human CD1d molecules modulates the

affinity of NKT cell TCR and the threshold of NKT cell activation. The Journal of experimental medicine, 204(5), 1131-1144.

McEwen-Smith, R. M., Salio, M., & Cerundolo, V. (2015). CD1d-dependent endogenous and exogenous lipid antigen presentation. Current opinion in immunology, 34, 116-125.

Medzhitov, R., & Janeway, C. A., Jr. (1997). Innate immunity: impact on the adaptive immune response. Curr Opin Immunol, 9(1), 4-9.

Merle, N. S., Church, S. E., Fremeaux-Bacchi, V., & Roumenina, L. T. (2015). Complement System Part I - Molecular Mechanisms of Activation and Regulation. Front Immunol, 6, 262.

Mollnes, T. E., Jokiranta, T. S., Truedsson, L., Nilsson, B., Rodriguez de Cordoba, S., & Kirschfink, M. (2007). Complement analysis in the 21st century. Mol Immunol, 44(16), 3838-3849.

Montoya, C. J., Pollard, D., Martinson, J., Kumari, K., Wasserfall, C., Mulder, C. B., . . . Wilson, S. B. (2007). Characterization of human invariant natural killer T subsets in health and disease using a novel invariant natural killer T cell-clonotypic monoclonal antibody, 6B11. Immunology, 122(1), 1-14.

Morgan, B. P., & Harris, C. L. (2015). Complement, a target for therapy in inflammatory and degenerative diseases. Nat Rev Drug Discov, 14(12), 857-877.

Morgan, H. P., Schmidt, C. Q., Guariento, M., Blaum, B. S., Gillespie, D., Herbert, A. P., . . . Johansson, C. M. (2011). Structural basis for engagement by complement factor H of C3b on a self surface. Nature structural & molecular biology, 18(4), 463-470.

Morris, K. M., Goldberger, G., Colten, H. R., Aden, D. P., & Knowles, B. B. (1982). Biosynthesis and processing of a human precursor complement protein, pro-C3, in a hepatoma-derived cell line. Science, 215(4531), 399-400.

Mueller-Ortiz, S. L., Wang, D., Morales, J. E., Li, L., Chang, J. Y., & Wetsel, R. A. (2009). Targeted disruption of the gene encoding the murine small subunit of carboxypeptidase N (CPN1) causes susceptibility to C5a anaphylatoxin-mediated shock. J Immunol, 182(10), 6533-6539.

Napier, B. A., Brubaker, S. W., Sweeney, T. E., Monette, P., Rothmeier, G. H., Gertsvolf, N. A., . . . Monack, D. M. (2016). Complement pathway amplifies caspase-11-dependent cell death and endotoxin-induced sepsis severity. J Exp Med, 213(11), 2365-2382.

Napolitani, G., Rinaldi, A., Bertoni, F., Sallusto, F., & Lanzavecchia, A. (2005). Selected Toll-like receptor agonist combinations synergistically trigger a T helper type 1–polarizing program in dendritic cells. Nature immunology, 6(8), 769-776.

Nikitin, P. A., Rose, E. L., Byun, T. S., Parry, G. C., & Panicker, S. (2019). C1s Inhibition by BIVV009 (Sutimlimab) Prevents Complement-Enhanced Activation of Autoimmune Human B Cells In Vitro. J Immunol, 202(4), 1200-1209.

Noris, M., & Remuzzi, G. (2013). Overview of complement activation and regulation. Paper presented at the Seminars in nephrology. 33(6), 479–492.

Oh, J., Wu, N., Barczak, A. J., Barbeau, R., Erle, D. J., & Shin, J. S. (2018). CD40 Mediates Maturation of Thymic Dendritic Cells Driven by Self-Reactive CD4(+) Thymocytes and Supports Development of Natural Regulatory T Cells. Journal of immunology (Baltimore, Md.: 1950), 200(4), 1399-1412.

Paget, C., Mallevaey, T., Speak, A. O., Torres, D., Fontaine, J., Sheehan, K. C. F., . . . de Moraes, M. L. (2007). Activation of invariant NKT cells by toll-like receptor 9-stimulated dendritic cells requires type I interferon and charged glycosphingolipids. Immunity, 27(4), 597-609.

Paixao-Cavalcante, D., Torreira, E., Lindorfer, M. A., Rodriguez de Cordoba, S., Morgan, B. P., Taylor, R. P., . . . Harris, C. L. (2014). A humanized antibody that regulates the alternative pathway convertase: potential for therapy of renal disease associated with nephritic factors. J Immunol, 192(10), 4844-4851.

Palm, F., Sjoholm, K., Malmstrom, J., & Shannon, O. (2019). Complement Activation Occurs at the Surface of Platelets Activated by Streptococcal M1 Protein and This Results in Phagocytosis of Platelets. J Immunol, 202(2), 503-513.

Pang, S. S., Wijeyewickrema, L. C., Hor, L., Tan, S., Lameignere, E., Conway, E. M., . . . Pike, R. N. (2017). The Structural Basis for Complement Inhibition by Gigastasin, a Protease Inhibitor from the Giant Amazon Leech. Journal of immunology (Baltimore, Md.: 1950), 199(11), 3883-3891.

Peng, Q., Li, K., Anderson, K., Farrar, C. A., Lu, B., Smith, R. A., . . . Zhou, W. (2008). Local production and activation of complement up-regulates the allostimulatory function of dendritic cells through C3a-C3aR interaction. Blood, 111(4), 2452-2461.

Peng, Q., Li, K., Patel, H., Sacks, S. H., & Zhou, W. (2006). Dendritic cell synthesis of C3 is required for full T cell activation and development of a Th1 phenotype. J Immunol, 176(6), 3330-3341.

Peng, Q., Li, K., Wang, N., Li, Q., Asgari, E., Lu, B., . . . Zhou, W. (2009). Dendritic cell function in allostimulation is modulated by C5aR signaling. J Immunol, 183(10), 6058-6068.

Pratt, J. R., Basheer, S. A., & Sacks, S. H. (2002). Local synthesis of complement component C3 regulates acute renal transplant rejection. Nat Med, 8(6), 582-587.

Prigozy, T. I., Naidenko, O., Qasba, P., Elewaut, D., Brossay, L., Khurana, A., . . . Kronenberg, M. (2001). Glycolipid antigen processing for presentation by CD1d molecules. Science, 291(5504), 664-667.

Purwar, R., Wittmann, M., Zwirner, J., Oppermann, M., Kracht, M., Dittrich-Breiholz, O., . . . Werfel, T. (2006). Induction of C3 and CCL2 by C3a in keratinocytes: a novel autocrine amplification loop of inflammatory skin reactions. Journal of immunology, 177(7), 4444-4450.

Ramarathinam, L., Sarma, S., Maric, M., Zhao, M., Yang, G., Chen, L., & Liu, Y. (1995). Multiple lineages of tumors express a common tumor antigen, P1A, but they are not cross-protected. Journal of immunology, 155(11), 5323-5329.

Reilly, E. C., Wands, J. R., & Brossay, L. (2010). Cytokine dependent and independent iNKT cell activation. Cytokine, 51(3), 227-231.

Reinink, P., & Van Rhijn, I. (2016). Mammalian CD1 and MR1 genes. Immunogenetics, 68(8), 515-523.

Reis, E. S., Barbuto, J. A. M., & Isaac, L. (2006). Human monocyte-derived dendritic cells are a source of several complement proteins. Inflammation Research, 55(5), 179-184.

Reis, E. S., Mastellos, D. C., Hajishengallis, G., & Lambris, J. D. (2019). New insights into the immune functions of complement. Nat Rev Immunol, 19(8), 503-516.

Rennick, D., Jackson, J., Moulds, C., Lee, F., & Yang, G. (1989). IL-3 and stromal cell-derived factor synergistically stimulate the growth of pre-B cell lines cloned from long-term lymphoid bone marrow cultures. J Immunol, 142(1), 161-166.

Ribot, J. C., Lopes, N., & Silva-Santos, B. (2020). gammadelta T cells in tissue physiology and surveillance. Nat Rev Immunol.

Ricklin, D., Reis, E. S., & Lambris, J. D. (2016). Complement in disease: a defence system turning offensive. Nat Rev Nephrol, 12(7), 383-401.

Risitano, A. M. (2012). Paroxysmal nocturnal hemoglobinuria and other complement-mediated hematological disorders. Immunobiology, 217(11), 1080-1087.

Risitano, A. M., Notaro, R., Luzzatto, L., Hill, A., Kelly, R., & Hillmen, P. (2010). Paroxysmal nocturnal hemoglobinuria--hemolysis before and after eculizumab. N Engl J Med, 363(23), 2270-2272.

Risitano, A. M., Notaro, R., Luzzatto, L., Hill, A., Kelly, R., & Hillmen, P. (2010). Paroxysmal nocturnal hemoglobinuria--hemolysis before and after eculizumab. N Engl J Med, 363(23), 2270-2272.

Rodriguez, E., Rallapalli, P. M., Osborne, A. J., & Perkins, S. J. (2014). New functional and structural insights from updated mutational databases for complement factor H, Factor I, membrane cofactor protein and C3. Biosci Rep, 34(5).

Rooijakkers, S. H., Wu, J., Ruyken, M., van Domselaar, R., Planken, K. L., Tzekou, A., . . . Gros, P. (2009). Structural and functional implications of the alternative complement pathway C3 convertase stabilized by a staphylococcal inhibitor. Nat Immunol, 10(7), 721-727.

Rudensky, A. Y. (2011). Regulatory T cells and Foxp3. Immunol Rev, 241(1), 260-268.

Sahu, A., & Lambris, J. D. (2001). Structure and biology of complement protein C3, a connecting link between innate and acquired immunity. Immunological reviews, 180(1), 35-48.

Salou, M., Legoux, F., Gilet, J., Darbois, A., du Halgouet, A., Alonso, R., . . . Lantz, O. (2019). A common transcriptomic program acquired in the thymus defines tissue residency of MAIT and NKT subsets. J Exp Med, 216(1), 133-151.

Savage, A. K., Constantinides, M. G., Han, J., Picard, D., Martin, E., Li, B., . . . Bendelac, A. (2008). The transcription factor PLZF directs the effector program of the NKT cell lineage. Immunity, 29(3), 391-403.

Scalise, M., Galluccio, M., Console, L., Pochini, L., & Indiveri, C. (2018). The Human SLC7A5 (LAT1): The Intriguing Histidine/Large Neutral Amino Acid Transporter and Its Relevance to Human Health. Front Chem, 6, 243.

Schmittgen, T. D., & Livak, K. J. (2008). Analyzing real-time PCR data by the comparative C(T) method. Nat Protoc, 3(6), 1101-1108.

Schulz, O., Edwards, A. D., Schito, M., Aliberti, J., Manickasingham, S., Sher, A., & e Sousa, C. R. (2000). CD40 triggering of heterodimeric IL-12 p70 production by dendritic cells in vivo requires a microbial priming signal. Immunity, 13(4), 453-462.

Serna, M., Giles, J. L., Morgan, B. P., & Bubeck, D. (2016). Structural basis of complement membrane attack complex formation. Nat Commun, 7, 10587.

Sheen, J. H., Strainic, M. G., Liu, J., Zhang, W., Yi, Z., Medof, M. E., & Heeger, P. S. (2017). TLR-Induced Murine Dendritic Cell (DC) Activation Requires DC-Intrinsic Complement. Journal of immunology (Baltimore, Md.: 1950), 199(1), 278-291.

Silk, J. D., Hermans, I. F., Gileadi, U., Chong, T. W., Shepherd, D., Salio, M., . . . Cerundolo, V. (2004). Utilizing the adjuvant properties of CD1d-dependent NK T cells in T cell-mediated immunotherapy. The Journal of clinical investigation, 114(12), 1800-1811.

Silk, J. D., Salio, M., Reddy, B. G., Shepherd, D., Gileadi, U., Brown, J., . . . Cerundolo, V. (2008). Cutting edge: nonglycosidic CD1d lipid ligands activate human and murine invariant NKT cells. Journal of immunology (Baltimore, Md.: 1950), 180(10), 6452-6456.

Smith, R. J. H., Appel, G. B., Blom, A. M., Cook, H. T., D'Agati, V. D., Fakhouri, F., . . . Nester, C. M. (2019). C3 glomerulopathy - understanding a rare complement-driven renal disease. Nat Rev Nephrol, 15(3), 129-143.

Smyth, M. J., Crowe, N. Y., Pellicci, D. G., Kyparissoudis, K., Kelly, J. M., Takeda, K., . . . Godfrey, D. I. (2002). Sequential production of interferon-gamma by NK1.1(+) T cells and natural killer cells is essential for the antimetastatic effect of alpha-galactosylceramide. Blood, 99(4), 1259-1266.

Souza, D. G., Esser, D., Bradford, R., Vieira, A. T., & Teixeira, M. M. (2005). APT070 (Mirococept), a membrane-localised complement inhibitor, inhibits inflammatory responses that follow intestinal ischaemia and reperfusion injury. Br J Pharmacol, 145(8), 1027-1034.

Speak, A. O., Cerundolo, V., & Platt, F. M. (2008). CD1d presentation of glycolipids. Immunology & Cell Biology, 86(7), 588-597.

Strainic, M. G., Liu, J., Huang, D., An, F., Lalli, P. N., Muqim, N., . . . Medof, M. E. (2008). Locally Produced Complement Fragments C5a and C3a Provide Both Costimulatory and Survival Signals to Naive CD4+ T Cells. Immunity, 28(3), 425-435.

Strainic, M. G., Shevach, E. M., An, F., Lin, F., & Medof, M. E. (2013). Absence of signaling into CD4 cells via C3aR and C5aR enables autoinductive TGF-[beta] 1 signaling and induction of Foxp3 regulatory T cells. Nature immunology, 14(2), 162-171.

Straub, T., Freudenberg, M. A., Schleicher, U., Bogdan, C., Gasteiger, G., & Pircher, H. (2018). Bacterial coinfection restrains antiviral CD8 T-cell response via LPS-induced inhibitory NK cells. Nat Commun, 9(1), 4117.

Takeda, K., & Akira, S. (2004). TLR signaling pathways. Semin Immunol, 16(1), 3-9.

Takeuchi, O., & Akira, S. (2010). Pattern recognition receptors and inflammation. Cell, 140(6), 805-820.

Thielen, A. J. F., van Baarsen, I. M., Jongsma, M. L., Zeerleder, S., Spaapen, R. M., & Wouters, D. (2018). CRISPR/Cas9 generated human CD46, CD55 and CD59 knockout cell lines as a tool for complement research. J Immunol Methods, 456, 15-22.

Thurman, J. M., & Yapa, R. (2019). Complement Therapeutics in Autoimmune Disease. Front Immunol, 10, 672.

Tuttle, K. D., Krovi, S. H., Zhang, J., Bedel, R., Harmacek, L., Peterson, L. K., . . . Gapin, L. (2018). TCR signal strength controls thymic differentiation of iNKT cell subsets. Nat Commun, 9(1), 2650.

Van Kaer, L. (2005). alpha-Galactosylceramide therapy for autoimmune diseases: prospects and obstacles. Nat Rev Immunol, 5(1), 31-42.

Van Kaer, L., & Wu, L. (2018). Therapeutic Potential of Invariant Natural Killer T Cells in Autoimmunity. Front Immunol, 9, 519.

van Vuuren, B. J., Bergseth, G., Mollnes, T. E., & Shaw, A. M. (2014). Electroluminescent TCC, C3dg and fB/Bb epitope assays for profiling complement cascade activation in vitro using an activated complement serum calibration standard. J Immunol Methods, 402(1-2), 50-56.

Verschoor, A., Karsten, C. M., Broadley, S. P., Laumonnier, Y., & Köhl, J. (2016). Old dogs—new tricks: immunoregulatory properties of C3 and C5 cleavage fragments. Immunological reviews, 274(1), 112-126.

Vincent, M. S., Gumperz, J. E., & Brenner, M. B. (2003). Understanding the function of CD1-restricted T cells. Nat Immunol, 4(6), 517-523.

Vogel, C. W. (2020). The Role of Complement in Myocardial Infarction Reperfusion Injury: An Underappreciated Therapeutic Target. Front Cell Dev Biol, 8, 606407.

Voskoboinik, I., Smyth, M. J., & Trapani, J. A. (2006). Perforin-mediated target-cell death and immune homeostasis. Nature Reviews Immunology, 6(12), 940-952.

Wang, S., Bartido, S., Yang, G., Qin, J., Moroi, Y., Panageas, K. S., . . . Houghton, A. N. (1999). A role for a melanosome transport signal in accessing the MHC class II presentation pathway and in eliciting CD4+ T cell responses. J Immunol, 163(11), 5820-5826.

West, E. E., Kolev, M., & Kemper, C. (2018). Complement and the Regulation of T Cell Responses. Annu Rev Immunol, 36, 309-338.

Wetsel, R. A. (1995). Structure, function and cellular expression of complement anaphylatoxin receptors. Current opinion in immunology, 7(1), 48-53.

Whaley, K. (1980). Biosynthesis of the complement components and the regulatory proteins of the alternative complement pathway by human peripheral blood monocytes. The Journal of experimental medicine, 151(3), 501-516.

Wittmann, M., Kienlin, P., Mommert, S., Kapp, A., & Werfel, T. (2002). Suppression of IL-12 production by soluble CD40 ligand: evidence for involvement of the p44/42 mitogen-activated protein kinase pathway. Journal of immunology (Baltimore, Md.: 1950), 168(8), 3793-3800.

Wolf, B. J., Choi, J. E., & Exley, M. A. (2018). Novel Approaches to Exploiting Invariant NKT Cells in Cancer Immunotherapy. Front Immunol, 9, 384.

Wu, J., & Sun, X. (2019). Complement system and age-related macular degeneration: drugs and challenges. Drug Des Devel Ther, 13, 2413-2425.

Xing, Y., Yao, X., Li, H., Xue, G., Guo, Q., Yang, G., . . . Meng, G. (2017). Cutting Edge: TRAF6 Mediates TLR/IL-1R Signaling-Induced Nontranscriptional Priming of the NLRP3 Inflammasome. J Immunol, 199(5), 1561-1566.

Yang, G., Artiaga, B. L., Lomelino, C. L., Jayaprakash, A. D., Sachidanandam, R., McKenna, R., & Driver, J. P. (2019). Next Generation Sequencing of the Pig alphabeta TCR Repertoire Identifies the Porcine Invariant NKT Cell Receptor. J Immunol, 202(7), 1981-1991.

Yang, G., Coffman, F. D., & Wheelock, E. F. (1994). Characterization and purification of a macrophage-triggering factor produced in Mycoplasma arginini-infected L5178Y cell cultures. J Immunol, 153(6), 2579-2591.

Yang, G., Hellstrom, K. E., Hellstrom, I., & Chen, L. (1995). Antitumor immunity elicited by tumor cells transfected with B7-2, a second ligand for CD28/CTLA-4 costimulatory molecules. J Immunol, 154(6), 2794-2800.

Yang, G., Hellstrom, K. E., Mizuno, M. T., & Chen, L. (1995). In vitro priming of tumor-reactive cytolytic T lymphocytes by combining IL-10 with B7-CD28 costimulation. J Immunol, 155(8), 3897-3903.

Yang, G., McIntyre, K. W., Townsend, R. M., Shen, H. H., Pitts, W. J., Dodd, J. H., . . . Watson, A. J. (2003). Phosphodiesterase 7A-deficient mice have functional T cells. J Immunol, 171(12), 6414-6420.

Yang, G., Mizuno, M. T., Hellstrom, K. E., & Chen, L. (1997). B7-negative versus B7-positive P815 tumor: differential requirements for priming of an antitumor immune response in lymph nodes. J Immunol, 158(2), 851-858.

Yang, G. X., Lian, Z. X., Kikuchi, K., Liu, Y. J., Ansari, A. A., Ikehara, S., & Gershwin, M. E. (2005). CD4- plasmacytoid dendritic cells (pDCs) migrate in lymph nodes by CpG inoculation and represent a potent functional subset of pDCs. J Immunol, 174(6), 3197-3203.

Yang, G. X., Lian, Z. X., Kikuchi, K., Moritoki, Y., Ansari, A. A., Liu, Y. J., . . . Gershwin, M. E. (2005). Plasmacytoid dendritic cells of different origins have distinct characteristics and function: studies of lymphoid progenitors versus myeloid progenitors. J Immunol, 175(11), 7281-7287.

Yang, G. X., Wu, Y., Tsukamoto, H., Leung, P. S., Lian, Z. X., Rainbow, D. B., . . . Ridgway, W. M. (2011). CD8 T cells mediate direct biliary ductule damage in nonobese diabetic autoimmune biliary disease. J Immunol, 186(2), 1259-1267.

Yang, J. Q., Kim, P. J., & Singh, R. R. (2012). Brief treatment with iNKT cell ligand alpha-galactosylceramide confers a long-term protection against lupus. J Clin Immunol, 32(1), 106-113.

Yu, K. K. Q., Wilburn, D. B., Hackney, J. A., Darrah, P. A., Foulds, K. E., James, C. A., . . . Seshadri, C. (2019). Conservation of molecular and cellular phenotypes of invariant NKT cells between humans and non-human primates. Immunogenetics, 71(7), 465-478.

Zajonc, D. M., & Girardi, E. (2015). Recognition of Microbial Glycolipids by Natural Killer T Cells. Front Immunol, 6, 400.

Zhang, W., Wang, G., Wang, Y., Jin, Y., Zhao, L., Xiong, Q., . . . Dai, Y. (2017). Generation of complement protein C3 deficient pigs by CRISPR/Cas9-mediated gene targeting. Sci Rep, 7(1), 5009.

Zipfel, P. F., & Skerka, C. (2009). Complement regulators and inhibitory proteins. Nature Reviews Immunology, 9(10), 729-740.

Zipfel, P. F., Wiech, T., Rudnick, R., Afonso, S., Person, F., & Skerka, C. (2019). Complement Inhibitors in Clinical Trials for Glomerular Diseases. Front Immunol, 10, 2166.

Zuniga-Pflucker, J. C. (2004). T-cell development made simple. Nat Rev Immunol, 4(1), 67-72.